JOURNAL OF APPLIED PHYSICS

JOURNAL
OF
APPLIED PHYSICS

Vol. 18, No. 12 DECEMBER, 1947

In This Issue

Page

Preliminary Study of a Physical Basis of Bird Navigation
HENRY L. YEAGLEY 1035

Inversion Applied to the Solution of 3-Dimensional Electromagnetic Problems
A. BLOCH 1064

Non-Linear Viscous Elasticity and the Eyring Shear Model
GEORGE HALSEY 1072

Magnetron-Resonator System
E. C. OKRESS 1098

Gyroscopic Effects in a Vibratory System
G. S. BENNETT 1110

Frequency Stabilization of Microwave Oscillators by Spectrum Lines
WILLIAM V. SMITH, JOSÉ L. GARCÍA DE QUEVEDO, R. L. CARTER, AND W. S. BENNETT 1112

Efficiency of Thermoelectric Generators. I.
MARIA TELKES 1116

Cesium Chromate Photo-Tube Pellets
H. A. LIEBHAFSKY AND A. F. WINSLOW 1128

Letters to the Editor:

Remarks on Some Recently Developed Devices for Summing Fourier Series for Crystal Structure Analysis
C. L. CHRIST 1133

Annual Indexes

Author Index to Volume 18 1140
Subject Index to Volume 18 1145
Volume Table of Contents III

In Every Issue

New Books 1134
New Booklets 1137
Here and There 1138
Calendar of Meetings 1139
Index to Advertisers XXXVI

BOARD OF EDITORS

ELMER HUTCHISSON, *Editor*

Associate Editors
R. BOWLING BARNES
OTTO BEECK
W. F. BUSSE
W. JAMES LYONS
PHILIP MORRISON
PAUL E. SABINE
FREDERICK SEITZ
J. R. TOWNSEND
JOHN VON NEUMANN

Publication of the American Institute of Physics

ADMINISTRATIVE STAFF

HENRY A. BARTON, *Director*

CLEVELAND NORCROSS, *Assistant Director*

RUTH F. BRYANS, *Publication Manager*

THEODORE VORBURGER, *Business Manager*

JOHN T. TATE, *Adviser on Publications*

GOVERNING BOARD

GEORGE R. HARRISON, *Chairman*

WALLACE WATERFALL, *Secretary*

GEORGE B. PEGRAM, *Treasurer*

E. U. CONDON
A. J. DEMPSTER
W. F. FAIR, JR.
FLOYD A. FIRESTONE
HARVEY FLETCHER
R. C. GIBBS
K. S. GIBSON
PAUL E. KLOPSTEG
A. H. PFUND
JOHN T. TATE
M. W. WHITE
A. G. WORTHING

The JOURNAL OF APPLIED PHYSICS, published monthly at Prince and Lemon Sts., Lancaster, Pa., is devoted to physics in its role as the science basic to other natural sciences and to the arts and industries. Previous to 1937 this publication was known as PHYSICS. The JOURNAL OF APPLIED PHYSICS publishes editorials, news of physicists, and reviews, as well as technical papers of applied physics.

Manuscripts should be submitted to Elmer Hutchisson, Editor, Case Institute of Technology, Cleveland 6, Ohio.

Subscriptions and orders for back numbers should be addressed to Prince and Lemon Streets, Lancaster, Pa. or to the American Institute of Physics, 57 East 55 Street, New York 22, N. Y.

Subscription Price

	U.S. AND CANADA	ELSEWHERE
To members and associate members of the American Institute of Physics	$6.00	$7.00
To all others	8.00	9.00

Back Number Prices

Complete set: Vol. 1, July, 1931–Vol. 17, 1946—$124.00
Yearly back number rate: $10.00
Single copies: $1.00 each.

Changes of address should be sent to the Business Manager, American Institute of Physics; **corrected proofs** should be sent to the Publication Manager, American Institute of Physics.

Advertising rates supplied on request. Orders, advertising copy, and cuts should be sent to the American Institute of Physics.

Entered as second class matter January 22, 1937, at the Post Office at Lancaster, Pennsylvania, under the Act of March 3, 1879.
Accepted for mailing at the special rate of postage provided for in the Act of February 28, 1925, authorized May 2, 1932.

Copyright 1947, by the American Institute of Physics.

Journal
of
Applied Physics

Volume 18, Number 12 December, 1947

A Preliminary Study of a Physical Basis of Bird Navigation

HENRY L. YEAGLEY
Department of Physics, The Pennsylvania State College, State College, Pennsylvania
(Received June 26, 1947)

Foreword

F. C. WHITMORE
Dean of the School of Chemistry and Physics, The Pennsylvania State College

The theory presented was formulated in 1942 at the Pennsylvania State College by Dr. H. L. Yeagley, Associate Professor of Physics. Its only public presentation is in a preliminary non-technical article in the October 1943 issue of The Penn State Engineer, a local student publication. The training of birds for the first experiments was begun in May 1943. The first actual field test was made November 7, 1943 with homing pigeons trained to navigate to Paoli, Pennsylvania. This experiment was witnessed by officers of the U. S. Army Signal Corps, including Major Otto Meyer, in charge of the Army Pigeon Service Agency of the U. S. Army Signal Corps. Because of the positive nature of the results and their importance to communication in the war, all subsequent work was reported only to the Army Service Forces:

Report on Bird Navigation, "Theory and confirming evidence" Decemder 12, 1944.

Report on Bird Navigation, "Hamlet experiment," April 24, 1945.

Report on Bird Navigation, "A continuation of experiments started at the Pennsylvania State College in December, 1942," January 4, 1946.

Report on Bird Navigation, "East-West experiment," June 30, 1946.

The bird navigation theory as presented implies an organ or organs in the bird's physiology which are sensitive to the effect of its motion through the vertical component of the earth's magnetic field and to the effort exerted to overcome the coriolis force, due to the earth's rotation. Both these influences involve a set of lines which together form a navigational gridwork. By correlating its instantaneous land speed with the two above effects, a bird can fly to its home which is a unique point in this gridwork, or to related companion points existing in the gridwork at positions other than its home. Experimentation with homing pigeons between the home and spurious home points (conjugate or companion points) has yielded data which supports the theory.

PROBABLY no natural phenomenon has intrigued man and held his interest more than the ability of the homing pigeon to fly long distances from a strange locality and across unfamiliar territory to its home loft. Many leading ornithologists believe that this same ability guides wild birds in their long migratory flights over land and water areas. Invariably, references made to this remarkable accomplishment in the bird world are in terms of "instinct," which is a way of saying "we don't know."

The over-all problem of bird navigation involves at least the following five factors:

1. A desire on the part of the homing pigeon

to go to the home loft or, in the case of wild birds, to go to their summer feeding and breeding grounds, or their warmer wintering areas during migratory periods.

2. The physical strength and endurance to fly the required distance.

3. A knowledge of familiar landmarks, within a minimum radius, for piloting to the exact spot. (This radius distance for homing pigeons is known to be about twenty-five miles.)

4. The ability to navigate. This implies the possession and use of an organ or organs as navigating instruments.

5. Considerable navigating experience in flying in and about the "home" region. With homing pigeons this experience is artificially built up by sending the birds to gradually increasing distances.

It is well known that many birds of the migratory species return to their breeding and nesting grounds after being trapped and sent hundreds of miles into strange territory. Many such flights have been arranged so that the birds must orient themselves and fly hundreds of miles over water routes out of sight of land. One species, the Golden Plover,[1] performs the remarkable feat of navigating 3000 miles from Alaska to the Hawaiian Islands with no landmarks over the broad expanses of the Pacific Ocean. Hundreds of individuals of the albatross family roam over thousands of square miles of the Southern Pacific area. Members of each species finally return to their own tiny island to breed and raise young. Hood Island[2] of the Galapagos Archipelago group, is headquarters for one species of these birds. Since there are no "sign posts" of any kind over the ocean wastes, the flights must involve true navigation until the home island comes into view. Other types of birds, including noddy and sooty terns, swallows, herring gulls, numerous varieties of ducks, hawks, storks, starlings, chimney swifts, have the homing or navigating ability developed to a high degree.

Thus, while man has been slowly and laboriously learning to navigate during the past six centuries, birds have been using a system of their own for perhaps millions of years.

Hundreds of papers have been written suggesting possible fragmentary explanations of the mystery of bird orientation. The more scientifically possible of these explanations involve sensitivity of the bird to one or more of the following:

1. The effect of motion through the earth's magnetic field.[3]

2. Gravitational differences due to variations in the earth's radius.

3. The Coriolis effect due to the earth's rotation.[4]

In order to set up a working system of bird navigation or, indeed, of any navigation, a combination of two or more overlapping fields of influence is necessary. Each of these must possess definite gradients. Possible grid patterns might represent repetitive, displaced fields of a single kind, or combinations of two or more of the following:

1. Light beams—limited, by horizon extinction, to comparatively small areas, and useful only in piloting.

2. Sound beams—too limited for long distances, conceivably available only for piloting.

3. Electric fields—extremely limited by small intensity factor, variable magnitudes, lack of permanence.

4. Electromagnetic radiations—network of radio or radar beams such as are used in the radio-range network system of navigation or, more properly, piloting.

5. Magnetic fields—the earth's natural magnetic field, a somewhat irregular function of distance from the magnetic poles.

6. Force fields, such as:

   a. Coriolis force,
   b. Gravitational force,
   c. Centrifugal force.

---

[1] Frederick C. Lincoln, *The Migration of American Birds* (Doubleday, Doran and Company, Inc., Garden City, New York, 1936).

[2] J. L. Peters, *Check-list of Birds of the World* (Harvard University Press, Cambridge, Massachusetts, 1931), Vol. 1 or 2; *ibid.*, Vol. 2, 1937; *ibid.*, Vol. 3, 1940; *ibid.*, Vol. 4.

[3] C. Viguier, "Le seus de l'orientation," Rev. Phil. **14**, 1 (1882); A. Thauzies, "Apropos d'une theorie sur l'orientation du pigeon voyageur," Rev. Sci. (series 5) **3**, 270 (1905); "L'orientation du pigeon voyageur," Ann. Med. Vet. **54**, 141 (1905).

[4] Dr. W. H. Thorpe and D. H. Wilkinson, "Ising's theory of bird orientation," Nature, December 21 (1946). Also, G. Ising, "The physical possibility of a biological sense of orientation based on the rotation of the earth," Ark. Math. Astrophys. **32A**, No. 4 (1946).

Appended is a bibliography of the fragmentary suggestions that have previously been made in explanation of bird navigation. Special attention is called to Dr. D. R. Griffin's paper,* "The sensory basis of bird navigation," and to W. M. Levi's book, *The Pigeon*,† for an excellent general coverage of the subject.

In setting up the present theory of bird navigation the following well-known facts pertaining to the flying and use of homing pigeons were considered:

1. When released at unfamiliar and distant points, they usually fly in large circles for a matter of minutes before moving off in a straight line. When training flights have been experienced once or twice daily for weeks, and pigeons are released individually from new locations around the compass, they often sense the correct direction, after having flown only one or a fraction of a complete circle.

2. Homing pigeons are unable to navigate in a thick haze or fog or in complete darkness. Blinded or hooded birds fly first in a large circle and then in a decreasing spiral, gradually decending until about six feet above ground level, after which a "crash" landing is made.

3. Pigeons are unable to navigate successfully in winds much over thirty-five miles per hour.

4. After reaching four or five weeks of age, homing pigeons can be trained "around the compass" for six or eight weeks at increasing distances of one, two, four, eight, sixteen, thirty-two miles (repeating each distance one or two times before increasing), after which they are easily capable of navigating flights of distances up to seventy miles and more. With a few more weeks of training, flights of one to two hundred miles, or even more, are readily accomplished. A year later, with some additional short training flights added to their experience, they can readily navigate home from four hundred miles, without previous experience of any kind in the new territory.

5. Written reports by the Army and Navy Communications[5] as well as numerous oral reports by representatives of flying clubs and individuals, indicate that pigeons are confused and are unable to orient themselves when released from points near powerful radio and radar broadcasting stations. There are some indications that the audiofrequencies rather than the carrier-frequencies are the disturbing factor.

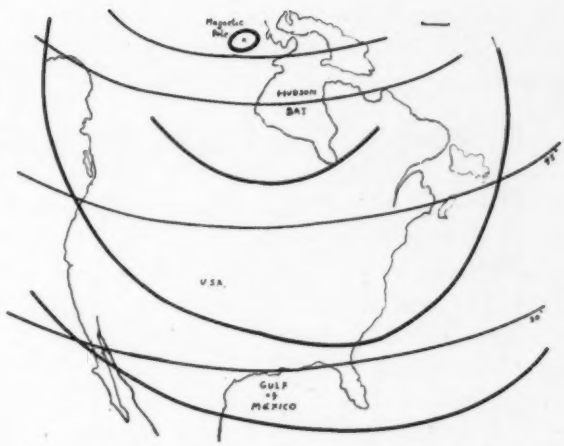

MAP I. North American section of earth-globe showing lines of equal magnetic vertical-Coriolis gridwork. South magnetic pole displacement from north terrestrial pole is roughly about 20° or 1400 miles.

The following theory is presented as the first complete working hypothesis to explain homing-pigeon navigation.

Three major factors are involved:

1. Sensitivity of birds to the effect of flying through a magnetic field.

2. Sensitivity to the forces, produced by the earth's rotation, acting on masses moving over its surface in a straight line (part of the well-known Coriolis effect which is a function of latitude).

3. Visual sensitivity to velocity over the earth's surface (land speed).

By correlating the results of the first and last of these sensitivities the bird can detect his "magnetic latitude." This differs from his true latitude because the magnetic poles are grossly and asymmetrically displaced from the earth's poles (Map I). By similar correlation of the second and last sensitivities it is possible to detect the true latitude.

The effective result of these two correlations is that the bird can recognize his home locality at the intersection of a characteristic line in the

* D. R. Griffin, "The Sensory Basis of Bird Navigation," Quarterly Review of Biology, 1 (1944).

† W. M. Levi, *The Pigeon* (R. L. Bryan Company, Columbia, South Carolina, 1944).

[5] *Experiments With Homing Pigeons' Sensitivity to Radio Frequency Waves*, conducted by 285th Signal Pigeon Company, March 1945.

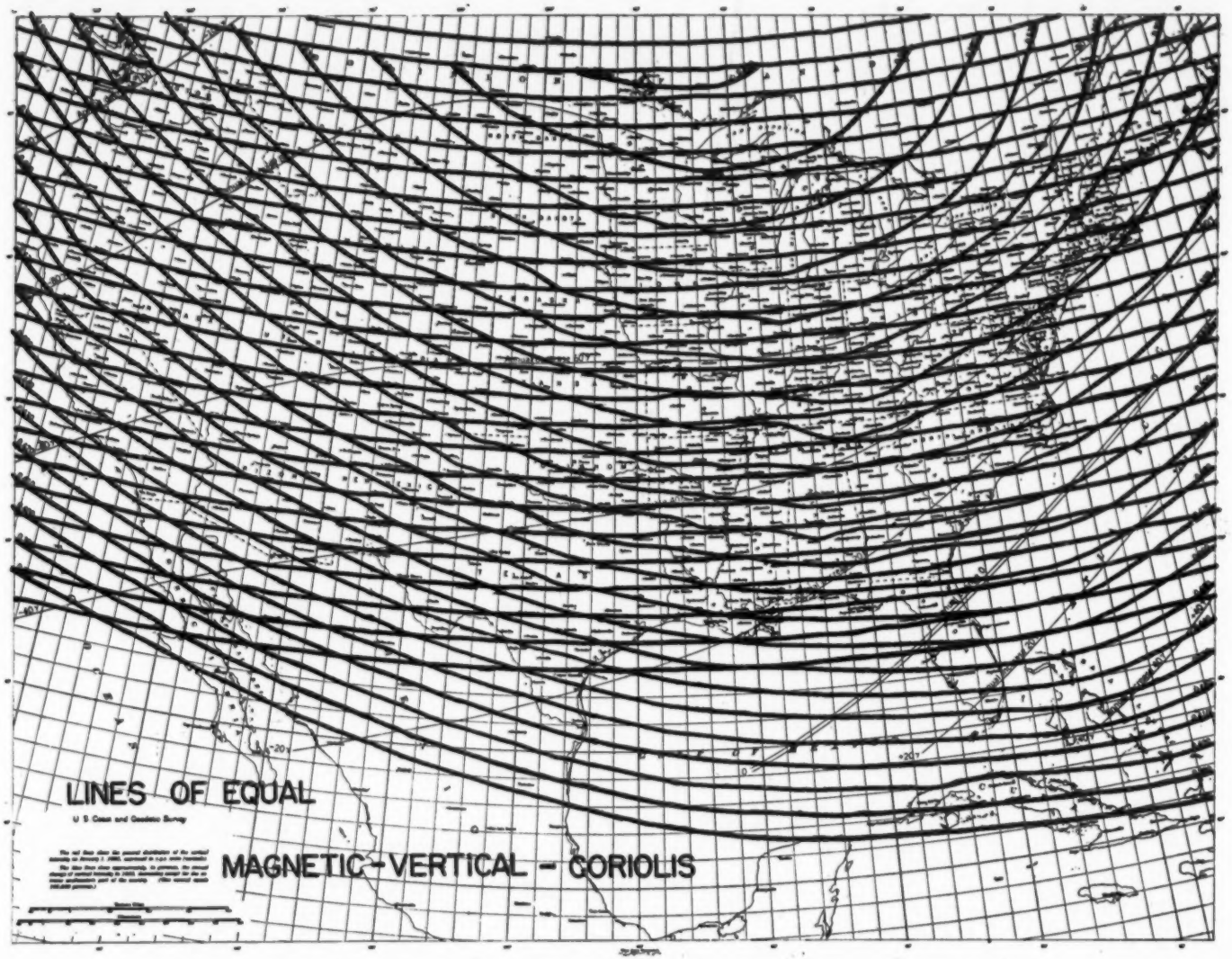

MAP II. Lines of equal magnetic vertical-Coriolis gridwork for the United States and bordering areas.

earth's magnetic vertical field with a characteristic line of latitude.

Thus it appears that the secret of bird navigation depends on the displacement of the magnetic poles from the rotational poles of the earth with the subsequent intersection of the lines of equal magnetic-vertical intensity with latitude lines (Maps I and II).

The fact is that it was a study of Map II in relation to the failure of homing pigeons near Indianapolis, Indiana,[6] which gave the first clue to the present theory. As will be noted, in that area the two sets of curves are essentially parallel. Thus in that section, the two sets of correlations guide the birds to a line many miles long instead of to an approximate point. It should be added that the study of maps involving lines of equal magnetic declination, equal magnetic dip, equal magnetic horizontal intensity, equal total magnetic intensity, or any combination of these failed to show such parallelism in southern Indiana.

In operation, the navigation may be as follows:

1. A bird is sensitive by virtue of some organ or organs to the magnitude of the effect of its motion in flight through the vertical component of the earth's magnetic field.[7] This effect which must be correlated with its land speed, is a direct function of the bird's horizontal velocity, and the distance from the magnetic poles. It is a maximum at the poles and decreases somewhat irregularly from each pole toward a line approximately half-way between. By this means, a bird, if flying in a location of magnetic vertical field intensity different from its home, can consciously fly in a direction which will bring its land-speed magnetic vertical-field effect[8] back to that to which it is accustomed during its normal flight around home territory. Since the lines of equal vertical magnetic-field intensity are irregular closed curves centering around the magnetic poles, it is evident that they represent one set of lines involving a velocity-magnetic vertical-field-gradient pattern which is part of our proposed navigational grid system.

2. A bird is sensitive by virtue of some organ or organs to the magnitude of the Coriolis effect. This latter results from a natural relationship between the earth's rotational velocity and motion of a body over the earth. The forces involved are a direct function of the earth's rotational speed, the speed of a body moving over the earth's surface, and the latitude of the moving body. As in the case of the electromagnetic effect, the bird must correlate its land speed with the magnitude of this force in order to use it as a guide. The lines of equal Coriolis force are true circles coincident with parallels of latitude. Hence, if a bird, usually subject to the Coriolis effect of normal flying around home territory, is displaced north or south, he need only fly in a direction which will bring the "feel" of the Coriolis land-speed relation back to normal and he will be back on his own latitude circle. These circles represent a second set of lines which in bird orientation involves a force land-speed-gradient pattern which is a part of our postulated navigational grid system.

Map I illustrates the existence on the earth of a gridwork of two distinct sets of curves, representing the land speed *vs.* electromagnetic effect and the land speed *vs.* Coriolis effect. For any horizontally moving body over the earth's surface these intersecting curves give rise to a system of unique pairs of conjugate points.

This conception offered an opportunity for the experimental testing of the theory. If a bird locates its home by navigating to the intersection of the proper magnetic vertical and the proper latitude, he should as readily navigate to the conjugate point as to his home, if released nearer the former. As can be seen on Map II the conjugate point of State College, Pennsylvania is in central Nebraska. A location near Kearney, Nebraska, has been used for checking the theory, as will be described below.

EFFECT OF MOTION THROUGH THE MAGNETIC FIELD

It is a well-known fact that whenever a continuous ring or circle of some material medium is rotated in a magnetic field, so that the lines of flux are cut, an e.m.f. is induced. This is said to result from a change of flux linkage and its magnitude is given by:

[6] F. J. Sauerteig, "Indianapolis," Am. Racing Pigeon News, Nov. 1942, p. 1.

[7] See reports to the U. S. Army Signal Corps listed in the Foreword.

[8] This effect may be the same phenomenon as the so-called "electromagnetic effect," it will subsequently be referred to as such for the sake of brevity.

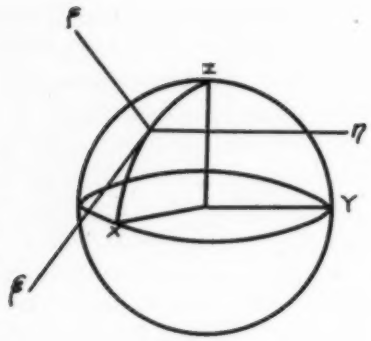

FIG. 1.

e.m.f. $= d\psi/10^8 dt$ (e.m.f. = induced voltage);
$d\psi/dt$ = rate cutting of flux in number of lines cut per second;
10^8 = factor needed to give result in volts or joules per coulomb.

Although it is quite customary in physics texts to give problems in which it is required to find the voltage induced when a straight wire of given length cuts a magnetic field of given strength and orientation at a given velocity, no known experiment has ever shown conclusively that an e.m.f. is induced under these latter conditions. Nevertheless, in dealing with bird navigational flight in this theory the assumption is made that the bird in some way senses the effect of flying normally through the vertical component of the earth's magnetic field, and the laws obeyed are the same or analogous to the electromagnetic effect. Whether or not it is the latter, as is ordinarily meant in the physical sense, or a phenomenon for which man has not yet conceived a picture, does not alter its general application to the theory involved. For if a bird navigates according to a pattern which fits exactly into the vertical, magnetic-field Coriolis gridwork, illustrated in Map II, some mechanism relating it to bird navigation exists, even though man does not yet comprehend its full import. A flying bird or any object moving at right angles to a magnetic field or its component would constitute a system comparable to a moving straight wire mentioned above rather than a rotating ring.

Should the sensitivity of the bird involve the ordinary laws of electromagnetism, the magnitude of the induced voltage for a bird flying forty miles per hour at State College, Pennsylvania, where the vertical component of magnetic field intensity is .556 oersted,[9] would be:

$$\text{e.m.f.} = \frac{d\psi}{10^8 dt} = \frac{H \cdot L}{10^8}\frac{ds}{dt} = \frac{.556 \times 1 \times 1798}{10^8}$$

$= 10^{-5}$ or 10 microvolts per cm of length.

$d\psi$ = lines of flux cut, H = field intensity, L = length of conductor, 40 mi./hr. = 59 ft./sec. or 1798 cm/sec. This voltage might make itself felt either across the nerves in the wings and other gross parts of the bird or across the eye, the ear, or any organ or parts of organs.

Not only sensitivity to the absolute value but also reaction to its variation is necessary to guide the bird in the compensatory direction. For this reason the increments of magnetic vertical-field intensity should be examined.

Average values of the vertical component of magnetic-field intensity are 0.60 oersted at a distance of 15° from the south magnetic pole in the Hudson Bay region, and 0.68 oersted at a distance of approximately 5 to 8 degrees from the South Magnetic Pole in the general region south of New Zealand. These values diminish to zero at points along great circles, approximately midway between. In equatorial regions the variation of the vertical intensity in a general north-south direction is about .01 oersted per degree. In the United States the corresponding variation is roughly .007 oersted per degree. Since all experimental work involved in this report has been done in this country the latter value will be considered for illustrative purposes.

$$\frac{d(\text{e.m.f.})}{d\varphi} = \frac{L}{10^8}\frac{ds}{dt}\frac{dH}{d\varphi} = \frac{1.798 \times 10 \times 7 \times 10^{-3}}{10^8}$$

$$= \frac{1 \times 1798 \times .007}{10^8} = \frac{1 \times 1.798 \times 7}{10^8} = 12.6 \times 10^{-8}$$

= .13 microvolt change for approximately each degree or seventy miles of flight (a change of 1.3 percent per degree).

$d\varphi$ = increment of "magnetic latitude"

[9] World values of H may be obtained from map No. 1702, "The vertical intensity of the earth's magnetic force," published by the Hydrographic Office, Washington, D. C. Values for the United States of America from Booklet and Serial number 602, as previously indicated.

EFFECT OF MOTION THROUGH THE CORIOLIS FIELD

The following equations represent the Coriolis acceleration or force per unit mass and were obtained from A. G. Webster's *Dynamics* (G. E. Stechert and Company, New York), p. 320–322.

$$d^2\xi/dt^2 = 2\Omega \sin\varphi(d\eta/dt), \quad \text{(see Fig. 1)} \quad (1)$$

$$d^2\eta/dt^2 = -2\Omega\{(d\xi/dt)\sin\varphi + (d\zeta/dt)\cos\varphi\}, \quad (2)$$

$$d^2\zeta/dt^2 = -g + 2\Omega\cos\varphi(d\eta/dt). \quad (3)$$

φ = latitude of place, Ω = angular rotational speed of the earth, $-g$ = acceleration of gravity, $\pm\eta$ = distance moved east or west on the earth surface, $\pm\zeta$ = distance moved north or south on the earth surface, $\pm\xi$ = distance moved toward zenith or nadir, t = time.

According to these equations, it is apparent that a bird might conceivably make use of Coriolis forces due to its motion in any direction (i.e., horizontal, vertical, or their resultant directions) as part of its system of navigation. Only horizontal motions are considered as part of this theory but if vertical motions were also included, no basic changes would be involved in the discussion, since in any case the magnitude of the resulting Coriolis forces will still be a function only of Ω, $\sin\varphi$ and ds/dt. Since the bird's continuous and normal motion in homing is horizontal, only the latter will be considered. Hence the following modified equation is obtained by combining (1) and (2):

$$a = [(d^2\xi/dt^2)^2 + (d^2\eta/dt^2)^2]^{\frac{1}{2}}$$

$$= 2\Omega\sin\varphi[(d\eta/dt)^2 + (d\xi/dt)^2]^{\frac{1}{2}}. \quad (4)$$

$$= 2\Omega\sin\varphi(ds/dt)$$

In (2) the term $(d\zeta/dt)\cos\varphi$ is zero since motion in the ζ (vertical) direction is considered zero. Equation (3) denotes that there will be a vertical force of Coriolis resulting whenever there is a component of horizontal velocity eastward or westward. When the motion is in the $+\eta$ (eastward) direction it is downward, and *vice versa*. The value of $d^2\zeta/dt^2$ (insofar as the bird is concerned) varies above or below $-g$ when it flies in any horizontal direction having a component of velocity either east or west. This vertical force could also be part of the bird's orienting mechanism and might operate to help maintain migrating birds on a true north or south course. In the bird's home territory where it recognizes local landmarks and awareness of direction is a factor, as in piloting operations, this vertical force may again operate in guiding him. As previously stated, even though this vertical force, or the term $(d\zeta/dt)\cos\varphi$ (in Eq. (2)), actually enters the picture, it in no way changes the over-all concept of the Coriolis land-speed relation to bird navigation as set forth in the theory. As homing pigeons are known to fly at rates of twenty to sixty miles per hour, a value of forty miles per hour, or fifty-nine feet per second, will again be used for making an illustrative calculation. A median value of 45° latitude will also be chosen arbitrarily to go with this arbitrary speed value. Substituting in Eq. (4):

$$a = 2\times\frac{2\pi}{86{,}400}\times.707\times59$$

$$= \frac{4\times3.14\times7.07\times5.9}{8.64\times10^4} = \frac{524}{8.64\times10^4} = 61\times10^{-4}$$

$$= .0061 \text{ feet per second per second.}$$

The direction of this Coriolis acceleration on the northern hemisphere is to the right and on the southern hemisphere to the left of the line of flight. This latter is commonly known to produce the counter-clockwise and clockwise whirlpools of moving fluids on the northern and southern hemispheres of the earth.

As a result of this accleration, the force per unit mass would be $F = ma = 1\times.0061$ or .0061 poundal per pound at 45° latitude, and a speed of forty miles per hour. Or in terms of rate change of Coriolis effect with respect to time:

$$\frac{da}{dt} = 2\Omega\frac{ds}{dt}\cos\varphi\frac{d\phi}{dt}.$$

But

$$\frac{d\phi}{dt} = \frac{1}{r}\cdot\frac{ds}{dt},$$

$$\therefore \frac{da}{dt} = \frac{2\Omega\cos\varphi(ds/dt)^2}{r} = \frac{2\times2\pi\times.707\times59\times59}{86400\times3955\times5280}$$

$$= \frac{4\times3.14\times7.07\times5.9\times5.9\times10^1}{8.64\times3.96\times5.28\times10^{10}}$$

$$= 1.72\times10^{-8} \text{ ft./sec./sec. each second,}$$

or about

$$10.8\times10^{-5}=.000108\frac{\text{ft./sec./sec.}}{\text{degree}}.$$

This 1.7 percent change of force per unit mass therefore occurs in flying one degree normal to the parallel circles of equal Coriolis effect at 45° latitude. The absolute value of Coriolis acceleration varies from maximum $1.00/.707\times.0060 = .0085$ ft./sec./sec. at forty mi./hr. at the poles to zero at the equator.

Judging by these tiny increments of Coriolis force and magnetic effect which the bird would have to correlate with land speed for navigational guidance, the tendency is to reject its validity.

Also it is certain that there is a physical basis for this ability to navigate which pigeons constantly demonstrate. It seems fair to assert that if the directives involved were of a gross magnitude, with modern scientific tools and mathematical means of investigation they would have been uncovered before now.

Examination of Maps I and II reveals that in the equal magnetic-vertical intensity Coriolis-force gridwork each pair of intersecting lines cross each other at least twice. In addition, about midway between the pairs of conjugate intersections, approximate parallelism often exists over a considerable portion of their lengths. These conditions also differ from a perfect pattern because large segregated surface deposits of magnetic materials on the earth prevent the equal magnetic-vertical lines from more than simulating the form of a true circle. On the United States Map II it can be seen that this condition of parallelism obtains over a fairly wide band of land area, including parts of Wisconsin, Illinois, Indiana, Kentucky, Tennessee, etc.

The above-mentioned relationships suggest that birds trained to navigate to one point of intersection of two lines toward the east, should, if released nearer to their conjugate point, fly preferentially toward the latter. Likewise, the region of parallelism or tangency should be one of confusion for navigating birds. If trained within this region their home would not contain a unique point with reference to the theory, or, if trained outside but released within this region, they would be in the dilemma of being apparently able to fly toward their home in either of two directions, approximately 180° apart. This suggests the experiments of training homing pigeons to navigate to one location and releasing them near the conjugate point of the location, or at points in between the two conjugates to see if they react to the home or conjugate positions.

Another suggested experiment arises from the idea that if birds are guided by the effect of flight through the vertical component of the earth's magnetic field, they should become confused if a sufficiently strong superimposed magnetic field moves upward and downward across their bodies simultaneously. These and the previously mentioned considerations led to the following set of experiments which will be described in chronological order.

TABLE I.

Nov.	Day	Two copper plates	Two magnets	Lost one magnet	Lost two magnets
7	1st	5	–	1	–
8	2nd	3	–	–	–
9	3rd	–	–	–	–
10	4th	–	1	2	2

EXPERIMENT I

The Magnetic Wing Experiment, November 7, 1943

The first experimental test of the theory was made by superimposing on homing pigeons while in navigational flight, a magnetic field moved up and down by their wing motion. This was accomplished by attaching hyflux-chrome magnets on the under side of the wings, between the first and second joints.

The normal magnetic effect would be the one due to the somewhat pulsating forward motion at right angles through the vertical component of the earth's magnetic field. If a number of homing pigeons with the superimposed moving experimental field were unable to home normally and a like number with identical training but with attached copper plates of the same approximate mass and size should home from the same release point in the normal fashion, it would be an indication that the earth's magnetic field plays a part in bird navigational guidance.

The birds used in this experiment were raised and trained for it by Mr. Lowell Gable of Paoli, Pennsylvania. Because he is an educated man with a scientific mind and one of the foremost in the field of homing pigeon racing, it was felt the experiment would be more significant than under other circumstances. Mr. Gable carefully trained twenty of his best young birds to pilot and navigate to his loft from distances up to one-hundred miles. The training flights were always from stations to the west, northwest, and north of Paoli so that the birds would not become familiar with land areas to the south and southwest over which the final experimental flights would be run. They were singly released many times at fifty to one-hundred airline miles or more to insure individual navigating skill and eliminate those that simply followed their loft-mates home. Between 10:05 A.M. and 12:04 P.M. on the morning of November 7, 1943, the twenty trained birds were released at a point eight miles southeast of Bellaire, Maryland. The airline distance to the loft at Paoli was about sixty-five miles. To the wings of each bird in turn was attached either a pair of magnetic or copper plates before it was set free. None was released until the previous one had been out of sight for five minutes. Its general direction of travel at time of disappearance was carefully noted. All even-numbered birds carried hyflux-chrome magnets, whereas the odd-numbered ones had copper plates attached to their wings. Both magnets and copper plates used were $1'' \times .218'' \times .025''$ and weighed approximately .8 gram. Attachments were made on the under side of the manus portions of the wings. Since any attachment involving the wing feathers or feather follicles would have caused rapid and serious irritations, a plan had been devised by which thin silk strands were threaded through the flesh between the third and fourth metacarpal bones. Previous and later tests showed that no soreness or injury resulted from long attachment or from hundreds of miles of flying with the plates remaining in position.

The record of their returns as supplied by Mr. Lowell Gable is shown in Table I.

The magnets on the wings of the birds were separated about 12″ between centers when in a horizontal, full-spread position. They were of such strength as to produce a horizontal intensity, half-way between them, about equal to that of the earth's magnetic horizontal component in the region of State College. This value is approximately .172 oersted.

TABLE II.

3	with copper plates deviated less than 10° from a direct line toward the home loft, sixty-five airline miles to the northeast.
4	with copper were less than 50° off from this line toward the north.
3	others with copper were less than 30° off from this line toward the east.
4	with magnets were about 45° off from this line.
2	with magnets were more than 90° from this line.
3	with magnets were approximately 130° off from this line.
1	with magnets flew in the exactly opposite direction from the home loft.

By assuming that the magnets move up and down with approximately simple harmonic motion and estimating the wing beats at 180 per second and their amplitude at $\frac{1}{8}$ foot, a value of .12 microvolt per centimeter was computed for the maximum induced e.m.f. per centimeter on the bird's anatomy.

This value of .12 microvolt per centimeter, as can be seen, is of the same order of magnitude as the change of e.m.f. involved in flying eighty miles toward or away from the normal magnetic-vertical line previously considered at 45° latitude. Both its magnitude and its pulsating character, i.e., changing three-hundred and sixty times per minute, from zero to .12 microvolt per centimeter and back to zero, might conceivably serve to confuse the bird and upset his navigating prowess during its occurrence.

The following important points should be noted:

1. Eight of ten birds with copper plates returned home during the first two days.

2. Of those returning, having originally had two magnets each and subsequently losing either one or both, only one with one magnet got home before the fourth day.

3. Only one bird with two magnets got home at all and it arrived on the fourth day.

4. None of the other birds, at this writing, has ever returned.

The final results of the experiment were well presaged by the directions in which the birds left the release point. Each was carefully watched out of sight before another was released. Table II

TABLE III. Showing release points and final locations of birds released.

Release	No.	Band	Place found	Date	Wind velocity, dir. to lofts, temp., storms, etc.
Release No. 1	1	AU43 PA11891	St. Paul	6/30	20 mi./hr. E.N.E. S.W.
St. Paul, Neb.,	2	WSC41 D2020	Grand Island	7/1	71°F
June 29, 1944,	3	IF431 5014	Grand Island	7/1	18 thunderstorms during day
distance 43 miles,	4	AU43 U5115	Ulysses	7/1	
14 birds,	5	IF43 K4994	Callaway	7/3	
7 reported	6	AU43 V50825	Franklin	7/4	
	7	IF43 K5013	Belgrade	7/5	
Release No. 2	1	AU44 P48107	Clay Center	7/2	22 mi./hr. S.E. N.W.
Hastings, Neb.	2	WB 31	Greeley	7/3	80°F
June 30, 1944,	3	AU44 P8113	Harrard	7/3	16 thunderstorms
distance 42 miles	4	AU43 V50824	Heartwell	7/2	
13 birds,	5	AU43 PA11886	Hastings	9/11	
5 reported					
Release No. 3	1	AU44 V35151	Sargent	7/3	20 mi./hr. S. S.E.
Broken Bow, Neb.,	2	AU44 V35165	Ericson	7/3	temperature?
July 1, 1944	3	AU44 P48110	Bassett	7/3	3 thunderstorms
distance 50 mi.	4	AU44 P48320	Mason City	7/2	
20 birds,	5	AU44 V35137	Ansley	7/8	
10 reported	6	AU44 V35160	Ansley	7/8	
	7	AU43 V58822	Comstock	7/2	
	8	IF43 BER414	Broken Bow	7/6	
	9	AU43 U5389	Taylor	7/3	
	10	AU43 V5111	12 W Loup City		
Release No. 4	1	WB26	Heartwell	7/4	24 mi./hr. S.S.W. N.N.W.
Minden, Neb.,	2	AU44 V35162	Kenesaw	7/5	93°F
July 2, 1944	3	AU44 P48117	Longpine	7/7	7 thunderstorms
distance 25 mi.,	4	*AU43 Y4794	5 mi. E. of Kearney	7/5	*AU43 Y4794—a Heitzman bird
15 birds,	5	AU43 X27252	Kenesaw	7/5	came within 3 miles of finding
7 reported	6	AU43 PA11780	Holredge	7/6	loft
	7	AU43 M4820	Lexington	7/7	
Release No. 5,	1	*WB 28	East Loft	7/5	21 mi./hr. S.E.
Havens, Neb.,	2	AU44 26649	Minden	7/4	91°F
July 3, 1944	3	AU44 V35141	Lexington	7/4	23 storms
distance 70 mi.,	4	AU43 PA11696	Ashton	11/23	*A Heissler (York, Pa.) bird flew 70
17 birds,					mi. and found loft. Direction was
4 reported					away from State College
Release No. 6	1	AU44 14356	Gothenburg	7/5	17 mi./hr. S.E.
Cozad, Neb.,	2	AU44 H48122	Burwell	7/6	81°F
July 4, 1944,	3	AU44 B335150	Cozad	7/6	11 storms
distance 48 mi.,	4	AU44 V35159	Cozad	7/6	
16 birds,	5	AU44 P48118	5 mi. N. Cozad	9/1	
9 reported	6	WB 27	Oconto	9/15	
	7	AU43 DC1486	Dunning	7/6	
	8	IF43 B518	Bertrand	7/26	
	9	AU43 J6506	11 mi. NW Miller	9/5	

indicates the general direction at which the birds went out of sight from the release point.

Since these birds were well trained and outstanding homing pigeons, Mr. Gable and others expert in the field of flying and racing homing pigeons expected at least two or possibly three of those with two magnets to home, just on the basis of their intelligence and ability to "hunt" their way home. On the basis of probability and chance a similar prediction would obtain.

EXPERIMENT II

The First Nebraska Experiment

With the positive though limited data for the electromagnetic phase of the theory secured, the groundwork was laid for testing the theory as a whole. Examination of the U. S. Coast and Geodetic Survey Map I revealed that the conjugate point of State College, Pennsylvania, (corrected for 1944) i.e., another position having

TABLE III.—*Continued.*

Release	No.	Band	Place found	Date	Wind velocity, dir. to lofts, temp., storms, etc.
Release No. 7 Columbus, Neb., July 7, 1944, distance 100 miles, 2 birds released, 1 reported	1	AU44 P48109	Thedford	7/10	21 mi./hr. 94° 25 storms
Release No. 8 20 mi. east Council Bluffs, Iowa, July 8, 1944, distance 185 mi., 1 bird released, 1 received in west loft	1	IF43 B1014	West loft	7/10	21 mi./hr. N.E. 77°F 18 storms—this bird flew 185 miles in a direction opposite from State College and found the west loft near Kearney
Special Release No. 1 Lincoln, Neb., May 14, 1944, distance 120 mi., 12 birds, 5 reported	1	RBC5951JF	15 mi. W. Grand Island	5/16	Day of release was clear, no winds, cool
	2	NPAB 3542	Lenora, Kan.	8/15	
	3	AU–A 13726	Fort Morgan, Col.	5/24	(Birds trained up to 50 and more miles)
	4	VE 14576	Odell, Neb.	5/22	
	5	AU–Y–6005	Freemont, Neb.	5/16	
Special Release No. 2 Lincoln, Neb., June 25, 1944, 12 birds released, 6 reported	1	E11712–43	Lincoln, Neb.	7/25	
	2	42W18225	Lincoln, Neb.	7/17	
	3	NPA43 B13239	Lincoln, Neb.	7/25	
	4	NPA44 B8117	Lincoln, Neb.	6/24	Weather clear
	5	41Z17857	Wahoo, Neb. later Lindwood, Neb.	6/26 7/6	Slight south wind
	6	NPA43–B13241	Hebron, Neb.	6/30	
Special Release No. 3 Berkeley Springs, Va., Cozad, Neb. birds September 16, 1944 distance 100 miles J. A. Rendle birds, 12 birds released, 6 reported	1	AU44 W8831	Pittsburgh, Pa.	9/20	
	2	AU44 W8849	Palmerton, Pa.	10/2	Weather was clear
	3	AU44 W8852	Freeland, Pa.	9/25	Very light breeze
	4	AU44 W8841	Near Berkeley Springs, Va.	9/19	Haze in distance
	5	AU43 A1436	E. Liverpool, Ohio	9/20	Birds released in sets of 3's
	6	AU44 W3851	Portage, Pa.	9/26	

identical values of magnetic vertical intensity and Coriolis force, lies in about the south-central portion of Nebraska (ten miles north of Kearney). A plan was worked out whereby a group of one hundred or more carefully selected homing pigeons would be settled[10] and trained at State College, after which the birds and lofts would be transferred to the above conjugate point. Tests would then be made to determine if they would fly from the surrounding regions toward that point instead of heading for State College, Pennsylvania.

With this plan in view, training flights up to fifty miles around State College were decided upon and the birds were housed in a conspicuously designed and painted loft so it could be seen from as great a distance as possible. In addition, it was moved[11] each day so that the occupants, returning from training flights, would become accustomed to looking for the loft and not for familiar landmarks nearby. A five-foot observation balloon was raised each day about one-hundred and fifty feet above the loft as an additional beacon or guide. All these plans were executed carefully. The loft had a peak resembling a church spire and the whole was painted a brilliant yellow. It was moved two hundred feet each day and during the training period traveled a distance, by tractor power, of about three miles in a zigzag path over and across the college farms. The birds were given initial

[10] Having been in full flight around loft, the bird returns and enters it. During his first free flight outdoors even though raised on the spot, it is easily frightened off in a panic, and may fail to take visual account of its surroundings. On a second release it is practically certain to return.

[11] Its location was shifted 200 feet each day for training flights of the birds, and never returned to a previous location.

piloting training flights[12] of one, two, four, eight, and sixteen miles in several directions around the compass. From then on for a period of three months they had practice flights twice daily up to fifty and more miles. There was seldom a half-day during which they were not released at some new point around the compass. Care was used to prevent repetitional flights which might either aid or hinder them in the Nebraska experiment. It is known that repeated training during the same part of the day and over the same terrain causes homing pigeons to fly habitually by the sun's direction. Near the end of the training period they were released from time to time in singles, doubles, and sets of five at twenty-five-mile airline distances.

On the day set for the start of the trip to Nebraska the birds were transported to Altoona by truck in one of the homing lofts. The shipment from there on was by express so the loft had been carefully designed to make it as large as possible and yet have it go inside the express car. During the entire 1100-mile trip the nests with eggs and young were cared for by the parent birds. On arrival in Kearney the loft was set on the fair grounds until magnetic measurements were made to check the values obtained from the U. S. Department of Commerce. Also a second loft had been built and previously shipped, to double the chance of the birds' finding one in case they navigated from the release points to the predicted conjugate point. Askania magnetometer measurements showed that the magnetic vertical-field intensity ten miles north of Kearney was the same as State College. Unfortunately, however, the field intensity gradually increased to about three times its normal value fifteen miles east and returned to its normal value ten miles beyond the anomaly. This condition meant that there were actually two conjugate points twenty-five miles apart, which called for a choice of placing the two lofts about 10 miles apart on either side of the point as planned according to the U. S. averages, or putting one at the normal conjugate point and the other twenty-five miles to the east at the anomalous conjugate point. The limited personnel and transportation facilities made the twenty-five mile separation impractical. In addition, magnetic anomalies exert most of their influence fairly near the ground surface and for all these reasons the former strategy was used. The lofts were carefully placed five miles east and west of the calculated position on as high ground as could be found in that flat country. The birds were allowed to rest one day to acclimate themselves to the immediate surroundings.

Beginning with June 28, groups of birds were taken out to release points around the compass forty and more airline miles away. Each bird carried an army-message capsule with the words.

Important
Telegraph Immediately (collect)
Wildlife Research Unit
cooperating with
The Army Pigeon Service
c/o Fort Kearney Hotel
Kearney, Nebraska
Give band number
Place found
Date

The data obtained from these experiments are set forth in Table III. Releases No. 1 through No. 8 show the direct result of the experiment proper carried out between June 29 and July 8. Releases labeled Specials No. 1 and No. 2 were performed before, and Special No. 3 after the main experiment and will be discussed later in the report. Map III, showing the state of Nebraska, contains a representation of the data shown on Table III except for that designated Special release No. 2 and No. 3. Each vector on the map represents graphically the sum total of the results for a given day or release number, the latter being in one-to-one correspondence on the map and table.

The flights of all birds reported were plotted as vectors on a preliminary work map and their vector sum obtained. The length of the latter was divided by the number of flights involved and the resultant vector represents the average result of all the recorded flights of that day. In referring to these in this report the term "total flight vector" will be used. A brief inspection of the total flight vectors for the eight days shows that numbers one, two, four, five, and eight not only point in the right direction but actually

[12] Short distance flights in which guidance could always be had by means of familiar landmarks.

MAP III. Flight vectors showing average flights of the various groups of pigeons released according to data on Table III.

terminate within ten miles of one or the other of the two predicted points (the normal and anomalous ones). In fact, four, five, and eight, and Special No. 1 terminate with good precision. It is a notable fact that one bird, a blue bar female, WB28, of flight number five, flew the seventy miles, and found and entered the loft, despite hot, twenty-seven-mile per hour winds at right angles to its line of flight. Another unusually significant flight was that of the light blue check female, band number IF43B1014, the only bird flown that day, and the only one released outside of Nebraska. Its flight started at 3:30 P.M. about twenty miles east of Council Bluffs, Iowa. Not only did it fly the one hundred eighty-five airline miles across hot winds averaging twenty miles per hour but, as with the seventy-mile flight described above, it flew in the opposite direction from its home in State College to find and enter its 4×4×5 foot loft displaced one thousand miles west of its home to the middle of a Nebraska grain field.

Total flight No. 6, representing nine reported birds, shows one of two anomalous results; these birds flew in an average direction 60° off the theoretical course. One possible explanation is that there was a violent thunder storm between the release and loft positions that come up swiftly just after the last bird had been released. An important fact about this flight (true for all releases), is that the birds did not fly toward State College nor in random directions. None of the nine flew in a direction as much as 90° off from the direction of the total flight vector. It is interesting to observe that, although the trend of this flight was not toward the home Coriolis line, it did follow almost the shortest route to the correct magnetic-vertical line of State College. Flight No. 3, also anomalous, has not the mitigating factor of an intervening electric storm, but it should be noted that the magnetic fields in the region involved are of the most distorted on record, according to Mr. James Affleck of The Gulf Research and Development Company. Release No. 7 is relatively unimportant since only one bird was reported of the two released. Actually, the flight direction is quite good, being only about 40° off theoretical, and the bird may have flown in and out of the twenty-five-mile error distance for homing pigeons. Further, the hot Nebraska wind that day varied from twenty-six to forty-eight miles per hour along the flight path, and the temperature averaged 94°F throughout.

Special release No. 1 represents an "advance guard" experiment in which twelve carefully trained homing pigeons were shipped to Lincoln, Nebraska, to be released by Professor P. A. Downs of the University of Nebraska. These birds, although not trained specifically for the experiment, had had several years of navigational and racing experience from points up to one hundred miles from State College, Pennsylvania. After they had been singly released and carefully watched out of sight, Dr. Downs later remarked that although they looked like good homers, unfortunately they went the wrong direction. Eight of the twelve had flown out of sight toward the west, exactly opposite from State College. Examination of the total flight vector for this group reveals that, for the five reported birds, making an average flight of one-hundred thirty miles, it ends practically on the predicted position.

On June 25, Dr. Downs again released twelve homing pigeons of excellent flying stock raised in State College, Pennsylvania, this time "prisoners" up to a year or more in age, and without flying experience except inside their home loft and fly-pen. In observing their behavior at the liberation, it was noted that they merely scattered in random directions. Of six subsequently reported by telegraph, four remained at Lincoln, two others went in directions neither toward State College nor its Nebraska conjugate. This serves to illustrate the fact that even good homing pigeons must have flying experience and training, in order to respond to the navigating influences.

Special release No. 3 was the outcome of a visit to Mr. J. A. Rendle of Cozad, Nebraska, an outstanding racing pigeon expert, whose name had been given us by Major Otto Meyer of the U. S. Army Signal Corps. Informed of our experiment, he straightway offered to train some of his best young birds for a reverse test of the theory. The conjugate point of Cozad is somewhat east of the middle of Pennsylvania, but the magnetic deposits in the mountains scatter it into several positions east and west along the

Coriolis line which is essentially the same (.04 of a degree north) as that of State College, Pennsylvania.

On September 15, we received from Mr. Rendle twelve young homing pigeons trained around the compass fifty miles from Cozad. The following day they were released in groups of three, at Berkeley Springs, Virginia. Inspection of Pennsylvania Map IV shows the total flight vector for the six reported: one stayed at or returned to Berkeley Springs but none followed a flight line more than 60° or so from the total flight vector, itself in a correct direction, and terminating within ten miles of the same Coriolis line through Cozad. This Cozad, Nebraska, to Pennsylvania result is a corroboration of the strongly indicative State College, Pennsylvania, Kearney, Nebraska, results.

Shortly before receiving these young Cozad birds Mr. Rendle shipped 10 old birds which had had 200 to 400 mile flights in their records. These were released at various places one hundred miles or more from the center of Pennsylvania. Closely paralleling Mr. Rendle's own predictions three of these birds homed across the 1400 or more miles to Cozad in from one to three weeks. Finally three of the remaining ones were reported found in the region of Michigan, western Pennsylvania, and eastern Ohio. A full discussion of these results requires more space than is available here and will appear in a later paper.

Salient Points of the First Nebraska Experimental Results

1. Of one-hundred twenty-two birds trained in State College and released in Nebraska, only one was ever reported east of Indiana. This was telegraphed in eight months later from Phillipsburg, Pennsylvania.

2. Of the eight main Nebraska releases, six of the total flight vectors support the validity of the theory, in addition to the indicative results obtained with the Cozad, Nebraska birds flown from south of Pennsylvania.

3. The Askania magnetometer readings on a sixty-mile line indicate there are two rather than one magnetic vertical-Coriolis conjugates in the Kearney, Nebraska, region. Two groups of total flight vectors (Special No. 1 together with Nos. 4, 5, and 8) and (Nos. 1 and 2), also show this to be true.

4. Two birds, one from seventy, the other from one-hundred eighty miles, flew in directions almost exactly opposite to their home area in State College, Pennsylvania, and found their lofts at the predicted conjugate point. An additional bird was found within three miles of the west conjugate and three were reported within less than ten miles of the anomalous conjugate point. Considering the fact that a homing pigeon should be familiar with landmarks twenty-five miles out from its home loft in order to assure a successful flight termination, it is evident that six of the reported birds (see data on releases Nos. 1–2 and 3, 4–4, 5–1, 8–1, Special No. 1–1) performed the equivalent of "homing" at their conjugate points. It is probable that a high percent of those used in the experiment flew into the regions involved, but, not seeing the loft or familiar landmarks, flew out again in random directions.

5. The results were good in the face of many adverse factors acting against success, such as:

(a) The birds were trained in green mountainous country but the experimental flights were over flat, brown terrain.

(b) The limited supply of five-foot signal balloons used in piloting the birds at the home loft were quickly blown down and punctured on stones during the first few minutes in the air during the first two days in Nebraska so their use had to be abandoned.

(c) The experimental flights were executed in hot, dry winds of from sixteen to forty-eight miles per hour velocity which blew continuously during the day. Experienced racing-pigeon men fear any wind velocities above twelve miles per hour even at normal temperatures. This was in direct contrast to low velocity winds or complete absence of winds during the training period in Pennsylvania.

(d) The birds of necessity were always liberated after 1:00 P.M., because of inadequate help and transportation. This is late in the day for the most successful flying and navigating results.

(e) Experience has shown the longer experimental flight to be more successful. Over-caution, especially at the beginning of the undertaking,

TABLE IV.

No. bird	Band No.	Year	Color		Age (months)
1	US44SC 4950	44	B.Ch.	4	B–Camp Crowder, M–Ft. Monmouth, S–Lebanon, RM–Ft. Monmouth
2	US44SC 20400	44	Dk.Ch.	—	B–Camp Edison, N. J., M–Ft. Monmouth
3	US44SC 25045	44	Griz.	7	B–Ft. Sam Houston, S & RN–W. Va., RS & RM–Ft. Monmouth
4	US44SC 24545	44	Red	6	B–Ft. Sam Houston, M–Ft. Monmouth, S, C, RM–Lebanon
5	US44SC 21496	44	B.Ch.	—	B–Camp Clairborne, M–Ft. Monmouth
6	US44SC 142	43	B.Ch.	—	B–Indio, Cal., S & F–Ft. Monmouth, S & M–Lebanon, RS & F–Ft. Monmouth
7	US44SC 22935	43	B.Ch.	10	B–Ft. Benning, S & M–Ft. Monmouth, RS & M–Lebanon, B–Camp Crowder
8	US44SC 21480	44	Blue	—	B–Camp Clairborne, M–Ft. Monmouth
9	US44SC 12255	43	B.Ch.	19	B–Camp Crowder, S & M–Ft. Monmouth, RS & RM–Lebanon
10	US44SC 20241	44	Red	—	B–Camp Clairborne, S & M–W. Va., RS & RM–Ft. Monmouth
11	US44SC 4369	44	B.Ch.	5	B–Camp Crowder, M–Ft. Monmouth, S–Lebanon
12	US44SC 25569	44	B.Ch.Spl.	5	B–Ft. Sam Houston, S & M–Lebanon, RS & RM–W. Va., RM–Ft. Monmouth
13	US44SC 37887	43	Blue	—	B–Baltimore, Md., S & F–Ft. Monmouth
14	US44SC 21946	44	Dk.Ch.	—	B–Camp Clairborne, M–Ft. Monmouth
15	US44SC 25520	44	Red	6	B–Ft. Sam Houston, S & M–Lebanon, RS & RM–W. Va., RM–Ft. Monmouth
16	US44SC 4904	44	Dk.Ch.	4	B–Camp Crowder, S & M–Lebanon, RM–Ft. Monmouth
17	US44SC 21479	44	Blue	—	B–Camp Clairborne, M–Ft. Monmouth
18	US44SC 21487	44	B.Ch.	—	B–Camp Clairborne, M–Ft. Monmouth
19	US44SC 24033	44	B.Ch.	8	B–Ft. Sam Houston, S & M–Lebanon, RS & RM–W. Va., RS & RM–Ft. Monmouth
20	US44SC 34217	43	Dk.Ch.	—	B–Elizabeth, N. J., M–Ft. Monmouth, RM–Lebanon
21	US44SC 21477	44	B.Ch.W.T.	—	B–Camp Clairborne, M–Ft. Monmouth
22	US44SC 21288	—	———	—	— — — —
23	US44SC 24084	44	B.Ch.	7	B–Ft. Sam Houston, S & M–Lebanon, RS, RM, C–Ft. Monmouth
24	US44SC 21178	44	Red	—	B–Camp Clairborne, M–Ft. Monmouth
25	US44SC 41183	44	B.Ch.	—	B–Camp Clairborne, S & M–Ft. Monmouth
26	US44SC 21465	44	Red	—	B–Camp Crowder, M–Ft. Monmouth
27	US44SC 5159	44	B.Ch.	4	B–Camp Crowder, M–Ft. Monmouth
28	US44SC 25208	44	Blue	6	B–Ft. Sam Houston, M–Ft. Monmouth, S & RM–Lebanon
29	US44SC 21950	44	Red	—	B–Camp Clairborne, M–Ft. Monmouth
30	US44SC 12134	43	Dk.Ch.W.F.Bl.	11	B–Camp Crowder, S & M–Ft. Monmouth, RS & RM–Lebanon
31	US44SC 40128	44	Blue Tk.	—	B, S & F–Camp Clairborne, RS & F–Ft. Monmouth
32	US44SC 22063	43	B.Ch.W.F.	11	B–Ft. Benning, S & M–Lebanon, RS & RM–W. Va., RS & RM–Ft. Monmouth
33	US44SC 5403	44	B.Ch.Spl.	4	B–Camp Crowder, S & M–Ft. Monmouth, RM–Lebanon
34	US44SC 1732	44	Blue	7	B–Camp Crowder, S & M–Lebanon
35	US44SC 46539	43	B.Ch.	—	B–Camp Clairborne, S & F–Hackettstown, N. J., RS & F–Ft. Monmouth
36	US44SC 2499	44	Red	7	B, S & F–Camp Crowder, RS & M–Lebanon
37	US44SC 4184	44	Mosaic	5	B–Camp Crowder, M–Lebanon
38	US44SC 41344	43	Red	—	B–Camp Clairborne, S & F–Ft. Monmouth
39	US44SC 41043	43	Blk.Ch.	—	B–Camp Clairborne, S & M–Ft. Monmouth
40	US44SC 40246	44	B.Ch.	—	B, S & F–Camp Crowder, RS & F–Ft. Monmouth
41	US44SC 1595	44	B.Ch.	7	B–Camp Crowder, S & M–Lebanon, RM–Ft. Monmouth
42	US44SC 22460	43	Blue	10	B–Ft. Benning, S & M–Lebanon
43	US44SC 23213	43	Blue Ch.	—	B–Ft. Storey, Va., S & M–Ft. Monmouth
44	US44SC 40990	43	Blue Tk.	—	B–Camp Clairborne, S & F–Ft. Meade, Md., S & F–Ft. Monmouth, RS & M–Lebanon
45	US44SC 24705	44	Silver	—	M–Ft. Monmouth, S–W. Va.
46	US44SC 20241	44	B.C.	—	B–Camp Clairborne, M–Ft. Monmouth
47	US44SC 22209	43	B.Ch.	—	B–Ft. Benning, S & M–Lebanon
48	US44SC 22191	43	Blk.	11	B, S & F–Ft. Benning, RS & M–Lebanon, RM–Ft. Monmouth
49	US44SC 44277	44	Blue	—	B, S & F–Camp Clairborne, RS & F–Ft. Meade, RS & F–Ft. Monmouth
50	US44SC 25116	44	B.Ch.Tk.	—	S & M–Lebanon, RS & RM–W. Va., RM–Ft. Monmouth

Glossary to Table IV

Bred (B)—includes mating of old birds, hatching and raising youngsters to flying stage (about four and one-half weeks or longer), but without any flying outside of the loft confines.

Settled (S)—involves letting birds fly outside of loft for the first time. Youngsters up to five or six weeks of age can be settled at a new loft, any distance whatever from the home cote, twenty-four hours after arrival.

Resettled (RS)—repeating operation (S) at a new loft or loft location. The Army was able to do this in seven or eight days by mobiling the birds at the initial settling station.

Flown (F)—this means that, in addition to regular daily exercise flights from the loft, the birds are each day released at progressively greater distances from the home location. Flights of under twenty-five miles are for the purpose of giving them knowledge of local landmarks for piloting to the exact loft locations, plus knowledge of magnitude and gradients of the directives for later use in navigating over unfamiliar territory.

Mobiled (M)—after settling to a portable loft, the latter is moved each day so birds, in their local flying and short training flights, search for it rather than for a particular spot on the land. In military mobiling operations the loft transfers are along a straight line. In the training operations of these experiments the successive locations were always on a circuitous route.

Remobiled (RM)—after settling and mobiling in a given region the birds are resettled, with the same or similar appearing portable lofts, at any desired distance from the last location. In the war, birds were mobiled in this country and remobiled in the European and Pacific war theatres.

caused us to keep the release distances on the short side.

At the completion of the first tests of the bird navigation theory just described, the data obtained were examined critically by the statistical group at the Iowa State College. These men, under Dr. George W. Snedecor, recommended that, in view of the indicative results, work should be continued and more data should be obtained. With this object in view plans with newly suggested procedures were carried out which resulted in the following experiments.

EXPERIMENT III

Hamlet Experiment, September 1944

The writer has talked to many persons, with much experience in racing homing pigeons, who contend that birds have a mysterious power to retrace a path over which they have been carried, even in darkness or in a drugged condition. Some tests of this contention[13] have been made and negative results obtained. There are also many experienced pigeon-racing men who claim that homing pigeons possess the remarkable ability to return to a loft from a distance, merely by virtue of their having lived in it. In the experiment of June, 1944, already recorded, the birds used in "Special release No. 2," had neither flying experience around their home loft at State College, Pennsylvania, nor navigational training. Although the data are far too limited to be conclusive, they do indicate an inability of such birds to make any effective attempt whatever at homing.

At the close of the first full-scale experiment in Nebraska it was found possible to secure, from mobile lofts of the Army Signal Corps at Fort Monmouth, New Jersey, three hundred pigeons, which (with one exception, as later learned) had had no training in navigation, although some had had limited "pilotage" experience from being settled and flown from short distances at the lofts where they were bred. These birds were bred and shipped from Fort Sam Houston, Texas, Camp Crowder, Missouri, and other stations indicated in Table IV and had been given only "mobile" training at Fort Monmouth. Upon arrival at the experimental headquarters at Hamlet, Nebraska, on September 29, 1944, they were placed in Army mobile lofts and permitted a twenty-four-hour rest before being transferred to the various release points. In order to take care of the slight possibility that they might be able to navigate even with the various types of training indicated, the releases were arranged from locations within a hundred and fifty miles radius of Hamlet, Nebraska. The latter is practically on the conjugate point for Fort Monmouth, New Jersey, and according to the theory and the Kearney, Nebraska, results, the point toward which the birds would fly, should their limited Fort Monmouth mobile training be adequate. On September 30, 1944, two hundred and fifty of these birds were re-

[13] G. Reynaud, "The laws of orientation among animals," Smith. Inst. Ann. Report of Board of Directors, p. 481, (translated from Rev. des Deux Mondes **146**) 380 (1898), also O. H. Mowrer, J. compar. Psychol. **19**, 177 (1935).

TABLE V.

Bird No.	Date	Place released	Place found	Distance traveled	
			Group No. 1		
1	Sept. 30, 1944	Ansley	Ansley	0 miles	
2	Sept. 30, 1944	8 mi. E. Goodland	5½ mi. E. Selden	60	
3	Sept. 30, 1944	Between Quinter and Ellis	Between Quinter and Ellis	0	
4	Sept. 30, 1944	9 mi. W. Burlington	5 mi. N.E. Kit Carson	40	
5	Sept. 30, 1944	17 mi. E. Goodland	17 mi. S.W. Burlington	55	
6	Sept. 30, 1944	Miller	Miller	0	
7	Sept. 30, 1944	13 mi. S. Alma	Alton, Kan.	40	
8	Sept. 30, 1944	3 mi. W. Bur. Stratton	3 mi. W. Bur. Stratton	0	
9	Sept. 30, 1944	Phillipsburg, Kan.	Stocton S.E.	23	
10	Sept. 30, 1944	Ansley	Ansley	0	
11	Sept. 30, 1944	Miller	Holstein	50	
12	Sept. 30, 1944	21 mi. E. Quinter	7 mi. S.W. Waukaneg, Kan.	7	
13	Sept. 30, 1944	3 mi. E. Goodland	Goodland	3	
14	Sept. 30, 1944	5 mi. E. Goodland	Winona	30	
15	Sept. 30, 1944	6 mi. N. Ansley	4 mi. S.E. Broken Bow	11	
16	Sept. 30, 1944	6 mi. E. Quinter	20 mi. S.E. Grainfield	17	
17	Sept. 30, 1944	Goodland, Kan.	Goodland, Kan.	0	
18	Sept. 30, 1944	12 mi. N. Ansley	4 mi. N. Wood River	58	
19	Sept. 30, 1944	Quinter	Quinter	0	
20	Sept. 30, 1944	23 mi. N. Miller	York, Neb.	100	
21	Sept. 30, 1944	3 mi. N. Phillipsburg	4 mi. N. Phillipsburg	1	
22	Sept. 30, 1944	Phillipsburg	Phillipsburg	0	
24	Sept. 30, 1944	5 mi. N. Miller	Juniata	50	
25	Sept. 30, 1944	Goodland	Goodland	0	
26	Sept. 30, 1944	17 mi. E. Goodland	8 mi. S. Monument	32	
27	Sept. 30, 1944	14 mi. S. Miller	Elm Creek	30	
28	Sept. 30, 1944	3 mi. W. Burlington	W. Eckley, Col.	57	
29	Sept. 30, 1944	20 mi. E. Goodland	19 mi. E. Goodland	1	
30	Sept. 30, 1944	Alma	E. Alma	1	
32	Sept. 30, 1944	Ellis, Kan.	Ellis, Kan.	0	
33	Sept. 30, 1944	18 mi. N. Ansley	8 mi. N.E. Broken Bow	7	
34	Sept. 30, 1944	Burlington	Burlington	0	
35	Sept. 30, 1944	Ogalla	Ogalla	0	
37	Sept. 30, 1944	6 mi. E. Quinter	11 mi. S.W. Stockton	47	
38	Sept. 30, 1944	18 mi. E. Waukeeny	Bazine, Kan.	40	
39	Sept. 30, 1944	3 mi. S. Alma	Republican City	0	
41	Sept. 30, 1944	12 mi. E. Quinter	5 mi. N.E. McCracken	40	
42	Sept. 30, 1944	Waukeeny	Utica	30	
43	Sept. 30, 1944	11 mi. N. Miller	1 mi. W. Heartwell	48	
44	Sept. 30, 1944	6 mi. W. Burlington	Stratton, Col.	19	
45	Sept. 30, 1944	3 mi. W. Burlington	10 mi. W. Burlington	7	
46	Sept. 30, 1944	Ansley	Ansley	0	
47	Sept. 30, 1944	Ellis, Kan.	Ellis, Kan.	0	
50	Sept. 30, 1944	Alma	Alma	0	
			Group No. 2		
23	Sept. 30, 1944	Goodland, Kan.	7 mi. E. Wallace, Neb.	110	(navigating experience at Ft. Monmouth. Flew toward conjugate point)
			Group No. 3		
31	Sept. 30, 1944	9 mi. W. Burlington	30 mi. N.E. Garden City, Kan.	120	
36	Sept. 30, 1944	12 mi. S. Alma	16 mi. N. Great Bend, Kan.	115	(made long flights in general direction of place bred)
40	Sept. 30, 1944	15 mi. E. Quinter	Sharon	150	
48	Sept. 30, 1944	9 mi. N. Phillipsburg	3 mi. W. Rozel	110	
49	Sept. 30, 1944	Phillipsburg, Kan.	Haviland, Kan.	145	

(Towns in Nebraska unless otherwise specified)

leased in four groups near Goodland, Kansas, Miller, Nebraska, Alma, Nebraska, and Quinter, Kansas, respectively. Small groups of twos, threes, fours, and fives were released, ten minutes apart, beginning at dawn. The weather was cool and clear with gusty winds of about fifteen miles per hour blowing during the day. Of two hundred and fifty birds released, fifty-four were reported on or before October 30, by telegrams.[14]

[14] Of the remaining fifty of the original three hundred, half were youngsters, the others yearlings. The twenty-five yearlings were released at Culbertson in a group most of

The performance of the birds released, as indicated by the telegrams reporting the flight terminals, seems to divide them into three natural groups (Table V) each of which will be dealt with separately.

Results

Group No. 1. These forty-eight birds flew in short random flights ranging from zero to sixty miles from the points of release. The arithmetical average of the forty-eight flights is about twenty miles. Of these, twenty were reported within a mile of the release point. An even more significant indication about the flight of these birds is that the average of the vector sum of their flight vectors (previously referred to as the "total flight vector") is less than ten miles. Since these flights, including distance and directions, are vector quantities, the vector sum and its average is the only one which has real meaning in this connection.

Group No. 2. This 110-mile flight seems significant in that this bird flew in a direct line for Hamlet, Nebraska, which is the conjugate point of Fort Monmouth, New Jersey, and stopped just thirty miles beyond. Of the fifty-two birds reported, it is the only one which had had the proper training in navigating to do this. It was later learned that it had been used in communications at Fort Monmouth, New Jersey, and inadvertently was shipped with the less experienced birds.

Group No. 3. These five birds are distinguished from the rest in that they made long flights averaging one hundred and fifteen miles in length, in addition to flying in directions quite accurately toward their original homes which are as follows:

Bird No.	Place bred
31	Camp Clairborne, Louisiana
36	Camp Crowder, Missouri
41	Camp Crowder, Missouri
50	Fort Benning, Georgia
51	Camp Clairborne, Louisiana

A check made with the head of the Army Pigeon Service revealed that they had been settled and had had considerable flying experience around their home loft before being shipped to Fort Monmouth, New Jersey, which may account not only for the length but also the direction of their flights.

It should be noted that any one of the fifty reported birds, having been bred from some of the world's finest homing pigeons, had the inherited qualities and the mental and physical make-up to fly a like distance toward Fort Monmouth or its conjugate point had they also possessed the means of so doing, brought about by the required type of navigational training. If the "retracement" contention had credence, they should have flown back along the path over which they had been transported by train two days before, or retraced the paths over which they had been taken by car from Hamlet to the various release points, during the hours previous to their release. In the latter case they should have flown toward Hamlet first and then started eastward to Fort Monmouth instead of the short random flights in forty-seven of fifty-four reported cases.

It is a well established fact that homing pigeons settled and trained to navigate at any point, will, in most cases, if physically able, return to it when released moderate distances away, such as one to three hundred miles. This experiment indicates, however, that just settling[15] and mobiling will not replace the training in navigation which they must have to home successfully from a distance. It therefore seems evident, whereas they may inherit the ability to navigate, that they must first have specialized and adequate training in order to accomplish it.

The results of the Hamlet experiment and Special No. 2 and all other tests of these experiments, indicate that homing pigeons do not retrace paths over which they have just been transported unless these latter happen to be directly in line from the home (or its conjugate point) to which they have been trained to pilot and to navigate.

which took up residence on the spot. The twenty-five youngsters were retained for "navigation" training at State College, Pennsylvania, for later experimentation.

[15] See explanation in Glossary appended to Table IV. Explains training which they must have to home successfully from a distance. It therefore seems evident, whereas they may inherit the ability to navigate, that they must first have specialized and adequate training in order to accomplish it.

TABLE VI. Showing release and terminal points of birds reported or which returned to the home loft at State College, Pennsylvania. Releases by Major Otto Meyer, Lt. A. M. Lehman, Dr. P. F. English, Jack Nesbitt, Roy Johnson, Donald Brenner, H. L. Yeagley, Dr. George O. Hendrickson. (X)—Birds released within 100 miles of the line of tangency and crossed over. E—Birds released east of line of tangency. W—Birds released west of line of tangency.

Yellow band number	U. S. Army Signal Corps band No.	Place of release	Date	Place found	Date	Designation
201	US45SC 68367	Marshaltown, Iowa	6/12	11 mi. E. of Sious Falls, S. D.	6/14	W
202	US45SC 68272	Joliet, Ill.	6/11	La Salle, Ill.	6/16	(X)
203	US45SC 68390	Arlington, Neb.	6/12	Nebraska City, Neb.	6/14	W
204	US45SC 68300	Ames, Iowa	6/12	Tennanet, Iowa	6/25	W
205	US45SC 68345	Morrison, Ill.	6/14	Marion, Ind.	6/14	(X)
206	US45SC 68343	Cedar Rapids, Iowa	6/12	Casey, Iowa	6/14	W
207	US45SC 68352	Carroll, Iowa	6/12	Not reported		
208	US45SC 68350	Arlington, Neb.	6/12	Not reported		
209	US45SC 68355	Morrison, Ill.	6/11	Gridley, Ill.	7/3	(X)
210	US45SC 68392	Tiffin, Ohio	6/11	Not reported		
211	US45SC 68368	Wadsworth, Ohio	6/10	State College, Pa.	6/20	E
212	US45SC 68369	Carroll, Iowa	6/12	Stuart, Iowa	6/24	W
213	US45SC 68356	Carroll, Iowa	6/12	Not reported		
214	US45SC 68380	Dunlap, Iowa	6/14	Fontanelle, Neb.	6/14	W
215	US45SC 68389	Altoona, Pa.	6/10	State College, Pa.	6/10	E
216	US45SC 68354	Tiffin, Ohio	6/11	Hartville, Ohio	6/14	E
217	US45SC 68382	Cedar Rapids, Iowa	6/12	Not reported		
218	US45SC 68185	Arlington, Neb.	6/12	Not reported		
219	US45SC 68239	Ottowa, Ohio	6/11	Not reported		
220	US45SC 68351	Arlington, Neb.	6/12	Not reported		
221	US45SC 68344	Valparizo, Ind.	6/11	Not reported		
222	US45SC 68341	Joliet, Ill.	6/11	Not reported		
223	US45SC 68372	Youngstown, Ohio	6/10	Loyalhanna, Pa.	6/11	E
224	US45SC 68353	Carroll, Iowa	6/12	Coon Rapids, Iowa	6/14	W
225	US45SC 68364	Van Wert, Ohio	6/11	Not reported		
226	US45SC 68391	Waterman, Ill.	6/11	Mt. Ayr, Iowa	6/14	W
227	US45SC 68362	Butler, Pa.	6/10	State College, Pa.	6/10	E
228	US45SC 68381	Youngstown, Ohio	6/10	State College, Pa.	6/11	E
229	US45SC 68385	Indiana, Pa.	6/10	Johnstown, Pa.	6/12	E
230	US45SC 68363	Ottowa, Ohio	6/11	Weirton, W. Va.	6/20	E
231	US45SC 68377	Waterman, Ill.	6/12	Chariton, Iowa	6/12	W
232	US45SC 68273	Arlington, Neb.	6/12	Garland, Neb.	6/26	W
233	US45SC 68394	Valparizo, Ind.	6/11	Kankakee, Ill.	6/13	(X)
234	US45SC 68393	Butler, Pa.	6/10	Cowansville, Pa.	6/18	E
235	US45SC 68141	Marshaltown, Iowa	6/13	Boxholm, Iowa	6/15	W
236	US45SC 68347	Indiana, Pa.	6/10	Gibsonia, Pa.	6/19	E
237	US45SC 68302	Not released	No record			
238	US45SC 68388	Ames, Iowa	6/12	Not reported		
239	US45SC 68348	Wadsworth, Ohio	6/10	Northfield, Ohio	6/11	E
240	US45SC 68349	Altoona, Pa.	6/10	State College, Pa.	6/10	E
241	US45SC 68387	Dunlap, Iowa	6/12	Dow City, Iowa	6/14	W
242	US45SC 68386	Not reported.				

EXPERIMENT IV

The East-West Experiment, June 1945

As previously stated, the orientation of the magnetic-vertical lines with respect to the Coriolis lines produce regions where the gridwork character tapers off and a pattern of irregular parallelism or tangency occurs. Reference to Map II indicates this relationship over a fairly wide strip of land through the region which includes the states of Wisconsin, Illinois, Indiana, Kentucky and continuing in a south-south-east direction. An irregular line including all the points of tangency in this region will subsequently be referred to as "the line of tangency."

It seems evident that if birds are guided to a unique point (their home or conjugate point) by conditions requiring grid representations of the fields of influence, they would lack that guidance in a region where the indicating lines approximate a condition of parallelism. Such has been thought to be the case by racing pigeon men in the region just referred to.[16] The procedures of

[16] F. J. Sauerteig, "Indianapolis," Am. Racing Pigeon News (November 1942).

TABLE VII. Showing classifications of birds with regard to their releases east and west of line of tangency (including those released within 100 miles of this line).

Yellow band No.	U. S. Army Signal Corps band No.	Place of release	Date	Place found	Date	±X	±Y
			Group (1) Eastern releases				
211	US45SC 68368	Wadsworth, Ohio	6/10	State College, Pa.	6/20	+197	+ 0
215	US45SC 68389	Altoona, Pa.	6/10	State College, Pa.	6/10	+ 33	0
216	US45SC 68354	Tiffin, Ohio	6/11	Hartville, Ohio	6/14	+106	− 7
223	US45SC 68372	W. of Youngstown, O.	6/10	Loyalhanna, Pa.	6/11	+ 73	−40
227	US45SC 68362	Butler, Pa.	6/10	State College, Pa.	6/10	+107	0
228	US45SC 68381	Youngstown, Ohio	6/10	State College, Pa.	6/11	+146	0
229	US45SC 68385	Indiana, Pa.	6/10	Johnstown, Pa.	6/12	+ 10	−20
230	US45SC 68363	Ottowa, Ohio	6/11	Weirton, W. Va.	6/20	+172	−33
234	US45SC 68393	Butler, Pa.	6/10	Cowansville, Pa.	6/18	+ 20	− 2
236	US45SC 68347	Indiana, Pa.	6/10	Gibsonia, Pa.	6/19	− 51	+61
239	US45SC 68348	Wadsworth, Ohio	6/10	Northfield, Ohio	6/17	+ 11	+20
240	US45SC 68349	Altoona, Pa.	6/10	State College, Pa.	6/10	+ 33	0
					TOTAL	$+X=908$	$+Y=81$
						$-X=51$	$-Y=102$
			Group (2) Western releases				
201	US45SC 68367	Marshaltown, Iowa	6/12	11 mi. East of Sioux Falls, S. D.	6/14	+165	−140
203	US45SC 68390	Arlington, Neb.	6/14	Nebraska City, Neb.	6/14	− 8	+57
204	US45SC 68300	Ames, Iowa	6/12	Tennant, Iowa	6/25	+ 92	+ 4
206	US45SC 68343	Cedar Rapids, Iowa	6/12	Casey, Iowa	6/14	+143	+ 8
212	US45SC 68369	Carroll, Iowa	6/12	Stuart, Iowa	6/24	− 14	+42
214	US45SC 68380	Dunlap, Iowa	6/12	Fontanelle, Neb.	6/14	+ 45	+ 4
224	US45SC 68353	Carroll, Iowa	6/12	Coon Rapids, Iowa	6/14	− 4	+12
226	US45SC 68391	Waterman, Ill.	6/11	Mt. Ayr, Iowa	6/14	+280	+45
231	US45SC 68377	Waterman, Ill.	6/11	Chariton, Iowa	6/12	+232	+30
232	US45SC 68273	Arlington, Neb.	6/12	Garland, Neb.	6/26	+ 41	+22
235	US45SC 68141	Marshaltown, Iowa	6/12	Boxholm, Iowa	6/15	+ 52	−20
241	US45SC 68387	Dunlap, Iowa	6/12	Dow City, Iowa	6/14	7 miles	
					TOTAL	$+X=1050$	$+Y=224$
						$-X=26$	$-Y=160$
			Group (3) Birds released within 100 miles of line of tangency				
202	US45SC 68272	Joliet, Ill.	6/11	LaSalle, Ill.	6/16	+ 50	+12
205	US45SC 68345	Morrison, Ill.	6/11	Marion, Ind.	6/14	+220	−58
209	US45SC 68355	Morrison, Ill.	6/11	Gridlev, Ill.	7/3	+ 47	−58
233	US45SC 68394	Valparizo, Ill.	6/11	Kankakee, Ill.	6/13	+ 30	+18
					TOTAL	$+X=347$	$+Y=+30$
						$-X=-0$	$-Y=-116$

this experiment were designed to test this phase of the theory.

On April 23, 1945, fifty five-week old youngsters were received from Fort Sam Houston, Texas. Pilotage and navigation training of these birds was started immediately. Their loft was not mobiled and training releases were made twice daily. These consisted of one, two, four, eight, sixteen, and twenty-five mile flights for pilotage experience, and many thirty-, fifty-, and seventy-mile flights, in several directions, for navigational training. On some of the longer flights they were liberated in twos, threes, and fives to make them more self-reliant and capable of independent navigational flights.

On June 10, 1945, when the experiment was to begin, there remained forty-two birds. The other eight were lost in the longer training flights, especially when released in small groups. They were transported by truck from State College to the points of liberation which were about equally spaced between State College, Pennsylvania, and Kearney, Nebraska. Table VI shows the time and place these birds were released as well as the time and place each was found and reported. Table VII shows the release

and terminal points of all the birds whose flight terminals were determined. These include all reported by telegraph and in the case of the eastern releases, five which actually arrived at the home loft. In addition it classifies them as follows:

Group 1—Those birds released east of the line of tangency (or region of confusion).
Group 2—Those birds released west of the line of tangency.
Group 3—Those birds which were released within a distance of one hundred miles east or west of the line of tangency and flew across it.

The column at the right on Table VII also shows the distances which each bird flew on a direct line toward the conjugate for the "western" releases and toward the home loft in the case of the "eastern" releases. The Y column shows the perpendicular distances flown either (+) counter-clockwise or (−) clockwise from the direct line to conjugate or home point, respectively.

Table VIII shows the computation of results from the data on Table VII. The algebraic sums of the X and Y components of both groups were divided by the number of flights contributing to their totals. These values of (ΣX/No. flights) and (ΣY/No. flights) were then added vectorily to determine the resultant "flight vector" for the group of birds involved.

As shown, the Eastern group (No. 1) on the average flew 1.8 miles in a counter-clockwise direction while averaging 71.4 miles toward the home (a deviation of approximately 1.0°) whereas the Western group (No. 2) deviated 5.8 miles in a clockwise direction while averaging 93.1 miles toward the conjugate point (a deviation of approximately 3.6°).

At the conjugate end of the experiment the birds, even without errors caused by large local magnetic anomalies, would be subject to errors of fifteen or twenty-five miles from the point, because of the natural errors of navigation to which they are subject. At the home end the pilotage training permits the bird, by means of local landmarks, to finish the last twenty-five or so miles of the journey to the loft. This probably accounts for the smaller angle of deviation for the eastern group.

Birds of group (No. 3) were deliberately liberated within the central two hundred-mile band, which should be a region of confusion insofar as the theory is concerned. It seems significant that the only birds to cross over the line of tangency were released in this band. More data will be obtained to check this indication.

EXPERIMENT V

Second Kearney Experiment, June 1945

This experiment deals with approximately two hundred homing pigeons trained at State College, Pennsylvania. In general, the preparations and procedures were the same as described in the previous experiment at Kearney, Nebraska. However, since the results of the previous tests had so thoroughly dovetailed with the requirements of magnetic-vertical Coriolis theory, at the suggestion of Major Otto Meyer and Lt. Arthur M. Lehman of the Army Signal Corps, it was decided to put a handicap in the way of these birds in order to give the theory the acid test. The plan involved training the birds by releasing them always north-west of State College, but when testing them for the conjugate point in the Kearney, Nebraska, region, making the releases well toward the north-east. In many of the pigeon races greater speed results from having the birds fly and refly over familiar territory and many believe the birds' ability to return depends on visual cues resulting from this careful training in the same direction.[17] Therefore, the significance of the above plane is self-evident.

During the first Kearney experiment in July 1944, five-foot meteorological balloons were used at State College and in Nebraska in an attempt to aid the birds in piloting the last ten or fifteen miles to the loft. The strong Nebraska winds, however, quickly blew them down and broke them so that their value was not determined. In this experiment eight-foot orange-colored box-kites were used for a similar purpose. The kites were flown during most of the training flights to the home loft at State College and during the two days the birds were released in Nebraska. Since no birds actually found the lofts this year, it is assumed that their effect was negligible.

[17] Ralph Gundlach, "Field study of homing pigeons;" Lucian H. Warmer, "The present status of the problems of orientation and homing by birds;" "Homing pigeons a puzzle to science," Am. Weekly (June 3, 1945).

TABLE VIII. Computations with diagrams of results.

Group (1)
Eastern releases

Distance traveled toward home loft	$X_e = +908$ miles (11 birds)
Distance traveled away from home loft	$-X_e = -\ 51$ miles (1 bird)
	$\Sigma X_e = +857$ miles (12 birds)
Deviation to left from the X direction	$Y_e = +\ 81$ (2 birds)
	$-Y_e = -102$ (5 birds)
	$Y_e = \ 0$ (5 birds)
	$\Sigma Y_e = -\ 21$ (12 birds)

$$\frac{\Sigma X_e}{\text{No. birds}} = \frac{+857}{12} = 71.4 \text{ miles}; \quad \frac{\Sigma Y_e}{\text{No. birds}} = \frac{-21}{12} = -1.8 \text{ miles}$$

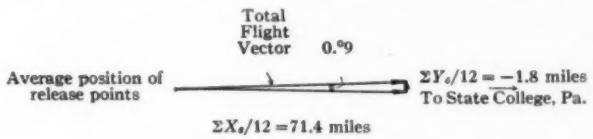

FIG. 2.

Group (2)
Western releases

Distance traveled toward conjugate point	$+X_w = +1050$ miles (8 birds)
Distance traveled away from conjugate point	$-X_w = -\ 26$ miles (3 birds)
	$\Sigma X_w = +1024$ miles (11 birds)
Deviation to left from X_w direction	$Y_w = +\ 224$ miles (9 birds)
Deviation to right from X_w direction	$-Y_w = -\ 160$ miles (2 birds)
Net (to left) deviation from X_w direction	$\Sigma Y_w = +\ 64$ miles (11 birds)

$$\frac{\Sigma X_w}{\text{No. birds}} = \frac{+1024}{11} = 93.1 \text{ miles}; \quad \frac{\Sigma Y_w}{\text{No. birds}} = \frac{+64}{11} = +5.8 \text{ miles}$$

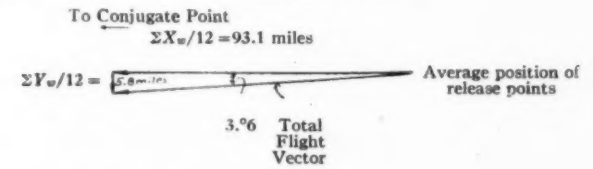

FIG. 3.

Procurement and Training of Birds

Of the two hundred homing pigeons trained for this experiment one hundred fifty-nine were six-week old youngsters supplied by the Army Service Forces from the Army breeding lofts at Fort Sam Houston, Texas. The remainder were birds secured from various racing pigeon men a year previous and held over to be used as two-year-olds.

All the birds were housed in two mobile lofts having tall peaked roofs, six-foot ceilings, and six- by twelve-foot floor spaces. Each contained one hundred and twenty nest boxes with adequate avaries for sunning and bathing. The lofts were mounted on standard farm wagons having Timken high speed bearings, 6:00×16 automobile tires, and were painted a bright yellow They were moved one hundred yards twice daily for receiving the birds from their training flights. The latter change in loft position was accomplished with a Fordson farm tractor.

Training flights were carried out morning and afternoon. After the initial short flights to the east, north, and west, to take care of their error in navigation, the birds were trained only from the north-west. Except for a few stormy days, training was continuous from the time the younger birds were received on April 14 until the day of departure for Kearney on June 10.

The navigation flights were extended to seventy miles airline. The birds flew the latter distance many times and on several occasions, when the wind velocity was practically zero, they homed in approximately seventy minutes.

TABLE IX.

X = distance bird flew toward conjugate point; $-X$ = away from point.
Y = distance bird flew to left; $-Y$ to right of line drawn from liberation point to conjugate point. Released by: E-L = English-Lehman, H-B = Hendrickson-Brewer, H-R = Hendrickson-Rendle.

Yellow celluloid band No.	U. S. Army or other seamless band No.		Color	Release date	Release by	Place released	Date found	Place found	$\pm X$	$\pm Y$
						Group A				
6	US45SC	68240	D.C.	6/17	E–L	Silver Creek, Neb.	6/20	Hampton, Neb.	+ 22	+ 27
8	US45SC	68247	DCWF	6/16	E–L	Silver Creek, Neb.	6/18	Spalding, Neb.	+ 22	− 40
22	AU44	W31805	G.riz	6/17	H–R	Hampton, Neb.	6/18	Southerland, Neb.	+166	− 37
26	US45SC	68241	R.C.	6/17	E–L	Silver Creek, Neb.	6/19	Chapman, Neb.	+ 32	+ 8
33	US45SC	68285	D.C.	6/16	E–L	St. Edward, Neb.	6/18	Trenton, Neb.	+187	− 34
35	US45SC	68278	B.CWF	6/17	E–L	St. Edward, Neb.	6/18	Stamford, Neb.	+132	+ 18
41	US45SC	68269	D.C.	6/16	E–L	Silver Creek, Neb.	6/18	Bucklin, Kan.	+208	+190
44	AU44	W31806	N.C.O.	6/17	E–L	Albion, Neb.	6/19	Sargent, Neb.	+ 51	− 67
49	AU44	W31901	N.C.O.	6/17	E–L	Albion, Neb.	6/19	Royal, Neb.	− 30	− 37
53	US45SC	68316	D.C.	6/16	E–L	St. Edward, Neb.	6/19	Stuart, Neb.	+ 3	− 98
54	US45SC	68357	B.C.	6/17	E–L	Silver Creek, Neb.	6/20	Trenton, Neb.	+193	− 7
56	US45SC	68249	B.B.	6/17	E–L	Albion, Neb.	6/20	Eads, Col.	+333	− 43
59	US45SC	68259	B.C.	6/16	E–L	Albion, Neb.	6/23	Benkelman, Neb.	+200	− 62
63	US45SC	68328	Griz.	6/16	E–L	St. Edward, Neb.	6/18	Leigh, Neb.	− 32	+ 12
65	US45SC	68280	B.C.	6/17	H–R	York, Neb.	6/20	Kearney, Neb.	+ 78	+ 7
80	US45SC	68200	B.C.	6/16	E–L	Albion, Neb.	6/19	Holbrook, Neb.	+142	− 12
89	US45SC	68242	CWF	6/16	E–L	McCook, Neb.	6/18	Des Moines, Iowa	+387	− 75
91	US45SC	68312	R.C.	6/17	E–L	Silver Creek, Neb.	7/23	Aurora, Neb.	+ 29	+ 20
92	US45SC	68251	R.C.	6/16	E–L	Silver Creek, Neb.	6/17	Wilson, Kan.	+112	+137
94	US45SC	68155	D.C.	6/17	H–R	York, Neb.	6/19	Concordia, Kan.	+ 8	+ 90
115	AU44V	35135	D.C.	6/17	H–R	Hampton, Neb.	6/18	Ellis, Kan.	+105	+127
116	AU44P	48145	R.C.	6/17	E–L	Silver Creek, Neb.	6/26	Ravenna, Neb.	+ 68	− 10
119	AU43P	11890	BCWE	6/17	E–L	Silver Creek, Neb.	6/19	Hildreth, Neb.	+ 98	+ 28
121	AU43P	11884	B.C.	6/17	E–L	Silver Creek, Neb.	7/19	Salem, S. Dak.	− 76	−142
122	AU40P	1799	B.S.	6/17	E–L	Silver Creek, Neb.	6/24	Hebron, Neb.	+ 29	+ 74
124	US45SC	68298	B.C.	6/17	H–R	York, Neb.	6/19	Grand Island, Neb.	+ 40	− 7
130	US44SC	4163	B.C.	6/17	E–L	Clarks, Neb.	6/22	Filley, Neb.	− 38	+ 87
134	AU44V	35136	D.C.	6/17	E–L	Silver Creek, Neb.	6/19	Grand Island, Neb.	+ 43	+ 9
136	—		D.C.	6/16	E–L	Silver Creek, Neb.	6/20	Wilsonville, Neb.	+152	+ 22
155	AU43	11899	B.C.	6/17	H–R	Hampton, Neb.	6/18	Steel City, Neb.	− 40	+ 63
157	AU43	Y157	B.B.	6/17	H–R	Strombsurg, Neb.	6/19	Milford, Neb.	− 20	+ 30
160	AU43	Y160	B.C.	6/17	E–L	St. Edward, Neb.	6/19	Linwood, Neb.	− 32	+ 39
162	AU44T	28634	R.C.	6/17	H–R	York, Neb.	6/18	Leoti, Kan.	+199	+145
167	AU44V	31005	B.B.	6/17	E–L	Clarks, Neb.	6/18	Grand Island, Neb.	+ 32	+ 9
170	AU440	3139	BCWE	6/17	H–R	Hampton, Neb.	6/19	Deshler, Neb.	− 4	+ 55
171	AU45W	31905	B.B.	6/17	C–L	St. Edward, Neb.	6/19	Wahoo, Neb.	− 36	+ 60
183	AU44V	31012	B.B.	6/17	E–L	Silver Creek, Neb.	6/18	Pierce, Neb.	− 32	− 53
188	US44	21158	D.D.	6/17	H–R	York, Neb.	6/20	York, Neb. (22 m. N.W.)	+ 18	− 12
190	US45SC	68258	B.C.	6/17	H–R	York, Neb.	6/20	Mullen, Neb.	+173	− 93
192	AU44V	31017	S.B.	6/17	H–R	York, Neb.	6/25	Cody, Neb.	+180	−155
193	AU43X	27255	B.C.	6/17	H–R	York, Neb.	6/23	Claflin, Kan.	+ 60	+160
197	US45SC	68248	B.B.	6/17	E–L	Silver Creek, Neb.	7/19	Ft. Logan, Colo.	+395	− 73
									$\Sigma X = +3557$	$\Sigma Y = +360$
						Group B				
47	US45SC	68274	BCWE	6/16	E–L	Silver Creek, Neb.	6/28	Topeka, Kan.	− 59	+210
101	AU44	24126	B.B.	6/17	E–L	Clarks, Neb.	6/28	Delmont, S. Dak.	− 40	−132
107	AU44D	32149	D.C.	6/17	E–L	Clarks, Neb.	7/3	North Riverside, Ill.	−440	+140
135	AU44V	35174	B.B.	6/17	E–L	Silver Creek, Neb.	6/27	Shelby, Neb.	− 7	+ 12
151	US44SC	20523	B.C.	6/17	E–L	Albion, Neb.	7/30	Bridgewater, Iowa	−100	+150
152	US45SC	68205	B.B.	6/17	H–R	Aurora, Neb.	6/29	Portis, Kan.	+ 43	+ 90
158	AU45W	31904	B.B.	6/17	H–R	Stromsburg, Neb.	7/14	Ashton, Iowa	−115	−100
163	AU45W	Y163	D.C.	6/17	E–L	Clarks, Neb.	6/26	Tilden, Neb.	− 16	− 57
									$\Sigma X = -734$	$\Sigma Y = +313$

Training releases were made in groups of threes and fives a few times, but in most cases the birds were flown in groups of fifty.

On the morning of June 9th the birds were given a seven-mile exercise flight from the northwest. Immediately following, one of the lofts was transferred from its farm wagon base to a two-ton International Truck owned by the Agri-

TABLE IX.—*Continued.*

X = distance bird flew toward conjugate point; $-X$ = away from point. Y = distance bird flew to left; $-Y$ to right of line drawn from liberation point to conjugate point. Released by: E-L = English-Lehman, H-B = Hendrickson-Brewer, H-R = Hendrickson-Rendle.

Yellow celluloid band No.	U. S. Army or other seamless band No.		Color	Release date	Release by	Place released	Date found	Place found	$\pm X$	$\pm Y$
					Group C					
10	AU44	1475	D.C.	6/16	H–B	McCook, Neb.	6/16	McCook, Neb.	0 mile	
19	US45SC	68287	R.	6/17	H–R	Stromsburg, Neb.	6/24	Stromsburg, Neb.	0 mile	
32	US45SC	68289	S.B.	6/16	E–L	Silver Creek, Neb.	6/22	Genoa, Neb.	10 miles	
73	US45SC	68295	D.D.	6/19	H–R	Stromsburg, Neb.	6/22	Stromsburg, Neb.	0 mile	
78	US45SC	68297	B.C.	6/16	H–B	McCook, Neb.		McCook, Neb.	0 mile	
132	US45SC	68157	B.C.	6/17	E–L	Silver Creek, Neb.	6/22	Genoa, Neb.	7 miles	
141	US44SC	68275	R.C.	6/17	E–L	St. Edward, Neb.	9/19	Genoa, Neb.	10 miles	
153	AU44V	31015	B.C.	6/17	H–R	Hampton, Neb.	6/21	Aurora, Neb.	7 miles	
199	AU44T	28631	B.C.	6/17	H–R	Stromsburg, Neb.	6/21	Osceola, Neb.	10 miles	

cultural Engineering Department of the College. The second was coupled to the back of the truck. All feed, kites, and other needed equipment was put under a false floor built in the latter loft.

On June 10th at 7 A.M. the trip to Kearney, Nebraska, was started. The party consisted of Roy Johnson, in charge of trucks, Jack Nesbitt, in charge of kites, Donald Brewer, in charge of birds, Major Otto Meyer, Lt. A. M. Lehman, P. F. English, and H. L. Yeagley. The trip of more than twelve hundred miles was made in three days. Two men, including the driver, handled the truck, and drivers were changed every two hundred or so miles, while the remainder of the party rode in a car belonging to the Pennsylvania Cooperative Wildlife Research Unit of the Pennsylvania State College and driven by Dr. English. At Ames, Iowa, Dr. George Hendrickson joined the party with a car owned by the Iowa Cooperative Research Unit. Mr. J. A. Rendle of Cozad, Nebraska, also joined the party at Kearney and assisted in the experimental procedures.

Upon arrival at Kearney the lofts were placed one and twenty miles, respectively, north of the town. This spaced them about equally north and south of the western State College conjugate. After one day for resting the birds, they were taken in groups and released on an average of seventy-five miles to the N.N.E. and E.N.E., and N.E. of the loft locations.

On June 15th at ten P.M. reports from the United States Weather Bureau indicated that the next day would be clear with scattered clouds and that wind velocities would average ten miles an hour or lower. About four o'clock the next morning (June 16th) Dr. English and Lt. Lehman took one hundred eighteen birds for liberation at points averaging seventy-five miles to the north-east of the conjugate. The birds were all released during the morning groups of threes and fives in the regions around the

TABLE X.

Group A
(Including al birds reported within 10 days of liberation)

ΣX for 42 birds = +3557 miles
$\Sigma X/42 = 84.7$ miles
ΣY for 42 birds = +360 miles
$\Sigma Y/42 = 8.6$ miles

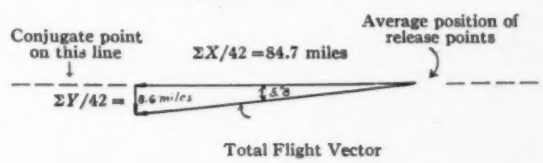

Total Flight Vector

FIG. 4.

Groups A and B
(Including all birds reported up to December 24, 1945)

ΣX for 50 birds reported = 2823 miles
$\Sigma X/50 = 56.5$ miles
ΣY for 50 birds reported = 673 miles
$\Sigma Y/50 = 13.5$ miles

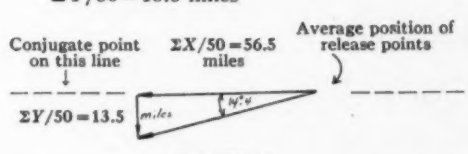

Total Flight Vector

FIG. 5.

TABLE XI. Showing flight vectors, X and Y distances flown ΣX and ΣY values and "total flight vector" for all Army pigeons reported within ten days of liberation. Number reported—20.

$\Sigma X = +2664$ miles	$\Sigma X/20 = +133.2$ miles
$\Sigma Y = -45$ miles	$\Sigma Y/20 = -2.3$ miles

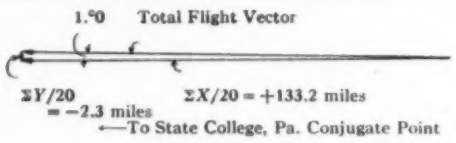

FIG. 6.

Band number	X	Y
6	+ 22	+ 27
8	+ 22	+ 40
26	+ 32	+ 8
33	+187	− 34
35	+132	+ 18
41	+208	+190
53	+ 3	− 98
54	+193	− 7
56	+333	− 43
59	+200	− 62
63	− 32	+ 12
65	+ 78	+ 7
80	+142	− 12
89	+387	− 75
91	+ 29	+ 20
92	+112	+137
94	+ 8	+ 90
124	+ 40	− 7
190	+173	− 93
197	+395	− 73
	$\Sigma X = +2664$ mi.	$\Sigma Y = -45$ miles

Nebraska towns of Clarks, Silver Creek, St. Edward, and Albion. Simultaneously Dr. Hendrickson and Donald Brewer released ten birds to the south-west (near McCook, Nebraska) for control purposes. As indicated by the weather reports, the day was unusually good for bird navigation.

The next morning, June 17th, with weather report and actual weather similar to that of the preceding day, Dr. Hendrickson and Mr. Rendle took the fifty-six remaining birds for liberation to regions around Stromsburg, York, and Hampton, Nebraska. The distance was about the same as the preceding day but the direction was more toward the east. Again the birds were released well before noon in groups of threes and fives. As in previous experiments the birds carried messages in Army message carriers asking the finder to report when and where the bird was found.

Results

Table IX lists all birds which were reported (thirty-two percent of total released) up to the present writing. It lists the time and place of release, persons in charge of liberation, time and place they were found, and the distances flown along and at right angles to a line drawn through the conjugate point and the release point.

From racing-pigeon men it has been learned that birds which do not arrive home from one- and two-hundred-mile flights within a few days are likely not to arrive at all. This is taken as an indication that they become discouraged or fly at random after that time. For this reason all birds reported more than ten days after liberation were listed separately (Group B, Table IX) and this data used in a subsequent calculation to test its effect on the more reliable early data. A second separate listing consists of birds which never left, or perhaps returned to the release areas (Group C, Table IX). In any case, they were reported found within a ten-mile radius of the release point. The complete listing of the birds on Table IX is as follows:

Group A–Birds reported within a nine- or ten-day period after liberation.
Group B—Birds reported after June 26th.
Group C—Birds which were reported less than ten miles from the release point.

In working out and interpreting the data of this experiment the same plan was followed as with the previous ones. The flight (release point to flight terminal) of each bird was plotted and a straight line drawn from the release point to the conjugate point. The algebraic sums ΣX and ΣY of the components of all the flights toward and at right angles to the theoretically required direction line were divided by the number of birds and added vectorily to obtain the "total flight vector" for the groups.

On Table X is shown the average angle of deviation obtained from the flight data of the birds listed in Table IX. Those of Group A show a counter-clockwise deviation of 5.8°. When the data from those reported later (Group B) are used in the computations, the average deviation is seen to be +13.5 degrees.

As in the case of the 1944 Kearney experiments, the experimental birds seemed to behave

MAP IV. Map of Pennsylvania with northern parts of Virginia and West Virginia. Arrow represents total flight vector for reported birds of Special release No. 3 on Table III.

according to the magnetic vertical-Coriolis theory by flying on the average, with only small deviation from a line toward the computed conjugate point. It is noteworthy that the angle of deviation for the birds reported within reasonable time limits is extremely small (5.8°), and this in spite of the fact the birds were trained in a manner devised to confuse them if possible. If the training flights around State College, Pennsylvania, had misled them into flying toward the sun or the south-eastern sky each day, then in the Nebraska liberations they would have flown toward the state of Missouri. This would have been roughly ninety degrees from both State College, Pennsylvania, and Kearney, Nebraska, directions.

During the study and computation of the data in this report it was noticed that the pigeons supplied by the Army Signal Corps, on the average, made more accurate flights in the direction of the conjugate point than those obtained from private sources. It therefore seemed desirable that a separate computation be made for these birds. The summation of their flight components ($\Sigma X, \Sigma Y$) and average components (ΣX/No. birds, ΣY/No. birds) are:

Algebraic sum of distance flown in the direction of the conjugate by the twenty Army birds reported up to June 26, $\Sigma X = 2664$ miles.

Algebraic sum of distance flown at right angles to the above direction, $\Sigma Y = -45$ miles.

As indicated on Table XI, this represents an average flight of 133.2 miles in the X direction and 2.2 miles in the $-Y$ direction or a deviation of only one degree from the average direct line to the conjugate point. This seems to indicate that the Army birds are superior navigators. The small angle of deviation also seems remarkable in view of the flatness of the Nebraska country as contrasted with the mountains in Pennsylvania where the birds were trained, and the anomalous set-up of the earth's magnetic field through which they had to fly in both regions.

REMARKS

The fundamental importance of the foregoing explanation of the long mysterious bird navigation problem and the experimental data obtained is fourfold:

1. The results furnish an experimental indication that a bird moving across a magnetic field experiences an awareness to the effect.

2. The age-old mystery of bird migrations may be clarified by the results of this and already planned future experiments with wild birds. The ability of the Golden Plover[18] to navigate from Hawaii to Alaska, 3000 miles one way over ocean vastness, may possibly have an explanation in the homing pigeon's technique.

3. The biologists and psychologists can make use of its findings in studying the effect of a moving magnetic field on living nerves, an effect lacking demonstration up to now. Part of the ills occurring to pilots in super-speed planes and other high velocity craft, and attributed entirely to large values of acceleration, may conceivably be due to moving rapidly through the earth's magnetic field.

4. There is evidence that wild birds and homing pigeons become confused when in the region of powerful broadcasting stations. Although there is much controversy on the subject, the evidence included in this report, both from the standpoint of the magnetic wing and the conjugate point experiments, indicates that the phenomenon could exist. Further evidence of this is also being sought with new experiments on homing pigeons now under way at The Pennsylvania State College.

ACKNOWLEDGMENTS

The experimental work has been supported by: the Department of Physics and The Department of Zoology and Entomology of The Pennsylvania State College; the Pennsylvania Wildlife Research Group at The Pennsylvania State College and the Army Service Forces of the United States Army Signal Corps.

The men mainly responsible for carrying out the experimental procedures are: Dr. H. L. Yeagley, Department of Physics, and Professor Merrill Wood, Department of Zoology, both at The Pennsylvania State College; Dr. P. F. English and Dr. Logan Bennett, both of the Pennsylvania Wildlife Research Unit; Dr. George Hendrickson, Associate Professor of Wildlife Management, Iowa State College, and Major

[18] F. C. Lincoln, The Migration of American Birds, p. 54.

Otto Meyer, in charge of the Pigeon Service Agency, Army Service Forces, U. S. Army Signal Corps, during World War II.

Note: Illustrative maps and tables are the same as those used in the Reports to the Army Service Forces.

BIBLIOGRAPHY

G. C. Aymar, *Bird Flight* (Garden City Publishing Company, Garden City, New York, 1935), p. 99.

C. E. Brown, "Homing pigeons exposed to radio frequency waves," Sci. Am. **160**, 45 (1939).

J. E. Brown, "The pigeon cooker," Radio News (April 1938).

J. Casamajor, "The mysterious 'seris de L'espace,'" Rev. Sci., Paris, **65**, 555 (1927).

E. Chamberlain, *The Homing Pigeon* (The Homing Pigeon Publishing Company, Manchester, England, 1907).

R. D. Chard, "Visual acuity in the pigeon," J. Exper. Psychol. **24**, 588 (1939).

H. E. Dodge, "The racing homer," Feathered World, London, (1922).

M. E. Duchatel, "Faculté de direction du pigeon voyageur," Ann. de Psychol. Zool. **1**, 22 (1901).

S. Exner, "Negative Versuchsergebnisse über das Orientierungsvermögen der Brieftauben," Sitz. Wien Akad. Wiss. **101**, 318 (1893).

Experiments with homing pigeons sensitivity to radio frequency waves, conducted by 285th Signal Pigeon Company, March 1945.

D. S. Farner, "The return of robins to their birthplaces," Bird Banding **16**(3), 81 (July 1945).

Dr. D. R. Griffin, "The Sensory Basis of Bird Navigation," The Quarterly Review of Biology, **19**, 1 (March 1944), pp. 15–31.

R. H. Gundlach, "A field study of homing in pigeons," J. Compar. Psychology. **13**, 397 (1932).

R. H. Gundlach, "A test of 'directional sense' in cats and pigeons," J. Compar. Psychol. **12**, 347 (1931).

J. Huie, "Orientation," Homing Pigeon **3**, 20 (1881). (Reprinted from J. Horticult.)

G. Ising, "The physical possibility of a biological sense of orientation based on the rotation of the earth," Ar. Math. Astrophys, 32A, No. 4 (1946).

Kingsley, "Orientation by inherited memory," Nature, **18** (June 1869).

Fredrick C. Lincoln, *The Migration of American Birds* (Doubleday Doran and Company, Inc., Garden City, New York, 1936).

W. M. Levi, *The Pigeon* (R. L. Bryan Co., Columbia, South Carolina. 1941).

O. H. Mowrer, "The nsytagmic response of the pigeon to constant angular acceleration at liminal and supraliminal intensities," Jour. Compar. Psychol. **19**, 177 (1935).

F. M. Packard, "The return of young robins to their birthplaces," Bird Banding **18**(1), 30 (January 1947).

J. L. Peters, *Check-list of Birds of the World* (Harvard University Press, Cambridge, Massachusetts, 1931), Vol. 1 or 2; *ibid.*, Vol. 2, 1937; *ibid.*, Vol. 3, 1940; *ibid.*, Vol. 4.

E. S. Starr, "Homing pigeons," Cent. Illust. Month. Mag. **31**, 361 (July 1886).

R. M. Strong, "On the olfactory organs and the sense of smell in birds," J. of Morphol. **22**, 619 (1911).

F. J. Sauerteig, "Indianapolis," American Racing Pigeon News, November 1942, p. 1.

G. Reynaud, "The laws of orientation among animals," Smith, Inst. Ann. Report of Board of Directors, p. 481 (translated from Rev. des Deux Mondes 146) 380 (1898), also O. H. Mowrer, J. Compar. Psychol. **19**, 177 (1935).

W. H. Thorpe and D. H. Wilkinson, "Ising's theory of bird orientation," Nature, December 21 (1946).

A. Thauzies, "L'orientation," Rev. Sci. **9** (series 4), 392 (1898).

A. Thauzies, "L'orientation du pigeon voyageur: donnes experimentales," Rev. Sci. **2** (series 5), 417, 453 (1904).

C. Viguier, "Le sense de l'orientation," Rev. Phil. **14**, 1–36 (1882).

G. J. Van Oordt, *Bird Migration* (Vogeltrek) (E. J. Brill) Leiden, Netherlands, 1944); Review in Bird Banding, **18** (1), 48 (1947).

J. B. Watson, "Recent experiments with homing birds," Harper's Month. Mag., 457 (May 1913).

J. B. Watson, and K. S. Lashley, "An historical and experimental study of homing," J. Carnegie Inst. of Washington (1915).

A. G. Webster, *Dynamics* (G. E. Stechart and Company, New York), second edition, pp. 320–322.

K. Wodzicki, et al., "Experiments on homing in birds," Nature, **35** (Jan. 1, 1938).

Inversion Applied to the Solution of 3-Dimensional Electromagnetic Problems*

A. Bloch
Research Laboratories, The General Electric Company (Ltd.), Wembley, England
(Received March 18, 1947)

This paper presents an extension of the method of inversion to certain electromagnetic problems and rectifies at the same time an error of long standing in the solution of an elementary problem which seems to have acted as a bar to just this extension.

If the image of a charge in a sphere is derived by the method of inversion, as is done in this paper, it becomes immediately obvious that the image of radially oriented dipole is another radial dipole plus a free charge proportional to the moment of the dipole. The potential caused by the free charge is not of negligible magnitude, and this indicates that the solution given by Sir J. Larmor and independently by S. P. Thompson and Miles Walker for the case of a magnetic dipole outside a sphere of infinite permittivity cannot be correct, for the image used therein consists of a simple dipole. However, it can be shown in addition that the latter image is not void of physical significance: the vector potential of such an image transforms in a simple manner and from this in turn follow simple laws of transformation for flux linked with loops and for mutual inductance between such loops.

This extension of the method of inversion is used in the second part of the paper to deal with a problem complementary to that of Larmor-Thompson, namely, with that of a spherical wall impermeable to magnetic flux. This problem is of practical importance as an idealization of an inductor used at radiofrequencies and placed inside a metal screen, and it has for this reason been dealt with by direct attack on several previous occasions. It is shown here that the action of such a screen on the field produced by the loop can be replaced by the introduction of a simple image loop. From this follows then a simple way of calculating the change in self and mutual inductance produced by such a screen, even in cases more general than considered heretofore. The losses caused by the screen can also be easily calculated by the use of H. A. Wheeler's concept of equivalent magnetic skin thickness.

SYMBOLS

O = center of inversion
K = constant of inversion
P = point at which a charge or current element is situated
P' = inverse of P $[OP \times OP' = K^2]$
N = point at which the value of a potential is considered
N' = point inverse to N
$l = PN$
$l' = P'N'$
r, r' = a distance from O and its inverse
q, q' = an electric or magnetic charge and its inverse
m, m' = a magnetic moment and its inverse
I, I' = an electric current and its inverse
V = an electric or magnetic potential
$\mathbf{A}$ = Vectorpotential
ϕ = magnetic flux
L = self-inductance
M, M_{12} = mutual inductance.

INTRODUCTION

THE purpose of this paper is to present an extension of the method of inversion to the solution of certain electromagnetic problems and at the same time to rectify an error of long standing which seems to have acted as a bar to just this extension. In 1888 Sir J. Larmor considered[1] the magnetic field caused by a circular current loop in the presence of a cocentric soft iron sphere and concluded that for infinite permittivity of this sphere its action on the field outside its boundary could be replaced by that of an "image" of the original loop in the sphere. An identical solution was given independently by Silvanus Thompson and Miles Walker[2] and is still referred to in modern textbooks. It does not seem to have been noticed so far that an image of this kind does not solve the problem given.

If these images are introduced by the method of inversion—as will be done hereafter—such failure will be immediately evident. At the same time it is then not difficult to see that such an image obeys a simple law of transformation for its vector potential, from which follow in turn simple laws of transformation for magnetic flux through loops and mutual inductance between loops.

* Communication from the Staff of the Research Laboratories of The General Electric Company, Limited, Wembley, England.

[1] Sir J. Larmor, "Electromagnetic and other images in spheres and planes," Quart. J. Pure and App. Math., 1–8 **24**, 94 (1889).
[2] S. P. Thompson and M. Walker, "Mirrors of magnetism," Phil. Mag. **34** (5th series) 213–224 (1895).

This extension is dealt with in the first part of the paper, to be followed in the second part by an application to a problem complementary to that of Larmor and Thompson and Walker, namely, to that of a sphere impermeable to magnetic flux. This case arises when we study the reaction of a screening can at radio frequencies on an enclosed loop, as has been done on several occasions. H. Kaden[3] considered a loop of very small dimensions situated at the center of a spherical screen. C. F. Davidson and J. C. Simmonds[4] have extended this solution to the case of a loop of finite dimensions. H. Buchholz[5] has given solutions for the self- and mutual-inductance of loops which are parallel to each other and coaxially situated in any position along the radius of the screening sphere. All these authors use a direct method of attack and require, therefore, a mathematical apparatus of some complexity.

The present papers show that the action of the screen can be represented as the action of a simple image loop and thus reduces all the problems mentioned to the well solved determination of the mutual inductance between two parallel and coaxial loops. Actually, the methods of the paper are capable of dealing with some slightly more general arrangement of the loops and with certain non-circular loops.

I. THE METHOD OF INVERSION AND ITS EXTENSION TO MAGNETIC IMAGES

Let O be a fixed point (the *center of inversion*) and P a variable one; determine on OP a point P' so that the distances OP and OP' fulfil

$$OP \times OP' = K^2 \tag{1}$$

(K = *constant of inversion*).

Then if P describes a line, or a surface, or a volume, P' will describe a corresponding geometrical element (the *inverse* or the *image* of the original element).

The most important properties of this well-known geometrical transformation are recalled by Figs. 1 and 2. Figure 1 shows that the inverse of a circle contained in a plane through the center of inversion is another circle in the same plane. Hence the inverse of a sphere must be another sphere, that of a circle in a general position—defined by the intersection of 2 spheres—must again be a circle, and the inverse of a plane (sphere through the infinitely distant point) a sphere through the origin. Figure 2 illustrates the "conformal" property of the transformation: the angles of intersection between lines and surfaces remain unchanged in the transformation.

To apply this method to the solution of problems of the theory of potential we have to add to this a law for the transformation of charges, as follows: A point charge of magnitude, say q, situated at a point, say P, shall be represented by another point charge of magnitude q' situated at the image P' of P, whereby

$$\frac{q'}{q} = \pm\frac{K}{OP} = \pm\frac{OP'}{K} = \left(\frac{OP'}{OP}\right)^{1}. \tag{2}$$

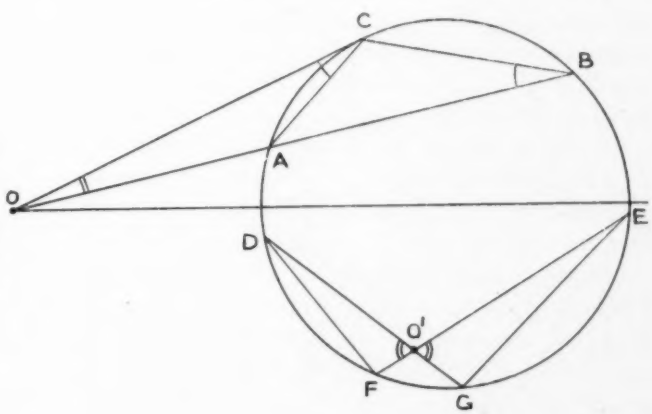

FIG. 1. The inverse of a circle is another circle. $\sphericalangle OCA = \sphericalangle CBA$ when OC is tangent to circle; hence $\triangle OCA$ is similar to $\triangle OBC$, and $OA \times OB = OC^2$. If $K = OC$, this means that the circle inverts into itself; if K is larger or smaller, the result of the inversion is correspondingly larger or smaller, but it will still be a circle. There is a similar proof if the center of inversion O' is situated inside the circle: $\triangle FO'D$ is similar to $\triangle GO'E$ and $DO' \times O'G = FO' \times O'E = \text{const.}$

[3] H. Kaden, E.N.T. **10**, 277 (1933).
[4] C. F. Davidson and J. C. Simmonds, W. Eng., **22**, 3 (1945).
[5] H. Buchholz, Archiv. f. Electrotechnik **28**, 556 (1934).

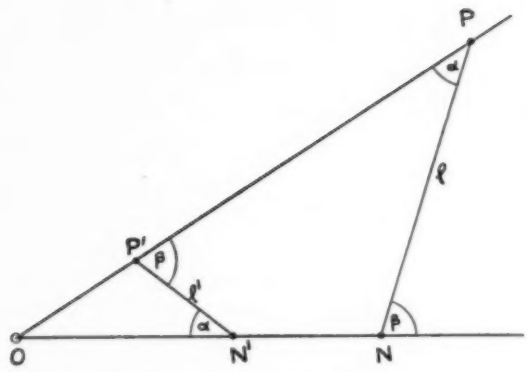

FIG. 2. If $OP \times OP' = ON \times ON' = K^2$, then $OP' : ON' = ON : OP$, i.e., $\sphericalangle OP'N' = \sphericalangle ONP$. From this follows (a) if l and l' are infinitesimally small, the angles formed by these line elements with their radii vectorii are equal; (b) $l : l' = ON : OP' = OP : ON' = \left(\frac{ON \times OP}{ON' \times OP'}\right)^{\frac{1}{2}} = \frac{ON \times OP}{K^2} = \frac{K^2}{ON' \times OP'}$.

The reason for selecting this particular relation will become clear when we inquire into the potential V, caused by such a charge at some point N, and compare it with the potential V' caused by the image charge at the image point N' (see Fig. 2).

In this case $V = q/l$, and $V' = q'/l'$, hence

$$\frac{V'}{V} = \frac{q'}{l'} \cdot \frac{l}{q} = \pm \frac{K}{OP} \cdot \frac{OP}{ON'} = \pm \frac{K}{ON'} = \pm \frac{ON}{K} = \pm \left(\frac{ON}{ON'}\right)^{\frac{1}{2}}. \quad (3)$$

The last equation shows that the transformed potential V' can be calculated from the original potential without the need for inquiring into the position of the charge which "caused" the potential. Hence the potential will still transform accordingly to the same rule if it is due not to a single charge but to an assembly of charges.

These relations allow us to deduce the solution of a problem for the inverse space from the solution of the corresponding problem for the original space and *vice versa*. As an example we recall the case of a point charge q in front of an infinite earthed plane. This problem is of course equivalent to that of the original charge, q, and of the mirror image, q_m, of this charge in this plane. By inversion from any point not coinciding with the plane the latter transforms into a sphere, with one charge q' inside and the other one q'_m outside its boundary. From Eq. (3) it is then seen that the potential of this sphere is again zero (for all points of the sphere not coinciding with the center of inversion the multiplier K/ON' is finite; with a finite gradient of the field in the neighborhood of the center of inversion the potential of this point must then be zero too). Thus, the transformed arrangement solves the problem of a point charge inside or outside an earthed sphere. The "answers" for this case can be obtained either by appropriate translation from the results of the "plane" case, or, simpler still, by noting directly the fact that here too the total field is due to the combined action of the charge q' and of the "image in the sphere" q'_m.

It is useful to note that we are led to this image charge also by a slightly different application of the method of inversion. If we invert the charge q' and the sphere from the center of the sphere as inversion center in such a way that the sphere changes into itself (constant K of inversion equal to the radius of the sphere) then q' transforms into the image q'_m previously found.*

From the fact that image and original charge are thus related by Eq. (2), it follows immediately, that in the case where we are given two charges of equal magnitude, forming a radially oriented dipole, the corresponding image charges cannot be equal. If the given charges are situated at, say r and $r+dr$, the image charges are in this case situated at

$$r' = \frac{K^2}{r}, \text{ and } r' + dr' = \frac{K^2}{r+dr},$$

* That this is so—at least geometrically—is easily seen if we consider what happens to all those spheres which are common to the two charges q and q_m of the "plane" arrangement. These intersect normally with the plane, and they transformed therefor, in the first inversion into all those spheres which pass through the two charges q' and q'_m and intersect normally with the earthed sphere. In the second inversion—with the center of the sphere as inversion center—each of these spheres transforms into itself, i.e., their first common point must change into their second common point. (Their points of intersection with the earthed sphere remain fixed, and we know also that the angle of intersection must be again 90°.) Electrically the transformed arrangement could differ from the original arrangement then only by having both charges increased or decreased by the same factor. However, it is seen at once that this factor must be equal to unity as the electrical displacement at the surface of the sphere (charge per unit area) remained unchanged in this transformation (see Eq. 2)).

and they differ in magnitude by

$$\Delta q' = \frac{q \cdot K}{r^2} dr = \frac{m \cdot K}{r^2}, \tag{4}$$

where $m = qdr$ is the moment of the original dipole.

The case of an isolated sphere (with the given charges outside the sphere) differs from the case of an earthed sphere only insofar that a further charge at the center of the sphere is added so that the sum total of all the charges inside the sphere equals zero whilst the surface of the sphere still remains an equipotential surface.

The case of a magnetic dipole outside a shell of infinite permittivity is perfectly analogous to this latter case. From this follows immediately that a solution which takes the image of a radial dipole to be simply another dipole is not a case of ordinary inversion and is unlikely to follow the transformation law of Eq. (3) for the potential. (The potential produced at the surface of the sphere by the neglected free charge $\Delta q'$ is evidently of the same order as that produced by the dipole itself.)

This conclusion can be easily confirmed if we go to the trouble of writing down explicitly the expression for the magnetic potential of such a dipole. This expression, however, suggests further that it is now the magnetic vector potential of the dipole that follows the simple transformation law of Eq. (3). The magnetic vector potential of a radial dipole of moment m situated at P (Fig. 2) has at point N the value

$$A = \frac{m}{l^2} \sin\alpha. \tag{5}$$

The direction of this vector is normal to the plane of the paper. The vector potential at N' caused by the image dipole situated at P' will be of magnitude

$$A' = \frac{m'}{l'^2} \sin\beta. \tag{6}$$

If we assume

$$\frac{m'}{m} = \frac{q' \cdot dr'}{q \cdot dr} = \frac{K}{OP} \cdot \frac{OP'}{OP} = \frac{K^3}{OP^3}, \tag{7}$$

we have

$$\frac{A'}{A} = \frac{m'}{m} \cdot \frac{l^2}{l'^2} \cdot \frac{\sin\beta}{\sin\alpha} = \frac{K^3}{OP^3} \cdot \frac{OP^2}{ON'^2} \cdot \frac{ON'}{OP'}$$

$$= \frac{K}{ON'} = \frac{ON}{K} = \left(\frac{ON}{ON'}\right)^3. \tag{8}$$

The foregoing finds an immediate application if we consider the fields produced by current loops. The magnetic effects of such a loop (not necessarily of circular shape), in which a current I flows, is equivalent to that of a magnetic shell bounded by the loop, the strength of this shell (i.e., the magnetic moment per unit area) being equal to I.

Transformation of this shell produces as image another shell; if the original shell was spherical with center O, the image shell will also be spherical, and again of constant strength. Since corresponding elements of these two shells are related as to their surface areas as

$$\frac{S'}{S} = \left(\frac{r'}{r}\right)^2, \tag{9}$$

we have

$$\frac{I'}{I} = \frac{(m'/S')}{(m/S)} = \frac{K^3}{r^3} \cdot \frac{r^2}{r'^2} = \frac{K}{r'} = \frac{r}{K} = \left(\frac{r}{r'}\right)^3. \tag{10}$$

This means that we may replace this shell in turn by another current loop, the image of the original loop, the strength of the image current being given by Eq. (10).

The last equation may be used to show independently that the vector potential of such a loop transforms as stated in Eq. (8).

We have for the vector potential of the original loop

$$\mathbf{A} = \oint d\mathbf{A} = \oint \frac{I d\mathbf{s}}{l}, \tag{11}$$

and for that of the transformed loop

$$\mathbf{A}' = \oint dA' = \oint \frac{I' \cdot d\mathbf{s}'}{l'}. \tag{12}$$

The two contours over which these two line integrals are to be taken correspond to each other element $d\mathbf{s}$ for element $d\mathbf{s}'$, and the ratio

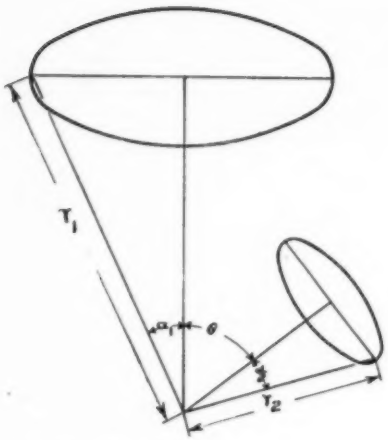

FIG. 3. The notation above γ_2 should read α_2. The point at which the radii of the loops intersect should be labelled O.

of corresponding contributions dA and dA' is

$$\frac{d\mathbf{A}'}{d\mathbf{A}}=\frac{I'}{I}\cdot\frac{d\mathbf{s}'}{d\mathbf{s}}\cdot\frac{l}{l'}=\frac{K}{OP'}\cdot\frac{OP'}{OP}\cdot\frac{ON}{OP'}=\frac{ON}{K}. \quad (13)$$

Hence the ratio of the two integrals themselves is given by the same constant.

From the transformation formula for the vector potential follows at once a simple formula relating the flux ϕ linked with a loop to the flux ϕ' linked with the image of this loop, provided each of the loops under consideration is again equidistant from the origin 0. The flux through such a loop can be calculated as $\phi=\oint\mathbf{A}d\mathbf{s}$, the integral being taken around the loop. The ratio of corresponding contributions to these integrals is (as $\mathbf{A}'\|\mathbf{A}$ and $d\mathbf{s}'\|d\mathbf{s}$)

$$\frac{\mathbf{A}'\cdot d\mathbf{s}'}{\mathbf{A}\cdot d\mathbf{s}}=\frac{ON}{K}\cdot\frac{ON'}{ON}=\frac{K}{ON}=\frac{\phi'}{\phi}. \quad (14)$$

This is again a relation in which only the position of the "point of observation" enters, and not the position of the "causes."

If the flux through the loop (say, loop 1) is due to the fact that another loop (say, loop 2) carries a current I_2, we are led to a transformation formula for the mutual inductance M_{12} between two such loops. It is

$$\phi_1=M_{12}\cdot I_2 \quad \text{and} \quad \phi_1'=M_{12}'\cdot I_2'. \quad (15)$$

Hence

$$\frac{M_{12}'}{M_{12}}=\frac{\phi_1'/I_2'}{\phi_1/I_2}=\frac{K\cdot K}{r_1\cdot r_2}=\left(\frac{r_1'\cdot r_2'}{r_1\cdot r_2}\right)^{\frac{1}{2}}. \quad (16)$$

The last formula is easily tested if we consider the mutual inductance between two circular loops, the axes of which intersect at an angle Θ. (This angle can of course be zero, in which case we have two parallel, coaxial loops.) The value of this mutual inductance is given by Maxwell[6] by an expression of the form

$$M=r_2\cdot\Sigma_n C_n\left(\frac{r_2}{r_1}\right)^n=r_1\Sigma_n C_n\left(\frac{r_1}{r_2}\right)^n, \quad (17)$$

where r_1 and r_2 denote the distances of the loops from the point 0 of intersection of the axes, and where the coefficients C_n depend on the angle Θ and on the angles α_1, and α_2 which the radii of the loops subtend at O (see Fig. 3).

When this configuration is inverted, with 0 as center of inversion, we have

$$r_1'=K^2/r_1, \quad r_2'=K^2/r_2$$

while α_1, α_2, and Θ remain unchanged. Hence

$$\frac{M'}{M}=\frac{r_2'\Sigma C_n\left(\frac{r_2'}{r_1'}\right)^n}{r_1\Sigma C_n\left(\frac{r_1}{r_2}\right)^n}=\frac{K^2}{r_1\cdot r_2}\,\frac{\Sigma C_n\left(\frac{r_1}{r_2}\right)^n}{\Sigma C_n\left(\frac{r_1}{r_2}\right)^n}=\frac{K^2}{r_1r_2} \quad (18)$$

as required by Eq. (16).

If the loops are coaxial, any point on the common axis can be chosen as center of inversion. This can be used to transform the general case into various special cases. For instance, if we chose as center one of the points at which the common axis penetrates the sphere common to both loops, the two transformed loops will be co-planar. Another special case would be the transformation into loops of equal diameter, which is achieved by using as center of inversion the point at which the axis penetrates a sphere around the vertex of the cone common to both loops, the radius of this sphere being the geometrical mean of the distances of the two loops from this vertex (see the second method of apply-

[6] J. C. Maxwell, *A Treatise on Electricity and Magnetism*, Vol. 2, Chapter 14.

ing inversion to the problem discussed in the next section). It is, however, easily seen (by application of the formula given in the caption to Fig. 2) that in any such transformation the ratio of the shortest and the longest distance between these two loops remains invariant, which means (see below) that such transformation will not aid in evaluating the elliptic integral occurring in the formula for the mutual inductance.

II. APPLICATIONS TO THE CASE OF A HIGH FREQUENCY SPHERICAL SCREEN

The theory developed in Section I can be usefully applied when we have to consider the screening effect of spherical metal "cans" at high frequencies. If the conductivity of such a screen is infinite, it is impermeable to magnetic flux at any frequency. Finite conductivity allows penetration of the field, though with the usual materials of construction such penetration is at radio frequencies limited to "skin depth." We may then either neglect this deviation from the ideal case altogether or take it into account by a simple approximation.

There are two ways in which the method of inversion can be applied to this problem, of which we shall consider first the more general one. Suppose that we are given a current loop—circular or otherwise—which is equidistant from the center of a hypothetical sphere, and further that we know the magnetic field produced by this loop. If we invert then from this center as center of inversion so that the sphere changes into itself, the loop will change into its image and we can predict from the theorems of Section I the field produced by this image. In particular, it follows from Eq. (14) that any test loop which we might draw on the surface of the sphere and that was linked with a certain amount, ϕ, of the flux of the original loop will be linked with an identical amount, ϕ, of flux produced by the image loop. Hence, if we take the correct sign for the current in the image loop, the sum total of the flux through the test loop will be zero. Thus the field produced by the combined action of original and image loop will have the property that none of its flux crosses the boundary of our hypothetical sphere, and we could introduce in its place an impermeable material screen without making any change to the field either inside or outside its boundary. Conversely, it follows that the effect of introducing such a screen on the field produced by the original loop could be simulated by the introduction of the image loop.

This allows us to calculate directly the change of self-inductance caused by the introduction of such a screen. We have, taking into account Eq. (10),

$$\Delta L = -M\cdot\frac{I'}{I} = -M\cdot\frac{r_0}{a}, \tag{19}$$

where M is the mutual inductance between the image and the original loop and r_0 the distance of the latter from the center of the sphere of radius a.

Similarly, the flux arising from the image loop causes a change in the mutual inductance between the original loop and any other loop (say, loop 2) inside the sphere of amount

$$\Delta M_{12} = -M_{12}'\cdot\frac{r_0}{a}, \tag{19a}$$

where M_{12}' denotes the mutual inductance between the image loop and the second loop.

In the case of circular loops formula (19) is easily evaluated, for the two loops are then coaxial and parallel (Fig. 4), and their mutual inductance is given (references 6 and 7) by

$$M = 8\pi\left(\frac{bb'}{k}\right)^{\frac{1}{2}}(K-E), \tag{20}$$

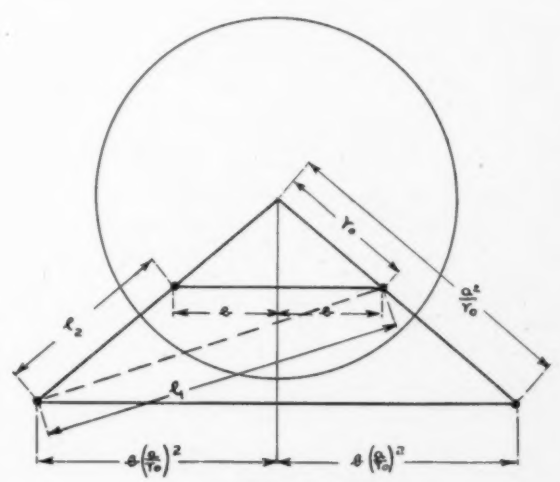

FIG. 4.

[7] A. Russel, J. Inst. Elec. Eng. **67**, 659 (1929).

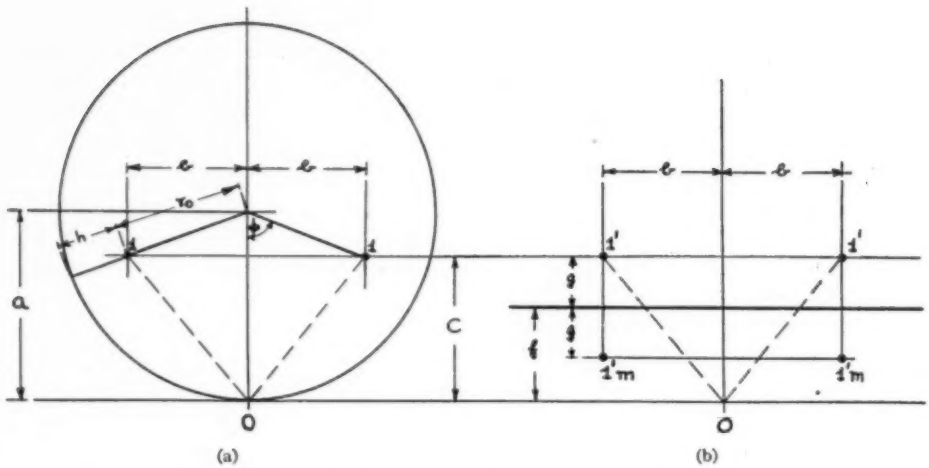

FIG. 5. Constant of inversion $K^2=b^2+c^2=b^2+(a-r_0\cos\phi)^2$
$f=\frac{b^2+c^2}{2a}$ and $g=c-f=\frac{a^2-r_0^2}{2a}\approx h$ for $h\ll a$.

where b and b' are the radii of the two loops and K and E are the complete elliptic integrals of the first and second kind to modulus k. This modulus itself is given by

$$k=\frac{l_1-l_2}{l_1+l_2}=\frac{\lambda-1}{\lambda+1}\left(\lambda=\frac{l_1}{l_2}\right), \tag{21}$$

where l_1 and l_2 denote the largest and the smallest distance between the elements of the two loops. In the present case $b'=ba^2/r_0^2$, and therefore

$$\Delta L=-\frac{8\pi b}{(k)^{\frac{1}{2}}}(K-E). \tag{22}$$

For the same reason we have, with $\alpha=a/r_0$, $\beta=b/r_0$ and $\nu=\alpha-1/\alpha$

$$\lambda=\left(1+\left(\frac{2\beta}{\nu}\right)^2\right)^{\frac{1}{2}}. \tag{23}$$

Evaluation of Eq. (20) is facilitated by extensive tabulation (references 6, 8, 9). There exists also a truly embarrassing number of approximations, (reference 9) so that it is perhaps useful to quote two which are simple but sufficient for slide-rule accuracy, (reference 7).

If $k<0.9$, that is $\lambda<20$ (that is in our case for loops which are not too close to the wall of the screen P) we have with an error of less than 6/10 of a percent

$$K-E=\frac{\pi k^2}{1+3(1-k^2)^{\frac{1}{2}}}. \tag{24}$$

If k is larger than 0.9 we have, with an error of less than $\frac{1}{3}$ percent,

$$K-E=\tfrac{1}{2}(k)^{\frac{1}{2}}\left[\log_e 4\cdot\frac{1+k}{1-k}-2\right]. \tag{25}$$

The case of a very small loop can of course be dealt with in an elementary way. If the loop should be in the center of the sphere (Kaden's problem) we have the specially simple case that the image loop is infinitely distant, producing an image field that is homogeneous. The strength of this field can be found directly from the condition that the combined flux across the sphere must be zero everywhere. As the loop creates there a field strength (for unit current) equal to $2b^2\pi/a^3$ at those places where the sphere is penetrated by the axis of the loop, this too must be the strength of the image field. The image field sends then

$$\phi=b^2\pi\cdot 2b^2\pi/a^3 \tag{26}$$

[8] Circular C74 of the Nat. Bur. Stand. Washington (1924), reprinted 1937. A similar table is contained in Terman's *Handbook for Radio Engineers*. Further and more extensive tables are given by F. W. Grover, "Tables for the calculation of the mutual inductance of circuits with circular symmetry about a common axis," Sci. Pap. Bur. Stand. **20**, (1926) and F. W. Grover *Inductance-Calculation* (D. Van Nostrand Company, Inc., New York, 1946).

[9] See the survey given by F. W. Grover in "Methods for the derivation and expansion for formulas for the mutual inductance of coaxial circles and of the inductance of single layer solenoids," Bur. Stand. J. Research 1, 487 (1928).

flux lines through the original loop, i.e.,

$$\Delta L = -2\pi^2 b\left(\frac{b}{a}\right)^3. \tag{27}$$

If the loop is placed eccentrically (distance r_0 from the center of the sphere) it follows similarly from Eq. (7) that

$$\Delta L = -2\pi^2 b\left(\frac{b}{a}\right)^3\left(\frac{\alpha^2}{\alpha^2-1}\right)^3. \tag{28}$$

The limiting case at the other end of the range is a loop that has from the screen only the very small clearance distance h. It can be shown that then the effect of the screen is identical with that of an impermeable plane that is parallel to the loop at a distance h. This particular case gives us an opportunity to illustrate shortly the second method of applying inversion which we mentioned at the beginning. Here we take as the center of inversion one of the points at which the axis of the loop penetrates the sphere. The sphere transforms then into a plane impermeable to flux. Without restricting the generality of the treatment we can select the constant K of inversion so as to have the original loop transform into itself. With this particular choice of K the current through the transformed loop will be of the same magnitude as in the original loop. The transformation is illustrated in Figs. 5a and 5b; this figure shows too how the transformed arrangement can be solved by the introduction of the mirror image l_m' of the transformed loop l'.

If the walls of the spherical screen are not of infinite conductivity, the high frequency field penetrates to skin thickness and causes losses. These losses are calculated by Davidson and Simmonds for the case of the centrally situated loop. They can be calculated in a more general way if we make use of Wheeler's concept of the equivalent magnetic skin thickness ($=\frac{1}{2}$ conducting skin thickness). If the walls of the container of infinite conductivity are receded by the equivalent magnetic skin thickness, the magnetic energy of the field is increased (for constant input current) by just the same amount as if the field had penetrated into the walls of finite conductivity. (This is the definition of equivalent magnetic skin thickness.) The increase in loop reactance caused by this increase in field energy can easily be calculated, and, as the phase angle of such surface dissipation is always 45 degrees, this increase in reactance is numerically equal to the ohmic impedance component caused by the field penetration (reference 10).

In the present case, if the radius of the screen a is increased by δa, the (negative) inductance increment ΔL previously found is varied by

$$\delta L = \left(\frac{\partial L}{\partial a}\right)\delta a. \tag{29}$$

Hence,

$$\delta R = 2\pi f\left(\frac{\partial L}{\partial a}\right)t_m, \tag{30}$$

where f frequency of the field and $t_m = t/2$ equivalent magnetic skin thickness. The latter can be expressed in terms of the surface resistivity R_s of the wall material. We have for the conducting skin thickness $t = 1/2\pi(\rho/f)^{\frac{1}{2}}$[$\rho$ = volume resistivity], and

$$t_m = \frac{t}{2} = \frac{R_s}{8\pi^2 f}$$

hence

$$t^2 = \frac{1}{4\pi^2}\frac{\rho}{f} = \frac{1}{4\pi^2}\cdot R_s \cdot t. \tag{31}$$

Equation (30) allows us to write down immediately Kaden's result for the resistance component. By differentiation of Eq. (27) we obtain

$$\delta R = \tfrac{3}{2}\pi\cdot\left(\frac{b}{a}\right)^4\cdot R_s.$$

There is no difficulty involved in evaluating Eq. (30) in a more general case, and, for instance, Davidson and Simmonds' result for δR can be obtained from their series for δL by term differentiation. Differentiation of the general expression given in Eq. (22) leads to a rather laborious expression which is therefore not given, as for all practical purposes it is sufficient to replace the differential quotient by a difference quotient, the latter being easily obtained by direct numerical calculation.

[10] H. A. Wheeler, Proc. I.R.E. **30**, 412 (1942). See also A. Bloch, W. Eng. **21**, 367 (1944).

Non-Linear Viscous Elasticity and the Eyring Shear Model*

GEORGE HALSEY**

(Received April 17, 1947)

Attempts to analyze stress-strain-time relationships observed in experiments with textile fibers have been reported in a series of papers. This work has led to some general conclusions: First, the simplest three element model (spring in parallel with another spring and a dashpot in series) is adequate for the approximate explanation of a wide range of the data obtained. Second, the viscous element (dashpot) almost always appears to be non-Newtonian while the springs less frequently are non-Hookean. Third, the most striking deviations from simple behavior indicate, not a more complex model consisting of many simple elements, but that the assumed laws governing the viscous, or less frequently, elastic elements are themselves too simple.

Frequently a more complex law or laws will restore the three-element model to approximate agreement with the experimental facts. Finally, any system so far investigated can be made to show the presence of a number or a distribution of relaxation times by prolonging the experiment over a period of time, or more positively, by going to a point of no instantaneous relaxation, and waiting for the inevitable long period of relaxation to appear. Procedures to deal with the general situation described here are presented.

The paper begins with a condensed but essentially self-contained summary of the theoretical portions of the series of papers that preceded it. The original presentation has been clarified and recast in a form more in harmony with the present work. For experimental evidence, and supplementary information, the reader is referred to the original series.

The paper continues with a discussion of the various aspects of non-linear viscous elasticity, including the topics: Six rules for analyzing stress-strain curves (presented at the meeting of the Division of High-Polymer Physics of the American Physical Society, January 31, 1947); the thixotropic viscous element, where for convenience, complex situations, in which the populations of various states enter into a time-variable viscosity, have been gathered under the name "thixotropy"; constant force springs, where a particularly non-Hookean behavior is described.

INTRODUCTION

TO make a beginning in understanding the stress-strain behavior of a material[1] like a textile fiber or a plastic, a simple mechanical analogy has much to recommend it. The stress-strain relationship of most materials is not independent of time; thus, a simple elastic element (a spring) does not suffice to duplicate the behavior. Since immediate elongation is generally observed upon increasing the load, however, a spring effect initially unrestrained by viscous forces at the rate of loading in question is required. The existence of hysteresis, which is almost never absent, indicates that a viscous element (dashpot) must be incorporated in the model. The viscous element is restrained from free motion, by a spring, because in a majority of cases, the flow at constant load does not continue at a constant rate, showing that the force initially concentrated on the viscous element ultimately shifts to a spring.

The arrangement of elements indicated by this qualitative analysis is shown in Fig. 1. The two arrangements are almost equivalent, and, when Hooke's law is written for both springs, they are represented by identical equations. When a model of this kind is elongated at a constant rate, the stress-strain curve will begin at a steep slope, and then bend over as the yield force of the dashpot is reached. In terms of the first arrangement of the three elements (Fig. 1*a*), the stress-strain curve is made up of a line of slope equivalent to the sum of the stiffnesses of both springs being elongated together, followed by a transition region, leading to a line of slope corresponding to

* Contribution of the Frick Chemical Laboratory, Princeton University and The Textile Foundation, Princeton, New Jersey

** Fellow of the Textile Research Institute.

[1] "Mechanical Properties of Textiles:" I. George Halsey, Howard J. White, Jr., and Henry Eyring, Textile Research J. **15**, 295 (1945). II. George Halsey and Henry Eyring, Textile Research J. **15**, 451 (1945). III. Henry Eyring and George Halsey, Textile Research J. **16**, 13 (1946), supplementary data: *ibid.* **16**, 284 (1946). IV. Richard Stein, George Halsey, and Henry Eyring, Textile Research J. **16**, 53 (1946). V. Henry Eyring and George Halsey, Textile Research J. **16**, 124 (1946). VI. H. D. Holland, George Halsey, and Henry Eyring, Textile Research J. **16**, 201 (1946). VII. George Halsey and Henry Eyring, Textile Research J. **16**, 329 (1946). VIII. Henry Eyring and George Halsey, Testile Research J. **16**, 335 (1946). IX. Sidney Katz, George Halsey, and Henry Eyring, Textile Research J. **16**, 378 (1946). X. C. H. Reichardt, George Halsey, and Henry Eyring, Textile Research J. **16**, 382 (1946). XI. C. H. Reichardt, and Henry Eyring, Textile Research J. **16**, 635 (1946). XII. C. H. Reichardt and George Halsey, Textile Research J. **17**, (1947) in preparation.

the stiffness of the spring in parallel with the dashpot (Fig. 2).

These relationships will be expressed mathematically. If the total force on the model is F, and its elongation (change in length/original length) is l, the condition of experiment is $l=\rho t$, where t is the time and ρ is the rate of elongation. The problem is to find F as a function of t. If f is the force on the dashpot, and l_1 its elongation, $F-f$ is the force on the spring in parallel, and $l-l_1$ is the elongation of the spring in series. Hooke's law will be assumed to hold for the springs, and Newton's law of viscosity will be written for the dashpot. Thus the problem being solved is the linear three-element model operating at a constant rate of elongation. The equations governing these elements are

$$F-f=k_2 l, \tag{1}$$

$$f=k_1(l-l_1) \tag{2}$$

for the two springs, and

$$dl_1/dt=f/\eta \tag{3}$$

for the dashpot, and

$$dl/dt=\rho, \tag{4}$$

the condition of experiment.

At this point, it is to be noted that the force F on the whole system can be separated into two parts easily recognizable on the stress-strain curve, shown in Fig. 2. The broken line in this figure represents a line parallel to the ultimate slope, and starting at the origin. This line gives the force, $F-f$, on the spring in parallel with the dashpot as a function of strain. $F-f$ is a very simple function of elongation alone, and attention can now be directed to the residue of the force on the system, the difference between the

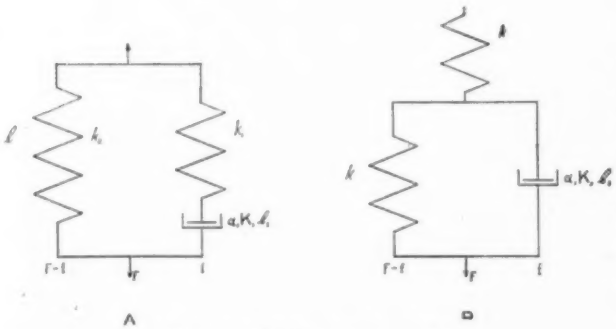

FIG. 1. Three-element model.

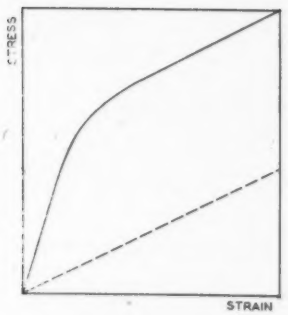

FIG. 2. A typical stress-strain curve.

ordinates of this line and those of the stress-strain curve itself. This difference, of course, is f, the force on the dashpot and spring in series, making up a Maxwell element. This function of f *versus* t is referred to as the "working curve." Eliminating l and l_1 from Eqs. 2–4 gives

$$(1/k_1\rho)(df/dt)=1-(f/\eta\rho). \tag{5}$$

Writing

$$f/\eta\rho=\phi \tag{6}$$

and

$$tk_1/\eta=\tau \tag{7}$$

to absorb constants gives the dimensionless equation

$$d\phi/d\tau=1-\phi \tag{8}$$

which can be integrated to

$$1-\phi=\text{const.}e^{-\tau}.$$

If $\phi=0$ when $\tau=0$ the constant becomes unity, and

$$\phi=1-e^{-\tau}. \tag{9}$$

Now at this time it becomes desirable to introduce the idea of reduced variables. Equation (9) can be written in the form

$$af=1-e^{-bt}, \tag{10}$$

where a and b are constants that must be adjusted to whatever units are selected for f and t. If some natural unit of the curve is selected as the unit of measurement, what is called a reduced variable is defined. A procedure of this kind is often adopted when working with equations of state and it will be used here. Thus, the ultimate value of f will be called unity, and t will be called unity when $f=\frac{1}{2}$, in the reduced units. The constants a and b can then be com-

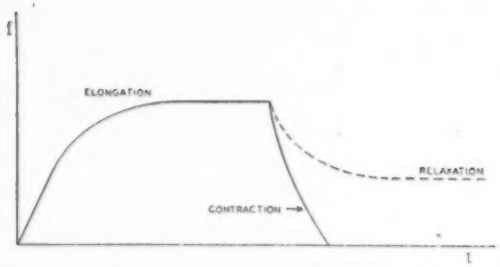

FIG. 3. Force on the dashpot as a function of time for elongation, contraction, and relaxation.

puted when

$$t=\infty, \quad f=1, \qquad (11)$$
$$f=\tfrac{1}{2}, \quad t=1.$$

Therefore, from (10), $a=1$ and $\frac{1}{2}=1-e^{-b}$, so

$$b=\log_e 2=\ln 2.$$

In reduced units, then,

$$f=1-e^{-t\ln 2}. \qquad (12)$$

The general nature of the curve is that of an exponential curve asymptotic to $f=1$, and for future reference, it should be noted that the force at the point $t=2$

$$f_2=1-\tfrac{1}{4}=0.75.$$

When the linear three-element model is relaxing at constant length, the problem is a very simple one, because $F-f$, the force on the parallel spring, is constant. Solving Eqs. (2) and (3) with l constant gives

$$(1/k_1)(df/dt)=-f/\eta \qquad (13)$$

which yields a simple unimolecular decay law.

The situation grows somewhat more complex when the usual repeated cycle stress-strain curve is considered. The separation of F into $F-f$ and f now has great utility. The force on the parallel spring is simply a function of elongation, and attention can be focused on the behavior of the dashpot and spring in series. Consider the working curve (Fig. 3) taken at a constant rate of elongation. If suddenly the elongation be halted, the relaxation curve begins, following Eq. (13). If the working curve be quite near its ultimate value, the dashpot is flowing at a rate equal to ρ, the over-all rate of elongation and the spring has ceased to elongate. This is shown by the constant value of the force. Therefore, when the elongation ceases, the dashpot will be flowing on at a rate equal to the over-all rate, and the force on the series spring will decay at exactly the same instantaneous rate as the initial slope near $t=0$ when the spring was being loaded at the over-all rate, ρ.

Now, if instead of stopping for relaxation the rate of elongation is reversed, at the ultimate value of f, then the force will be decaying for two reasons. The dashpot is still elongating at an instantaneous rate ρ, and the series spring is being shortened by another ρ. The total rate of decay is 2ρ, and so, the instantaneous slope upon reversal when $f_{\text{reduced}}=1$ is twice the initial slope. As the contraction at rate ρ proceeds, the slope decreases, for obviously, when $f=0$ the slope must be the initial slope, because the dashpot is no longer moving at all. As further contraction into the region of negative tension occurs, the situation is the same as in the initial elongation except that the sign of f becomes negative.

The equation for this region is still the familiar (12). Then, because the region of steep slope occurs without an intervening reversal at a time preceding the familiar region, it becomes apparent that the equation for this region is also (12), but in the region of negative time. The slope at any value of ϕ is obtained from (8), and it is seen that at $\phi=-1$, the slope is twice that of $\phi=0$.

The working curve for positive and negative values of time is shown in Fig. 4. Using this curve, the stress-strain curve for many cycles of elongation and contraction is easily constructed with a pair of dividers and a ruler. The sawtooth pattern of the force on the spring in parallel is first marked out, putting in a horizontal sec-

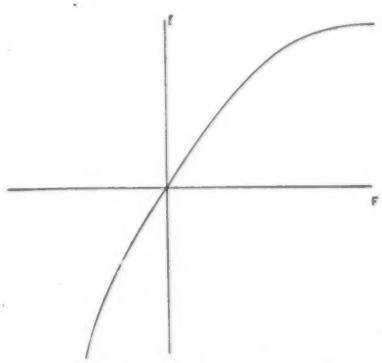

FIG. 4. The working curve.

tion for every relaxation. Then, starting at any point when f is known to be zero, the curve is laid out measuring the f value from the working curve. Whenever the direction of elongation reverses, the force value is measured from the other branch of the working curve, that is, where the value of f is the same except for sign. Now it is quite clear that if the shape of the working curve is known, this process of calculation of a complex curve can be generalized. None of the laws has to be linear. The only restriction, at the moment, is that the viscous drag at a given rate be the same for moving the dashpot forward as for moving it backward. Actually, to calculate the working curve depends on the ability to integrate the equation, but this integration can always be found by numerical means.

With this generality available, the question arises "when is the three-element arrangement itself permissible?" The answer to this question lies in a study of the points where $f=0$, that is, when the stress-strain curve crosses the line ($F-f$ *vs.* l) representing the force on the spring in parallel. At this point, there will be no relaxation. On either side of it, relaxation will occur in opposite directions, tending toward it. These "points of no relaxation" lie on a line that is a function of elongation alone. By a study of experimental points of no relaxation, it can be ascertained that they are a function of elongation, alone. If they are, their totality of points forms the line representing $F-f$, the force on the parallel spring, which for convenience is referred to as the "spring line."

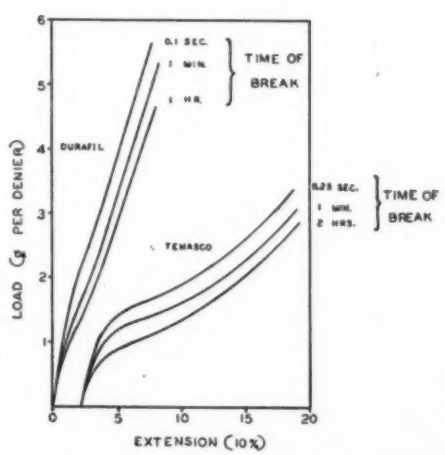

FIG. 5. Effect of rate of loading on load-elongation properties of regenerated cellulose rayons at 20°C and 65 percent R.H.

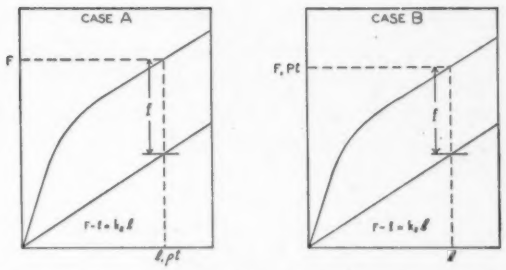

FIG. 6. The manner in which the various quantities are determined from the stress-strain curve; A, at constant rate of elongation, and B, at constant rate of loading.

A change in rate of experiment produces quite striking results. On the assumption of the Newtonian viscous element the force at a given elongation should be a linear function of the rate of elongation. Contrary to this, the function is found to be more nearly logarithmic. For example, D. Entwistle, in the third John Mercer Lecture,[2] publishes a curve (Fig. 5) showing the rate of elongation changed over a factor of 28,800 with the curves arranged in such a manner that he states: "Over a considerable range there is an approximately linear relationship between breaking load and the logarithm of the time of break." Because the breaking elongation is relatively independent of rate, this is equivalent to stating that the logarithmic law holds at any given elongation, since the curves parallel one another. This situation is entirely incompatible with any linear model, but harmonizes very well with the Eyring viscous element, or for that matter, any exponential law of flow.

In 1936 Eyring[3] proposed his law for viscosity in shear:

$$\text{rate of shear} = 2(V_h/V_m)(kT/h)e^{-\Delta F^{\ddagger}/kT} \sinh fV_h/2kT, \quad (14)$$

where V_h is the volume of the flow "hole," V_m is the volume of the molecule, k is Boltzmann's constant, T is temperature, h is Planck's constant, $\Delta F^{\ddagger}$ is the free energy of activation for flow, and f is the shear stress. This can be written for the present as

$$dl_1/dt = K \sinh \alpha f. \quad (15)$$

[2] D. Entwistle, J. Soc. Dyers and Colourists **62**, 261 (1946).
[3] Henry Eyring, J. Chem. Phys. **4**, 263 (1936).

The problem of the three-element model incorporating this viscous element will now be solved. It is a quite general law, and it includes the Newtonian law as a special case. The equations governing the model are:

$$F-f=k_2 l,$$
$$f=k_1(l_1-l_1),$$
$$dl_1/dt=K\sinh \alpha f,$$

and, for the condition of experiment,

$$pF+ql+rt=0.$$

This equation represents the most general restraint that can be integrated conveniently. It includes, as special cases, a constant rate of elongation, ρ, and a constant rate of loading, P. For these two cases the various variables are measured in the manner shown in Fig. 6. Also governed by this equation are the results of the pendulum-type tester, if the movement of the upper jaw is proportional to the load. Solving these equations for f as a function of t yields the equation

$$-\left(\frac{1}{k_1}+\frac{p}{pk_2+q}\right)\frac{df}{dt}-\frac{r}{pk_2+q}=K\sinh \alpha f. \quad (16)$$

This equation is of the form

$$\beta-d\phi/d\tau=\sinh\phi, \quad (17)$$

which is integrated to give

$$\frac{2}{(1+\beta^2)^{\frac{1}{2}}}\tanh^{-1}\left\{\frac{e^{+\phi}-\beta}{(1+\beta^2)^{\frac{1}{2}}}\right\}=\tau-c.$$

Solving this equation for ϕ gives

$$\phi=\ln\left\{\beta+(1+\beta^2)^{\frac{1}{2}}\tanh\left[\frac{(1+\beta^2)^{\frac{1}{2}}}{2}(\tau-c)\right]\right\}. \quad (18)$$

When $\tau=0$, $\phi=0$, so

$$c=\frac{2}{(1+\beta^2)^{\frac{1}{2}}}\tanh^{-1}\left\{\frac{\beta}{(1+\beta^2)^{\frac{1}{2}}}\right\}. \quad (19)$$

Now, it is desired to obtain a reduced equation, so following a procedure like that employed in the linear case, the equation

$$af=\ln\left\{\beta+(1+\beta^2)^{\frac{1}{2}}\tanh\left[\frac{(1+\beta^2)^{\frac{1}{2}}}{2}(bt-c)\right]\right\} \quad (20)$$

is solved for a and b, under the conditions that when $t=\infty$, $f=1$, and when $t=1$, $f=\frac{1}{2}$. After a series of algebraic manipulations the reduced equation

$$f=\frac{\ln\left\{\dfrac{1+\dfrac{1+\beta}{(1+\beta^2)^{\frac{1}{2}}}\tanh(At)}{1+\dfrac{1-\beta}{(1+\beta^2)^{\frac{1}{2}}}\tanh(At)}\right\}}{\ln\left\{\dfrac{1+\dfrac{1+\beta}{(1+\beta^2)^{\frac{1}{2}}}}{1+\dfrac{1-\beta}{(1+\beta^2)^{\frac{1}{2}}}}\right\}} \quad (21)$$

is obtained, where

$$A=\tanh^{-1}\left\{\frac{\left[\left(\dfrac{1+\beta}{(1+\beta^2)^{\frac{1}{2}}}+1\right)\left(\dfrac{1-\beta}{(1+\beta^2)^{\frac{1}{2}}}+1\right)\right]^{\frac{1}{2}}-1}{\left(\dfrac{1+\beta}{(1+\beta^2)^{\frac{1}{2}}}+1\right)\left(\dfrac{1-\beta}{(1+\beta^2)^{\frac{1}{2}}}+1\right)-1}\right\}. \quad (22)$$

With this function of t and β it is possible to calculate a whole family of working curves, depending on the shape factor, β. The larger β is, the more non-Newtonian is the behavior of the working curve. To compute β from the working curve, the behavior of the reduced force at some suitable value of t_{red} can be investigated. It was shown above that for the Newtonian case for $t=2$, $f=0.75$. In the non-Newtonian case this force is always larger, approaching unity as β increases indefinitely. The quantity f_2 *versus* β is shown in Fig. 7.

The meaning of the increase of f_2 with β is found in the fact that the more non-Newtonian a dashpot is, the more insensitive it is to forces below the yield force. In the limit, the com-

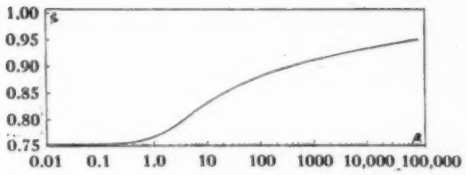

FIG. 7. Diagram for evaluating β from the reduced force, f_2, acting on the dashpot at a time, t_2, which is twice the time elapsed from the application of the load until it reaches one-half its final value.

pletely non-Newtonian dashpot yields quite sharply at a given force, independent of the rate of elongation, and does not move below this force. For practical purposes of constant evaluation the shape factor is only of the roughest significance, but at this point it is appropriate to give the constants of the viscous law as a function of the observed quantities. For the case of a constant rate of elongation $K=\rho/\beta$ and $\alpha=1/f_\infty \operatorname{arc\,sinh}\beta$. The ultimate value of the force on the dashpot is written f_∞. Similarly for the case of constant rate of loading, P, $K=P/\beta k^2$ and

$$\alpha=1/f_\infty \operatorname{arc\,sinh}\beta.$$

Various other ways of evaluating β are given in the original references, along with a treatment of relaxation and creep and a more detailed discussion of the Eyring viscous element.

The practicable way of evaluating β is found when the change of the ultimate force, f_∞, with rate of elongation is considered. If r_n is the ratio of f_∞ at a speed n times a basic speed β, to f_∞ at the unit speed, then one has

$$r_n=f_\infty(n)/f_\infty(1)=\phi_n/\phi_1, \tag{23}$$

$$\phi_1=\operatorname{arc\,sinh}\beta,$$
$$\phi_n=\operatorname{arc\,sinh}n\beta,$$

and, therefore,

$$r_n=\operatorname{arc\,sinh}n\beta/\operatorname{arc\,sinh}\beta. \tag{24}$$

Therefore, β can be determined as a function of r_n. If β is large, the approximation $\operatorname{arc\,sinh}\beta \approx \ln 2\beta$ holds, and β can be found explicitly:

$$\beta=\tfrac{1}{2}n^{(1/r_n-1)}. \tag{25}$$

This equation provides a way to determine β as a function of scale factors alone, and independent of shape.

The three-element non-Newtonian model is quite successful in accounting, qualitatively at least, for many stress-strain curves. It should be emphasized that the non-Newtonian nature of the dashpot is responsible for its remarkable qualitative fidelity. In complicating the three elements, very little progress can be made merely by having many Newtonian elements hooked together. Most existing material concerning the visco-elastic behavior of materials, however general and formal, has in it somewhere the assumption that the governing equations are linear. This is particularly true of the so-called superposition principle. The utility of such schemes is thus strictly limited. In fact, linear systems are usually found only in highly plasticized systems where the stresses are in the region of 10^7 dynes per square centimeter. In textiles, where stresses are of the order of 10^9 dynes per square centimeter, no case has come to the author's attention. Further discussion of this topic is found in the original references. The most fruitful complications are found when the elements themselves are changed, retaining the three element model.

In deriving the Eyring viscous law, the assumption is made that flow is retarded by a symmetrical potential barrier. It was always realized that this simplification might be unjustified, and it has been observed that it is often not available. That is, the force, notably in the case of wool, is much more effective in producing flow in one direction than in the opposite one. Clearly, if the potential barrier is unsymmetrical, the rate of reaction up the steep side will be less affected by the force than the rate up a more gradual slope. This, then, is in harmony with the experimental observation. With an unsymmetrical barrier, the expression for the rate of shear is

$$dl_1/dt=(K/2)(e^{2\mu\alpha f}-e^{-2(1-\mu)\alpha f}), \tag{26}$$

where μ is the symmetry coefficient. The form

$$dl_1/dt=Ke^{+(2\mu-1)\alpha f}\sinh\alpha f \tag{27}$$

is equivalent to this expression, which shows the perturbing influence of the lack of symmetry on the original hyperbolic sine law. For convenience, σ is written for $2\mu-1$.

Using this new viscous law, the equation governing the working curve becomes

$$\beta-(d\phi/d\tau)=e^{+\sigma\phi}\sinh\phi, \tag{28}$$

which gives

$$-\tau=\int\frac{d\phi}{\beta+e^{\sigma\phi}\sinh\phi}, \tag{29}$$

which is not integrated. The measurement of the ratio

$$(f_n/f_1)_\infty=(\phi_n/\phi_1)_\infty$$

still permits determination of the constants, even if the exact shape of the working curve is not calculated.

Using the notation ϕ_1^{out} for the ultimate value of ϕ with the dashpot going forward at speed 1, and similarly ϕ_n^{out}, ϕ_1^{in}, and ϕ_n^{in} for the other three ultimate values, the equations when $d\phi/d\tau$ becomes zero, are

$$\begin{aligned}\beta&=e^{+\sigma\phi_1^{\text{out}}}\sinh\phi_1^{\text{out}},\\ n\beta&=e^{+\sigma\phi_n^{\text{out}}}\sinh\phi_n^{\text{out}},\\ \beta&=e^{-\sigma\phi_1^{\text{in}}}\sinh\phi_1^{\text{in}},\\ n\beta&=e^{-\sigma\phi_n^{\text{in}}}\sinh\phi_n^{\text{in}}.\end{aligned} \tag{30}$$

Using the approximation $\sinh x\approx e^x/2$ for large x, these equations become

$$\begin{aligned}\ln 2\beta&=(1+\sigma)\phi_1^{\text{out}},\\ \ln n+\ln 2\beta&=(1+\sigma)\phi_n^{\text{out}},\\ \ln 2\beta&=(1-\sigma)\phi_1^{\text{in}},\\ \ln n+\ln 2\beta&=(1-\sigma)\phi_n^{\text{in}}.\end{aligned} \tag{31}$$

From this set of equations, a set of ratios may be derived as follows:

$$R^{\text{out}}=(\ln 2\beta+\ln n)/\ln 2\beta=R^{\text{in}}, \tag{32}$$

$$R_n=(1+\sigma)/(1-\sigma)=\phi_n^{\text{in}}/\phi_n^{\text{out}}; \tag{33}$$

where

$$\begin{aligned}R^{\text{out}}&=\phi_n^{\text{out}}/\phi_1^{\text{out}}=f_n^{\text{out}}/f_1^{\text{out}},\\ R^{\text{in}}&=\phi_n^{\text{in}}/\phi_1^{\text{in}}=f_n^{\text{in}}/f_1^{\text{in}},\\ R_n&=f_n^{\text{in}}/f_n^{\text{out}}.\end{aligned}$$

From these equations for large ϕ $\beta=\frac{1}{2}n^{1/R-1}$ (as is found for this approximation when $\sigma=0$), and

$$\sigma=\frac{R_1-1}{R_1+1}=\frac{R_n-1}{R_n+1}, \tag{34}$$

or

$$\mu=\frac{R_1}{R_1+1}=\frac{R_n}{R_n+1}, \tag{35}$$

where the formulas with R_n are obviously better approximations.

In the other approximation, where ϕ is small, the four equations become so simple that σ disappears completely, in harmony with the necessary equality at the rates of reaction at equilibrium, satisfying the principle of detailed balancing.

As a second degree of approximation, consider that $\beta=\beta_0+\beta_1$, $\sigma=\sigma_0+\sigma_1$, and $\phi_1^{\text{out}}=\phi_0+\phi_1$, where $\phi_0=(1+\sigma_0)^{-1}\ln 2\beta_0$. Upon expansion in the small correction factors, using the approximate equation for the zero-order values, closer values for the constants can be found.

Of some utility is the limiting concept of the completely unsymmetrical barrier, where $\mu=1$. Flow in one direction is not affected by force at all. The equation for shear becomes

$$dl_1/dt=(K/2)(e^{2\alpha f}-1). \tag{36}$$

If the slightly altered definitions $\phi=2\alpha f$, $\beta=(2\rho/K)+1$, and

$$\tau=k_1\alpha Kt$$

are made, the differential equation for the working curve becomes

$$\beta-(d\phi/d\tau)=e^{\phi}, \tag{37}$$

which yields

$$\tau+\text{const.}=(1/\beta)[\phi-\ln(\beta-e^{\phi})]. \tag{38}$$

A reduced equation will be obtained, subject to the conditions, that when

$$\begin{aligned}t&=0, &f&=0\\ t&=\infty, &f&=1\\ t&=1, &f&=\tfrac{1}{2}.\end{aligned}$$

The equation is

$$t=\frac{(f\ln\beta-\ln(\beta-e^{f\ln\beta})+\ln(\beta-1))}{(\ln\sqrt{\beta}-\ln(\beta-\sqrt{\beta})+\ln(\beta-1))}, \tag{39}$$

an equation which changes when $-f$ is substituted for f.

The only type of experiment considered above was one in which a linear relationship existed between force, elongation, and time:

$$pF+ql+rt=0,$$

because only this restraint makes the equations amenable to simple treatment. In practice, it is often desirable to calculate behavior that is characterized by its dependence on any restraint, assuming in this discussion that the constants of the model have been evaluated from simple experiments and hence are available for computation. However, in solving even the simplest cases analytical difficulties are met, and it is of interest to consider here simple point-by-point methods. The method of synthesizing the total force, F, from the partial forces, f, on the dashpot and spring in series, and $F-f$, on the single spring will be employed, as before. If the restraint is of the form $l=R(t, F)$, then $F-f=k_2l=k_2R(t, F)$. The value of f must be considered with more care. First the case of constant rate is considered. The value of ϕ is

$$\phi=\ln\left\{\frac{1+\dfrac{1+\beta}{(1+\beta^2)^{\frac{1}{2}}}\tanh\dfrac{\tau}{2}(1+\beta^2)^{\frac{1}{2}}}{1+\dfrac{1-\beta}{(1+\beta^2)^{\frac{1}{2}}}\tanh\dfrac{\tau}{2}(1+\beta^2)^{\frac{1}{2}}}\right\} \quad (40)$$

with a new set of normalization conditions.

The time values were normalized previously to the half-value of the ultimate force (that is, when $t=1, f=\frac{1}{2}$), but now the ratios between the initial slopes must be preserved in their proper values. This is made necessary by the new variable that is now considered. Thus, the three conditions defining the old reduced variables variables were as follows: when

$$\begin{aligned} f&=0, \quad & t&=0,\\ f&=\tfrac{1}{2}, \quad & t&=1,\\ f&=1, \quad & t&=\infty, \end{aligned}$$

and the definitions of the new reduced variables are as follows: when

$$\begin{aligned} f&=0, \quad & t&=0\\ K\alpha k_1&=1,\\ \alpha&=1. \end{aligned}$$

This curve, or family of curves, depending on β, is adequate to predict the value of f from its initial value, f_0, as long as f_0 is below f_∞ in value. For values of f_0 greater than f_∞ it is necessary to determine the family of curves where the extreme boundary value $f_0=\infty$ is employed. The general solution

$$f=1/\alpha\ln[\beta+(1+\beta^2)^{\frac{1}{2}}\tanh(bt+c)] \quad (41)$$

yields at $f=\infty$, $t=0$

$$\begin{aligned} \infty&=\ln[\beta+(1+\beta^2)^{\frac{1}{2}}\tanh c],\\ c&=\pi/2(-1)^{\frac{1}{2}}. \end{aligned}$$

This yields, as a special solution,

$$\phi'=\ln\left\{\beta+\frac{(1+\beta^2)^{\frac{1}{2}}}{\tanh bt}\right\}. \quad (42)$$

(The constant b is then $(1+\beta^2)^{\frac{1}{2}}$ to agree in scale with f.) This equation represents a family of curves asymptotic to $t=0$ and $f'=f_\infty$, because when $t=\infty$

$$\phi_\infty'=\ln[\beta+(1+\beta^2)^{\frac{1}{2}}], \quad (43)$$

and for the other set of curves passing through $t=0, f=0$

$$\phi_\infty=\ln\left\{\frac{1+\dfrac{1+\beta}{(1+\beta^2)^{\frac{1}{2}}}}{1+\dfrac{1-\beta}{(1+\beta^2)^{\frac{1}{2}}}}\right\}, \quad (44)$$

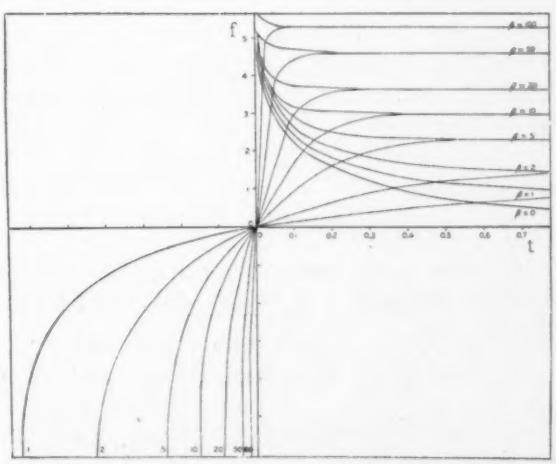

FIG. 8. The working curves for various values of β from 1 to 100.

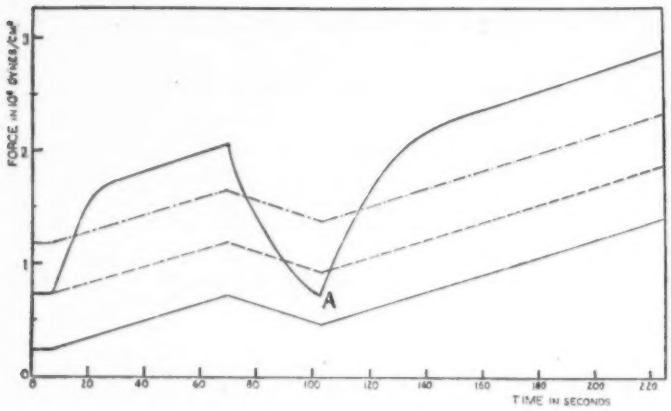

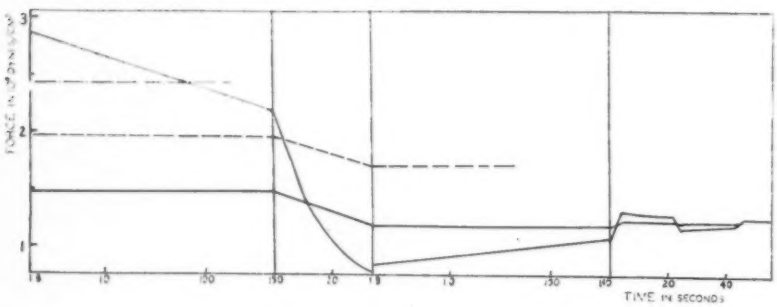

FIG. 9. A typical stress-strain curve showing the inadequacy of the three-element model. It is 6-denier textile rayon, elongated at a rate 6.5×10^{-4} per second at 0.35 R.H.

and, since

$$\beta+(1+\beta^2)^{\frac{1}{2}}=\frac{1+\dfrac{1+\beta}{(1+\beta^2)^{\frac{1}{2}}}}{1+\dfrac{1-\beta}{(1+\beta^2)^{\frac{1}{2}}}}=e^{\text{arc sinh}\beta},$$

$$\phi_\infty'=\phi_\infty.$$

These two families, which together cover the entire range of f from $-\infty$ to ∞, are plotted in Fig. 8. Thus with a given velocity and initial conditions, subsequent conditions can be predicted at that velocity by following the proper curve. But since

$$l=R(F,t),$$

or

$$dl/dt=\rho=R'(F,t) \tag{45}$$

is no longer a constant, it is possible to predict the initial velocity if f_0, F_0 and the constants are known to be

$$\beta_0=\rho_0/K=R'(F_0,0)/K. \tag{46}$$

Proceeding along the proper curve β_0 an amount Δt_1, from f_0 gives

$$\Delta(F-f)_1=\rho_0 k_2\Delta t. \tag{47}$$

Here k_2 is the force constant of the parallel spring. ΔF_1 is obtained from Fig. 8

$$\Delta l_1=\rho_0\Delta t_1.$$

Then a new β is determined:

$$\beta_1=\rho_1/K=R'[(F_0+\rho_0 k_2\Delta t_1+\Delta f_1),\ \Delta t_1]/K. \tag{48}$$

Then, from the point $f_0+\Delta f_1$, curve β_1 is followed for a time Δt_2, and another point is thus constructed. This process is repeated until the required curve is produced.

Now, in order to work a specific problem where the values of the constants are presented in centimeter-gram-second units, it is necessary to reduce the units. First, the value of the force unit is taken, so that α becomes unity in terms of the new force variable. Then, time is taken so that the product $K\alpha k_1$ equals unity, whereupon the variables are reduced. Then β_{initial} is computed from ρ_{initial} and K, and k_2 are expressed in terms of reduced force, and the computation begins. The only numbers that characterize a given computation, then, are the experimental restraints such as inertia (which must again be in reduced units), the value of k_2 in reduced units, and ρ_{initial}.

Although a large amount of material can be explained with the three-element model, almost any material can be made to show the presence of a distribution of relaxation times by a suitably prolonged experiment. Before going into the general theory of complex arrangements of non-linear elements, it will be helpful to consider a simple system that shows some of the qualitative features of the distribution.

The use of any sort of model containing more than one viscous element is a difficult undertaking. However, the most rudimentary considerations of the molecular structure of a fiber make it seem highly unlikely that the fiber can be described with a single viscous element, no matter how involved its law of operation. Nevertheless, a single element serves to a remarkable degree to reproduce the behavior of materials which do not exhibit plastic flow to an appreciable extent. The "distribution" used here contains only two elements; no particular significance, however, can be attached to this, except perhaps that the data do not warrant further extension. The actual fiber, no doubt, involves a continuous distribution. It is necessary to remark that this distribution has nothing in common with the Wiechert distribution of linear elements; this latter is totally inadequate to explain the experiment. It is much farther from the facts than the three-element, non-Newtonian model.

In the analysis of a large number of stress-strain curves, using the method of the three-element model of previous papers, certain persistent difficulties have been encountered. The curve of Fig. 9 shows an extreme case. The ultimate slope is well defined. Therefore, simple permanent set cannot be a factor over moderate time ranges. Repeated cycles could then be expected to yield a limiting curve. In order to place the line of ultimate relaxation, three procedures are resorted to, using the well-defined ultimate slope. First, the line is drawn from the origin. This is unsatisfactory for two reasons: the line does not cut the experimental curve with constant angle and it does not agree with the position of ultimate relaxation as determined at the end of the experiment. An attempt to draw a line through the points of constant slope meets with even less success. Using the established slope, it is impossible to go through all of the points. The line is too high for the relaxation curve, and, of course, it fails completely to agree with the determination of the point of ultimate relaxation. Projecting the line back from this point also fails completely. It leaves the point *A*, which is obviously a point below the spring line, hopelessly above it.

These considerations obviously lead to the conclusion that the model is not a correct picture of this fiber. However, the qualitative as-

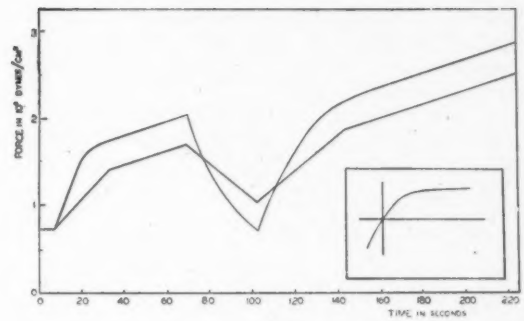

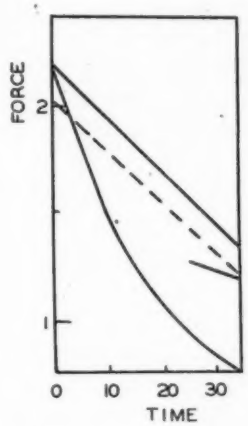

FIG. 11. The curve of Fig. 9 here is analyzed on the basis of the model of Fig. 10. Only a small excerpt from the second part of Fig. 9 is shown.

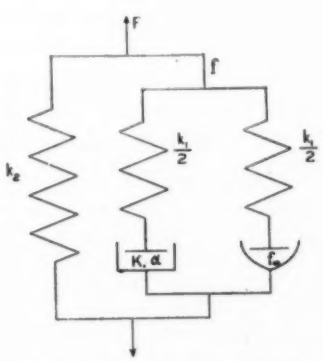

FIG. 10. The five-element model used in this paper to explain the curve of Fig. 9.

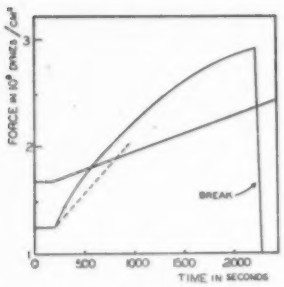

FIG. 12. The experiment of Fig. 9 carried out at one twenty-fifth the former rate. It shows the presence of a distribution but is interrupted by breakage of the fiber.

pects of the diagram are the same as a curve produced by a perfect three-element model. No widely separated processes exist. The sharpness of the initial yield point completely disallows a wide distribution of yield forces of a simple non-thixotropic character. These yield forces must be within perhaps 10 percent of one another. Equally impossible is any type at all of three-element model. A single dashpot, even if unsymmetrical and thixotropic, cannot explain point *A*. That is, a true point of ultimate relaxation cannot always be achieved by finite process.

The model suggested by these considerations is one containing a number of elements of the same yield strength. A simple method of this type suffices to explain the curve in Fig. 9. This model (Fig. 10) contains two dashpots of equal yield value. One is quite non-Newtonian and the other is more nearly Newtonian. The effect of this arrangement is that the non-Newtonian dashpot reinforces the spring when it is not at the yield force. When the point of ultimate relaxation is found by hunting, it does not represent the place where the force on the compound element is zero, but the place where the force on the Newtonian dashpot is zero. Therefore, the slope to be used in leaving this point to connect with other similar points is not the well-defined slope but a steeper slope calculated by connecting several points of the proper slope. This slope must yield to the well-defined slope when the yield value is reached. That this model accounts for the curve is apparent (Fig. 11). During the relaxations, the model must be abandoned in favor of a smoother distribution of some unknown character. At a finite rate, however, this crude model is the most complicated that can be justified. Its importance is that it is the *simplest* model that possibly can give rise to the experimental facts.

When the force is divided among several viscous elements, there are at least two ways to express the constants. If the actual force on an element is used to compute the constant, then this represents the exact mechanical element that would reproduce the behavior when combined with its fellow springs and dashpots. However, if constants are based on the total viscous force along with a "concentration," then the situation is conceptually clearer. Thus, if one desires to make a three-element model with two identical dashpots instead of one, it seems desirable that the constants should be the same as if he had used only one because the behavior would be identical.

So far as a single rate of elongation is concerned, the model of Fig. 10 seems quite adequate. Figure 12 shows the effect of changing the rate of elongation to one twenty-fifth of its former value. Unfortunately, the viscose rayon fiber soon broke. The shape of the curve, however, shows that the hypothesis of equal yield forces is no longer good. The presence of a distribution of relaxation times is clearly indicated. This is as it should be, for if at one speed the yield force of the dashpots is equal, then at other speeds the yield forces must diverge from one another. Figure 12 shows that the dashpot of the more Newtonian character is almost completely yielded at all times, and that the yield force is approximately accounted for by the completely non-Newtonian dashpot if that yield force, by hypothesis, is considered constant. The gradual nature of the yielding process shows that this hypothesis is only qualitatively correct, and that the completely non-Newtonian dashpot is beginning to split into several more or less non-Newtonian dashpots.

Proceeding in a manner similar to that described above and observing the convention therein described, one obtains the following results:

Springs: $k_1 = 0.94 \times 10^{11}$ dyne/cm^2,
$k_2 = 1.19 \times 10^{10}$ dyne/cm^2;
First dashpot: 0.66 concentration
$f_\infty = 0.874 \times 10^9$ dyne/cm^2;

Second dashpot: 0.34 concentration

$\rho = 6.5 \times 10^{-4}$,

$\beta = 3$ (from shape),

$k = 2.2 \times 10^{-4}$,

$\alpha = 2.09 + 10^{-9}$,

$\Delta F^{\ddagger} = 23{,}650$ calories,

$V_h = 5.5$ A cubed.

In Fig. 11, second part, the agreement with the established line of no relaxation is shown by the difference between the dashed line and the solid line. In Fig. 12, the dashed line gives the slope used before to represent the single dashpot. At this new speed, it no longer has meaning.

SIX RULES FOR ANALYZING STRESS-STRAIN CURVES

In the analysis of the stress-strain properties of a material there is a certain advantage to the making of haphazard stress-strain curves, following no particular pattern and depending, almost, on the whim of the experimenter. Then these curves are subjected to an analysis that must meet many novel conditions of experiment. For path-finding purposes this procedure is very useful. Until the present writing, stress-strain work in the laboratory has followed such a pattern, or lack of pattern. However, as more painstaking analyses are attempted, and as the model is refined, this procedure becomes very wasteful and the results meager. An attempt has been made to improve the situation by setting up a series of six rules for the analysis of the stress-strain curves of a material.

In the present paper, the general distribution of non-Newtonian relaxation times is included in the scheme of analysis. The introduction of the distribution has been avoided in previous papers because its great complexity obscured the exposition of simpler ideas, such as non-Newtonian behavior and the unsymmetrical potential barrier. The importance of the distribution is realized when more complex experiments are performed. It is seldom if ever found absent when experiments are devised that accentuate it. Similarly, the existence of multiple equilibrium positions at the same value of the flow coordinate (thixotropy) is of very great importance. The protein fibers seem especially thixotropic. Because both of these complications are introduced here, the scheme is more general in application than the analysis given in previous papers.

Each of the proposed six rules contains a simplifying criterion. If the criterion in the first rule is satisfied, then the procedure of the second rule becomes usable, and so on through the rules. If all six criteria are obeyed, then the material under study is representable by a hyperbolic sine-law model. When a criterion is violated, the notes to the rules suggest the proper procedure. At times this procedure can only be sketched, because the mechanics of the complex analysis is still being worked out. However, the principles governing the calculation are usually clear. The six rules suggest an orderly mode of experiment which is outlined in a note. The language of the rules is that of experiments conducted at a constant rate of elongation, but obvious modifications will occur to those interested in the other types of experiments. It also seems pertinent to observe that whenever the general criterion for the existence of a simple system (the three-element model) has been established, the single dashpot has its kinetics, however peculiar, completely bared, and the necessity for employing the rules vanishes. The concept of compound models, because of its great difficulty from the experimental standpoint and its complicated and involved nature from the theoretical standpoint, is reserved for a final note.

The typical experimental material available is a complex stress-strain curve like Fig. 13, which consists of many cycles of elongation, relaxation, and contraction. In Fig. 13 the curve is plotted, for compactness, on a load-elongation plane, rather than the alternative plot on the load-time plane. The six rules are as follows.

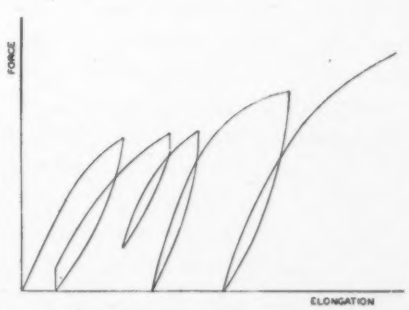

FIG. 13. A complex stress-strain curve. Relaxation is indicated by a straight vertical line.

THE SIX RULES

I. The complex stress-strain curve is compared with simple experiments in which samples of the material under study are elongated to break at the rates of elongation under study (Fig. 14). The complex stress-strain curve at a given rate on the load-elongation plane must lie within the simple curve taken at the rate considered as an envelope (criterion I) (Fig. 15). Any portion of the complex curve lying outside of the envelope (Fig. 16) must be analyzed on the basis of a theory of thixotropy.

An obvious exception to this rule is encountered when the rate is changed rapidly enough to leave the stress-strain curve within the envelope at the old, faster rate, but outside of the envelope at the new, slower rate (Fig. 17).

II. A large number of points of no relaxation is determined. A point of no relaxation is determined by finding an elongation where the force decreases upon relaxation, then contracting the sample until a point is reached where the force increases with relaxation, eventually bracketing the force value when the initial rate of relaxation is zero (Fig. 18). Out of the totality of points so determined, a special group is defined as follows: a member is taken directly by one contraction starting from a point where the complex curve lies on its envelope. This definition will have to be approximated by doing as little searching as possible, and a certain amount of discretion must be used in placing a point in the special class.

Because there is only one defined way of achieving a member of this group from a definite elongation on the envelope, the totality of these points will form a line underneath the envelope that is a function of the elongation. Consider the difference in force between the envelope and these points. If this difference increases monotonically and becomes constant, then, in terms of spring-dashpot language, the elements that are determining the point of no relaxation are the same after this constancy has been achieved. When this condition of constancy is satisfied early in the experiment, criterion II is obeyed. The group of elements that determine the points of no relaxation can then be investigated as an entity. Before criterion II is satisfied the region,

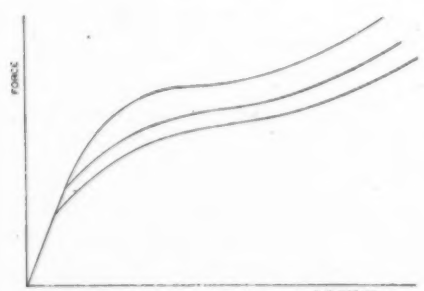

FIG. 14. Samples elongated to break at several rates.

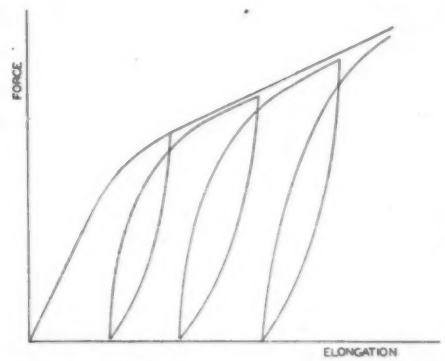

FIG. 15. A complex curve lying completely within the envelope (conforming to criterion I).

if it is satisfied ultimately, is to be treated under the rules given below concerning the return (contraction) curves. Data in this region, for most practical cases, are fragmentary and unimportant.

When this condition of monotonic increase and constancy is not satisfied, then some change in the determining flow process with elongation is implied.

III. *The residue of points* of no relaxation, after the special group is considered, is divided into sections totally separated from one another by any relaxation occupying a longer time than is the criterion of direction of movement, for determining the point of no relaxation. It is, of course, also separated by any determination of a point of the special class or any return to the envelope. The process described in this rule is repeated for each group of points isolated by these occurrences. Within such a section, a spring line is drawn from the terminal point of such a long relaxation or from the point of a determination of the special group, with a slope that makes it pass as closely through the points

in the section (Fig. 19) as possible. If it is possible to pass this line through all the points in the section, and if it is possible to do this with the same slope in every section, then the concept of a single relaxing dashpot for determining the point of no relaxation is applicable. (Criterion III.) The example of a simple "distribution" given above is of this kind.

IV. If the previous criteria are observed, it remains to consider the shape of the return loops. A simplifying criterion is the existence of a well-defined slope in the region of no relaxation. If this constant elastic slope exists throughout the experiment, then it is established that the same totality of Hookean springs is operating throughout the experiment. (Criterion IV.) When this criterion is not observed, some condition of thixotropic flow or non-Hookean elasticity is implied.

V. When the elastic slope of rule IV is established, the working curves are transcribed, using the slope of rule III as spring line and the points of no relaxation as origin. If a well-defined working curve exists, the appropriate theory can be applied. (Criterion V.)

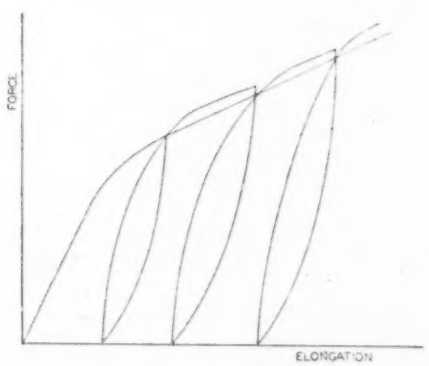

FIG. 16. A complex curve with a portion outside the envelope (violating criterion I).

VI. If the working curve is the same for elongation and contraction and the constants determined from relaxation agree with those from shape and rate change, then the simple hyperbolic-sine model can be employed. (Criterion VI.)

NOTES AND EXCEPTIONS TO THE RULES

I. When only a certain small portion of the curve appears outside of the envelope, this part

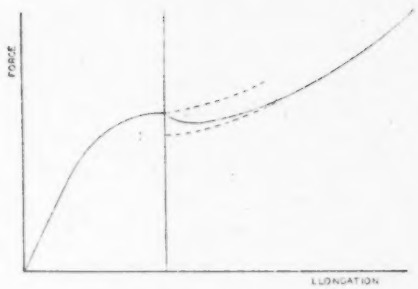

FIG. 17. The case of a change from a fast to a slow rate in which the curve can be said to obey criterion I because it approaches the envelope, although from the outside.

can often be neglected, and points of no relaxation taken from it excluded from the special class. Usually this "hump" is observed just as the curve reaches the envelope after a series of elongations and contractions confined to the interior of the permitted area. By a careful study of when the humps appear, a proper thixotropic scheme can be devised (see below). Although the special class of points of no relaxation is not affected, the behavior of the other points must be carefully studied in the light of the thixotropic scheme. When, however, the position of the curve is a complete departure from the envelope ("strain hardening"), an extremely thorough study of the effect of order of succession in the performing of experiments becomes necessary. This complication of experiment is required because the great simplification of the possibility of proceeding to a reproducible state (the envelope) at will, is no longer available. When the general thixotropic scheme has been devised for the envelope, it is still a much greater task to go to the return loops and points of no relaxation. There is no example where this has been done.

Certain deviations from the envelope in the sense that the complex curve lies below the envelope when it is obviously parallel to it and therefore unable to reach it, can be ascribed to true permanent set, or quasi-permanent set from a later relaxation process. Because of the usual highly non-Newtonian nature of the yielding process, it is not an important occurrence. Even when the first criterion is not satisfied, as long as the curve over a given range conforms within appropriate limits, the procedures of the following rules can be applied with caution. When the general thixotropic scheme has been elucidated,

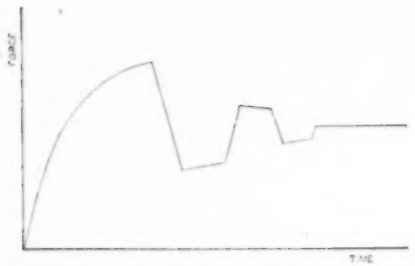

FIG. 18. The determination of a point of no relaxation.

then more general modifications of subsequent rules can be applied.

When thixotropy is established, it is quite apparent that for the envelope curves themselves whenever a dashpot is changing its rate of flow, thixotropy is likely to enter. Therefore, there might be some advantage in constructing a hypothetical, experimentally unrealizable envelope curve calculated on the basis of all of the dashpots continuously having their ultimate viscosity. The obvious reason for rejecting this procedure is the uncertainty of any theory that might be used to calculate such a curve.

The essential nature of the envelope criterion is that all curves should approach a common curve when the sample is pulled for a length of time with no reversals or halts. It is conceivable that the nature of the multiple state flow might be rheopectic, and at first the viscosity be lower than its ultimate value. No striking test for this situation is apparent, and a careful study of the consequent varying rate of approach to the envelope is required. A curve that almost parallels the envelope at a distance for a time and then ultimately approaches, indicates rheopexy, but this criterion is necessarily more vague than the corresponding one for thixotropy. When a large number of points of no relaxation are not experimentally available, then a study of the envelope curves themselves is of some use. At first, the curves at the varying rates are coincident, corresponding to the action of spring forces alone, and then they diverge as the rate-dependent dashpots come into action. The lines will then roughly parallel one another, until further yielding processes are discovered, when they will separate farther or perhaps, because of a non-Hookean parallel spring, come closer together.

II. It is to be observed that the selection of slope in rule III has no effect on the special group of points of no relaxation. The adherence to the criterion merely implies that whatever the elements that are important in the inside area, they remain the same. No assumptions of independent action of relaxation or simplicity of moving dashpot enter. When the criterion holds, it is possible to treat the single contraction curve starting at the envelope as an individual. If it, transcribed as a working curve, does not maintain constant shape while the criterion continues to hold, then a change in symmetry of potential barrier with elongation is implied.

When the compression force on the other side of the line of points in the special class is considered, it becomes quite conceivable that, while the contraction curve from the envelope to the line of the special class may be of unchanging shape and length, the prolongation of the curve may deviate from this constancy on the compressive side of this line. When this situation is encountered, it is proper to define some minor special classes, supplementing what can be called the major special class, of rule II. A suitable member would be defined as the points determined directly after going to a given line parallel to the envelope, and below the major class line. This new line would be parallel to the major line, because, by hypothesis, criterion II is already satisfied. Then if the new line of points of no relaxation is also parallel, the determining elements are identical with those determining the major line. It is apparent that very peculiar elements indeed would be implied if these lines were not parallel.

Other improper special classes can be designated by using the line of no forces as a reference. These special classes are improper because they involve both the envelope and the line of no force as references. These lines diverge as elongation increases, and so the points determined are not comparable at differing elongations. The significance of any special class is that the points it comprises are obtained from a fixed reference (the envelope) by a defined procedure. Then elongation becomes the only variable. For example, the improper class of points taken directly after a contraction from the envelope to zero force will ultimately parallel, not the envelope, but the line of zero force when the determining

dashpot system is flowing at a constant rate. It is apparent that for most purposes, the major special group is sufficient and that for any situation this group is of paramount importance.

The point of no relaxation with the greatest value of force at a given elongation is attained by going into relaxation at the envelope for as short a time as is found to be necessary, contracting a very little, and looking for reversed relaxation. A similar process at zero forces finds the point with the lowest value of force.

When the second criterion fails to hold, and the envelope is a straight line when it is failing to hold, it is reasonable to assume that the cause of the failure is not the discovery of any new dashpots, but a change in the dashpots already concerned. The dashpot is of the quasi-viscous type, and the proportion of the energy dissipated to the energy stored is changing as a function of elongation, or perhaps even of history (thixotropy). Dashpot systems of this type are of fundamental importance when recycling experiments reveal dissipation with perfect elasticity (Nylon rubber).

III. While it would appear on first glance that the slope determined in III enters into the position of the points in the special group, it is nevertheless true that one of the residual points is necessary to fix this slope. The special class depends only on the envelope slope. The slope of III can often be guessed by passing the spring line through the points where the elongation and contraction curves have equal slopes (the "well-defined" slope of IV). This process depends, of course, on the adherence to criterion IV.

IV. In the case of wool, a lowering of slope because of continued working in the region of no relaxation shows that the molecular chains are resting in temporary positions of high energy when it becomes easy to coil and uncoil them. A relaxation of sufficient time restores the original slope. The initial slope is often steeper than subsequent ones. This can be ascribed to a deep-seated thixotropy, or to a non-Hookean behavior.

V. If there is definite evidence for the presence of a distribution, the transcription of a working curve will probably fail, unless the singleness of the determining dashpot is established. Then, over moderate ranges, a working curve for this single element can be established. In a recycling within a short time after being on the envelope, the yield to the envelope will be very sharp, no matter how broad the distribution, because all of the elements are in phase. Under these conditions the securing of a working curve for the determining element is facilitated. However, after a long relaxation, the yield is very gradual because the more non-Newtonian dashpots have held the compression of the associated springs. Here the hypothesis of singleness of determining dashpot is most likely to break down.

To treat the relaxation curve quantitatively, the first portion of it is ascribed to the determining element. From this portion, the constants of the determining element are estimated, and the result compared with those from shape. Then the change in envelope with rate is investigated, and the amount ascribable to the finding element subtracted. The remainder of the relaxation curve is split into enough parts to absorb the residue. This process can be made to yield a number which characterizes the distribution. The number of independently acting dashpots to which the relaxation curve must be attributed to make the non-Newtonian flow ratio, determined from speed change, come out right, is a measure of the extent of the distribution. Then, this distribution must be harmonized with the shape factor by postulating a distribution in activation energy instead of yield value. Because the determining dashpot changes with rate, this briefly indicated process must be a matter of cut and try, with a gradual assimilation of all of the data.

NOTE CONCERNING THE TYPE OF EXPERIMENT TO BE PERFORMED

Except for certain path-finding experiments, the effort should be made to test the criteria in

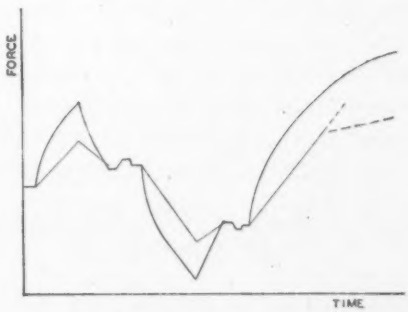

FIG. 19. The determination of the spring line.

the order given. First, a number of elongations to break, at differing rates, should be performed. These serve as general guides to the shape of the curves, and indicate the presence of the various yielding mechanisms. To find the difference in yield force because of rate, the effect of sample variation must be obviated. This is done by changing the rate, while at a point of no relaxation, on a single sample. Then the complete elongations at one rate are used to extrapolate to various elongations not covered by the complex rate experiment. The order in which the rates are applied must be permuted to determine if any strain hardening exists. (See the note to I.) If it does, then this portion of the experimental investigation must be prolonged until the rules governing the hardening can be ascertained and incorporated on a thixotropic scheme.

Then, experiments must be performed to get representative members of the special group at no relaxation points. These can be performed at one rate for each experiment, and keyed to one another by the earlier experiments at differing rates. In these experiments, the first proofs of thixotropy may be discovered, if thixotropy does not depend on backward relaxation, and manifests itself by a passing outside of the envelope. Thixotropy can be neglected until criterion II can be proved or disproved. If this criterion is obeyed, then the treatment is simplified.

Next, the experiments consisting of return cycles and the determination of the residue of relaxation points must be performed. If thixotropy is indicated, these experiments must contain many attempted returns to the envelope to elucidate the thixotropic scheme. In the presence of thixotropy, little more can be accomplished because the thixotropic working curves remain to be calculated although the principles governing the calculation are clear. However, even in the presence of thixotropy, the finding dashpot may not be thixotropic, and thus can be studied more easily if return loops starting at a thixotropic peak are not present. Last, a study of relatively long time relaxation should be undertaken.

NOTE CONCERNING THE REPRODUCIBILITY OF THE EXPERIMENTS

Extremely poor reproducibility enormously complicates single fiber work. A trivial type is lack of scale reproducibility. If two constant-rate-of-elongation experiments differ only by the scale of the force, then a suitable area correction can be applied.

The most significant type of deviation is encountered in the early part of most curves. The first yield value may be abnormally low. This can be ascribed to greater than usual initial tension or lack of over tension ever occurring in the preparation. On the other hand, much more commonly the initial yield force may be very high, showing that at some time in the preparation the sample received an over tension that more or less permanently moved some highly non-Newtonian elements, leaving them in compression in the unstressed state. Because of the long-term relaxation, or probably more precisely creep recovery, the yield in this case is high but gradual. Because of the almost endless possibility of the concealment of progressively less Newtonian elements, it is wise to neglect and adjust for the first cycle in the early experiments. Thus, after the first good approach to the envelope, the curves will reproduce. Later on, long-time creep and relaxation studies will be required to elucidate the first part of the curve.

For this reason in analyzing stress-strain curves the position of the curve as a function of rate is known very accurately, while the position of the true spring line must be estimated by an unsure speculation. The formula for calculating β from two rates and the position of the spring line is thereby limited in accuracy to the precision with which the spring line can be placed. It seems a logical step to replace this formula involving two rates and the spring line by the formula based on three rates alone. If β is the value of this constant referred to the lowest rate, then for rates m and n times as fast, the corresponding values are $m\beta$ and $n\beta$. Thus $f_1=(1/\alpha)\ \text{arc sinh}\beta$, $f_m=(1/\alpha)\ \text{arc sinh}m\beta$, $f_n=(1/\alpha)\ \text{arc sinh}n\beta$.

The measured ratio R_{mn} is defined

$$R_{mn}=\frac{f_n-f_1}{f_m-f_1}$$

$$=\frac{[\text{arc sinh}n\beta-\text{arc sinh}\beta]}{[\text{arc sinh}m\beta-\text{arc sinh}\beta]}.$$

To the approximation that

$$\text{arc sinh}\beta = \ln[\beta + (1+\beta^2)^{\frac{1}{2}}] \approx \ln 2\beta,$$

this equation becomes, for large β

$$R_{mn} = \ln n / \ln m.$$

That is, to a good approximation, this measured ratio remains independent of β and thus this method of calculating β fails. Hence, it is apparent that if only the experimental values of the curve envelopes are being considered, the carrying of the constant β is redundant. The one-constant non-Newtonian element is immediately suggested. Taking the dimensional datum $f_n - f_1$ as the measured quantity, a dimensioned α can be directly computed from:

$$f_n - f_1 = (1/\alpha)(\text{arc sinh}n\beta - \text{arc sinh}\beta).$$

If the spring line is sufficiently far away to make β large, then the approximation for arc sinh can be employed, and

$$f_n - f_1 = 1/\alpha_\infty \ln n$$

or

$$\alpha_\infty = (\ln n)/(f_n - f_1).$$

The symbol α_∞ then denotes a limiting value of dimensional α as β becomes very large. It should not be confusing that α in reduced units reaches no limiting value but goes on increasing. The new α_∞ has been computed directly in the units of force used for $f_n - f_1$. The utility of this reduction in the number of constants is increased when it is applied to the more complex models for viscous elements described under the heading "The Thixotropic Viscous Element."

Any other lack of reproducibility at present is ascribed to essential differences in the samples.

Having eliminated the spring line, it is now possible to apply the formula for α to cases where it is known that the three-element model is inapplicable. Whenever the envelope curves taken at the varying rates are parallel, the quantity $f_n - f_1$ in the equation for α_∞ can be measured. The constant so obtained applies to whatever dashpots are affected by rate. Now if criterion III is obeyed, so that a single dashpot determines the major special group, then it follows that this dashpot is markedly more affected by rate than the others, and therefore the constant α_∞ applies almost exclusively to it. Even when the criterion has not been established, this method of dealing with a group of envelope curves is satisfying and a good approximation.

It is in reality a first viscous datum for any material, because, while the value of the yield force is a function of history and generally increases after a few cycles to meet any stress situation, the constant α_∞ is always applicable to define the effect of changing rate, and therefore impact, on the material.

NOTE ON COMPOUND MODELS

Higher Order Experiments

If in a stress-strain experiment a point of no relaxation is found and then a relaxation curve is taken starting at this point, a definite relaxation, although at a very low rate, is encountered. At a given elongation this second-order relaxation can be either upwards or downwards depending on the force on the fiber. By a judicious interpolation of relaxations the median force where this relaxation is neither up nor down, and constants for this second-order dashpot can be found. The position of the median can be followed as a function of elongation and the second order version of rule II can be used, if some definite mode of finding the median be adopted. If the position of the median is independent of the mode of finding it, at a given elongation, then the second-order analog of the three-lement model has been established. As the rudiments of a third-order investigation, the very slow relaxation of the median itself can be investigated as a function of a second-order length parameter.

Lower Order Experiments

Although certain of the criteria may fail for the stress-strain curve as a whole, in the region of the plane bounded by the envelope a small stress-strain curve that contains no part on the envelope can be investigated. It may be found that among the easily moved elements that come into play in this region, definite yield envelopes can be identified.

The curves inside these sub-envelopes can then be investigated exactly like the gross stress-strain curve, except that experiments must be refined. The same rules have a greater chance of success in this region of less drastic forces. If

various sub-sections, separated by stretches of curve on the gross envelope, yield to the same analysis, up to and including rule V, then with these constants of a simple hunting element sub-curve, a gross curve with a doubly compound hunting element can be defined. In fact, a gross curve that did not yield to rule II could be satisfactorily analyzed if its sub-curves yielded to the rules. The constants so obtained for the sub-curves would show how the make-up of the determining or hunting element of the gross curve varied with elongation.

THE THIXOTROPIC VISCOUS ELEMENT

It is possible to construct a viscous element with a dependence on history of treatment, and with a state that changes in time by postulating a double (or multiple) series of potential energy curves, one of which represents the molecules in a rest state when flow is difficult, and the others repeated promoted states revealed by flow and by thermal agitation. In this development of the simple thixotropic element, the volume of flow displacement, α, will be considered constant.

The equations developed will be for true viscous elements, that is, the external force will be the sole agent causing flow, and when it is removed flow will stop. Several forbidden systems will be discussed to show that this is not always the case. The second condition for a true viscous element, namely, the identity of behavior at any value of the flow measuring coordinate, will be observed in all cases. When several intercommunicating positions of rest (potential wells) at one value of the flow coordinate are available, then the rate of flow of the system is not a simple function of the force on the system alone. The population of the wells becomes a factor.

To take a specific example, if two positions of rest are available, transformations can conceivably be of importance along all of the paths indicated in Fig. 20 where the circles designate positions of rest and the lines, transformations. Transformations along these lines are governed by laws of the type

$$K=(kT/h)(F^2/F_1)e^{-\epsilon/kT},$$

where K is a "rate constant." There will be two of these equations for each connecting path. The total rate of shear is the sum of the rates of reaction in the forward direction minus the sum of the rates in the backward direction. If n is the population of the top state, and $1-n$ the population of the bottom state, then similarly dn/dt equals the sum of the k's going upward minus the sum of the k's going down.

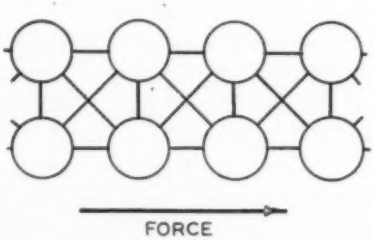

FIG. 20. A schematic representation of a complex flow system. The circles denote positions of rest while the lines represent flow processes.

The equations for the complex two-position model could be written out, but they quite obviously contain too many parameters to be readily used. Two principles hold: First, the assignment of constants must be symmetrical with respect to plus and minus force, or otherwise, when the force is removed from the element and the populations are in any state but the equilibrium one, there will be residual motion associated with the assumption of the equilibrium state. Second, if this symmetrical assignment is made, the force will exert no influence on the populations (the populations will remain at rest equilibrium) unless the potential barriers of the diagonal transformations are unsymmetrical.

In order to simplify the treatment, certain transformations are given sufficiently high activation energies to make them unimportant. This is symbolized in the diagram by the absence of the line representing this transformation. This transformation then is "forbidden" in both directions.

It is contrary to the principle of detailed balancing to forbid a transformation in one direction alone. A satisfactory substitute is found in the completely unsymmetrical barrier. In the normal symmetric barrier if the forward rate is increased by a multiplicative factor $\Phi\equiv e^{\phi}\equiv e^{\alpha f}$, then the backward reaction is retarded by the same factor. In the case of the completely unsymmetrical barrier, the reaction in one direction is affected by Φ^2, while the reaction in the other direction is unaffected. This is diagrammatically expressed

by a line with an arrow head on the end toward which reaction is affected by the force.

The simplest true viscous element will now be formulated (Fig. 21). The undisturbed rate along the horizontal arrow will be denoted by K. Then

$$\begin{aligned} k_{\rightarrow} &= (1-n)K\Phi, \\ k_{\leftarrow} &= (1-n)K\Phi^{-1}, \\ k_{\nearrow} &= (1-n)KD, \\ k_{\nwarrow} &= (1-n)KD, \\ k_{\searrow} &= nKD\Phi^{2}, \\ k_{\swarrow} &= nKD\Phi^{-2}, \end{aligned} \tag{49}$$

when D is a factor for the difference between the diagonal passage rate and the horizontal rate. Then the rate of elongation is

$$dl/dt = K[(1-n)(\Phi-\Phi^{-1})+nD(\Phi^{2}-\Phi^{-2})], \tag{50}$$

and

$$dn/dt = KD[2(1-n)-n(\Phi^{2}+\Phi^{-2})]. \tag{51}$$

In these equations it has been assumed that the two available positions are at equal energies, and thus at equilibrium with no force applied, $n=0.5$.

To calculate working curves, the condition of experiment must be specified. At a constant rate of elongation from (2)

$$\begin{aligned} dl/dt &= \rho-(1/k_1)(df/dt) \\ &= K[(1-n)\sinh\alpha f+nD\sinh 2\alpha f)], \end{aligned} \tag{52}$$

where the factor $\frac{1}{2}$ in the definition of sinh has been adsorbed in K, and

$$dn/dt = KD[(1-n)-n\cosh 2\alpha f]. \tag{53}$$

In reduced units

$$\beta-d\phi/d\tau = (1-n)\sinh\phi+nD\sinh 2\phi. \tag{54}$$

Now, if the constants are known, a point-by-point calculation will give the working curve. To calculate the constants from the experimental working curve is more difficult.

If experiments are available at high rates of shear, when the ultimate population of the upper state $n_\infty \approx 0$, then it is simple to calculate all of the constants but D from the law governing the change of yield force with rate of experiment, utilizing the ultimate force values at two or more rates of experiment. At high rates it can be assumed that when the maximum in force occurs, sufficient reaction has not taken place to alter n appreciably from its initial value if D is small. If this value is the equilibrium value,

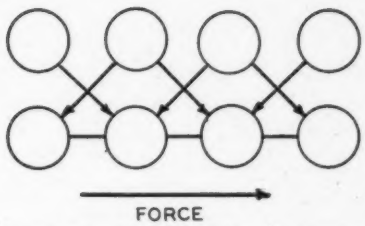

FIG. 21. The simplest true viscous element with two positions of rest.

then at the point of maximum force $n=\frac{1}{2}$. If D is very small, then

$$\beta = \tfrac{1}{2}\sinh\phi_{max}. \tag{55}$$

Now, by hypothesis

$$\beta = \sinh\phi_\infty. \tag{56}$$

Because β is large, by hypothesis

$$\begin{aligned} \phi_{max} &= \ln 4\beta, \\ \phi_\infty &= \ln 2\beta, \end{aligned}$$

and if

$$r = \phi_{max}/\phi_\infty$$

then

$$r = \ln 4\beta/\ln 2\beta = 1+(\ln 2/\ln 2\beta). \tag{57}$$

If the contribution of D is of importance

$$\beta = \tfrac{1}{2}\sinh\phi_{max}+2D\sinh 2\phi_{max}, \tag{58}$$

and replacing hyperbolic sines with exponentials and using

$$\begin{aligned} \phi_{max} &= r\phi_\infty = \ln(2\beta)^{r}, \\ 4\beta &= (2\beta)^{r}+D(2\beta)^{2r}, \end{aligned}$$

or

$$D = 4\beta-(2\beta)^{r}/(2\beta)^{2r}. \tag{59}$$

It is quite apparent that a model wherein the lowest state $n=0.5$ is not adequate except when thixotropy is slight. The largest permissible value of r is 2, and practical values will be much lower because β is usually high.

If it is desired to express the results solely in terms of force difference, analagous to the one constant treatment of non-Newtonian viscosity above, the argument is as follows:

$$\begin{aligned} \beta &= \sinh\phi_\infty, \\ \beta &= \tfrac{1}{2}\sinh\phi_{max}+\tfrac{1}{2}D\sinh 2\phi_{max}. \end{aligned} \tag{60}$$

Replacing the hyperbolic sine with the exponential form

$$\begin{aligned} 2\beta &= e^{\phi_\infty}, \\ 4\beta &= e^{\phi_{max}}+De^{2\phi_{max}}. \end{aligned} \tag{61}$$

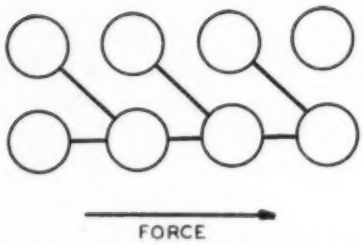

FIG. 22. A viscous system of the forbidden type.

Then

$$\phi_\infty = \ln 2\beta,$$

$$\phi_{\max} = \ln\left[\frac{(1+16D\beta)^{\frac{1}{2}}-1}{2D}\right], \tag{62}$$

$$\Delta f = \frac{1}{\alpha}(\phi_{\max}-\phi_\infty) = \frac{1}{\alpha}\ln\left[\frac{(1+16D\beta)^{\frac{1}{2}}-1}{4D\beta}\right];$$

whence

$$D\beta = [2-e^{\alpha\Delta f}]/[e^{2\alpha\Delta f}]. \tag{63}$$

This depends on rate, and the final expression of the answer takes the form

$$D/K = \rho[2-e^{\alpha\Delta f}]/[e^{2\alpha\Delta f}] \tag{64}$$

when α comes from the change in f_∞ with rate, and ρ is the rate of elongation. This formula applies only when $e^{\alpha\Delta f}<2$ as otherwise the model is invalidated.

This limitation could be removed by placing the upper state at an advantage thermodynamically, but this modification would introduce another constant. A permissible system, having no more constants, which does not have $n_0=0.5$ can be designed by modifying the previous system by making D a difference in well energy rather than an activation energy factor. The activation energy for the diagonal process, from the bottom state, will be the same as that for horizontal flow along the bottom states. The equations expressing this are

$$\begin{aligned} k_{\rightarrow} &= (1-n)K\Phi, \\ k_{\leftarrow} &= (1-n)K\Phi^{-1}, \\ k_{\nearrow} &= (1-n)K, \\ k_{\nwarrow} &= (1-n)K, \\ k_{\searrow} &= nKD\Phi^2, \\ k_{\swarrow} &= nKD\Phi^{-2}, \\ 1-n_0/n_0 &= D, \\ n_0 &= 1/D+1. \end{aligned} \tag{65}$$

The equation for dl/dt remains the same. But repeating the approximation for

$$\begin{aligned} \beta &= (1-n_0)\sinh\phi_{\max}+n_0 D\sinh 2\phi_{\max} \\ &= (D/D+1)(\sinh\phi_{\max}+\sinh 2\phi_{\max}). \end{aligned} \tag{66}$$

Then

$$D = [(2\beta)^{2r-1}+(2\beta)^{r-1}-1]^{-1}.$$

In terms of force differences

$$2\beta = e^{\phi_\infty},$$

$$2\beta = (D/D+1)(e^{2\phi_{\max}}+e^{\phi_{\max}}), \tag{67}$$

whence

$$\phi_\infty = \ln 2\beta,$$

$$\phi_{\max} = \ln\frac{[1+8(D+1/D)]^{\frac{1}{2}}-1}{2}, \tag{68}$$

$$\alpha\Delta f = \tfrac{1}{2}\ln 2/\beta D, \quad (\beta \text{ is very large}),$$

$$D/K = 2\rho e^{2\alpha\Delta f}. \tag{69}$$

A system which is of interest is shown in Fig. 22. It is of the forbidden unsymmetrical type and, for this reason, can function without unsymmetrical potential barriers. The equations governing its motion are

$$\begin{aligned} k_{\rightarrow} &= (1-n)K\Phi, \\ k_{\leftarrow} &= (1-n)K\Phi^{-1}, \\ k_{\searrow} &= nKD\Phi, \\ k_{\nwarrow} &= (1-n)KD\Phi^{-1}, \\ dl/dt &= K[(1-n)(\Phi-\Phi^{-1}) \\ &\qquad +nD\Phi-(1-n)D\Phi^{-1}], \\ dn/dt &= KD[(1-n)\Phi^{-1}-n\Phi]. \end{aligned} \tag{70}$$

At a constant rate of elongation, when $d\phi/dt=0$,

$$\begin{aligned} \beta = (1-n)\sinh\phi_{\max} &+ nD(e^{\phi_{\max}}/2) \\ &-(1-n)D(e^{-\phi_{\max}}/2). \end{aligned} \tag{71}$$

If n has its equilibrium value $\frac{1}{2}$, following a similar procedure gives

$$\beta = \tfrac{1}{2}\sinh\phi_{\max}+\tfrac{1}{2}D\sinh\phi_{\max},$$

or

$$\begin{aligned} 2\beta &= (1+D)\sinh\phi_{\max} = (1+D)\beta^r, \\ D &= (2\beta/\beta^r)-1. \end{aligned} \tag{72}$$

If n has the extreme value, unity,

$$\beta = \frac{De^{\phi_{\max}}}{2} = \frac{D(2\beta)^{r\max}}{2},$$

$$D = (2\beta)^{1-r\max}. \tag{73}$$

For this third "forbidden" case the argument based on force differences is as follows:

$$\begin{aligned} 2\beta &= e^{\phi_\infty}, \\ 2\beta &= \tfrac{1}{2}e^{\phi_{max}} + \tfrac{1}{2}De^{\phi_{max}}, \quad \text{if } n = \tfrac{1}{2}, \\ \phi_\infty &= \ln 2\beta, \\ \phi_{max} &= \ln(4\beta/1+D), \\ -\alpha\Delta f &= \ln(1+D/2), \\ D &= 2e^{-\alpha\Delta f} - 1. \end{aligned}$$

If $n = 1$,

$$\begin{aligned} 2\beta &= De^{\phi_{max}}, \\ \phi_{max} &= \ln 2\beta/D, \\ -\alpha\Delta f &= \ln D, \\ D &= e^{-\alpha\Delta f}. \end{aligned} \tag{74}$$

The simplest of all models is an improper one, containing an unsymmetrical barrier (Fig. 23). The equations governing this model are, assuming all activation energies and energy levels equal,

$$\begin{aligned} k_{\rightarrow} &= (1-n)K\Phi, \\ k_{\leftarrow} &= (1-n)K\Phi^{-1}, \\ k_{\searrow} &= nK, \\ k_{\nwarrow} &= (1-n)K\Phi^{-2}, \\ dl/dt &= K[(1-n)(\Phi-\Phi^{-1}) + n - (1-n)\Phi^{-2}]. \end{aligned} \tag{75}$$

At a constant rate of elongation, when ϕ is maximized

$$\beta = (1-n)\sinh\phi_{max} + n - (1-n)e^{-2\phi_{max}}. \tag{76}$$

Because there is no extra constant, n can be fixed as a function of r

$$n = 1 - 1/(2\beta)^{r-1}. \tag{77}$$

For the last and simplest case, the following argument holds in terms of force differences:

$$\begin{aligned} 2\beta &= (1-n)e^{\phi_{max}} + n, \\ \phi_{max} &= \ln 2\beta/1-n, \\ -\alpha\Delta f &= \ln(1-n), \\ n &= 1 - e^{-\alpha\Delta f}. \end{aligned} \tag{78}$$

These equations will be employed in the analysis of some typical thixotropic curves.

Rules for Analyzing the Working Curves

The examples of special two-position working curves given above make clear the principles governing the calculation of curves of this type, and indicate methods of calculating the constants when the curve is found experimentally.

The complexity introduced with only one new constant, and in one case with no new constants, is apparent. Realizing that these cases were selected for their simplicity rather than for their reality, it becomes apparent that the selection of the particular multiple-position model is a difficult task.

A series of rules is set up for analysis, assuming that the over-all analysis has been carried to such a point that the working curve of the element in question is known at least to an extent of uncertainty no greater than the presence of an unknown additive factor.

I. The working curve must have a constant slope at and near the origin (criterion I).

II. The working curve is investigated at several velocities and the behavior of the ultimate value of the force investigated. If this force is a function of the velocity alone, strain-hardening is absent (criterion II).

Using these ultimate forces, a value of β is computed for the bottom process of flow. Similarly, the behavior of the hump itself is investigated as a function of the treatment after leaving a steady value of ultimate force. The shape should depend only on this recent history (criterion IIA).

III. The difference between the maximum force (at the hump) and the ultimate force is investigated after cycles of elongation and contraction followed by periods of no force. If the largest maximum force always follows the longest period of no force, other conditions being equal, then a symmetrical model is indicated (criterion III).

IV. The maximum value of r is compared with the value $r = \ln 4\beta/\ln 2\beta$. If r is ever greater than this value, it is necessary to employ a model with the difficult-to-flow state thermodynamically favored.

V. If r is not greater than $\ln 4\beta/\ln 2\beta$, the

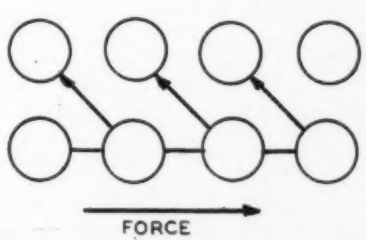

FIG. 23. The simplest (improper) model.

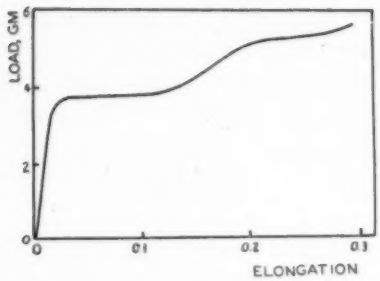

FIG. 24. Elongation *vs.* load to break for the chicken keratin fiber, diameter of 90μ, $\rho = 0.402 \times 10^{-3}$.

single constant can go into an activation energy factor to hinder the diagonal reaction.

These rules have been carried only far enough to provide for a single new constant. They could be expanded to include tests of a quantitative nature to employ more constants. No radically different behavior would be encountered within the framework of two equilibrium positions.

If the first criterion is disobeyed, it becomes necessary to employ a "thixotropic spring" model; if the second criterion is disobeyed, strain hardening is involved. If the third criterion is disobeyed, an unsymmetrical model is implied, and, in any one of the three cases, the simple definition of a viscous element fails.

Experiments with Chicken Keratin

When Dr. Harold P. Lundgren of the Department of Agriculture's Western Regional Research Laboratory visited the Textile Research Institute Laboratories, he left a sample of the fiber prepared from chicken feather keratin in his laboratory. This material shows many interesting properties, including flow thixotropy, constant force springs, and the presence of a complex distribution of relaxation times. The fiber is very sensitive to humidity. When it is wet, it is very soft. At 40 percent relative humidity, it has a stress-strain curve that does not have any thixotropic hump but which shows very clearly the constant force spring. Figure 24 shows an elongation to break. At 50 percent humidity the thixotropic hump appears, and all of the curves of this section except Fig. 24 were made at this humidity. The region of flatness is moved up and is correspondingly longer than the flat region of Fig. 24. At 60 percent relative humidity, the fiber becomes so stiff that it often breaks before the yield point; therefore, long-range experiments become impossible except in the region below the yield point.

Because the fiber was prepared in a small-

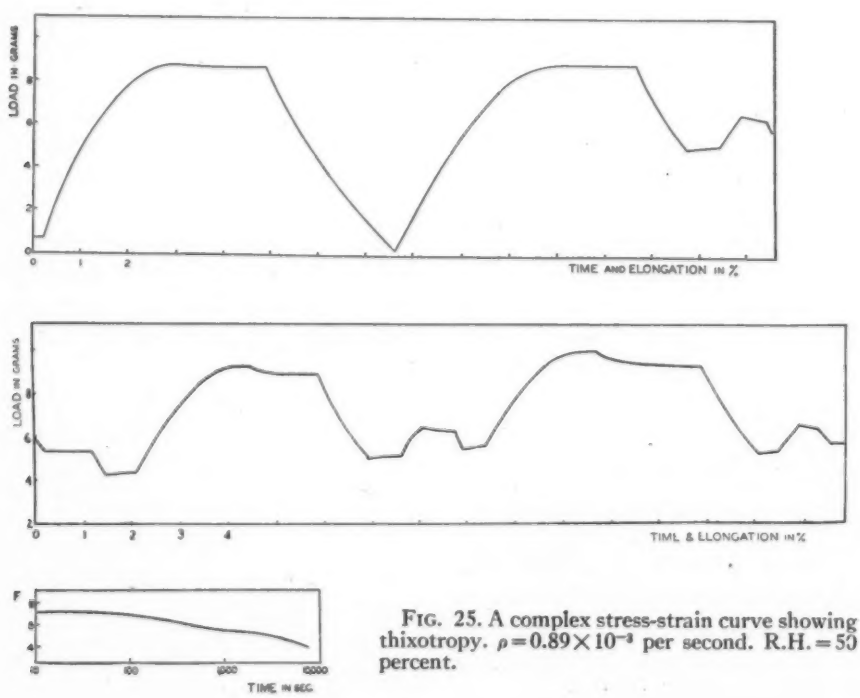

FIG. 25. A complex stress-strain curve showing thixotropy. $\rho = 0.89 \times 10^{-3}$ per second. R.H. = 50 percent.

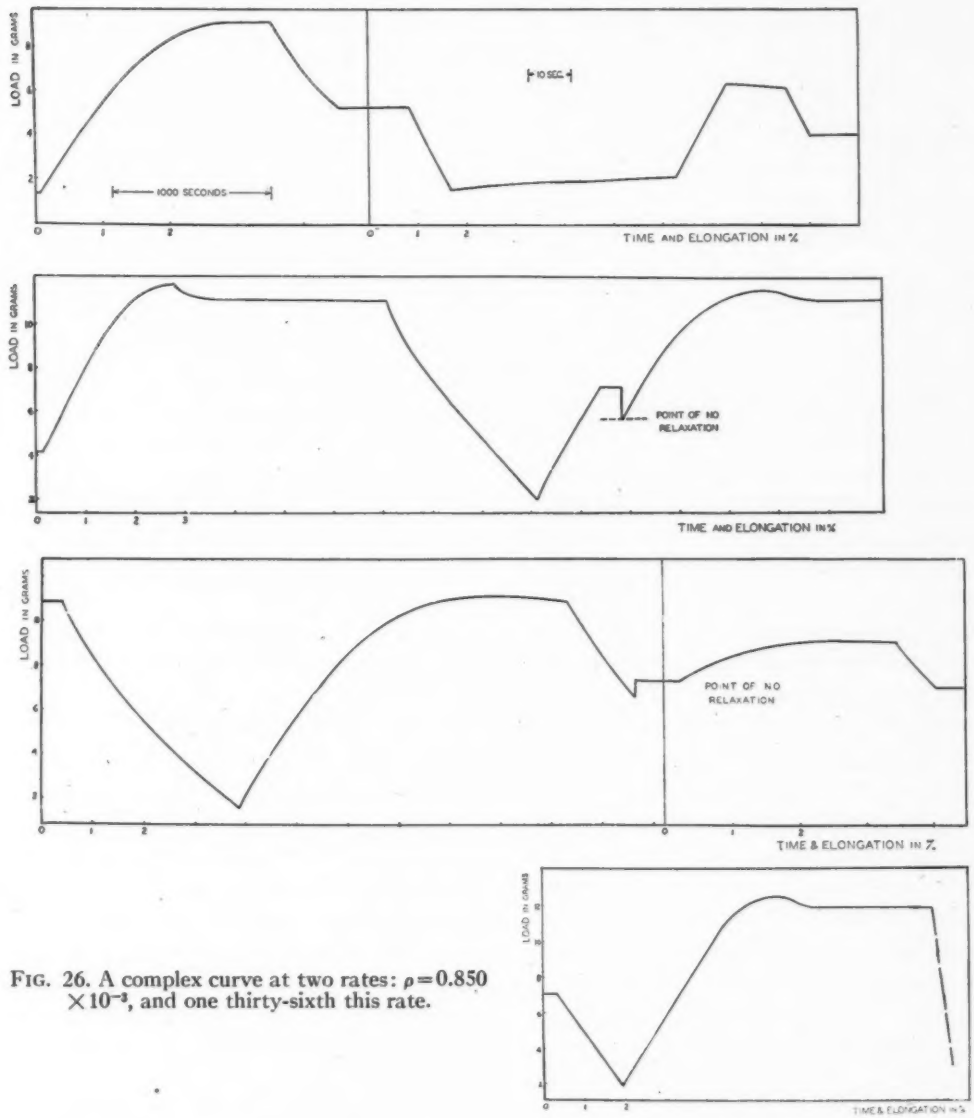

FIG. 26. A complex curve at two rates: $\rho = 0.850 \times 10^{-3}$, and one thirty-sixth this rate.

scale experimental fashion, it was quite irregular in behavior. Therefore an investigation to determine the exact components of its visco-elastic system would have been very trying. For that reason, the method of expressing constants that depends only on differences in force and not on the position of the ultimate spring line will be employed.

Figure 25 shows results of an experiment. The first panel shows that in the beginning of the experiment there was very little hump in the curves. After working some time to determine a point of no relaxation, a pronounced hump of about one gram has developed. A situation of this nature shows that the unsymmetrical "forbidden" type of element must be employed. As will be shown later, the meaning of the unsymmetrical element can be expressed in configura-

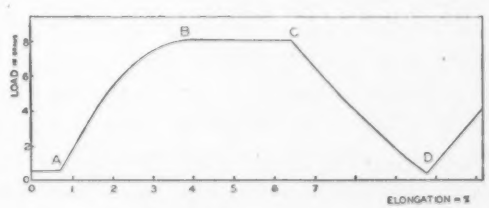

FIG. 27. A portion of the stress-strain curve for chicken feather keratin. The diameter of the fiber is approximately 90μ, and $\rho = 0.835 \times 10^{-3}$ per second, R.H. = 50 percent.

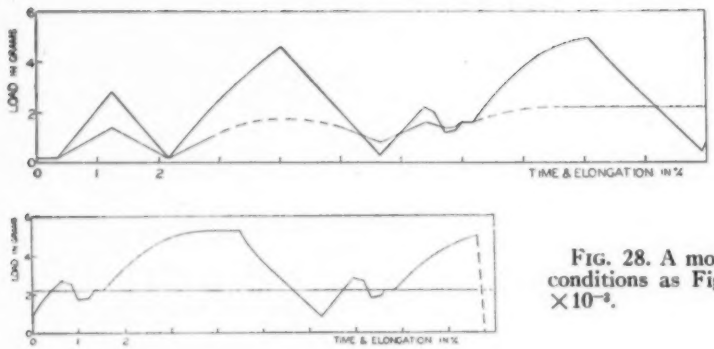

FIG. 28. A more complex curve prepared under similar conditions as Fig. 27 except R.H.=60 percent, $\rho=0.40\times10^{-8}$.

tion space. Hence, there is no uncertainty about the use of such an element.

Now a very long experiment with many differing treatments would be necessary to justify a very complex picture of the flow system in configuration space. Because of the fragility of the fiber, this is very difficult to realize. The two-constant improper thixotropy theory is adequate to explain the curves here which are of a fair degree of complexity. The last panel of Fig. 25, in which the relaxation over a long period of time, starting with a point of no (instantaneous rate of) relaxation, shows clearly that a complex distribution of relaxation times enters into a complete description of the fiber. By using the one-constant method, the analysis of this feature of the curves can be avoided and attention focused on the problem of thixotropy.

The stress-strain curve of Fig. 26 is complex enough to allow a computation of some constants. The change in ultimate force caused by a rate change of a factor of 36 was 2.0 grams. Thus $\alpha_\infty=\ln 36/2.0=1.8$ per gram. ΔF is very close to 1.0 gram when carefully taken from a point of no relaxation. Therefore, $\alpha\Delta F=1.8$, $e^{-\alpha\Delta F}=0.17$. Because this is a rather small quantity, denoting a large thixotropy, the over-simplification of the simplest forbidden case is not appropriate. The other forbidden case discussed in the text had an equilibrium value of n_0 of one-half and is similarly only slightly thixotropic.

A slight modification of this treatment can be made in which, instead of the rate of flow between states differing by a factor D from the forward and backward rates, the inaccessible state is made a factor D lower than the state when forward flow is direct. That is the two states differ by $\Delta F'$, and $D=e^{-\Delta F'/RT}$. Then the equilibrium value

$$n_0=1/D+1,$$

and in terms of the infinite force expressions one finds by arguments similar to those given in the section above

$$D/D+1=2e^{-\alpha\Delta F}. \tag{79}$$

From this experiment, at 300°K, the difference in energy is found to be 1410 calories.

CONSTANT FORCE SPRINGS

The only requirement that a true spring must satisfy is that it should store energy completely reversibly. This in turn means that the energy of a spring must be a monotonic function of the elongation. The force on the spring is the slope of the energy function, and it is expected that the force can rise, go through a maximum, and descend to zero, but never become negative. Although it is easy to construct springs of this sort artificially, there are few illustrations of them in nature.

In the analysis of the stress-strain curves of protein fibers it has been found necessary to employ non-Hookean springs in which, if it does not descend, it reaches a constant value. In Fig. 27 a portion of a stress-strain curve for the chicken feather keratin fiber is shown. At point B the fiber is completely yielded to zero slope. If at point B the direction of elongation had been reversed, then the contraction would have taken place quite reversibly but not to such an extent that the elongation was any less than that at point A. Indeed, as the strain at the reversal was decreased, recovery would asymptotically approach A from the B side. In the actual experiment, the reversal of direction was not made at point B, but the fiber was elongated

at constant force, for several percent of elongation, to point *C*. Because there was no increase in force, one would expect that the entire portion of the curve from *B* to *C* would be completely dissipative and, therefore, all reversal curves from this point onward would be superposable. That this is not the case is manifest in that the elongation *CD* is greater than *BA*. That is, between *B* and *C* energy was being stored at a constant rate of elongation. This shows that a spring system was present that was operative at constant force. In Fig. 28 a more complex curve of the same type is analyzed on the basis of the three-element model incorporating for the spring in parallel a non-Hookean element of the type described. It is quite apparent that the spring cannot operate at constant force throughout its entire range, but that it must start at some Hookean slope. That slope is determined here by connecting the first point of no relaxation with the origin using a line of the proper constant slope. It is to be noted that even if at times the resulting line passes above the ultimate force of the spring, as long as the first point of no relaxation is sensibly below this ultimate, then the determined slope is valid below the ultimate, and must be rounded off when it approaches the ultimate. This is shown in Fig. 28 by the dashed lines. The working curve, which is well defined for the whole experiment, is shown in Fig. 29. However, it is known that this fiber cannot be successfully represented under every condition by the three-element model and

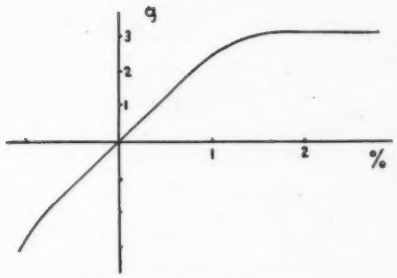

FIG. 29. The working curve for Fig. 28.

obviously all of the points of no relaxation determined belong to the special class.[2] The three-element model is quite satisfactory over this particular range and any constants determined would be average values of some unspecified nature.

The important point, however, is that no combination of non-Newtonian, unsymmetrical and/or thixotropic elements coupled with Hookean springs could reproduce this behavior. A spring operating at *constant force* is definitely demonstrated. These springs obviously could not exist uncoupled in the free state because the elongation at the ultimate force would be undefined. But when they are coupled with viscous elements this difficulty is removed.

ACKNOWLEDGMENTS

I wish to thank Mr. Charles H. Reichardt for valuable suggestions, and Dr. J. H. Dillon for reading the manuscript and clarifying the presentation.

A Magnetron-Resonator System

E. C. Okress
Westinghouse Electric Corporation, Lamp Division, Bloomfield, New Jersey
(Received May 26, 1947)

The present exposition deals with the fundamental multiplet spectrum of a multi-sectorial cavity or vane-type magnetron and specific applications involving the evaluation of the π-mode wave-length thereof. The consequence of mutual coupling between the sectorial cavities through the interaction space of an infinitely long anode is evaluated for the linear case and subsequently applied to the cylindrical case. Although both the qualitative and quantitative results are reasonable in the limit for relatively very long anodes, in practice the latter are relatively short and since the mode separation, order thereof, and hence the component wave-lengths are more or less influenced by the actual relative anode and end cavity lengths at each end of the anode, the results naturally differ from "cold" test data. Predictions of π-mode wave-length have been obtained to about 10 percent, depending upon the degree to which the parameters of the actual vane magnetron approximate the assumptions on which the present treatment is based. With the aid of "cold" test data the preliminary theoretically derived resonator geometry may be appropriately "trimmed" to produce the exact π-mode wave-length desired.

Included in this article is a discussion of the need and function of straps of the resonator system and dimensional scaling, which preserve certain desirable properties of the prototype at the new wave-length, or operating point, in terms of magnetron performance-chart parameters. Finally, in Part III, a brief consideration is allotted to the derivation of the rectangular cavity or slot-type resonator system from the more general relation for the sectorial cavity in this article.

I. INTRODUCTION

THE subject of this paper is based on a Westinghouse radar report[1] concerning an investigation of the symmetrical multi-sectorial-type cavity, commonly referred to as the vane magnetron illustrated essentially by Fig. 3 and practically by Fig. 9.

The analytical evaluation of the wave-length spectrum of the fundamental multiplet for the resonator system of the vane magnetron was initiated some time prior to its invention,[2] with the original object of developing a cheaper, lighter, more readily manufacturable product possessing excellent electrical properties, in contrast to the parallel slot or hole- and slot-type of resonator systems. Eventually these objectives were realized during the war, aided by the cooperative efforts of other laboratories; the vane magnetron was and is being continually introduced to many important uses to which it is especially suited.

Prior to August 1942 no results on the evaluation of the principal wave-length of the vane magnetron were known or available, so that in order to establish some basis for a preliminary design of a 10-centimeter, 8-vane magnetron the aforementioned work[1] was initiated and reported upon.

[1] C. C. Wang and E. C. Okress, "The vane type magnetron," Radar Report B-1, Bloomfield-29, August 1942.
[2] Patent applied for.

M.K.S. units are used throughout this paper unless otherwise noted.

It is appropriate to point out that only the travelling-wave magnetron oscillator is considered in this article. These oscillations are also referred to in the pre-war literature, as the transit time oscillation of higher order and type *B*. The characterization of this oscillator lies in the fact that the electronic interaction and phase relations are incorporated with the tangential and radial components of the rotating electromagnetic field in the interaction space, between the cathode and anode, respectively, in accordance with the Slater, Hartree, and Block theories of oscillation.

II. THE RELATION FOR THE NORMAL MODES OF OSCILLATION

Consider an isolated, infinitely long sectorial cavity, with metallic confining walls, with a longitudinal slot adjoining the cylindrical hole shown in Fig. 1. Note that this cavity represents the generalization of the rectangular case to be commented on later. A mode of oscillation of future utility is chosen such that the associated components of the electromagnetic field in the sectorial cavity satisfy the conditions:

$$E_r = E_z = 0,$$
$$H_r = H_\phi = 0,$$
$$E_\phi = E_\phi(r),$$
$$H_z = H_z(r).$$

Since Maxwell's equations in cylindrical coordinates may be expressed as:

$$\frac{\partial E_z}{r\partial\phi}-\frac{\partial E_\phi}{\partial z}=-i\omega\mu H_r, \qquad \frac{\partial H_z}{r\partial\phi}-\frac{\partial H_\phi}{\partial z}=(\rho+i\omega\epsilon)E_r,$$

$$\frac{\partial E_r}{\partial z}-\frac{\partial E_z}{\partial r}=-i\omega\mu H_\phi, \qquad \frac{\partial H_r}{\partial z}-\frac{\partial H_z}{\partial r}=(\rho+i\omega\epsilon)E_\phi,$$

$$\frac{\partial}{r\partial r}(rE_\phi)-\frac{\partial E_r}{r\partial\phi}=-i\omega\mu H_z,$$

$$\frac{\partial}{r\partial r}(rH_\phi)-\frac{\partial H_r}{r\partial\phi}=(\rho+i\omega\epsilon)E_z,$$

which, for the conditions enumerated, become

$$\frac{\partial}{\partial r}(rE_\phi)=-i\omega\mu rH_z, \tag{1a}$$

$$-\frac{\partial}{\partial r}H_z=i\omega\epsilon E_\phi, \tag{1b}$$

for a perfect dielectric medium in the cavity of Fig. 1. The angular frequency, velocity of light, permeability, and dielectric constant are denoted by ω, c, μ, and ϵ, respectively. By eliminating E_ϕ in Eqs. (1a) and (1b), Bessel's equation is obtained in the form

$$\frac{\partial^2}{\partial r^2}H_z+\frac{1}{r}\frac{\partial H_z}{\partial r}+k^2H_z=0, \tag{2a}$$

where the wave number $k=\omega(\epsilon\mu)^{\frac{1}{2}}=\omega/c$.

By a similar process, eliminating H_z from Eqs. (1a) and (1b), is obtained Bessel's equation in another form

$$\frac{\partial^2 E_\phi}{\partial r^2}+\frac{1}{r}\frac{\partial E_\phi}{\partial r}+\left(k^2-\frac{1}{r^2}\right)E_\phi=0. \tag{2b}$$

In compact form the complete solution of (2a) may be written as:

$$H_z=aJ_0(kr)+bN_0(kr), \tag{3a}$$

wherein $J_0(kr)$ and $N_0(kr)$ denote the usual Bessel functions of zero order, first and second kinds, respectively.

Similarly in compact form the complete solution of (2b) or the result of the substitution of (3a) in (1b) may be written as:

$$\frac{i}{z_0}E_\phi=aJ_1(kr)+bN_1(kr), \tag{3b}$$

wherein $J_1(kr)$ and $N_1(kr)$ denote the usual Bessel functions of the first order, first and second kinds, respectively. z_0 denotes the intrinsic impedance of the confined space, $(\mu/\epsilon)^{\frac{1}{2}}$.

Relations (2a) and (2b) constitute all possible solutions of (1a) and (1b).

Now, applying the boundary conditions at

$$r=r_b, \quad E_\phi=0,$$
$$r=r_a', \quad H_z=0,$$

wherein r_a' denotes the uncoupled sectorial cavity radius, to (3a) gives

$$H_z=aJ_0(kr_a')+bN_0(kr_a')=0, \tag{4a}$$

and to (3b) gives

$$\frac{i}{z_0}E_\phi=aJ_1(kr_b)+bN_1(kr_b)=0. \tag{4b}$$

So that from (4a) and (4b) $T_0(kr_a)$ and $T_1(kr_b)$ are defined and related at $r=r_a'$ by:

$$-\frac{J_0(kr_a')}{N_0(kr_a')}=T_0(kr_a')=\frac{b}{a}=-\frac{J_1(kr_b)}{N_1(kr_b)}=T_1(kr_b),$$

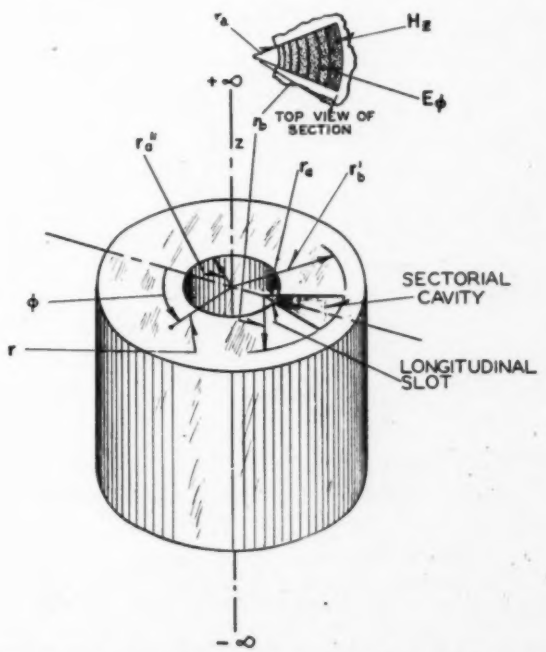

FIG. 1. A section of an infinite length sectorial cavity and adjoining chamber.

or

$$T_1(kr_b) = T_0(kr_a'). \tag{4c}$$

Equations (3a) and (3b) may be rewritten, with $E_\phi = E_{r_a}$ (and $H_z \neq 0$) at $r = r_a$, as

$$z_0 H_z = E_{r_a} \cdot i \cdot \frac{J_0(kr) + T_1(kr_b)N_0(kr)}{J_1(kr_a) + T_1(kr_b)N_1(kr_a)}, \tag{5a}$$

$$E_\phi = E_{r_a} \cdot \frac{J_1(kr) + T_1(kr_b)N_1(kr)}{J_1(kr_a) + T_1(kr_b)N_1(kr_a)}, \tag{5b}$$

where r_a represents the radius of the sectorial cavity coupled to the interaction space such that $(r_a - r_a') = \Delta/k$, where Δ is a small quantity.

Now consider the linear magnetron with an array of sectorial resonators as shown in Fig. 2. The electromagnetic fields in the interaction space (between the cathode and anode along the y axis) must be constructed, and then E_y and H_z matched at the slots. The match or continuity of E_y at the slot is exact, whereas for H_z only an approximate continuity condition will be resorted to, although this is quite satisfactory for narrow slots ($d \ll Y$). In the interaction space a solution of Maxwell's equations,[3] for the electromagnetic field, of the type

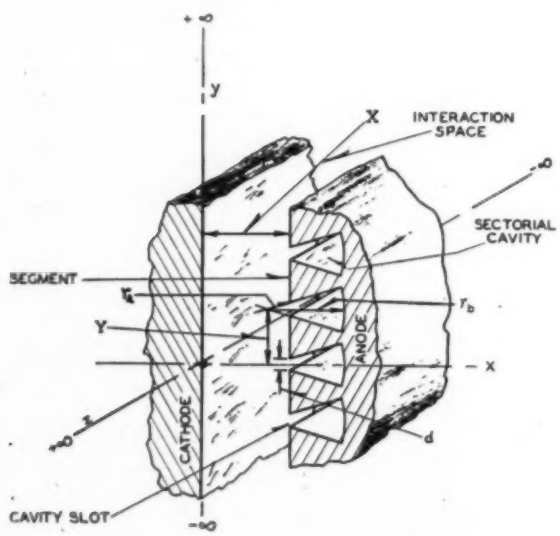

FIG. 2. A section of infinite linear multi-sectorial cavity magnetron.

[3] J. C. Slater, "The theory of the magnetron oscillator," M.I.T. Radiation Laboratory Report D-1-9, Office of Publications Board, Report PB-3777, p. 23, 1941. It may be procurable from the Department of Commerce, Washington 25, D. C. Slater's method, for the multi-rectangular cavity case described in his report, serves as a guide in our subsequent analysis.

$$E_y = \sum_{m=0,\ \pm 1 \cdots} -ik_{xm} \times \frac{c^2}{\omega} B_m \sinh k_{xm} X e^{i(k_{ym}y - \omega t)}, \tag{6a}$$

$$B_z = \sum_{m=0,\ \pm 1 \cdots} B_m \cosh k_{xm} X e^{i(k_{ym}y - \omega t)} \tag{6b}$$

is used. k_x and k_y denote the magnitudes of the imaginary and real components of the complex propagation vectors, k_i and k_r, along the abscissa and ordinate in Fig. 2, respectively. The coefficient $B(=\mu H$ in rationalized M.K.S. units) denotes the magnitude of the real component of the flux density normal to both components of the complex propagation vectors. The relation between k_{ym} and k_{xm} may be expressed as

$$k_{xm}^2 = k_{ym}^2 - k^2.$$

Observe that the electromagnetic wave in the interaction space is damped along k_i and propagated along k_r. The electromagnetic field in the jth slot of the sectorial resonator by (5a) and (5b), in corresponding notation, becomes

$$E_{yj} = -i\frac{kc^2}{\omega} B\{J_1(kr_a) + T_1(kr_b)N_1(kr_a)\}e^{i(k_{y0}jY - \omega t)}, \tag{7a}$$

$$B_{zj} = B\{J_0(kr_a) + T_1(kr_b)N_0(kr_a)\}e^{i(k_{y0}jY - \omega t)}, \tag{7b}$$

wherein the propagation vector k_{y0} is related to k_{ym} by the relation $k_{ym} = k_{y0} + 2\pi m/Y$, in which m is a positive or negative integer.

The boundary conditions imposed are

$$E_y = E_{yj} \left(jY - \frac{d}{2} \right) \leq y \leq \left(jY + \frac{d}{2} \right), \tag{8a}$$

$$E_y = 0, \quad \text{for} \quad (jY - Y/2) \leq y \leq (jY - d/2), \tag{8b}$$

$$\text{for} \quad (jY + Y/2) \geq y \geq (jY + d/2),$$

$$B_z = B_{zj} \quad \text{at} \quad y = jY. \tag{8c}$$

The equality in (8c) is not strictly valid within

$$(jY - d/2) \leq y \leq (jY + d/2).$$

Although the field varies sinusoidally with y, it is small provided $d \ll Y$.

Hence, equating the electric and magnetic components of the electromagnetic fields, (6a, 6b,

7a, 7b) in the interaction space and sectorial cavities at the slots, and applying the associated boundary conditions (8a, 8b, 8c), the solution of (6a, 6b) and (7a, 7b) assumes the form

$$\sum_{m=0,\ \pm 1\cdots} -\frac{d}{Y}\frac{k}{k_{xm}}\left[\frac{J_1(kr_a)+T_1(kr_b)N_1(kr_a)}{J_0(kr_a)+T_1(kr_b)N_0(kr_a)}\right] \times\frac{1}{\tanh k_{xm}X}\frac{\sin\left(k_{y0}+\frac{2\pi m}{Y}\right)\frac{d}{2}}{\left(k_{y0}+\frac{2\pi m}{Y}\right)\frac{d}{2}}=1. \quad (9)$$

Recalling that

$$\Delta=kr_a-kr_a', \quad (10)$$

and introducing the contraction $Z_0(kr_a')$ in (4a),

$$J_0(kr_a')+T_1(kr_b)N_0(kr_a')=Z_0(kr_a')=0. \quad (11)$$

Observing that

$$Z_0'(kr_a)=-[J_1(kr_a)+T_1(kr_b)N_1(kr_a)].$$

Now, applying Taylor's expansion to (11), since Δ/k is sufficiently small, gives

$$Z_0(kr_a')=Z_0(kr_a-\Delta) =Z_0(kr_a)-Z_0'(kr_a)\cdot\Delta+\cdots=0,$$

so that

$$-\frac{J_1(kr_a)+T_1(kr_b)N_1(kr_a)}{J_0(kr_a)+T_1(kr_b)N_0(kr_a)}\simeq\frac{1}{\Delta}.$$

In addition it will be assumed that

$$k_{x0}\simeq k_{y0}=\frac{\pi}{Y}-\delta; \quad k_{x,-1}=\frac{\pi}{Y}+\delta$$

where δ is a small quantity,

$$\frac{\sin\left(k_{y0}+\frac{2\pi m}{Y}\right)\frac{d}{2}}{\left(k_{y0}+\frac{2\pi m}{Y}\right)\frac{d}{2}}\simeq 1,$$

and

$$\tanh k_{xm}X\simeq 1,$$

which implies in sequence that $k^2\ll(\pi/Y)^2$; $(Y/2(r_b-r_a))^2\ll 1$, and d and X are sufficiently small and large, respectively, to justify these assumptions. With these assumptions, using but two terms of (9) in the region of large k_{y0}, Eq. (9) reduces to

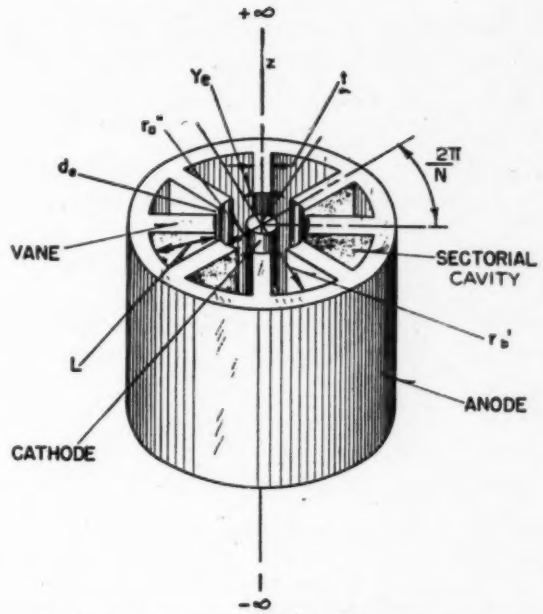

FIG. 3. A section of infinite length multi-sectorial cavity or vane magnetron.

$$\frac{d}{\pi}\frac{k}{\Delta}-[(1-Y\delta/\pi)^{-1}+(1+Y\delta/\pi)^{-1}]=1, \quad (12)$$

which on applying the Binomial theorem, introducing $kL=kr_b-kr_a$, with the definition $(\pi/2)\Lambda(kL')=(kr_b-kr_a')$ where $L'=(r_b-r_a')$ and by virtue of (10), (12) reduces to the closed form for the wave-length

$$\lambda=\frac{1}{\Lambda(kL')}\left[4L+\frac{8d}{\pi}\{1+(\delta Y/\pi)^2\cdots\}\right], \quad (13)$$

which is valid for $k_{y0}(=\pi/Y-\delta)$ between $\pi/2Y$ to π/Y for the linear case.

Now on the premise that only the region near the anode is of material consequence and that the velocity of propagation in the interaction space is unaltered, these results may be applied to the cylindrical magnetron, illustrated by Fig. 3. Incidentally, only discrete modes of oscillation are permitted in contrast to the linear case. Now, note that

$$\delta=\frac{\pi}{Y_e}-k_{y0}, \quad Y_e=\frac{2\pi r_a}{N},$$

where Y_e denotes the arc length between centers of adjacent cavities at r_a''.

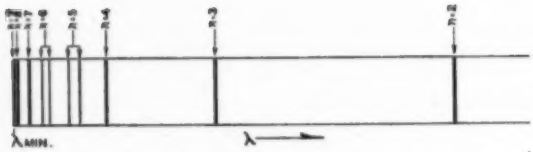

FIG. 4. An example of the fundamental multiplet band structure of modes measured on a Westinghouse 18-vane magnetron ($n_{max}=N/2=9$; $n_{min}=1$).

$k_{y0}r_a=n$
$=1, 2, \cdots N/2$ modes of oscillation for even N
$=1, 2, \cdots (N-1)/2$ modes of oscillation for odd N

and

$$\delta=\frac{\pi}{Y_e}\left(1-\frac{2n}{N}\right)$$

(12) for the cylindrical case, becomes

$$\lambda=\frac{1}{\Lambda(kL')}\left\{4L+\frac{8d_e}{\pi}\left[1+\left(1-\frac{2n}{N}\right)^2+\cdots\right]\right\}. \quad (14)$$

Since the $n=N/2$ or π mode of oscillation is invariably sought, for reasons to be revealed presently, and the remaining modes of the fundamental multiplet receive consideration only from a competitive aspect, (14) may be simplified to read

$$\lambda=\frac{1}{\Lambda(kL')}\left(4L+\frac{8d_e}{\pi}\right), \quad (15)$$

which for the sake of brevity suffices in the subsequent discussions, although one can readily derive the complete spectrum of the fundamental multiplet from (14).

It is now appropriate to comment on the characteristics of the mode spectrum of a multicavity cylindrical magnetron in order to present a pictorial interpretation of the analytical results culminating in (14) for the vane magnetron.

The allowed modes of oscillation of the symmetrical cylindrical multicavity magnetron are grouped on a wave-length scale similar to band spectra. The longest wave-length band is referred to as the fundamental multiplet, its band structure or mode components are defined by Eq. (14) for the vane magnetron. It may be characterized by variations in ϕ of the electromagnetic field in the plane normal to the axis of the magnetron, for which edge effects are neglected. The modes of the band are characterized by phase differences between alternating potentials on the successive segments in the interaction space. Other bands of the spectrum have shorter wave-lengths, and their electromagnetic fields vary longitudinally as well. Each component of the fundamental multiplet has a different wave-length, although the differences are relatively small and depend upon the effective circuit constants of the cavity and the number of them. Figure 4 presents a pictorial

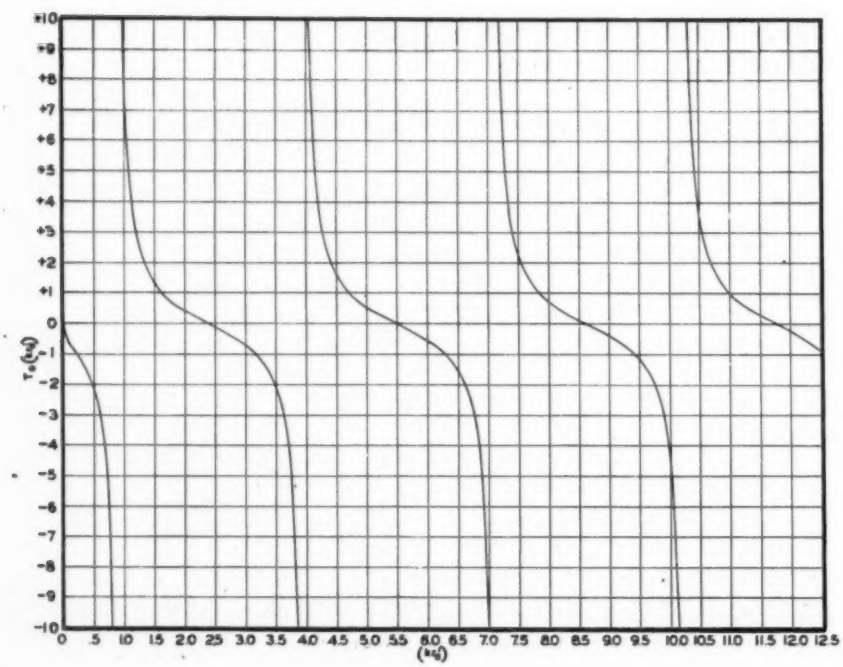

FIG. 5. Graph of the Bessel function, $T_0(kr_a')$, *versus* its argument (kr_a'). Values of $T_0(kr_a')$ for arguments less than 0.20 were evaluated from

$$T_0(kr_a')=-\frac{1}{\frac{2}{\pi}\ln\left[\frac{2}{\delta(kr_a')}\right]},$$

where $\delta=e^{\gamma}=1.781$, and γ is Euler's constant.

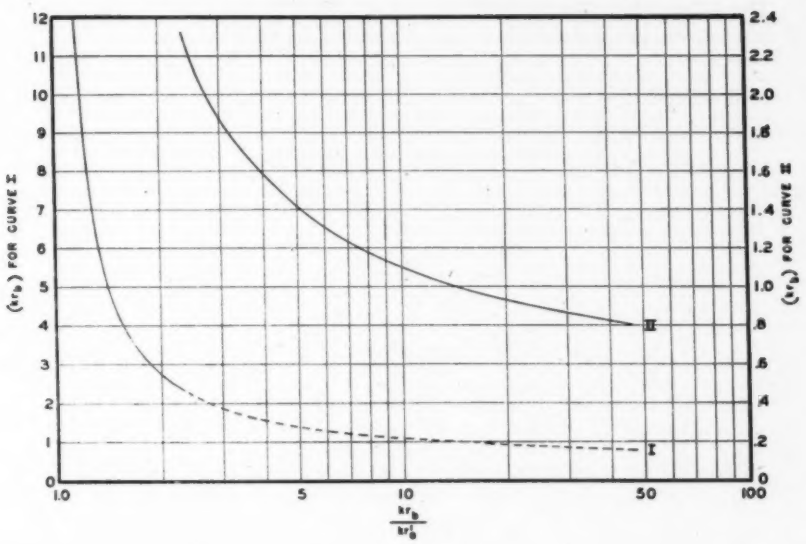

FIG. 6. Solution of Eq. (4c), $T_0(kr_a') = T_1(kr_b)$. Curve II is a single dimensional magnification of the dashed portion of Curve I.

representation of the band structure or mode components of the fundamental multiplet from "cold" measurements for an unstrapped Westinghouse 18-vane magnetron. Modes 5 and 6 have been split into doublets by inherent unsymmetries. The relative intensities of the components in the fundamental multiplet are governed by the respective coupling between the resonators and the electronic system *via* the interaction space.

All except one of the modes in the fundamental multiplet for which the number of component resonators, N, of the magnetron is even, are doubly degenerate when the resonant system is completely symmetrical, whereas all the modes in the fundamental band, for which N is odd, are doubly degenerate under the same conditions. The term doubly degenerate refers to the number of linearly independent modes, with the degenerate frequency, which in turn is defined as having more than one mode of oscillation though only one frequency. [It may be recalled however, that there are at least two exceptions for which certain unsymmetries do not result in removal of the degeneracy]. Such a split mode is known as a doublet and is characterized by two identical opposite traveling waves around the anode in the interaction space. For a symmetric magnetron with an even number of resonators there are, in the fundamental multiplet, $N-1$ modes with $n=1, 2, \cdots N/2$ separate wave-lengths, whereas for an odd N there are $N-1$ modes though only $n=1, 2\cdots(N-1)/2$ separate wave-lengths. The non-degenerate mode is referred to as the $n=N/2$ or π mode. Besides this non-degenerate mode there is an abnormal one, which is associated with the interaction space exclusively and is negligibly influenced by the multi-cavity geometry in a symmetrical multi-cavity system. This abnormal mode is referred to as the $n=0$ or zero mode and is usually well separated on a wave-length scale from the normal components of the fundamental multiplet. For these and other reasons its influence is negligible for symmetrical multi-cavity magnetrons. The electromagnetic field in the interaction space associated with these two modes is of the stationary type, though the zero-mode field is independent of the angular coordinate, whereas the π mode field is periodic in this respect. The lower order modes of the fundamental multiplet of the infinite length symmetrical multi-cavity magnetron are ideally found at longer wave-lengths. The π mode of the fundamental multiplet is characterized by non-degenerate property and highest conversion efficiency and for these reasons is invariably sought in practice.

In deriving Eq. (14) approximations which are explicitly or implicitly referred to were used. Hence, the present results must not be accepted unconditionally, though quantitatively they are not seriously in error.

Sometime after the completion of this work further efforts by others (in their unpublished

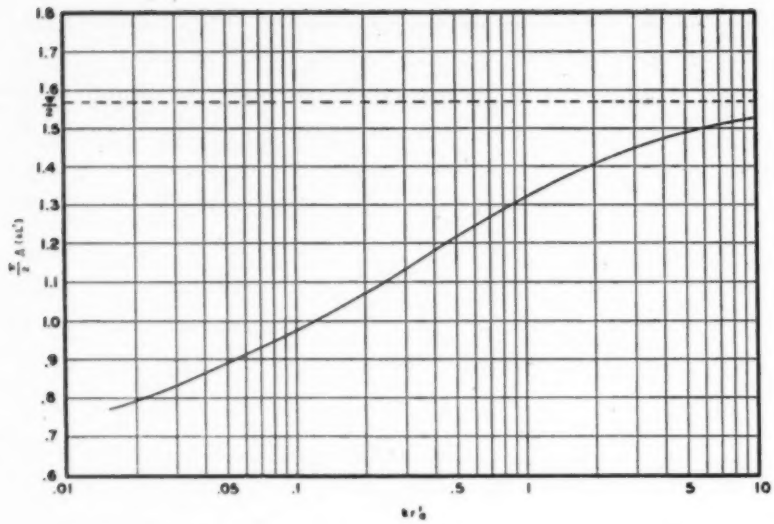

FIG. 7. A graph for the evaluation of the geometry of the sectorial cavity in terms of a given wave-length. It is derived from Fig. 5.

works),[4] concerning the infinite cylindrical case of the vane magnetron were able to be directed by the utilization of a method developed and applied by Clogston to the slot, and hole- and slot-type magnetrons in his unpublished thesis.[5] However, the influence of actual lengths of the end cavities and anode, which influence the order of the modes, their mutual separation, and consequently the wave-length of the π mode are not explicitly included. Hence, predictions made in accordance with them, though more accurate in the ideal case than the results of the present method, are also inaccurate when applied to actual magnetrons by about the same percentage in some cases. Generally, however, they[4] are more accurate.

III. APPLICATIONS

In order to utilize (13) it is necessary to first evaluate (4c). Figures 5 and 6 portray the results of this evaluation. Figure 7 is derivable from the results of Fig. 6. Incidentally, examination of Fig. 7 in conjunction with trigonometric expansions[6] for the components of Bessel functions (4) reveals that the transformation from the sectorial to the rectangular cavity, as r_a and r_b approach infinity together, provides that

$$kr_b - kr_a \rightarrow \pi/2$$

as the limit. So that

$$r_b - r_a \rightarrow \lambda/4,$$

which is the condition for the rectangular cavity.

Note that the solution of kr_a' nearest to kr_b is chosen by virtue of the mode considered in the sectorial cavity $\delta=0$ in (13) for $n=N/2=\pi$ mode.

In order to evaluate the radial vane length, L, or major cavity radius, r_b', when the anode radius, r_a'', free space wave-length of a desired mode of oscillation, λ_π, vane thickness, t, and number of resonators, N, are known, the following procedure is convenient. Refer to Fig. 3 for identification of symbols.

Given data:

wave-length, $\lambda_\pi=9.46$ cm

$$\left(k=0.664\frac{1}{\text{cm}},\right)$$

number of sectorial cavities, $N=18$,
vane thickness, $t=0.263$ cm,
anode diameter, $2r_a''=3.46$ cm,
effective anode length $=3.36$ cm,
cathode diameter, $2r_c=1.100$ cm,
cathode to anode ratio, $r_c/r_a''=0.318$.

Determine L or r_b' by the following procedure:

the coupled cavity radius,

$$r_a=r_a''-\frac{t}{2\sin\pi/N}=0.972 \text{ cm},$$

[4] W. Altar, Westinghouse Research Report SR-133, September 15, 1942, and later by H. Goldstein, M.I.T., Ph.D. thesis of 1943.
[5] A. M. Clogston, M.I.T., Ph.D. thesis of 1941.
[6] Jahnka-Emde, *Tables of Functions* (B. G. Teubner, Leipzig and Berlin, 1938), p. 138.

equivalent slot width,

$$d_e=\frac{\pi 2r_a''}{N}-t=0.441 \text{ cm},$$

from relation (12), for the π mode $\delta=0$, so

$$\Delta=\frac{2d_e k}{\pi}=0.1867,$$

from Fig. 7, for $kr_a'=kr_a-\Delta=0.459$;
$(\pi/2)\Delta(kL')=(kr_b-kr_a')=1.20$,
hence $kL=(kr_b-kr_a')-\Delta\simeq 1.013$ cm,
so that $L=1.525$ cm
and $2r_b'=6.51$ cm,
which differs by about 6 percent from its experimental value on a magnetron (Westinghouse VA-1) possessing these dimensions.

In order to evaluate the wave-length for the π mode of oscillation when the anode radius, major cavity radius, vane thickness, and number of resonators are known, it is merely necessary to evaluate the ratio (kr_b/kr_a') and kr_b with the aid of Fig. 6, as illustrated by the following results for the previous Westinghouse magnetron. Refer to Fig. 3 for identification of symbols.

Given data:

number of sectorial cavities, $N=18$,
vane thickness, $t=0.263$ cm,
anode diameter, $2r_a''=3.46$ cm,
effective shell diameter, $2r_b'=6.90$ cm,
effective anode length $=3.36$ cm,
cathode diameter, $2r_c=1.100$ cm,
cathode to anode ratio, $r_c/r_a''=0.318$.

Determine π mode wave-length, λ_π, by the following procedure:

$$d_e\simeq\frac{\pi 2r_a''}{N}-t=0.341 \text{ cm}$$

$$r_b=r_b'-\frac{t}{2\sin\pi/N}=2.693 \text{ cm}$$

$$r_a=r_a''-t/2\sin\pi/N=0.973 \text{ cm}$$

$r_a'=r_a-2d_e/\pi$, {from (10) and (12) $\delta=0$ for $n=\pi$ mode}, $=0.756$ cm

$r_b/r_a'=3.54$

(kr_b) from Fig. 6 $=1.70$

$\lambda_\pi=2\pi r_b/(kr_b)=9.95$ cm

percent difference $\simeq 5$ percent from operating wave-length of 9.46 cm for $n=9$ or π mode. (Westinghouse VA-1.)

Because of assumptions, such as infinite anode length, linear approximation, etc., inherent in the present method it is not surprising to be confronted with differences of the order of 10 percent more or less between the experimental and theoretical values of π mode wave-length. For instance, the length of the anode and end cavity

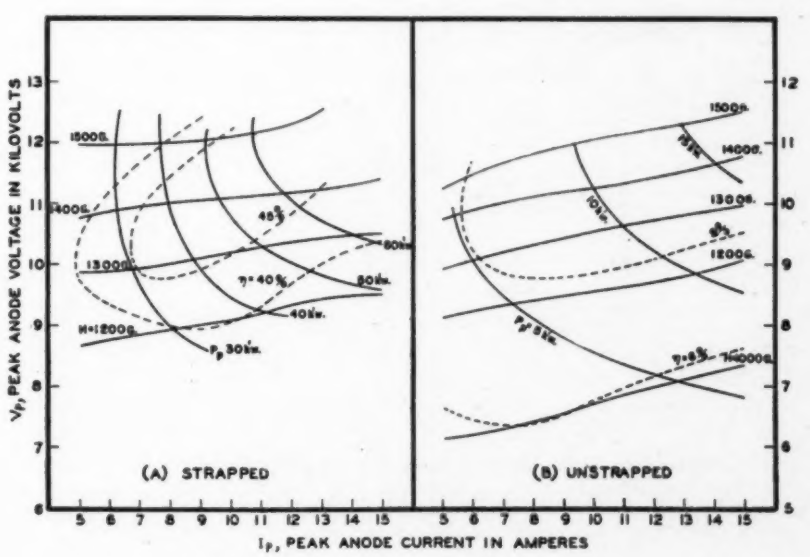

FIG. 8. Performance charts of Westinghouse 8-vane magnetrons, WX-3256, illustrated in Fig. 9. The magnetrons are terminated by a 50-ohm matched coaxial line. The operating unstrapped and strapped wavelengths are 8.0 and 9.6 cm, respectively.

in terms of free space wave-length will have more or less of an influence on the order and separation of the modes in the multiplet and obviously on the wave-length of the π mode.[7] The method, nevertheless, provides reasonable approximate data for a preliminary design, which can then be corrected accordingly by "cold" test.

After examining "cold" test data of a number of similar 8-vane unstrapped 10-centimeter magnetrons constructed with the aid of the preceeding theory, it was discovered that for end cavity and effective anode lengths of the order of $\lambda/10$ and $\lambda/4$ of free space wave-length, respectively, that the perimeter of the sectorial cavity normal to the axis of the magnetron, was nearly equal to half the free space π-mode wave-length. Since the end cavity and anode lengths have a more or less influence on the order, mode separation, and wave-lengths of the modes of the fundamental multiplet in a practical magnetron, this perimeter index is useful only as a guide in deriving the magnitude of the π-mode wave-length for a vane magnetron.

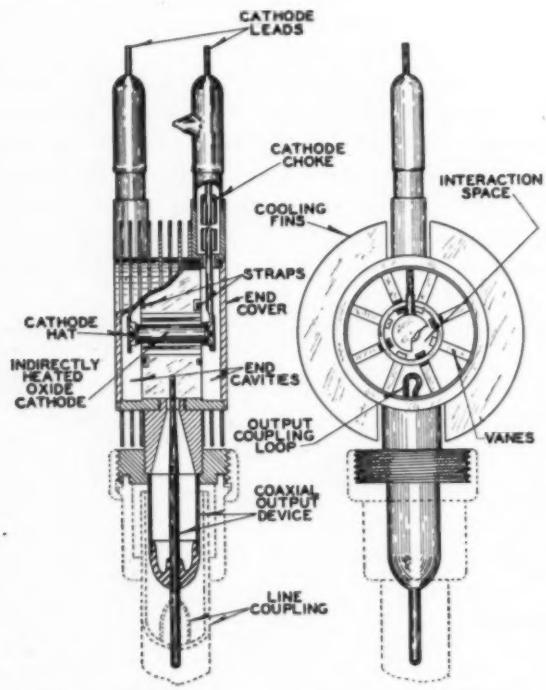

FIG. 9. Westinghouse vane magnetron, WX-3256.

[7] J. C. Slater, M.I.T. Radiation Laboratory Report No. 182, "Resonant modes of the magnetron." It may be procurable from the Office of Publications Board, previously referred to.

IV. APPLICATION OF STRAPPING TO THE RESONATOR SYSTEM

Because of the inherent assumptions in the theoretical methods for the determination of mode-frequency spectrum of a multi-cavity magnetron, varying degrees of error result in application so that one often uses the theoretically derived values only as a guide in obtaining a magnetron-resonator system possessing mode-frequency spectrum in the desired wave-length range, for subsequent "cold" tests. From such tests are derived the actual mode spectrum; and if undesirable for one reason or other the resonator system is modified in order to achieve the desired mode separation (about 5 percent or more) and distortion of competing modes, for efficient operation. When the modes are too close together, ($\ll$5 percent say) as is the case with symmetrical multi-cavity magnetrons (for $N \gg 2$) without straps, the competing modes cause the efficiency of the desired mode to be low, as illustrated by Fig. 8. In order to achieve the requisite mode separation between the desired mode (usually the π mode since it is non-degenerate and associated with the highest theoretical conversion efficiency) and competing ones in the fundamental spectrum of a symmetrical magnetron, in contrast to the "rising sun" type, strapping is resorted to. Strapping is a mechanical means of joining segments of like phase, usually at one or both ends of an anode, adjacent to the interaction space, in such manner as to increase the normal coupling between resonators and hence the effective capacity of the resonator system. Strapping usually distorts the competing mode patterns so that their interaction with the space-charge field at the slot is poor. The π mode is not significantly distorted by proper strapping, so that efficient electronic interaction ensues for this mode. The coupling between cavities for a particular mode may be selective with straps and thereby further increase mode separation.

Essentially two types of strapping are utilized. The symmetrical type of strapping, such as the "echelon,"[7] separates the components of the fundamental multiplet but actually does not split the degenerate modes, whereas the unsymmetrical type of strapping, such as the "Y–B,"[7] which adequately distorts the competing modes, only slightly influences the π-mode pattern. The type

TABLE I. Magnetron scaling.

Ratio of initial to final parameter	General scaling $Q_L'/Q_{L-1}\, r_c'/r_c = \left(\frac{\sigma}{\sigma'}\right)\left(\frac{r_a'}{r_a}\right)$; $\sigma_{opt} = \frac{1+4/N}{1-4/N}$ (see reference 3 and Section VI)	Restricted scaling $\frac{N'}{N}=1; \frac{Q_L'}{Q_L}=1, \frac{n'}{n}=1; \frac{\sigma'}{\sigma}=1$
$\frac{H'}{H}$	$\frac{\lambda}{\lambda'}$	$\frac{\lambda}{\lambda'}$
$\frac{V'}{V}$	$(r_a'/r_a)^2(N/N')(\lambda/\lambda')^2\left[\frac{1-\frac{1}{\sigma'}}{1-\frac{1}{\sigma}}\right]$	$(r'/r)^2(\lambda/\lambda')^2$
$\frac{I'}{I}$	$(L'/L)(r_a'/r_a)^2(N/N')(\lambda/\lambda')^3$	$(L'/L)(r'/r)^2(\lambda/\lambda')^3$
$\frac{J_e'}{J_e}$	$(r_a'/r_a)(N/N')(\lambda/\lambda')^3(\sigma'/\sigma)$	$(r'/r)(\lambda/\lambda')^3$
$\frac{P'}{P}$	$(L'/L)(\lambda/\lambda')^5(r_a'/r_a)^4(N/N')^2\left[\frac{1-\frac{1}{\sigma'}}{1-\frac{1}{\sigma}}\right]$	$(L'/L)(r'/r)^4(\lambda/\lambda')^5$

of assymmetry and degree of coupling or "tightness" of strapping will govern the mode separation and number of degenerate modes which are split by unsymmetrical strapping.

The use of unsymmetrical straps provides one of several necessary conditions for efficient operation in the π mode. Figure 8(a) illustrates a typical improvement in performance over that of Fig. 8(b) for the same 10-centimeter, 8-vane magnetron after straps and strap-breaks are incorporated, as illustrated by Fig. 9. "Single recess ring" straps at both ends of the anode are illustrated. The cathode "hat" illustrated, serves to establish an axial component of electric field in order to reduce the number of electrons which would otherwise leave the interaction space and bombard the end covers.

The ratio between the unstrapped, $\lambda_{\pi U}$, and strapped, $\lambda_{\pi S}$, wave-lengths may be expressed

$$\left(\frac{\lambda_{\pi U}}{\lambda_{\pi S}}\right)^2 = \frac{1}{1+\frac{C_S}{C_T}},$$

in terms of C_S and C_T, which denote the total lumped effective values of strap to vane- and resonator-system capacities, including mutuals. The resonator-system capacity is a product of the number of resonators and the effective lumped capacity of each cavity, less straps. The strap capacity will obviously vary with the number and type of straps used and the geometry at the strap-vane intersection. Both C_T and C_S may be derived either by simple electrostatic approximations, by means of models in the electrolytic tank, or by the more elaborate conformal transformations. Practical results are available.[8]

To increase further effectiveness of straps, strap-breaks over the segments are incorporated at judicious places with respect to the load coupling in order to distort the unwanted mode by proper phasing and reduce the tendencies to mode shifts during load variations. With proper type of strapping and number and orientation of strap-breaks, relatively stable competing-mode free operation may be realized.

Since the ratio of equivalent effective capacity to inductance of the cavity (which is a product of the reciprocal of the number of cavities and the effective inductance of one of them) of a magnetron-resonator system is altered by strapping, the frequency pulling characteristics are also

[8] E. Everhart, M.I.T. Radiation Laboratory Report 223, "Magnetron strapping, wave-length calculations for strapped magnetrons." Office of Publications Board Report, PB-2850, 1943. W. V. Smith, M.I.T. Radiation Laboratory Report 226, Office of Publications Board Report, PB-8327, 1943, "Practical considerations of magnetron design." These reports may be procurable from the Office of Publications Board previously referred to.

TABLE II. Restricted scaling in wave-length and voltage.

Ratio of initial to final parameter	Wave-length scaling (shape, invariant) $\lambda'/\lambda = r'/r;\ L'/L = \lambda'/\lambda$	Voltage scaling (wave-length invariant) $\lambda'/\lambda = 1;\ L'/L = 1$
H'/H	λ/λ'	1
V'/V	1	$(r'/r)^2$
I'/I	1	$(r'/r)^2$
J'/J	$(\lambda/\lambda')^2$	r'/r
P'/P	1	$(r'/r)^4$

altered. Of course, altering the anode length and end cavity length of a symmetrical magnetron with or without straps will influence the mode separation, mode wave-length, and order or distribution between components of the fundamental multiplet. For instance, by altering the anode length of an unstrapped anode, of given end cavity geometry, the order between the components may be completely reversed and consequently wave-lengths changed.

V. APPLICATION OF DIMENSIONAL SCALING[9]

After incorporation into the magnetron of all the necessary features known to be desirable and after obtaining performance characteristics, a suitable prototype may be obtained which may be dimensionally scaled to other wave-lengths, voltages, powers, etc., while the original efficiency is retained during the transformation. Scaling of vane magnetrons requires that the geometry of the straps, its vane recess, and position on the vane be scaled so as to maintain the strap in the original relative position on the vane. Scaling of a prototype is a very profitable design procedure since it avoids the expensive and time consuming development which would otherwise be required. Since these scaling relations are very useful and appropriate to the present subject, they will be briefly considered herein, though without derivation. Approximate scaling relations have been derived,[10] on the basis of Newton's and Maxwell's differential equations applied to the electrons in the interaction space of the magnetron, and provide conditions for which two magnetrons, differing by some scaling factor, possesses the same efficiency or equivalent operation. These conditions of anode voltage, V, and magnetic field, H, for constant ratio of anode to cathode radii, σ, mode of oscillation, n, or number of cavities, N, and loaded, Q, Q_L, may be expressed as the invariant magnetron scaling relations,

$$H\lambda;\ V\cdot\left(\frac{\lambda}{r_a}\right)^2;\ \frac{I\lambda^3}{r_a{}^2L},$$

in which V and H are frequently expressed in kilovolts and Gauss, respectively; anode current, I, is expressed in amperes, anode length, L, anode radius, r_a, and wave-length, λ, in centimeters. This restricted type of scaling is illustrated in terms of the performance chart parameters, for constant σ, n, N, and Q_L, in Table I. Note that the scaling is valid for either input or output values of anode voltage, V, and power, P. The current density, J, is applicable at either the cathode or anode.

Table I also illustrates the general scaling relations, in which the restraints on the restricted type of scaling have been removed. Note that for the general scaling the current density is applicable only at the cathode. Another relation can be derived for the anode. Very often it is desirable to wave-length, voltage, or power scale a desired operating point of a magnetron under the conditions of the restricted case. For this purpose, the corresponding restraints on the shape and wave-length of the magnetron are inserted into the expressions for the restricted (N fixed) case. The result of which is illustrated by Table II. For both the restricted and general types of scaling, end effects are neglected such that the anode current, I, per unit length is independent of length.

With the aid of the scaling relations illustrated by Tables I and II it is possible to scale a selected operating point on the performance chart of a magnetron, as the prototype, to another point in terms of the operational parameters. This process may or may not involve a change of the number of cavities,[11] depending upon whether the general or restricted forms of scaling are applied. Though very often it is only necessary to apply the

[9] J. A. Stratton, *Electromagnetic Theory* (McGraw-Hill Book Company, Inc., New York, 1941), Section 9, p. 488.

[10] A. M. Clogston, M.I.T. Radiation Laboratory Report 52. This was later extended by H. C. Hu in Radiation Laboratory Report 1043-3. These reports may be procurable from the Office of Publications Board, previously referred to.

[11] When a large change in the number of cavities, N, is contemplated, in general scaling, the error may be significant, so that one ought to consult reference 10 by H. C. Hu for details.

restricted type of scaling in the forms illustrated by Table II.

The application of the scaling processes illustrated by Table I is readily acquired. For example, consider the often used restricted scaling process in the form illustrated by Table II, which is to be applied to a prototype in order to permit operation at another wave-length and power output. The first step is to make a wave-length scale by altering the effective magnetron's dimensions linearly, in proportion to the new to the old wave-length, in accordance with column two of Table II Then voltage scale by evaluating the anode radius of the interaction space from a knowledge of the desired power by the appropriate relations given under the restricted voltage scaling column. Obviously, one must use the physical and operational parameters derived from wave-length scaling for voltage scaling. This two-step scaling process is convenient, since it affords an inspection of the change in parameters from the prototype to the fully scaled magnetron. Sometimes both power and wave-length must be increased so much above that of the prototype that the consequence of increased physical size may be undesirable; then the prototype may be only wave-length scaled to the desired region according to Table II. After this the desired power may or may not be achieved with undesirable characteristics by mere extrapolation of the applied fields above the chosen operating point of the prototype. In scaling or extrapolation involving a change of the cathode-current density one should, for economic and stability considerations, maintain this as near its stable value as possible. The extent to which simple extrapolation of this sort is practical is usually unknown in advance of tests, because of various implicit properties of the magnetron. Obviously, the performance characteristics of such a "new" magnetron, if operable, are no longer those of the prototype since the above invariance conditions are not satisfied by such an extrapolation.

VI. RELATED TOPICS AND PRACTICAL CONSIDERATIONS

The distribution of the electric component of the electromagnetic field in the sectorial cavity may be plotted from (5b) as a function of $(r-r_a)/(r-r_b)$, with r_b/r_a as a parameter.

Using (5a) and 5(b), together with the boundary conditions (4a) and (4b), enables the evaluation of the total stored energy per unit length and hence the Q.

Practically, for symmetrical magnetrons having $N=6$ to 16 inclusive, the reduced cathode radius, $1/\sigma$, varies from 0 to 17 percent greater than Slater's[3] theoretical optimum value, $(=(1-4/N)/(1+4/N))$, and for $N=18$ this reduced cathode radius amounts to about 5 percent less than this theoretical optimum value. However, the reduced cathode radius may radically deviate from its theoretical optimum value when considerations related to oscillation build-up time and maximum π-mode (applied) voltage or current in pulsed and C.W. magnetrons are of paramount importance. For example, the 5J26 magnetron possesses a reduced cathode radius amounting to 64 percent greater than the theoretical optimum value, and this at 48 percent over-all efficiency, which incidentally is a product of 58 percent electronic and 82 percent circuit efficiencies.

In voltage scaling symmetrical, strapped magnetrons one must consider the alteration in mode separation, $(\lambda_{n_\pi}-\lambda_{n_\pi\pm1})$, by virtue of the alteration in strap lengths. Since there exists an optimum mode separation (except possibly for rising sun structures with large N) for the attainment of the maximum π-mode input voltage (or current), aside from any further curtailment under pulsed conditions by virtue of inadequate oscillation build-up time, one should determine whether or not the resultant mode separation will seriously curtail the desired π-mode input voltage or current, under either C.W. or pulsed conditions, after voltage scaling.

Gyroscopic Effects in a Vibratory System*

G. S. BENNETT**
Naval Research Laboratory, Washington, D. C.
(Received June 18, 1947)

An analytical investigation is made to determine the influence on a vibrating elastic system of a high speed rotating element. A fundamental condition for the presence of any gyroscopic effect is that the vibration be such as to produce a tilt of the spin vector of the rotor. Equations are derived showing (a) that if precession be prevented, no gyroscopic effects are present, and (b), that if precession be permitted, the gyroscopic action contributes a force opposed to the tilt, and proportional to the angle of tilt, in effect increasing the stiffness of the elastic system. Calculations based on an arbitrarily chosen rotor intended to approximate a typical small motor armature indicate that this additive spring force is small, and that the increase in natural frequency caused by the added stiffness is exceedingly small—on the order of 0.1 percent—in the case where the precessional motion is not restrained.

IN many cases, especially aboard aircraft, equipments subjected to vibration have as component parts dynamotors or other rotating elements. It is the purpose of this investigation to determine whether gyroscopic effects caused by rotating elements exert any marked influence on the vibration characteristics of the equipment.

The fundamental condition necessary for gyroscopic action to appear is that a torque be applied tending to change the direction of the axis of rotation of a spinning body. A pure translation will produce no such effects. Assuming such a torque, and using Euler's angles (see Fig. 1) as coordinates for a rigid body in space, we can write Euler's equations for the applied torques about the three principal axes as[1]

$$M_1 = A\dot{\omega}_1 - (B-C)\omega_2\omega_3, \tag{1a}$$

$$M_2 = B\dot{\omega}_2 - (C-A)\omega_3\omega_1, \tag{1b}$$

$$M_3 = C\dot{\omega}_3 - (A-B)\omega_1\omega_2, \tag{1c}$$

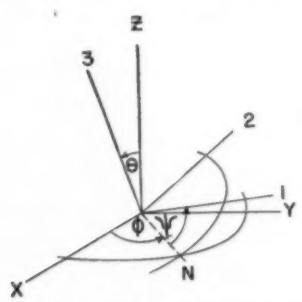

FIG. 1. Euler's angles as coordinates of a rigid body in space.

* Paper presented at the 277th meeting of the American Physical Society.

** Now at Michigan State College, East Lansing, Michigan.

[1] Slater and Frank, *Introduction to Theoretical Physics* (McGraw-Hill Book Company, Inc., New York, 1933), first edition, Chapter 10.

where A, B, and C are the moments of inertia about the principal axes 1, 2, and 3, respectively.

Consider the case of a rigid object symmetrical about one axis, and identical with respect to the other two, such as a cylinder rotating about its axis of figure, or a motor armature. Specifying the principal axes and moments of inertia as in Fig. 2, it is apparent that $A=B$. Writing $(B-C) = -(C-A) = H$, and stipulating that $M_3=0$, by use of the equations

$$\omega_1 = \dot{\theta}\cos\psi + \dot{\phi}\sin\theta\sin\psi, \tag{2a}$$

$$\omega_2 = \dot{\theta}\sin\psi + \dot{\phi}\sin\theta\cos\psi, \tag{2b}$$

$$\omega_3 = \dot{\psi} + \dot{\phi}\cos\theta \tag{2c}$$

substituted in Eqs. (1), we easily find

$$M_1 = \cos\psi[A\ddot{\theta} + \dot{\phi}\dot{\psi}C\sin\theta - H\dot{\phi}^2\sin\theta\cos\theta] + \sin\psi[A(\partial^2\phi/\partial t^2)\sin\theta - C\dot{\theta}\dot{\psi} + (A+H)\dot{\phi}\dot{\theta}\cos\theta] \tag{3a}$$

$$M_2 = \cos\psi[B(\partial^2\phi/\partial t^2)\sin\theta - C\dot{\theta}\dot{\psi} + (B+H)\dot{\phi}\dot{\theta}\cos\theta] - \sin\psi[B\ddot{\theta} + \dot{\phi}\dot{\psi}C\sin\theta - H\dot{\phi}^2\sin\theta\cos\theta] \tag{3b}$$

$$0 = C\ddot{\psi} + C(\partial^2\phi/\partial t^2)\cos\theta - C\dot{\phi}\dot{\theta}\sin\theta]. \tag{3c}$$

From Eqs. (1c) and (2c), in place of Eq. (3c), we may write

$$\omega_3 = K = \dot{\psi} + \dot{\phi}\cos\theta. \tag{4}$$

Examination of Eqs. (3a) and (3b) shows immediately that the torques about the moving principal axes 1 and 2 may be considered as the projections of two torques not rotating with the principal axes; one lying along the nodal line N and designated as P, the other perpendicular to this line but in the 1, 2 plane and designated as

Q. Thus,

$$P = A\ddot{\theta} + \dot{\phi}\sin\theta(CK - A\dot{\phi}\cos\theta), \tag{5a}$$

$$Q = B(\partial^2\phi/\partial t^2)\sin\theta - \dot{\theta}(CK - 2B\dot{\phi}\cos\theta). \tag{5b}$$

The first term of Eq. (5a) is recognized as the usual Newtonian torque, while the second term is gyroscopic in nature. The first term of Eq. (5b) is, similarly, the Newtonian torque about the precession axis making an angle $(\pi/2-\theta)$ with the 1, 2 plane caused by a torque lying in that plane. Again, the second term of Eq. (5b) is gyroscopic in nature.

There are two cases to be considered; (I) precession is prevented by suitable restraints, and (II) the torque Q is zero (precession not restrained).

For case I, Eqs. (5) reduce to

$$P = A\ddot{\theta}, \tag{6a}$$

$$Q = -CK\dot{\theta}, \tag{6b}$$

where Q is then the torque exerted by the restraint in order to prevent precession, and P the torque which produces tilting—the Newtonian torque.

For case II, rewriting Eqs. (5) with the aid of Eq. (4), and setting $Q=0$,

$$P = A\ddot{\theta} + (K-\dot{\psi})\tan\theta[CK - A(K-\dot{\psi})], \tag{7a}$$

$$O = B(\partial^2\phi/\partial t^2)\sin\theta - C\dot{\theta}(2K-\dot{\psi}) + 2B\dot{\theta}(\dot{\psi}-K). \tag{7b}$$

Substituting θ for $\tan\theta$ (for small θ) and letting $\dot{\psi}$ be constant, we can write

$$P = A\ddot{\theta} + R\theta, \tag{8a}$$

$$O = B(\partial^2\phi/\partial t^2)\sin\theta - S\dot{\theta}. \tag{8b}$$

Equation (8a) shows that the gyroscopic effect is that of adding a spring stiffness to the inertia torque. If the system be mounted on springs in the θ direction, the effect is that of raising the natural frequency. Equation (8b) shows that the torque producing precession is proportional to the velocity of tilt.

Let us now examine the relative importance of the constants R and S. Equations (7) and (8) give

$$R = CK(K-\dot{\psi}) - A(K-\dot{\psi})^2, \tag{9a}$$

$$S = C(2K-\dot{\psi}) - 2A(K-\dot{\psi}). \tag{9b}$$

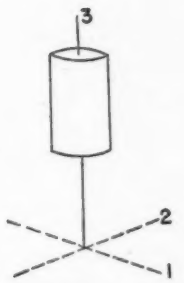

FIG. 2. Arbitrarily chosen rotor. 1, 2, and 3 are principal axes about which the moments of inertia A, B, and C are taken, respectively. Rotor is taken to be 5 inches long, 2 inches in diameter, and with the lower end 5 inches from the 1, 2, plane. The weight of the rotor is 5 lbs. and the spin velocity chosen as 6000 r.p.m.

Now in general, for systems of the sort here considered, the resultant angular velocity K will be only slightly greater than the spin velocity $\dot{\psi}$, so that $(K-\dot{\psi})$ is small.

From Eq. (9a), R is a quadratic function of $(K-\dot{\psi})$, and is zero when $(K-\dot{\psi})=0$, and when $(K-\dot{\psi})=CK/A$, or $(K-\dot{\psi})/K=C/A$. Between these limits, R reaches a maximum at $(K-\dot{\psi})/K=C/2A$, and for values outside these limits R is negative. Now a negative value of R is physically absurd, as this would indicate a gyroscopically produced torque tending to aid the external torque, which is contrary to all experience. Thus $(K-\dot{\psi})/K$ must lie between O and C/A.

For a rough estimate as to the magnitude of R, let us assume the rigid body as is shown in Fig. 2 with the axes of rotation as shown. This is thought to be a fair representation of a typical motor armature. Assuming the dimensions and weight shown, and a motor speed of 6000 r.p.m., the maximum value of $(K-\dot{\psi})/K=C/A=0.019$ and the value of $(K-\dot{\psi})/K$ for maximum R is $C/2A=0.0095$. Putting these values in Eq. (9a), the maximum value R can assume is found to be 10,500 lb. in./sec., which gives for a natural frequency about the fixed point (in the θ plane) approximately 0.95 c.p.s. This is much lower than the usual run of vibration frequencies, implying that the added apparent spring stiffness is small compared to the actual springs present.

S can be rewritten as

$$S = CK - (K-\dot{\psi})(2A-C), \tag{10}$$

which is a linear function of $(K-\dot{\psi})$. Again, S

must be always positive, or the limiting value of $(K-\dot{\psi})/K=C/(2A-C)$, which is somewhat larger than the value found above giving the maximum value of R. As C becomes small compared to A, the value of $(K-\dot{\psi})/K$ approaches the value for maximum R, and as C approaches A, the value of $(K-\dot{\psi})/K$ approaches the value found above as an upper limit. It is to be noted that S is a direct function of K, the resultant angular velocity—as the spin velocity increases, the torque-producing precession increases. For the particular values here chosen, (for maximum R) S is 35.5 in lb.^{2}/sec.^{2}.

The rotor might well be mounted on springs such that the stiffness would be four-hundred times the apparent stiffness calculated here. For the rotor alone this would mean a natural frequency of 19 c.p.s., which is not uncommon. The effect of added inertia would be to reduce both natural frequencies (real and gyroscopic) without affecting the spring stiffness. In this case then, the gyroscopic effect will be to raise the natural frequency in the ratio

$$\frac{f_{g+s}}{f_s}=\left(\frac{401}{400}\right)^{\frac{1}{2}}=1.0012,$$

and the change is on the order of 0.1 percent.

Frequency Stabilization of Microwave Oscillators by Spectrum Lines*

WILLIAM V. SMITH, JOSÉ L. GARCÍA DE QUEVEDO, R. L. CARTER, AND W. S. BENNETT
Department of Physics, Duke University, Durham, North Carolina

(Received June 25, 1947)

A 2K50 microwave oscillator has been electronically coupled to the NH_3 3,3 rotational spectrum line at 23,870 megacycles in such a manner as to maintain the frequency of the oscillator at the spectrum-line frequency. The theory of the "spectrum-line discriminator" designed to produce this frequency stabilization is developed.

INTRODUCTION

THE possibility of stabilizing the frequency of a microwave oscillator by means of a spectrum line has already been mentioned in the literature.[1] The present article deals with one form of "spectrum-line stabilizer" which has been used to tie the frequency of a 2K50 klystron to the NH_3 3,3 spectrum line at 23,870 megacycles. It is believed that this is the first time any oscillator has been thus "tied to a spectrum line" although variations in the absorption properties of gases have been previously used to modify the properties of cavity stabilizers.[2] Since the first laboratory model of the stabilizer is relatively simple and reliable, it is to be anticipated that engineered versions of the stabilizer will be of considerable importance not only as frequency standards substantially independent of temperature, but also as frequency controlling elements of communications devices, since transmitter and receiver can be set unerringly on the same frequency merely by tying each to the same spectrum line.

THEORY

In developing the theory of this spectrum-line stabilizer, frequent reference will be made to Pound's article on the stabilization of microwave oscillators,[1] as the present stabilizer design is in some features similar to his direct-current cavity stabilizer circuit. The comparable elements of the two stabilizers, i.e., the discriminators, are shown in Figs. 1a and 1b. The operation of both circuits is, essentially, that an input signal of variable frequency is reflected from the terminations of the two tee sections, finally being rectified by crystals A and B. The reflections are frequency sensitive, particularly the reflection from arm 2 of tee A, which can be so designed that the rectified output of crystals A and B, suitably added, is a linear function of frequency near the resonant frequency ν_0 of the element terminating arm 2. In general, the output is adjusted to be zero at ν_0, and is amplified and applied to the re-

* The research described in this report was supported by Contract No. W-28-099-ac-125 with the Army Air Forces, Watson Laboratories, Air Materiel Command.

[1] R. V. Pound, Rev. Sci. Inst. **17**, 490 (1946).

[2] A. Roberts, Y. Beers, and A. G. Hill, Phys. Rev. **70**, 112 (1946).

flector electrode of a microwave oscillator. Since the frequency of oscillation of the oscillator is a linear function of the voltage applied to the reflector electrode, it is possible to feed back the output of the discriminator circuit in such a phase as to correct for any tendency of the oscillator to drift away from the resonant frequency ν_0 of the discriminator.

The only apparent difference between the two discriminators consists in replacing Pound's cavity at $x-\lambda_g/8$ by a short circuit and inserting symmetrical windows C and D in the tee near its junctions, so that one or both of the lengths of guide can be evacuated and filled with gas at a low pressure. (These windows may conveniently be made of mica, and if window D is reflectionless and arm 1 is filled with air, window C can be omitted.) If, then, the gas in arm 2 is resonant at a frequency ν_0, it can be shown that the combined reflections from arms 1 and 2 are the same as for a cavity of frequency ν_0 terminating arm 2, when no gas is present in the arm. Physically, the phenomena occurring in the case of the spectrum-line discriminator are different from those in the cavity discriminator. Energy is absorbed all along arm 2 in the first case, and only in the terminating cavity in the second case. Also, for the spectrum-line case arms 1 and 2 must be long enough so that appreciable absorption takes place at ν_0, but not so long that the incident wave is completely absorbed at ν_0, as then complete absorption may also take place at frequencies in the immediate vicinity of ν_0. For the cavity discriminator, on the other hand, the optimum condition is a match at ν_0, i.e., complete absorption of incident energy. Finally, it should be noted that in the spectrum-line case the two arms differ by $\lambda_g/8$ in electrical length, which is not necessarily the same as the physical length as the dielectric constant (at a frequency well removed from ν_0) may differ in the two arms.

The mathematical analysis will be undertaken for arms 1 and 2 of equal electrical lengths l, and the reciprocal of the difference in input impedances to the two arms will be shown to be the same as the input admittance of a cavity. It then follows that if the lengths differ by $\lambda_g/8$, the electrical properties of Fig. 1b will be those of the cavity discriminator of Fig. 1a. Expressing the input impedances Z_1 and Z_2 to arms 1 and 2 in terms of the characteristic impedance Z_0 of the guide, and ignoring the small change in Z_0 caused by the gas in comparison with the change in propagation constant, then

$$\begin{aligned} Z_1 &= Z_0 \tanh\gamma_0 l, \\ Z_2 &= Z_0 \tanh\gamma l, \end{aligned} \tag{1}$$

where γ_0 and γ are the propagation constants in vacuum and in gas.

If α_0 is the attenuation of the guide walls in nepers per cm, and ϵ_1 and ϵ_2 are the real and imaginary parts of the dielectric constant of the gas,

$$\begin{aligned} \gamma_0 &= \alpha_0 + \frac{2\pi}{\lambda_g} j, \\ \gamma &= \gamma_0 + \frac{\pi}{\lambda_g}[j(\epsilon_1 - 1) + \epsilon_2]. \end{aligned} \tag{2}$$

Also, according to Van Vleck,[3] if the line breadth $\Delta\nu$ is caused solely by collision broadening

$$\begin{aligned} \epsilon_1 - 1 &= \frac{A\nu_0}{2} \frac{\nu_0 - \nu}{\Delta\nu^2 + (\nu - \nu_0)^2}, \\ \epsilon_2 &= \frac{A\nu_0}{2} \frac{\Delta\nu}{\Delta\nu^2 + (\nu - \nu_0)^2}, \end{aligned} \tag{3}$$

where A is a constant.

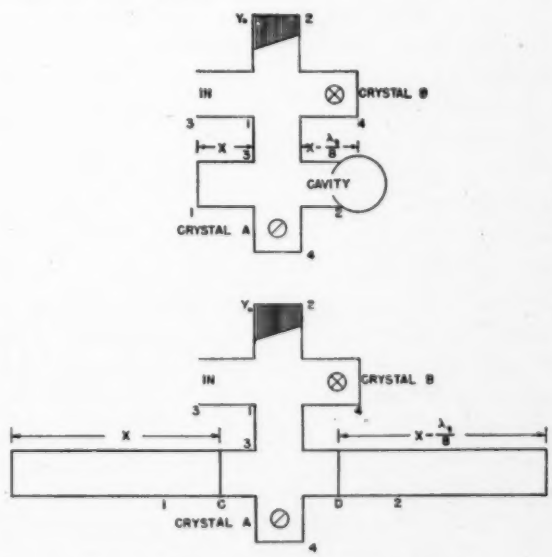

FIG. 1. Spectrum-line discriminator and frequency stabilizer.

[3] J. H. Van Vleck, "The relation between absorption and the frequency dependence of refraction," Report 735, M.I.T. Radiation Laboratory.

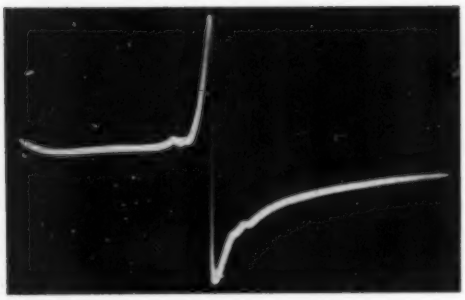

FIG. 2. NH_3 3,3 discriminator characteristic, showing fine structure. The spacing between the center of the linear portion of the discriminator curve and the first satellite is 1.72 megacycles, establishing the frequency scale.

Expanding Eqs. (1), (2), and (3) for ϵ_1-1, ϵ_2, $\Delta\nu/\nu_0$ and $\tanh\gamma l$ all very small compared to 1

$$Y=\frac{1}{Z_2-Z_1}=\frac{2\lambda_g\Delta\nu}{\pi lA\nu_0}\left[\frac{2jQ_0(\nu-\nu_0)}{\nu_0}+1\right]Y_0, \quad (4)$$

where

$$Q_0=\frac{\nu_0}{2\Delta\nu}. \quad \text{If} \quad \alpha=\frac{\pi lA\nu_0}{2\lambda_g\Delta\nu} \quad \text{and} \quad a=\frac{2Q_0(\nu-\nu_0)}{\nu_0},$$

Eq. (4) may be rewritten as

$$Y=\left(\frac{1}{\alpha}+j\frac{a}{\alpha}\right)Y_0, \quad (5)$$

which is Eq. (1) of reference 1 describing the admittance properties of a resonant cavity.

For collision broadening, $A/\Delta\nu$ is independent of pressure.[3] Thus, for a cell of fixed length, as the pressure is lowered the parameter α remains constant while Q_0 increases until at sufficiently low pressures effects other than collision broadening begin to influence the line breadth. A discussion of these effects is given by Townes.[4] He states that Doppler effect and collisions with the wave guide walls should begin to affect the line width at $2\Delta\nu=150$ kilocycles, while saturation effects causing an increase in line breadth with input power may limit the line breadth to over one megacycle for high input power.

Townes' data indicate that these saturation effects are just noticeable for an input power of 1.8 milliwatts into an absorption tube of 10.7-mm by 4.3-mm cross section for a pressure of 4×10^{-2} mm of mercury. At this pressure he gets for the ammonia 3,3 line a peak absorption of 5×10^{-4} neper per cm in wave guide and a line width of $2\Delta\nu=1.9$ megacycles. Since the attenuation in nepers/cm $=(2\pi/\lambda_g)\epsilon_2$, the parameters of Eq. (4) are found to be

$$Q_0=\frac{23{,}879}{1.9}=12{,}500, \qquad \alpha=\left(\frac{\pi l\epsilon_2}{\lambda_g}\right)_{\nu=\nu_0}=\frac{l}{3200}. \quad (6)$$

The slope $dv/d\nu)_{\nu_0}$ of the discriminator curve as derived by Pound is

$$\frac{dv}{d\nu}\Big)_{\nu_0}=DP_0\frac{Q_0}{\nu_0}\frac{2\alpha}{(1+\alpha)^2} \quad (7)$$

volts per megacycle, where P_0 is the input power to the discriminator and D is a constant. Typical cavity constants are $Q_0=12{,}500$, $\alpha=1$, and $P_0\approx1$ milliwatt, where the upper limit to P_0 is set by the amount of decoupling necessary to prevent frequency discontinuities in tying the discriminator to the oscillator. For the spectrum-line discriminator with a 2-meter cell, the constants are $Q_0=12{,}500$, $\alpha=\frac{1}{15}$, and again $P_0=1$ milliwatt, the limit on P_0 this time being set by saturation effects. The ratio $dv/d\nu_{\text{spectrum line}}$ to $dv/d\nu_{\text{cavity}}$ can therefore be made at least 1 to 4.5. If Pound's value of $DP=1$ volt is applicable to 1-cm oscillators and crystals as well as to the 3-cm ones to which he applied it, this gives $dv/d\nu=250$ millivolts per megacycle for a cavity and 55 millivolts per megacycle for a spectrum line.

OBSERVATIONS

Figure 2 is a photograph of the NH_3 3,3 discriminator characteristic at a pressure of about one one-hundredth of a millimeter of mercury. The fine-structure satellites of the line are clearly visible, two on each side of the discriminator. The spacing between the center of the linear portion of the discriminator curve and the first satellite is 1.72 megacycles,[5] establishing the frequency scale. The slope of a similar characteristic measured at a somewhat higher pressure was 70

[4] C. H. Townes, Phys. Rev. **70**, 665 (1946).

[5] B. P. Dailey, R. L. Kyhl, M. W. P. Strandberg, J. H. Van Vleck, and E. B. Wilson, Jr., Phys. Rev. **70**, 984 (1946).

millivolts per megacycle, comparing favorably with the rough theoretical estimate of 55 millivolts per megacycle.

For purposes of comparison of spectrum-line discriminators and cavity discriminators, the above measured slope $dv/d\nu$ is all the data needed. The ultimate purpose of such a discriminator, however, is to actually stabilize an oscillator. To this end, the microwave oscillator which had been frequency swept to obtain the discriminator characteristic was operated *CW*, and the discriminator output fed into a d.c. amplifier similar to that described by Pound. The amplifier output was fed to the reflector electrode only, and the oscillator frequency was observed as a function of the setting of a potentiometer controlling the reflector voltage. Thus the actual voltage on the reflector was the sum of the potentiometer control and the error signal from the amplifier. It was observed that if the pressure of ammonia in arm 2 was a centimeter or more, or if the ammonia were frozen out at liquid air temperatures, the oscillator frequency was a continuous function of the potentiometer control. If, however, the pressure was in the range corresponding to a line width of one-half to two megacycles, approximately, the frequency would "lock in" to the line frequency of 23,870 megacycles over a range of potentiometer settings, jumping discontinuously to a different frequency when the limit of control of the discriminator was exceeded. At approximately optimum conditions as the potentiometer was continuously varied in such a direction as to tend to increase the oscillator frequency, the oscillator tuned continuously up to 23,841 megacycles, jumped to the line frequency of 23,870 megacycles, remaining constant within one megacycle until it again jumped to 23,892 megacycles. Control was thus maintained for variations in reflector voltage equivalent to a frequency spread of just under 51 megacycles. The measured variation of potentiometer voltage over which the frequency remained constant was 14 volts (of a total reflector-cathode voltage of 75 volts).

The Efficiency of Thermoelectric Generators. I.*

MARIA TELKES
Department of Metallurgy, Massachusetts Institute of Technology, Cambridge, Massachusetts
(Received July 28, 1947)

The generation of electrical energy from thermal energy by thermoelectric means cannot be accomplished with thermocouples made of the available alloys generally used for temperature measurements, their efficiency being less than one percent.

A review of the theoretical efficiency calculations shows that higher efficiencies can be attained with thermocouple materials to which the Wiedemann-Franz-Lorenz relation is applicable, when their thermoelectric power is greater than 200 microvolts/°C. Some zinc-antimony alloys with added metals approach the above conditions and have produced an experimental efficiency in excess of five percent, in accordance with the theoretical calculations.

The criteria of higher efficiency are applied to semiconductors, deriving the optimum conditions. Lead sulfide with excess lead was found to be the only suitable material at present, which in combination with the zinc-antimony alloy produces an efficiency of seven percent.

Higher thermoelectric efficiencies can be produced only by developing new materials which can attain the theoretically required high values of thermoelectric power, low heat conductivity, and low specific resistance.

SYMBOLS

T temperature (°abs.)
T_h hot junction temperature (°abs.)
T_c cold junction temperature (°abs.)
$\Delta t = T_h - T_c$ temperature difference (°C)
E open circuit e.m.f. of thermocouple, Seebeck e.m.f. (volt)
$e = \frac{E}{T_H - T_C}$ the average thermoelectric power in the temperature range of $\Delta t = T_h - T_c$ (volt/°C)
$\theta = dE/dT$ the instantaneous thermoelectric power at T temperature (volt/°C)
I current flowing in thermocouple and external load circuit (amp)
R resistance of thermocouple (ohm)
R_e external load resistance, $R_e = R$ (ohm)
W_0 output in external circuit (watt)
W_i thermal energy absorbed at the hot junction (watt)
Q_c heat conductance of thermocouple (watt)
$\rho' \rho''$ specific electric resistance of thermocouple materials average between T_h and T_c (ohm cm)
σ specific electric conductivity at T temperature (ohm^{-1} cm^{-1})
$k'k''$ specific heat conductivity of thermocouple materials averaged between T_h and T_c (watt cm^{-1} deg.$^{-1}$)
$s's''$ cross-sectional area of thermocouple materials (cm^2)
L length of thermocouple materials, both of same length, (cm)
$d'd''$ form factors of thermocouple materials denoting s'/L and s''/L (cm)
$\Delta\epsilon$ energy level difference (electron volt)
k_0 Boltzman's constant (0.8617×10^{-4} electron volt/°C)
l_0 mean free path (cm)
n_b the number of bound impurity electrons/cm^3
e_0 electronic charge

* Publication No. 20, M.I.T. Solar Energy Conversion Research Project.

HISTORICAL REVIEW

VARIOUS types of thermoelectric generators have been constructed in the past with the aim of producing a gas-heated low voltage direct-current source of relatively small but constant power output. The early efforts have been summarized in book form by F. Peters in 1908.[1] This summary shows that most of the thermoelectric materials then known have been used experimentally in a large variety of empirical designs. Only very few types of thermoelectric generators have reached the production stage. The best-known commercially produced apparatus was Gülcher's gas-heated thermoelectric generator with an over-all efficiency of one-half of one percent.

In more recent times the construction of thermoelectric generators was revived with the aim of producing a gas-heated power supply for radio receivers and for charging storage batteries. Koch's[2] antimony and German silver thermoelectric generator attained an efficiency of 0.5 percent. Wall[3] used iron-constantan thermoelements, attaining an efficiency of less than 0.05 percent. Milne[4] used thermocouples made of nickel and an alloy of copper-silver-selenium in a gas-heated battery charger for radio re-

[1] F. Peters, *Thermoelemente und Thermosäulen*, Halle 1908.
[2] E. Koch, Helios **28**, 557 (1922).
[3] T. F. Wall, The Electr. Rev. 847 (1927).
[4] H. R. Milne, Brit. Patent 510, 410, and 501, 411 Feb. 24 (1939).

ceivers, producing an efficiency less than one percent.

THE EFFICIENCY PROBLEM

For the purpose of electrical power production an efficiency of one percent is definitely unsatisfactory. It is true that relatively small electrical power generators used at present are comparatively inefficient. Small steam-electric power generators operate with an efficiency of five percent or less. Power plants used on farms for the generation of electricity for household purposes operate with an efficiency of less than ten percent, which compares with the twenty-five percent efficiency rating of large modern electric power generating stations.

What is the cause of the low efficiency of thermoelectric generators? This question has been analyzed repeatedly in the literature. One of the suggested causes was the relatively imperfect heat transfer from the fuel burner to the hot junctions of the thermoelements. It is obvious that only that part of the heat of combustion is effective which is actually transferred to the hot junctions. Considerable heat may be lost in the flue gases and through the structural elements which are necessary to hold the thermoelements.

Peters[1] described numerous empirical designs which attempted to improve the heat transfer conditions, but there are relatively few measurements available concerning this phase of the problem. The over-all efficiency of the thermoelectric generator is best analyzed as the efficiency of the thermoelectric process itself as distinct from the efficiency of the heat transfer to the hot junctions.

The purely thermodynamic treatment of the thermocouple considers the thermocouple as a reversible heat engine (recent summary by W. F. Roeser[5]). The thermodynamic consideration establishes correlations between the Seebeck, the Peltier, and the Thomson effects disregarding the irreversible processes caused by heat conduction, lateral heat losses, and the Joule heat generated in the operating thermoelements. The thermodynamic treatment alone is insufficient to account for the performance of the thermoelectric generator, because the irreversible effects are unavoidable and predominant in the calculation of the efficiency.

The efficiency of the thermoelectric process (eff.) is defined as the ratio of useful electrical power output (W_0) delivered to an external load, to the electrical equivalent of the thermal energy absorbed at the hot junctions of the thermoelements (W_i)

$$\text{eff.} = W_0/W_i.$$

This definition has been used in previous calculations by Lord Rayleigh,[6] Kollert,[7] and Altenkirch.[8] The knowledge of the following physical properties of the thermoelectric materials is required: the thermoelectric power (e), the specific electrical resistance (ρ), and the specific heat conductivity (k) which are functions of the temperature. The above factors are the material constants of the thermoelements. The form factors (cross section, length, shape factors) may be selected according to certain conditions of best design. The previous calculations failed to produce any correlation between the calculated and the observed efficiency, which was primarily due to the inadequate data concerning the material constants.

In recent years the construction of radiation-measuring thermopiles has been improved considerably. Radiation-measuring thermocouples or thermopiles may be regarded as miniature thermoelectric generators, operating at a relatively small temperature difference. In most cases a high voltage output is desired at the expense of the efficiency. The efficiency calculations for thermoelectric generators and radiation-measuring thermopiles are otherwise identical. Such calculations have been published by Johansen,[9] Firestone,[10] Harris,[11] Cartwright,[12] Jones,[13] Kovalenko,[14] Emmons,[15] and others.

The theoretical calculations mentioned above are revised on the following pages, with the aim of deriving equations and conclusions concerning

[5] American Institute of Physics, *Temperature, Its Measurement and Control in Science and Industry* (Reinhold Publishing Corporation, New York, 1941), p. 180.

[6] Lord J. W. Rayleigh, Phil. Mag. **34**, 481 (1892).
[7] J. Kollert, Elektrotech. Zeits. **11**, 333 (1890).
[8] E. Altenkirch, Physik. Zeits. **10**, 560 (1909).
[9] E. S. Johansen, Ann. d. Physik **33**, 517 (1910).
[10] F. A. Firestone, Rev. Sci. Inst. **1**, 630 (1930).
[11] L. Harris, Phys. Rev. **45**, 635 (1934).
[12] C. H. Cartwright, Rev. Sci. Inst. **1**, 592 (1930).
[13] R. V. Jones, J. Sci. Inst. **11**, 247 (1934).
[14] V. Kovalenko, Tech. Phys. U.S.S.R. **5**, 789 (1938).
[15] H. Emmons, J. Frank. Inst. **229**, 29 (1940).

the theoretical efficiency and the best design criteria of thermoelectric generators. During these calculations several assumptions are made which are now considered in detail.

1. Thermocouple Materials

The thermoelectric generator consists of a number of thermocouples, which are identical. The theoretical efficiency is not influenced by the number of the thermocouples and therefore in the following calculations only one thermocouple is considered. The couple is formed of two thermoelectric materials, with hot and cold junctions maintained at definite temperatures. The materials are assumed to be in the polycrystalline state. Their specific electric resistance ($\rho'\rho''$), specific heat conductivity (k', k''), and thermoelectric power (e) are known functions of the temperature (T). The materials should be suitably annealed and their physical properties should not change during the operation of the thermocouple.

2. Junctions

A selection of solders, fluxes, or welding techniques is available for the preparation of satisfactory junctions. It is important that the junction should be free of any additional electric resistance, caused by imperfect soldering or welding, due to the presence of oxide layers or other causes. It is assumed that the "junction resistance" is negligible compared to the total resistance of the thermocouple. This condition is relatively easily attained at the cold junction, but difficulties may arise at the hot junctions. During prolonged operation at relatively higher temperatures, thermal corrosion and deterioration may occur at the hot junction, increasing the electrical resistance and thereby decreasing the efficiency.

It is obvious that the hot junction cannot be operated above a certain temperature, limited by the melting points of the thermoelements. Actually the operating temperature of the hot junction is further limited by the nature of the thermoelectric materials and the contact at the hot junction. Even if oxidation is avoided by limiting the hot junction temperature, changes may occur during prolonged operation because of the diffusion of the two thermoelectric materials and the connecting layer. If the hot junctions are formed with the help of a solder, the components of the solder may diffuse into the thermoelectric materials, with the possibility of changing their composition and properties. Such changes may not be noticed except during prolonged life tests. The effect of thermal diffusion may be minimized by using welding techniques or by limiting the amount of solder to a minimum, using a soldering material which does not interfere with the physical characteristics of the thermoelectric materials.

3. Heating the Hot Junctions

The experimental determination of the efficiency of thermocouples requires a controlled heating arrangement delivering measured amounts of thermal energy to the hot junctions. For experimental purposes electrical heating of the hot junctions is preferable.

4. Cooling the Cold Junctions

Because of the irreversible heat conduction occurring in the thermoelectric materials a considerable amount of heat is conducted from the hot junction to the cold junction. If this energy is not removed by suitable cooling, the temperature of the cold junction will increase. The temperature of the cold junctions can be maintained at or near room temperature by using suitable water or air cooling. The use of higher cold junction temperatures is not desirable in thermocouples made of metallic conductors, because their electrical resistance increases with increased temperature, decreasing their efficiency.

5. Lateral Heat Losses

It is obvious that the lateral or radial heat losses from the surface of the thermoelements should be as small as possible. In a thermoelectric generator, consisting of a large number of thermoelements, these losses may be minimized by arranging the thermocouples in a closely packed assembly, with the unavoidable minimum of insulating material between the couples. Experimental tests made with relatively few or with individual couples may minimize the lateral heat losses, by surrounding the thermocouples

with adequate thermal insulation, or the lateral heat losses may be determined experimentally and corrections applied. During the efficiency calculations it is assumed that the lateral heat losses are negligible.

6. Form Factors

The thermoelectric materials are generally in the form of cylindrical or rectangular bars, wires, or sheets. Some constructors used wedge-shaped or tubular thermoelements with the aim of improving the performance. Actually, however, such forms failed to increase the efficiency. The construction is simplified if the lengths of the thermoelectric materials are equal, as in this case the distance between the hot and cold junction zones is fixed, facilitating the structural arrangement. Complex shape or form factors alone cannot improve the efficiency.

It can be shown by calculation that optimum conditions will prevail if the shape factor of the thermoelements is selected in such a way that equal amounts of heat are conducted away by the two thermoelectric materials, while at the same time the electric resistance of the two elements is also equal.

7. Internal and External Resistance

The maximum power output of a thermoelectric generator is obtained when its internal resistance is nearly equal to the external load resistance. This criterion can be derived by calculation and has been proven by experiments.[3]

8. Joule Heat

During the operation of a thermoelectric generator with current flowing through the thermoelements, an internal Joule heat will be generated. Part of this heat will be removed at the cold junctions. This effect may be disregarded as long as the efficiency of the thermocouple is rather low.

9. Thomson Effect

During the operation of a thermoelectric generator on closed circuit the Thomson effect should influence the thermal distribution conditions. The effect is of relatively slight importance in most cases and therefore it is not considered in the following calculations.

EFFICIENCY CALCULATIONS

The calculations apply to a definite operating temperature interval $\Delta t = T_h - T_c$.

The open circuit e.m.f. is $E = e\Delta t$. When the circuit is closed through an external resistance (R_e) which is equal to the internal resistance (R) of the thermocouple a current (I) will flow in the circuit: $I = E/2R$. The load e.m.f. will drop to $\frac{1}{2}E$. The Watt output in the external circuit will be:

$$W_0 = \tfrac{1}{2}EI = E^2/4R. \tag{1}$$

The total electrical energy produced in the thermocouple and the external load circuit is $2W_0$. A part of the thermal energy (W_i) absorbed at the hot junction will be used for the production of $2W_0$ electrical energy, while the larger part of W_i will be conducted away by the thermocouple elements in accordance with their heat conductivity (Q_c) (irreversible loss). Applying the second law of thermodynamics, the amount of thermal energy required for the production of $2W_0$ electrical energy is:

$$\frac{2W_0T_h}{T_h - T_c} = \frac{2W_0T_h}{\Delta t}. \tag{2}$$

The efficiency is obtained by combining Eqs. (1) and (2):

$$\text{eff.} = \frac{W_0}{W_i} = \frac{W_0}{\dfrac{T_h 2W_0}{\Delta t} + Q_c} = \frac{1}{\dfrac{2T_h}{\Delta t} + \dfrac{Q_c}{W_0}} = \frac{1}{\dfrac{2T_h}{\Delta t} + \dfrac{Q_c 4R}{E^2}}. \tag{3}$$

We proceed substituting the values of the specific resistance, the specific heat conductivity $k'k''$, and the form factors $d'd''$ into the above equation:

The electric resistance

$$R = \rho'/d' + \rho''/d''. \tag{4}$$

The heat conductance

$$Q_c = \Delta t(k'd' + k''d''). \tag{5}$$

TABLE I. Calculated efficiency of thermocouples (percent); cold junction temperature 27°C; Wiedemann-Franz-Lorenz relation applicable.

Temp. diff. t°C	Thermoelectric power in microvolts/°C									
	100	150	200	250	300	400	500	600	800	1000
100	0.75	1.56	2.53	3.54	4.55	6.3	7.7	8.7	10.1	10.8
200	1.30	2.70	4.35	6.04	7.69	10.5	12.7	14.3	16.0	17.4
300	1.72	3.57	5.71	7.92	10.0	13.6	16.2	18.2	20.6	22.0
400	2.06	4.25	6.78	9.35	11.8	15.8	18.8	21.0	23.8	25.3
500	2.34	4.80	7.63	10.5	13.2	17.6	20.9	23.2	26.2	27.8

From Eqs. (4) and (5) it follows that:

$$\frac{4RQ_c}{E^2}=\frac{4\Delta t(k'd'+k''d'')\left(\frac{\rho'}{d'}+\frac{\rho''}{d''}\right)}{e^2\Delta t^2}$$

$$=\frac{4\left(k'\rho'+k''\rho''+\frac{k'\rho''d'}{d''}+\frac{\rho'k''d''}{d'}\right)}{e^2\Delta t}. \quad (6)$$

Before proceeding further we examine the optimum conditions for the selection of the form factors. It was stated above that the form factors should be selected in such a way that equal amounts of heat should flow through the two elements and that their electrical resistance should be the same. This condition will prevail if:

$k'd'=k''d''$ or $d''/d'=k'/k''$ (from Eq. 5),

$\rho'/d'=\rho''/d''$ or $d''/d'=\rho''/\rho'$ (from Eq. 4),

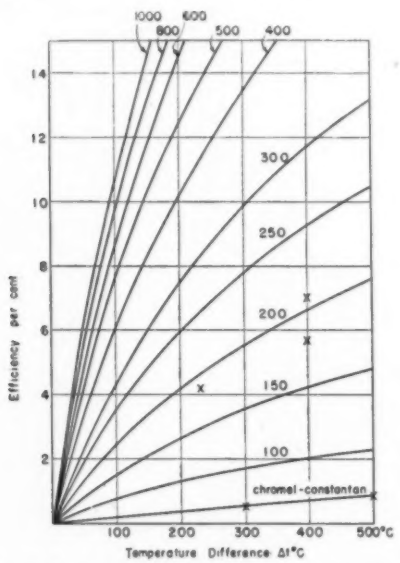

FIG. 1. Calculated efficiency of thermocouples as a function of the temperature difference; x-experimental results. The figures indicate the thermoelectric power in microvolts/°C.

combining the above

$$\frac{d''}{d'}=\left(\frac{k'\rho''}{k''\rho'}\right)^{\frac{1}{2}} \quad (7)$$

substituting Eq. (7) into (6) we obtain:

$$\frac{4RQ_c}{E^2}=\frac{4\{k''\rho''+k'\rho'+2(k''\rho''k'\rho')^{\frac{1}{2}}\}}{e^2\Delta t}$$

$$=\frac{4\{(k''\rho'')^{\frac{1}{2}}+(k'\rho')^{\frac{1}{2}}\}^2}{e^2\Delta t}. \quad (8)$$

Combining Eq. (3) and (8) the efficiency is:

$$\text{eff.}=\frac{1}{\frac{2T_h}{\Delta t}+\frac{4\{(k'\rho')^{\frac{1}{2}}+(k''\rho'')^{\frac{1}{2}}\}^2}{e^2\Delta t}}. \quad (9)$$

Examining the efficiency equation (9) we find the expressions $k'\rho'$ and $k''\rho''$. On the basis of experimental observations, Wiedemann-Franz found (in 1853) that for many metals and alloys the ratio of the heat conductivity (k) and the electric conductivity (σ) is constant at room temperature, $k/\sigma=7.3\times10^{-6}$. As the specific resistance $\rho=1/\sigma$ it equally follows that $k/\sigma=k\rho=7.3\times10^{-6}$.

The specific resistance of many metals and alloys was found to increase with temperature. On the basis of further experimental evidence Lorenz (in 1877) found the general relation (Wiedemann-Franz-Lorenz-constant):

$$k/6=k\rho=2.45\times10^{-8}T. \quad (10)$$

The theoretical explanation for the value of this constant has been given by Sommerfeld (in 1927).

The experimental evidence shows that the Wiedemann-Franz-Lorenz relation is applicable to most metals and many alloys (within the temperature range of thermocouple use). No metal or alloys have been found to show a lower value. Some alloys show a higher value, a deviation (D) from the normal Wiedemann-Franz-Lorenz constant. The deviation (D) may be explained by a consideration of the heat conductivity (k). The heat conductivity is due to two factors: the atomic part, which is of the same order of magnitude as that of insulators, and the electronic

part, which in good heat conductors is preponderant. Metals (Bi, Sb) or alloys of low heat conductivity generally show a deviation (D) from the normal Wiedemann-Franz-Lorenz constant.

According to Eq. (9) the efficiency will be high if $k'\rho'$ and $k''\rho''$ are small, that is, if the Wiedemann-Franz-Lorenz constant is applicable to the thermocouple.

Optimum condition: *Wiedemann-Franz-Lorenz relation* applicable. Assuming that Eq. (10) is applicable to a thermocouple operating at an average temperature of $1/2(T_h+T_c)$ it follows that $\rho'k'=\rho''k''=2.45\times10^{-8}1/2(T_h+T_c)$.

In this case Eq. (9) is changed to:

$$\text{eff.}=\frac{1}{\frac{2T_h}{\Delta t}+\frac{16\rho k}{e^2\Delta t}}=\frac{1}{\frac{2T_h}{\Delta t}+\frac{19.7\times10^{-8}(T_h+T_c)}{e^2\Delta t}}. \quad (11)$$

This equation contains only the junction temperatures and the thermoelectric power. The cold junction temperature, T_c, may be regarded as fixed near the ambient or room temperature, which is about 300°abs. (27°C). Equation (11) permits the calculation of the efficiency for definite temperature differences and thermoelectric powers. The results of this calculation are summarized in Table I and Fig. 1.

It should be emphasized that the above efficiencies represented in Table I and Fig. 1, are based upon the assumption that thermoelectric materials can be produced to which the Wiedemann-Franz-Lorenz relation is applicable. At higher efficiencies (>10 percent) the Joule heat cannot be neglected and therefore these values should be regarded as tenative indications.

The applicability of the Wiedemann-Franz-Lorenz relation for most metallic materials and alloys can be determined if the specific resistance and specific heat conductivity are known. For a temperature of 27°C (300°abs.) the Wiedemann-Franz ratio $\rho k=7.35\times10^{-6}$. For most materials the specific resistance is known, but the heat conductivity may not be available. In such cases the following rule may be applied to determine whether a large deviation from the Wiedemann-Franz-Lorenz relation can be expected. The specific heat conductivity may be assumed to be as low as that of certain insulators, which average

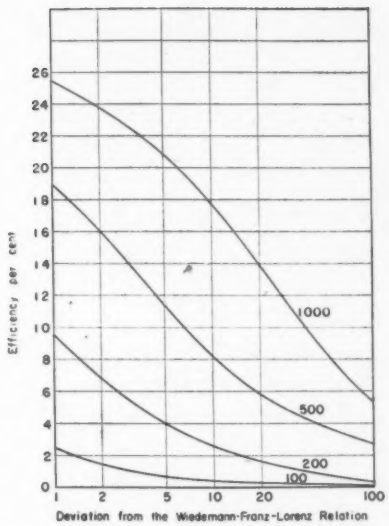

FIG. 2. Calculated efficiency of thermocouples in relation to their deviation from the Wiedemann-Franz-Lorenz relation; temperature difference 400°C; the figures indicate the thermoelectric power in microvolts/°C.

$k=0.01$. With this assumed value the corresponding ρ value will be 7.35×10^{-4}. *Any material which shows a specific resistance larger than 0.001 ohm-cm at room temperature probably cannot be expected to follow the Wiedemann-Franz relation.*

General condition: *Wiedemann-Franz-Lorenz relation not applicable.* Many thermoelectric materials of high thermoelectric power show a considerable deviation (D) from the Wiedemann-Franz-Lorenz relation. If the specific resistance, ρ', and the specific heat conductivity, k', of such materials is known, the deviation (D) at an average temperature (T) will be:

$$D=\frac{\rho'k'}{2.45\times10^{-8}T}.$$

A thermocouple formed of a thermoelectric material showing a deviation (D) in combination

TABLE II. Calculated efficiency of thermocouples (percent); cold junction temperature 27°C, temperature difference 400°C; D = Deviation from the Wiedemann-Franz-Lorenz relation.

Thermoelectric power microvolt/°C	$D=1$	2	5	10	20	100
100	2.1	1.3	0.8	0.5	0.3	0.07
250	9.4	6.7	4.2	2.7	1.6	0.4
500	18.8	15.8	11.6	8.3	5.5	1.6
1000	25.3	23.7	21.0	17.8	14.0	5.4

TABLE III. Commercially available temperature indicating thermocouples.

	Thermoelectric power (e) microvolts/°C Temp. range 27–727°C
Platinum alloys	less than 20
"Pallaplat" couple[15]	55
Chromel–alumel	42
Iron-constantan	57
Chromel P–constantan	76

with another material showing no deviation will show a diminished efficiency, as computed in Table II and shown in Fig. 2. The calculations were made for a cold junction temperature at 27°C, using a temperature difference of 400°C.

Table II indicates the importance of the deviation from the Wiedemann-Franz-Lorenz relation, which is very pronounced for the 100- to 250-microvolt/°C thermoelectric power values; the efficiency of such couples diminishes to half of the theoretical maximum with a deviation of two to five. For the 500- to 1000-microvolt/°C range the efficiency decreases to half of the theoretical value with a 10- to 20-fold deviation. Assuming that such materials would have a low specific heat conductivity of $k=0.01$, the corresponding ρ value will be about 0.03 ohm-cm. *It is probable that in the above indicated temperature range thermoelectric materials with a specific resistance greater than 0.03 ohm-cm could not attain an efficiency in excess of 10 percent, even if their thermoelectric power were as high as 1000-microvolt/°C.*

THERMOCOUPLE MATERIALS

Recent reviews[5,16,17] tabulate the properties of thermoelectric materials used for temperature measurements. Some of the best materials of this type are summarized in Table III.

As shown in Table III, the thermoelectric power of the commercially available thermocouples is considerably below 100-microvolt/°C. Even if the Wiedemann-Franz-Lorentz relation of these materials would not deviate from its normal value, the expected efficiency could not be greater than 2 percent, operating them at relatively high temperatures.

The Chromel P–Constantan Thermocouple

This couple produces the highest thermoelectric power and may be regarded as the best commercially available couple. It was used, therefore, to verify the efficiency calculations, comparing them with the experimentally attainable efficiency. Chromel P (approximately 90 nickel–10 chromium) and constantan (55 copper–45 nickel) were used in the form of flat bars with welded hot and cold junctions. The hot junctions were electrically heated, the cold junctions water-cooled. The specific resistance, heat conductivity, and thermoelectric power of these alloys are shown in Table IV together with their calculated and experimentally observed efficiencies.

The calculated and observed efficiencies are in good agreement and show that the efficiency is less than one percent with the hot junctions operating at 520°C. This is approximately the highest temperature at which constantan can be used continuously without undue thermal corrosion. Assuming that constantan could be protected against oxidation at higher temperatures, the calculations show that an efficiency of two percent could be attained with a temperature difference of about 1000°C.

The Bismuth-Antimony Couple

The use of this couple is limited by the melting point of bismuth (271°C). Instead of bismuth, an

TABLE IV.

	Temperature range 20–320°C	20–530°C
Constantan*		
specific resistance ρ	49×10^{-6}	49×10^{-6}
heat conductivity k	0.29	0.33
ρk	14.3×10^{-6}	16.2×10^{-6}
deviation D	1.30	1.20
Chromel P		
specific resistance ρ	75×10^{-6}	78×10^{-6}
heat conductivity k	0.19	0.22
ρk	14.3×10^{-6}	17.2×10^{-6}
deviation D	1.30	1.28
Chromel P–constantan		
thermoelectric power (volt/°C)	71×10^{-6}	73×10^{-6}
calculated efficiency (percent)	0.64	0.96
observed efficiency (percent)	0.58	0.92

* Constantan and alloys of nearly identical composition are manufactured under various trade names: Advance, Ideal, Copel.

[16] A. W. Smith, Ohio State Univ. Bull. No. 20. Eng. Exp. Station (1921).
[17] G. Borelius, Handbuch der Metallphysik 1, 185 (1935).
[15] A. Schulze, *Metallische Werkstoffe für Thermoelemente* (N. E. M.-Verlag Dr. G. Lüttke, Berlin, 1940).

alloy of 91 Bi–9 Sb can be used which shows a slightly better performance. The electrical properties of these materials have been determined by Gehlhoff and Neumeier[19,20] and are summarized in Table V, giving the calculated efficiency.

THERMOELECTRIC PROPERTIES OF ELEMENTS AND ALLOYS

The thermoelectric power and the specific resistance of various alloys have been summarized.[5,16,17,19–23]

According to the literature the thermoelectric power of most elements is considerably less than 100-microvolt/°C, with the exception of Te, Se, Si, and Ge.

The thermoelectric power of most alloys was found to be considerably less than 100-microvolt/°C, therefore these alloys could not be expected to produce efficiencies higher than two to three percent, even when operated at relatively high temperature differences.

Thermoelectric power values in excess of 100-microvolt/°C apparatently are found only in alloys containing Sb, Bi, Se, Te, Si (group IVB, VB, VIB of the periodic table), in combination with other metals.

The following general rules have been derived from the study of binary alloy systems;

In a binary alloy series a high value of the thermoelectric power and a high value of the specific electric resistance generally occurs at or near an intermetallic compound.

A relatively small amount of added metal ("impurity") may diminish the specific resistance of an element or an intermetallic compound to a considerable extent, while the thermoelectric power is changed relatively slightly, the heat conductivity remaining practically unchanged.

TABLE V.

		Temperature range 260–20°C
Bismuth		
specific resistance	ρ	185×10^{-6}
heat conductivity	k	0.096
	ρk	17.8×10^{-6}
deviation	D	1.74
Antimony		
specific resistance	ρ	86×10^{-6}
heat conductivity	k	0.205
	ρk	17.8×10^{-6}
deviation	D	1.74
91 Bi–9 Sb		
specific resistance	ρ	212×10^{-6}
heat conductivity	k	0.073
	ρk	15.4×10^{-6}
deviation	D	1.51
Bismuth-antimony couple		
thermoelectric power (volt/°C)		111×10^{-6}
calculated efficiency (percent)		1.00
91 Bi–9 Sb *vs.* antimony couple		
thermoelectric power (volt)e		123×10^{-6}
calculated efficiency (percent)		1.31

Operating at the highest attainable temperature difference, these thermocouples show a calculated efficiency at 1.00 and 1.31 percent.

TABLE VI. Properties of tellurium and tellurium alloys.

Composition weight percent	Spec. resist. ρ (at room temp.)	Heat cond. k	Thermoelectric power microvolt/°C ref. Cu 100–20°C temp. range	References (see Bibliography)
Te (pure)	0.04	0.014	70	24
Te (pure)	0.025		70	25
Te (impure)	0.035	0.018	300 to 500	24, 25
Te (impure)	0.009 to 0.40		300 to 550	24
1 Bi bal. pure Te	0.0024		220	24
0.5 Sb bal. pure Te	0.0032		215	24
Bi_2Te_3(52Bi–48Te)				
impure	0.0020		120	27
impure	0.0010		170	26
pure	0.0008		−150	26
42Bi–58Te pure	0.0009		−160	26
42Bi–58Te impure	0.00084		−100	27

A thermocouple formed of 1Bi–99Te and 42Bi–58Te shows a thermoelectric power of 380-microvolt/°C. Efficiency experiments are in progress.

Tellurium and Tellurium Alloys

The general rules indicated above can be illustrated by tellurium and its alloys. The thermoelectric power of pure tellurium is rather low, while its specific resistance is high. Impure tellurium generally shows a high thermoelectric power, with variable specific resistance. Certain small additions (Bi, Sb) diminish the specific resistance about 100-fold, increasing the thermoelectric power of pure tellurium. The intermetallic compound Bi_2Te_3(52 Bi–48 Te) when

[19] G. Gehlhoff and F. Neumeier, Verh. d. D. Phys. Ges. **15**, 1069 (1913).
[20] G. Gehlhoff and F. Neumeier, Verh. d. D. Phys. Ges. **15**, 876 (1913).
[21] W. Guertler, Zeits. f. Metallkunde **22**, 78 (1930).
[22] W. Meissner, Thermoelektrizität in Vol. 11, part 2, in Wien-Harms *Handbuch der Experimentalphysik* (Akademische Verlagsgesellschaft, Leipzig 1935).
[23] M. A. Hunter, p. 1227 of reference 5.
[24] C. H. Cartwright, Ann. d. Physik **18**, 656 (1933).
[25] C. H. Cartwright, Proc. Roy. Soc. London **A148**, 648 (1935).
[26] M. Telkes, unpublished.
[27] W. Haken, Ann. d. Physik **32**, 291 (1910).

TABLE VII. Properties and efficiency of Zn–Sb alloys; temperature interval 20 to 420°C.

	Spec. resist. (ρ)	Spec. heat conductivity (k)	Thermo-electric power ref. constantan (ε)	Efficiency (percent) observed	Efficiency (percent) calculated
ZnSb	0.0072	0.014	250	2.7	2.7
ZnSb with small amounts of Sn, Ag	0.0027	0.015	250	5.6	5.7
ZnSb with other additions	0.0022	0.015	220	4.8	4.8
	0.0044	0.015	280	5.2	5.1

pure has a negative thermoelectric power, which changes sign when impurities are present. Another alloy 42 Bi–58 Te shows the highest negative thermoelectric power of this series. The properties of some Te alloys are shown in Table VI.

Zinc-Antimony Alloys

It has been known[1] that an alloy of Zn and Sb forming the intermetallic compound ZnSb (35 Zn–65 Sb) is a suitable material for thermoelements. The specific resistance, specific heat conductivity, and thermoelectric power as a function of the temperature has been measured.[28,29] Relatively small amounts of metals added to the ZnSb compound diminish its specific resistance considerably, while the thermoelectric power and the specific heat conductivity are altered only slightly. Efficiency measurements have been made with thermocouples of ZnSb with constantan, at a temperature difference of 400°C, the maximum allowable operating range. The observed efficiency values agree with the calculated values (Table VII).

A thermocouple formed of the above alloys in combination with an alloy of 91 Bi+9 Sb, Table V, attained an efficiency of 4.2 percent operating at a temperature difference of 230°C (hot junction at 250°C) which is the highest allowable temperature due to the low melting point of the bismuth alloy (near 270°C). At this relatively low temperature thermal corrosion is entirely absent. The Zn–Sb alloy thermocouples in combination with constantan or with the Bi–Sb alloy show a considerable improvement in efficiency (4.2 to 5.6 percent) compared with Chromel P–constantan and the Bi–Sb couples (about 1 percent).

[28] M. Telkes, U. S. patent 2,229,482 (1941).
[29] M. Telkes, U. S. patent 2,366,881 (1945).

Cadmium-Antimony Alloys

The Cd–Sb series of alloys form an unstable intermetallic compound. This condition influences greatly the electrical properties, as reported in the literature.[30,31] Efficiency tests failed to produce favorable results.

Silicon and Silicon Alloys

The thermoelectric power and the resistivity of silicon is very markedly influenced by impurities. Relatively small changes in the amount of the impurities may result in a reversal of the sign of the thermoelectric power.[32–34] The specific heat conductivity of impure silicon is comparable to that of nickel, while the specific resistance of silicon is at least 1000 times greater. The Wiedemann-Franz-Lorenz relation, therefore, is very unfavorable and a high efficiency could not be expected.

Sulfides, Oxides, Semi-Conductors

The sulfides and oxides as thermoelectric materials may be classified according to the nature of their electrical conductivity.

Metallic conductors of high conductivity, which decreases at increasing temperatures. Their temperature coefficient of resistivity is negative, as it is in most metals and alloys.

Semi-conductors of comparatively low electrical conductivity, which increases considerably at higher temperatures; the temperature coefficient of resistivity is negative. The thermoelectric power of semi-conductors is generally in the range of 100- to 1000-microvolt/°C.

A large group of semi-conductors show pure electronic conductivity, and only these are considered. Their electrical properties are usually

[30] A. Eucken and G. Gehlhoff, Ber. d. D. Phys. Ges. **14**, 169 (1912).
[31] F. Fischer and G. Pfleiderer, Ges. Abh. Kennt. Kohle **4**, 409, 440 (1919).
[32] Broniewski and Smialowski—Rev. Met. **29**, 542, 602 (1932).
[33] M. Schulze, Zeits. f. Metallk. **23**, 261 (1931); Physik. Zeits. **31**, 1062 (1930); Zeits. f. tech. Physik **11**, 443 (1930).
[34] F. Fischer and Dehn, Ges. Abh. Kenntn. Kohle **12**, 526 (1937).

influenced by the presence of small amounts of impurities. With the exception of the elements Te, Se, Si, and Ge the semi-conductors are chemical compounds or intermetallic compounds. In their pure and stochiometrically exact form their electrical conductivity shows a minimum, approaching that of insulators.

Semi-conductors of the oxide and sulfide group are usually prepared by compressing and sintering. This procedure generally does not furnish solid compacts, a certain porosity remains, which decreases the conductivity, although it does not influence the thermoelectric power. With suitable treatment the semi-conductors can be prepared in a non-stochiometric form, with the electropositive or the electronegative element in excess as impurity (homogeneous or intrinsic impurity). Added foreign atoms in a similar way can act as heterogenous (extrinsic) impurities. The impurities may supply free conduction electrons or may combine with free electrons, altering the conductivity of the pure stochiometric compound. In some cases the conductivity may increase 10^3- to 10^6-fold. The thermoelectric power is generally not affected in a similar manner; in some cases it is hardly influenced at all.

The semi-conductors are classified as:

a. excess electron conductors containing a stochiometric excess of a metallic element; they generally show a negative thermoelectric power. The excess metal may be obtained through a reducing heat treatment.

b. defect or hole conductors containing a stochiometric excess of a non-metallic element; they generally show a positive thermoelectric power. The excess non-metal may be obtained by heat treatment in a suitable gas.

The theoretical treatment of the electrical conductivity and the thermoelectric power of semi-conductors[35–40] results in the following correlation:

The electrical conductivity

$$\sigma = A \exp(-\Delta\epsilon/2k_0T),$$

where

$$A = 0.024 l_0 n_b^{\frac{1}{3}} T^{\frac{1}{2}} (\text{ohm}^{-1}\,\text{cm}^{-1}).$$

The thermoelectric power

$$\theta = \pm[(\Delta\epsilon/2Te_0) + \text{const.}].$$

The value of the constant is $5k/4e_0 = 108 \times 10^{-6}$ volt for extrinsic conductors and $2k/e_0 = 172 \times 10^{-6}$ volt for intrinsic conductors.

The above equations may be verified experimentally by measuring the electrical conductivity (σ) as a function of the temperature ($1/T$) and deriving the values of A and $\Delta\epsilon$. The experimental determination of θ as a function of the temperature ($1/T$) should result in the same $\Delta\epsilon$ value.

Several attempts have been made to correlate the theoretical calculations with the experimental evidence. Hochberg[41] found a reasonable agreement in the case of V_2O_5 and WO_3, but only a qualitative agreement with MoS_2, CuO and a mixture of cobalt oxides. Borelius[42, 43] found satisfactory agreement for Se.

The equations for σ and θ are now examined from the point of view of the efficiency of the thermoelectric process. The requirement for a high thermoelectric power θ implies that $\Delta\epsilon$ must

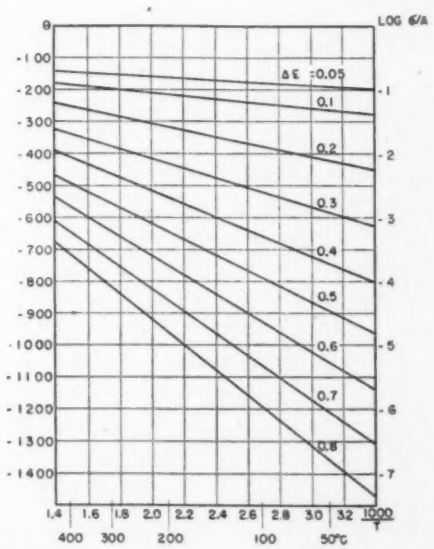

FIG. 3. Thermoelectric power θ and electric conductivity σ of semi-conductors as a function of the temperature T and the energy-level difference $\Delta\epsilon$; θ in microvolt/°C.

[35] A. H. Wilson, Proc. Roy. Soc. **133**, 458 (1931); **134**, 277 (1931).
[36] A. H. Wilson, Semi-Conductors and Metals (Cambridge 1939).
[37] B. Gudden, Ergeb. d. exakt. Naturwiss. **13** (1934).
[38] F. Seitz, J. App. Phys. **16**, 553 (1945).
[39] R. J. Maurer, J. App. Phys. **16**, 563 (1945).
[40] C. Wagner and E. Koch, Zeit. f. physik. Chemie **B32**, 439 (1936).
[41] B. M. Hochberg and M. S. Sominski, Physik. Zeits. Sowjetunion **13**, 198 (1938).
[42] G. Borelius, F. Pihlstrand, J. Andersson, and K. Gullberg, Ark. Mat. Astr. Fys. Svenska Vetens. **2**, No. 14, 30 (1944).
[43] G. Borelius and K. Gullberg, Ark. Mat. Astr. Fys. Svenska Vetens. **2**, No. 17, 31 (1945).

TABLE VIII.

Material	Electric cond. room temp. ohm^{-1} cm^{-1} σ	A	$\Delta\epsilon$	Thermo-electric power θ microv/°C ref. Cu near room temp.	Author
V_2O_5 monocrystal	10^{-5}		0.9	−900	41
V_2O_5 reduced (?)	0.03			−800	43
WO_3 sintered	10^{-5}		0.9	−900	41
TiO_2 sintered	0.2	9	0.06		43
TiO_2 reduced	5	22	0.08		44
TiO_2 further reduced	130	150	0.008		45
Fe_2O_3 reduced	210	25	0.01		45
SnO_2 reduced	6		0.1	−200	46
ZnO sintered reduced	5	5	0.03	−400	47
PbS pure	10^{-4}			700	49
PbS excess Pb	76			−300	49
PbS excess S	8			100	49
PbS melted	1000			−104	50
PbS reduced	455			−148	50
PbS excess S	30			71	50
PbS almost pure	0.3			530	26
PbS excess Pb	800			−150	26
PbS excess Pb (max.)	2000			−100	26
Ti sulfides sintered	0.15			−500	26
Ti excess S	100			−160	26
Cu_2S fused or sintered	20			280	26
Cu_2S excess Cu	0.03			620	26
Cu_2S excess S	200			80	26

be high. With increasing temperature the thermoelectric power decreases, therefore higher temperatures are less advantageous. The electrical conductivity is subject to the opposite condition, it increases considerably at higher temperatures and decreases at higher values of $\Delta\epsilon$. The value of A should be large, as the electrical conductivity is directly proportional to it. It should be noted that the porosity of pressed and sintered compacts should alter the value of A, but should not influence $\Delta\epsilon$.

Using various values of $\Delta\epsilon$, the conductivity in the form of $\log\sigma/A$ and the thermoelectric power θ can be plotted as a function of the temperature $1/T$. This is shown in Fig. 3. If the values of $\Delta\epsilon$ and A are known for any semiconductor, its conductivity as a function of the temperature can be obtained from Fig. 3, by inserting A into the corresponding σ/A values found on the particular $\Delta\epsilon$ line.

The efficiency calculations indicated that higher efficiencies can be expected only with thermoelectric powers in excess of 300-microvolt/°C, with a low heat conductivity of the order of magnitude $k=0.01$ with low specific resistance of the order of $\rho=0.001$ to 0.03 (conductivity $\sigma=1000$ to 33).

Figure 3 shows that near room temperature $\Delta\epsilon=0.2$ would correspond to a thermoelectric power of 440-microvolt/°C, with a corresponding $\log\sigma/A=-1.7$ or $\sigma/A\leqq 0.02$. For higher efficiency σ should be 33 to 1000 and therefore A should be at least 1500 or greater. At a temperature of 200°C $\Delta\epsilon=0.2$ would correspond to a thermoelectric power of 310-microvolt/°C, with $\sigma/A\eqq 0.1$ requiring an A value >1000.

The application of the efficiency calculations indicates that higher efficiencies may be obtained only from those semi-conductors, which show $\Delta\epsilon$ of the order of 0.2, with corresponding $A>1000$.

Table VIII shows the properties of some oxides and sulfides with relatively higher thermoelectric power values. The thermoelectric power of some other oxides or sulfides is rather high, but as their conductivity is excessive they were not included in this table.

Mixtures of oxides have been investigated by F. Fischer.[51, 52] The electrical conductivity of certain mixtures is much higher than the conductivity of the components; the thermoelectric power of the highly conducting mixtures is somewhat lower than that of the components.

Lead Sulfide Thermoelement

Inspecting Table VIII the material of highest conductivity is PbS with excess lead. This mixture shows metallic conduction, the conductivity decreasing at increasing temperatures. PbS thermoelements containing a slight excess of lead may be prepared by hot pressing and sintering. A thermocouple made of PbS and the ZnSb alloys of Table VII shows a thermoelectric power of 330 to 390 microvolt/°C. The specific heat conductivity of PbS was found to be

[44] W. Meyer, Physik. Zeits. **36**, 749 (1935).
[45] W. Meyer and H. Nedel, Physik. Zeits. **38**, 1014 (1937).
[46] G. Bauer, Ann. d. Physik **30**, 433 (1937).
[47] O. Fritsch, Ann. d. Physik **22**, 375 (1935).
[48] I. K. Krch, Abh Staats Univ. Saratov **14**, 54 (1938).
[49] H. Hintenberge, Zeits. f. Physik **119**, 1 (1942).
[50] L. Eisenmann, Ann. d. Physik **38**, 121 (1940).
[51] F. Fischer *et al.*, Ann. d. Physik **15**, 109 (1932).
[52] F. Fischer *et al.*, Ges. Abh. Kenntn. Kohle **12**, 516 (1937).

$k = 0.015$. The calculated efficiency of this couple, operating at a temperature difference of $\Delta t = 400°C$, is approximately 10 percent. The experimentally observed efficiency was 7 percent because of difficulties in attaching suitable end contacts to the PbS, which should be free of any contact resistance.

Efficiency tests made with Cu_2S failed to produce any noteworthy results.

CONCLUSIONS

The efficiency calculations establish a definite relationship between the thermoelectric power (e or θ), the specific electric resistance (ρ) or conductivity (σ), and the specific heat conductivity.

Higher efficiencies may be expected only with materials which show a constant Wiedemann-Franz-Lorenz relationship or a relatively small deviation from it. This criterion requires that the average specific resistance (ρ) should not be greater than 0.002 ohm cm ($\sigma = 500$) for materials of medium thermoelectric power (around 200-microvolt/°C). For high thermoelectric power values (around 500- to 1000-microvolt/°C, the maximum permissible average specific resistance (ρ) is about 0.03 ohm cm ($\sigma = 33$).

The thermoelectric power of most normal metals and alloys is less than 100-microvolt/°C, therefore their calculated efficiencies cannot exceed two to three percent even when operating at a temperature difference of 500 to 900°C. The observed efficiency of the best commercially available thermocouple (Chromel P–constantan) was only 0.9 percent, operating at the highest allowable temperature difference (500°C).

In the medium thermoelectric power range (200- to 300-microvolt/°C) some of the recently developed zinc-antimony alloys (containing small amounts of added metals) forming a thermocouple with constantan, produced an efficiency of 4.8 to 5.7 percent, at the highest allowable temperature difference (400°C). The same zinc-antimony alloy forming a thermocouple with a bismuth-antimony alloy, produced an efficiency of 4.2 percent at a much lower temperature difference (230°C). For these thermocouples the calculated and observed efficiencies showed very good agreement.

A survey of various alloys failed to produce any thermoelectric materials of higher calculated efficiency, with the exception of the tellurium-bismuth alloys and tellurium, with small amounts of some other metals.

Materials of higher thermoelectric power were found to contain Si, Sb, Bi, O, S, Se, Te (groups IV*B*, V*B*, VI*B* of the periodic table). Some of these materials are semi-conductors. The theoretical correlation of the electric conductivity (σ) and the thermoelectric power (θ) were applied to derive the criteria of high efficiency for this group of materials. A survey of published data failed to reveal suitable materials of high efficiency, with the exception of PbS containing excess lead, which in this form is actually a metallic conductor. Thermocouples made with PbS (with excess lead) and some of the zinc-antimony alloys mentioned above, produced an efficiency of 7 percent, with a possible expectation of 10 percent indicated by the calculation. The discrepancy is due to a junction-resistance.

Some of the semi-conductor material showing high thermoelectric powers are greatly affected by relatively small amounts of impurities. The presence of impurities may increase the conductivity very considerably, while the thermoelectric power is changed only slightly, the heat conductivity remaining practically uninfluenced. Further study of the effects of impurities may improve the properties of some materials showing high thermoelectric power values.

The theoretical calculations indicate that the problem of producing thermoelectric generators of higher efficiency can be solved only by continued search for materials of high thermoelectric power, low specific electric resistance (high electric conductivity) and low specific heat conductivity.

Cesium Chromate Photo-Tube Pellets

H. A. Liebhafsky and A. F. Winslow
Research Laboratory, General Electric Company, Schenectady, New York
(Received September 10, 1947)

The following results have been obtained in an exploratory investigation of the cesium chromate pellets used in the manufacture of photo-tubes: (1) hydrogen evolution or titration can be used to measure the yield of cesium with reasonable precision. Each method has limitations. (2) The theoretical yield could be obtained from cesium chromate-silicon pellets. (3) Within limits, the actual yield increases with the rate of heating; the maximum yield is not highly sensitive to composition in the range investigated. (4) No marked advantage was observed when titanium or zirconium was substituted for silicon as reducing agent. (5) An excess of hydrogen above the theoretical was consistently observed with nickel pellet holders, which points to a reaction of water vapor with reactive nickel formed during the heating and flashing of the pellet. The substitution of the less volatile molybdenum for nickel eliminated this difficulty. An excess of hydrogen was formed also when the reducing agent in the pellets was titanium.

It was suggested for purposes of further study that the complex process occurring when such pellets are induction heated be subdivided into two reactions of elementary silicon: (1) a preliminary exothermic reduction of hexavalent chromium, which initiates (2) a rapid reduction of monovalent cesium. The two reactions may proceed concurrently. This picture explains several observations made in the laboratory or in the factory.

THE function of the photo-tube pellet is to supply the alkali metal required for the light-sensitive surface. Such a pellet is usually made by compressing an intimately mixed powder containing a reducing agent and a compound of the metal, the metal being liberated in the tube by induction heating. Cesium chromate is a good compound for this purpose, and silicon is a good reducing agent; but little is known about the reaction between them.

Manufacturing processes could be considerably simplified if the pellets gave a reproducible yield. At the present time the only way of providing for enough metal is to make sure of an excess, though an excess is objectionable and must be removed in a subsequent bake-out. This investigation was undertaken in order (1) to find a reliable method of measuring the alkali metal produced when a pellet is "flashed," (2) discover under what conditions cesium chromate-silicon pellets give their maximum yield, and what this maximum is, (3) see how other reducing agents compared with silicon in effectiveness. The results given below were obtained before the war forced the work to be suspended.

EXPERIMENTAL DETAILS

Materials

Purified cesium chloride from the laboratory stock, made from pollucite ore by Dr. R. W. Moore, was the starting material for the preparation of cesium chromate. The sparingly soluble dichromate was precipitated out of a chloride solution and redissolved in cesium hydroxide electrolytically prepared, acetone finally being added to obtain the finely divided chromate. Chloride, which is objectionable in a chromate photo-tube pellet, was virtually absent from the product, the principal impurity present being sodium in small amount.

The silicon, titanium, and zirconium were commercial materials of good quality. The titanium was a "hydride;" that is, a product of indefinite composition which liberates hydrogen when heated to a low temperature (*ca.* 200°C) in vacuum. The hydrogen thus liberated did not falsify the experimental results since the system was always pumped out very carefully after the flashing of all pellets (see below).

Since all materials were powders, the particle size is an important variable. The silicon, titanium, and cesium chromate passed a 325-mesh sieve. The zirconium passed 100-, but was caught on 200-mesh. The thoroughly mixed pellet mixture containing silicon or titanium was put through 200-mesh; the zirconium mixture passed 100-mesh.

All pellets were prepared by subjecting about 25 mg of mixture to high pressure in a die. Before being used each pellet was weighed to 0.1 mg on an analytical balance.

Apparatus

The apparatus in Fig. 1 is designed to produce a mirror of alkali metal in high vacuum when a pellet is heated at a pre-determined rate, to make possible the reaction of this mirror with water vapor, and to permit measurement of the hydrogen thus liberated and titration of the alkali hydroxide formed. The operation of the apparatus is obvious and need not be described in detail. The weight of alkali metal and the pressure of hydrogen will be of the order of 10 mg and 100 microns, respectively; all manipulations were planned to give a precision near 1 percent of these quantities.

The rate of heating the pellet determines the "heating interval," which is the time, measured on a stop watch, that elapses between the closing of the induction-heating circuit and the explosive liberation of metal from the pellet to form a mirror on the enclosing bulb. (The metal escapes around the periphery of the pellet holder, which is held together by 3 or 4 spot welds.) The relationship between the setting of the induction heater and the heating interval had to be established in advance of the actual investigation; since this relationship, which will differ for each experimental arrangement, is sensitive to the relative position of induction coil and pellet, care was taken that this position did not vary from one run to the next. This position was so chosen that the periphery of the pellet holder was heated uniformly in the field. Consistent heating intervals were obtained only when the pellet was held in close contact with the metal, which ensured satisfactory heat transfer.

Pellet holders made of nickel had to be discarded because yields greater than 100 percent cesium were consistently obtained from silicon pellets by the hydrogen method (see below) when they were used; presumably the action of water vapor on active nickel formed during the heating period was responsible. This difficulty disappeared when molybdenum was substituted for nickel.

Evaluation of Yields

Cesium yields were always calculated according to the gas laws from the hydrogen liberated. To corroborate results thus obtained, the cesium hydroxide was occasionally titrated as follows. 5 cc of standardized 0.02 *N* perchloric acid was pipetted into the reaction bulb *H* (Fig. 1) at the end of the run, and the sides of the bulb were washed down with a little distilled water. After carbon dioxide had been expelled from the acid solution by boiling, the titration was carried out with 0.02 *N* sodium hydroxide containing methyl red. The acid was added to the bulb as soon as possible in order to minimize attack of the glass by cesium hydroxide.

Results from the hydrogen and from the titration method were calculated as percent yield for the pellet, whose weight and initial composition were known. A summary of all pairs of results obtained is given by Fig. 2, those in which the heating intervals were below 4 sec. being distinguished from the others. Inspection of Fig. 2 shows (1) that, three erratic points excepted, the agreement with the 45° line is generally satisfactory, (2) that for the low heating intervals the yield by the hydrogen method tends to exceed that obtained by titration. This tendency probably has the following cause. As the heating interval is decreased, the liberation of cesium becomes more and more explosive, with the result that some metal escapes the reaction bulb.

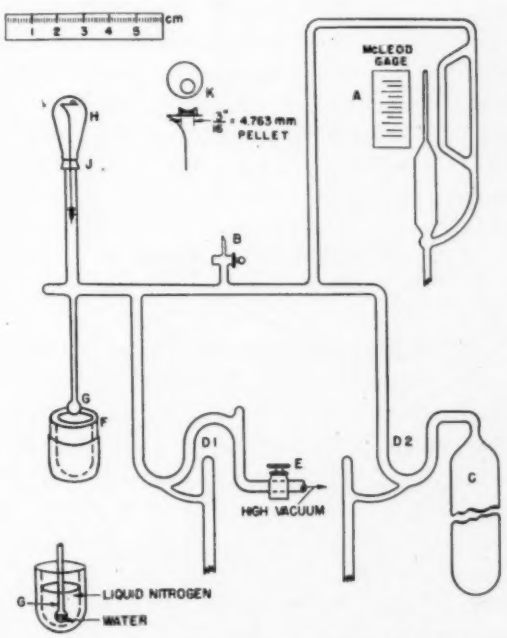

FIG. 1. Apparatus for studying activity of photo-tube pellets.

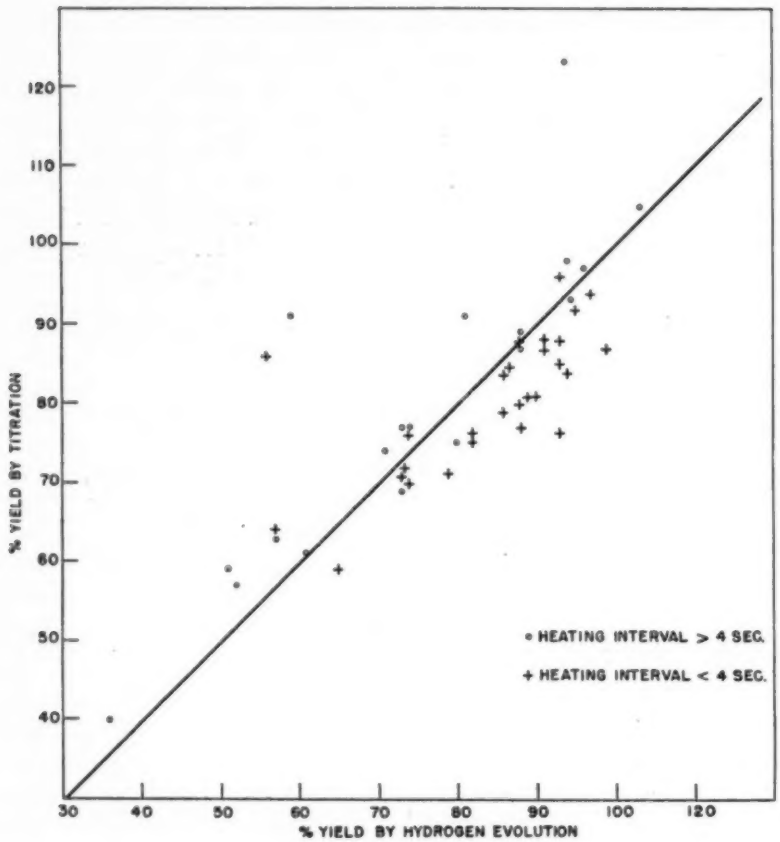

FIG. 2. Comparison of cesium yields as measured by hydrogen evolution and by titration.

Such metal would liberate hydrogen, but the corresponding cesium hydroxide would not be titrated. (Redesigning the apparatus might minimize this difficulty.) On this basis, we consider the hydrogen method to be the more reliable, provided there is no complicating liberation of excess hydrogen.

EXPERIMENTAL RESULTS

Silicon

The yields obtained by the hydrogen method on silicon-cesium chromate pellets of five compositions are shown in Fig. 3. The lowest abscissa plotted is 2 sec., because that is the heating interval corresponding to the maximum heating rate of which our experimental arrangement was capable. (In one instance a pellet flashed at 1 sec. and gave a 57 percent yield, as is recorded in Fig. 3. This result could not be duplicated.) It is noteworthy that the shortest heating interval becomes longer as the ratio Si/Cs_2CrO_4 increases; this is clear in spite of the scattering of the results, for the shortest interval at each composition was obtained with the maximum heating rate.

Figure 3 supports the following conclusions: (1) The yields fluctuate appreciably so that many measurements (more than in Fig. 3) are needed to establish all the characteristics of these pellets. (2) The theoretical yield, 100 percent, can be realized or very closely approached. (3) The yields tend to increase as the heating interval decreases. (4) The maximum yield is not highly sensitive to pellet composition in the range investigated. (If the heating rate could be increased, the yield for compositions such as $Si/Cs_2CrO_4=4$ would probably increase also.)

Titanium

The striking feature of the titanium results is how frequently the calculated yields exceed 100 percent. This excess of hydrogen cannot be de-

rived from titanium hydride, for, as has already been mentioned, the system was always thoroughly pumped out after each pellet was flashed. The most likely source of this hydrogen is the reaction of water vapor with highly reactive material, either titanium or one of its compounds, produced during the heating interval.

It will be remembered that a similar evolution of excess hydrogen was observed when nickel pellet holders were used. There the reacting material was probably evaporated or sputtered metal, since the pellet holder is not likely to be involved in a chemical reaction. With titanium, however, the possibility of a lower valent compound that is a powerful reducing agent must be considered, especially since titanium is more likely to form such compounds than is silicon or zirconium.

Because of the formation of this excess hydrogen, which may have occurred no matter what the yield, there is little point in discussing the titanium results. They appear to be more erratic than those obtained with silicon, but that seems to be the principal difference. Titration ought to supplement the hydrogen method in further work with titanium; in any case, there seems to be no reason for replacing silicon by titanium in photo-tube pellets.

Zirconium

Five experiments with $Zr/Cs_2CrO_4 = 1$ gave the following results: 82 percent at 5.0 sec., 81 per-

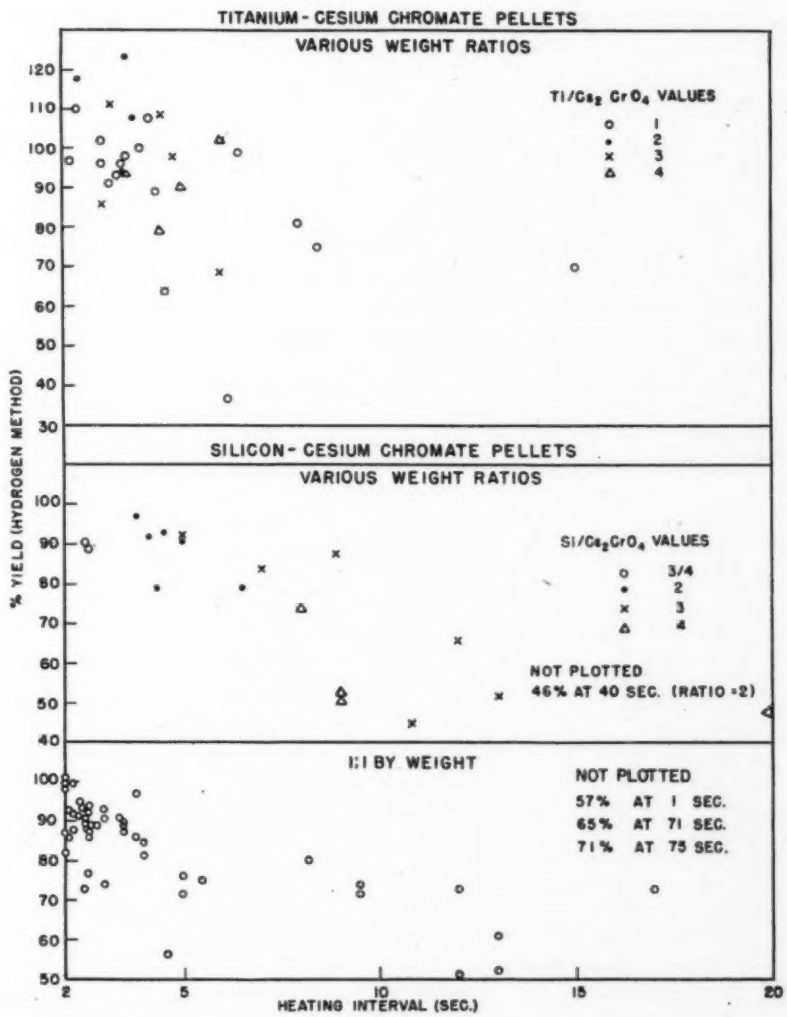

FIG. 3. Cesium yields for various compositions and various heating intervals as measured by hydrogen evolution.[1]

cent at 4.6 sec., 75 percent at 4.2 sec., 68 percent at 4.8 sec. Under our conditions, zirconium probably is a less effective reducing agent than silicon.[1]

DISCUSSION

The present investigation is only an approach to the problem of cesium chromate photo-tube pellets, but it has shown how their yields can be measured and revealed several of their more important characteristics. The stoichiometry involved needs to be established by examining pellet residues; meanwhile, however, the equation

$$4Cs_2CrO_4+5Si=2Cr_2O_3+8Cs+5SiO_2 \quad (1)$$

may serve as a basis for a brief discussion intended primarily to point the way to future work. In reaction 1, 1 gram of silicon is equivalent to 11 grams of cesium chromate; hence, every silicon pellet investigated contained the reducing agent in large stoichiometric excess.

The heating interval may be subdivided into a relatively long initial heating period, and a short final period in which the cesium is liberated almost explosively. With the heating rate at its maximum, the heating interval lengthens as the proportion of the chromate decreases (Fig. 3). This indicates that the induction heating is being supplemented by an exothermic reaction, limited by the chromate present but evolving no cesium. For this reaction, we shall naively write

$$4Cs_2CrO_4+3Si=2Cr_2O_3+3SiO_2+4Cs_2O. \quad (2)$$

Cesium oxide would, of course, never exist free in contact with the two other oxides. But reaction 2 does emphasize that the action of hexavalent chromium on silicon supplies the heat that facilitates cesium liberation; this point of view is logical also because monovalent cesium, the other oxidizing agent present, is bound to be far the less reactive toward silicon.

For the cesium liberation we then write

$$4Cs_2O+2Si=2SiO_2+8Cs. \quad (3)$$

Actually, each silicon grain probably becomes covered, during the initial heating period, by a matrix containing the three resultants of reaction 2; cesium liberation occurs when the temperature is high enough to make possible the reaction of this matrix with silicon.

Reaction 2, if it proceeds too slowly, can give a matrix that blocks reaction 3. At least, this seems the best explanation for these observations: (1) Cesium yields tend to decrease as the heating interval increases (Fig. 3). (2) It has been observed in the factory that pellets stored near 100°C for long periods tend to give erratic yields. (3) Pellets containing dichromate, which would form more matrix since it contains more hexavalent chromium than does chromate, are more erratic than those made with chromate.

[1] In this connection, cf. de Boer, Broos, and Emmens, Zeits. f. anorg. allgem. Chemie, **191**, 113 (1930).

Letters to the Editor

Remarks on Some Recently Developed Devices for Summing Fourier Series for Crystal Structure Analysis

C. L. CHRIST
Stamford Research Laboratories, American Cyanamid Company, Stamford, Connecticut
August 6, 1947

THERE appeared in a recent issue of this journal a paper entitled, "An electronic computer for x-ray crystal structure analysis," by R. Pepinsky.[1] The author states that the method is based upon Huggins' modification[2,3] of Bragg's earlier method[4] for photographically summing Fourier series. In the Huggins method the necessary sinusoidal distribution of bands for each Fourier term is referred to a square cell in order that the masks prepared may be used for the study of any crystal. Thus the Huggins method differs from the Bragg method in that a set of masks once prepared may be used repeatedly. With the present electronic computer the bands representing each term are oriented and spaced according to the dictates of the actual shape of the unit cell of the crystal under study.[1] This method seems, therefore, to be more closely related to the original Bragg method than to the Huggins modification.

In the electronic computer paper it is further stated[1] that the sand deposition method of McLachlan and Champaygne for summing Fourier series[5] does not permit the computation of projections having various axial ratios and angles. The fact that the "sand machine" gives projections having the same shape as that of the unit cell being studied, with regard to both the ratios of the edges of the cell and the inter-edge angle, is explicitly stated in the abstract preceeding the body of the publication cited[5] and is, of course, implicit in the detailed description of the theory of the method. In this connection it is interesting to compare the electron density projection of hexamethyl benzene given in the paper of Brockway and Robertson[6] with that obtained using the same data, with the McLachlan-Champaygne method,[5] and with the Huggins method.[3] Such a comparison shows that the use of the square lattice necessary to the Huggins method introduces distortion of the projected molecule over and above that introduced by the non-parallelness of the plane of the molecule and the plane of projection, as was pointed out by Huggins.[3] In contrast, the sand deposition method gives a projected molecule essentially the same as that obtained by Brockway and Robertson.

All three of the summation devices discussed above are based upon an equation of the type:[4]

$$\rho(x, y)' = |F_{hko}| + \sum_{h=-\infty}^{\infty} \sum_{k=-\infty}^{\infty} |F_{hko}| \cos[2\pi(hx+ky) - \alpha_{hko}]. \quad (1)$$

Any term $(S_{xy})_{hko}$ of this series, involving the phase angle α_{hko}, may be represented by the sinusoidial band distribution

$$(S_{xy})_{hko} = |F_{hko}| + |F_{hko}| \cos 2\pi(hx+ky) \quad (2)$$

displaced in the positive direction along the normal to the wave crests by the linear amount δ_{hko}, which may be represented by the equation

$$\delta_{hko} = \frac{\alpha_{hko}\lambda_{hko}}{360}. \quad (3)$$

Here λ_{hko} is the distance between wave crests, and α_{hko} is expressed in degrees. The electronic computer, at present, is confined to projections having a center of symmetry at the origin,[1] i.e., α_{hko} has the value 0 or 180°. In the case of the sand deposition method α_{hko} may have any value whatsoever,[5] and since the true unit cell is projected, λ_{hko} is precisely the interplanar spacing d_{hko}. There seems to be no reason why the Huggins method cannot also be used for non-centrosymmetric projections, since the use of Eq. (3) is compatible with the method. The desired result may be obtained, for example, in the case of non-centrosymmetric projections, by shifting the photographic film or paper on which successive exposures for each term $(S_{xy})_{hko}$ are being made[2] before each exposure by the amount δ_{hko}, according to the value of α_{hko}. It follows that for centrosymmetric cases, if this method of shift is used, only positive masks are necessary since their negative counterparts are obtained, in projection, by a shift of $\delta_{hko} = \lambda_{hko}/2$. In the case of the Huggins method it is necessary to remember that λ_{hko} is not, in general, equal to d_{hko}.

[1] R. Pepinsky, J. App. Phys. **18**, 601 (1947).
[2] M. L. Huggins, J. Am. Chem. Soc. **63**, 66 (1941).
[3] M. L. Huggins, J. Chem. Phys. **12**, 520 (1944).
[4] W. L. Bragg, Zeits. f. Krist. **A70**, 475 (1929).
[5] D. McLachlan, Jr. and E. F. Champaygne, J. App. Phys. **17**, 1006 (1946).
[6] L. O. Brockway and J. M. Robertson, J. Chem. Soc. 1324 (1939).

New Books

When the Earth Quakes

By JAMES B. MACELWANE, S.J., Pp. 283, Figs. 251, 15½×23 cm. The Bruce Publishing Company, Milwaukee, 1947. Price $5.00.

This book presents in non-technical language an introduction to seismology in all its phases. This is a popular treatment of an extensive field. Neverthless the book can command the interest of the technically trained reader.

Eleven chapters are devoted to natural earthquakes. Among the subjects discussed are: kinds of earthquakes, mechanisms of earthquakes, immediate and ultimate causes of earthquakes, isostasy, earthquake prediction, field studies, instrumental studies of earthquakes, location of epicenters, sea quakes, seismic sea waves, and the principles of seismographs. Twenty modern earthquakes are described in considerable detail. Each description is accompanied by a map of the epicentral region and there are many good reproductions of photographs showing the effects of earthquakes. There is reproduced also an excellent collection of photographs of seismographs. Older types as well as the most recently developed instruments are represented.

The remaining six chapters present several less-publicized branches of seismology.

Two chapters outline the purpose, methods, and instruments of engineering seismology which is the study of buildings and structures from the point of view of resistance to damage by earthquakes. There are excellent descriptions and illustrations of accelerographs, strong motion seismographs, and vibration meters. Also explained and illustrated are the shaking machines used to generate vibrations in the ground and in buildings or other structures.

One chapter deals with seismological engineering—a term used to cover the study of industrial problems arising from man-made disturbances, such as quarry blasts or machinery vibrations, and the laboratory study of those rock properties involved in natural or artificial earthquakes.

The author describes rock bursts which constitute a serious safety problem in underground workings in some areas. He explains the rock properties which make bursts possible and shows how the seismological attack on the problem has achieved at least partial success.

In another chapter is presented an easily understood explanation of the seismic refraction and reflection methods of mapping buried structures. The machanism of petroleum accumulation is outlined and several illustrations of instruments and equipment as well as good reproductions of commercial field records.

The final chapter, entitled "Microseisms and storms at sea", is based upon recent work. The nature of the relation between large microseisms and storms at sea has been established for only a few years. The author decribes the first application of this newly acquired knowledge. During the latter part of World War II special seismograph stations were set up in the Carribean area to aid in the detection and location of storm centers at sea.

Appendix A discusses briefly the geological forces at work on the earth and explains many geological terms.

There is an extensive bibliography to which references are made in the text and a glossary of terms which may be new to the average reader.

This well written book by a famous authority in seismology gives an interesting informative account of earthquake study. In addition, it does a good service for the literature by introducing aspects of modern seismology which are less familiar to workers in other fields.

The author is Dean of the Institute of Geophysical Technology of St. Louis University.

JOHN N. ADKINS
Massachusetts Institute of Technology

Mechanism of Reactions at Carbon-Carbon Double Bonds

By CHARLES C. PRICE. Pp. 120, 16×23 cm. Interscience Publishers, Inc., New York., 1946. Price $2.50.

This book is based on a series of lectures presented by the author at the Polytechnic Institute of Brooklyn, and is the first volume of a series of *Lectures on Progress in Chemistry* edited by H. Mark. It is clearly pointed out in the introduction and preface that the book is not intended to be a complete detailed review of all published work on the subject, but rather a brief treatment of the pertinent information together with the author's personal interpretation of the material.

The book deals ultimately with the subject of polymerization and the various mechanisms involved. However, more than half of the book is devoted to background material on structure and reactions of unsaturated compounds in general. Modern concepts of electronic structure are presented in the first chapter together with their relation to reactivity, orientation, and reaction mechanisms. The concept of a pulsating resonant mesomerism is compared to the fixed hybrid theory of resonance, and it is apparent that the author is somewhat skeptical of certain aspects of the resonance concept as applied to organic molecules. Evidence is presented to show that an electrostatic approach may be more fundamental than the resonance hypothesis in explaining many reactions such as the orientation of substitution in benzene derivatives in which the substituent already present is one of those which do not appear to be capable of mesomeric interaction with the unsaturation of an aromatic ring or a double bond.

The second and third chapters deal with the mechanisms of ionic and free radical reactions, respectively, at double bonds. Aromatic as well as olefinic reactions are included in both chapters.

The last four chapters deal with the mechanisms involved in the various types of polymerization. The free radical mechanism of addition polymerization is discussed in Chapter 4; and the various factors involved in copolymerization are presented in Chapter 5. The author's theory that the polarity of the double bond is an important determining factor in copolymerization, is of particular interest.

Polymerization in emulsion and in suspension are treated in Chapter 6, with the function and fate of the emulsifying agent receiving particular attention. Chapter 7 concludes the book with a discussion of the polar mechanism of polymerization, and the catalysts which promote this type of reaction.

The book is well written and fully illustrated throughout with specific formulae and reactions. There are a few minor errors in the printing such as the apparent omission of certain substituent groups in formulae on pages 86 and 102. The personal manner of presentation lends interest to the book, and the author's frank appraisal of various theories and mechanisms contributes much to its value. However, the reader should keep in mind that other authorities may not be in complete accord with all of the author's interpretations. The book should be of great interest to all who are concerned with the modern concepts of organic chemistry in general, and will be of particular value to those who are concerned either with high polymer chemistry or with the general question of reaction mechanisms involving unsaturation in both aliphatic and aromatic compounds.

J. Reid Shelton
Case Institute of Technology

Cosmic Radiation

Edited by W. Heisenberg. English translation by T. H. Johnson. Pp. 192, 16×24½ cm. Dover Publications, New York., 1946. Price $3.50.

We may welcome the advent of any opus edited by and contributed to by so competent a physicist as Heisenberg. Because the subject of the cosmic radiation has so few adequate, modern treatises, this one is doubly welcome. The book has come at a time to help meet the fast-growing need for good compendia in this field.

The book represents the views of a number of authors, and is a condensation of a series of lectures by these persons. Each chapter is written by a different author, the majority of whom are well-known investigators in this field. Hence the book is certainly authoritative.

The book starts with a review of the present state of cosmic-ray knowledge by Heisenberg. Next, the soft component is considered, with chapters on cascade theory by Heisenberg and on large showers by Moliere. Turning to the hard component, the bulk of the book is devoted to various phases of mesotron studies. Klemm discusses the production of mesotrons, Klemm and Heisenberg the showers with penetrating particles, Voltz the absorption of mesotrons, and Weiszacker the excitation of bursts by mesotrons. The decay is next treated by Heisenberg, the decay electrons by Bopp, and the theory of mesotrons by Weiszacker. Next follow chapters on the mesotron theory of deuterons by Flugge and the theory of explosive showers by Heisenberg. The final three chapters deal with nuclear disruptions as discussed by Bagge, the production and distribution of neutrons as treated by Flugge, and the geomagnetic effects which are summarized by Meixner. At the end a rather extensive bibliography is appended.

As would be inevitable in a work of this sort, the chapters vary somewhat in the degree of sophistication expected of the reader. Naturally, each author writes of his own specialty from his own point of view, and with varying mathematical complexity, the theoretical chapters being the most complex. The style of each author varies, but the skillful editing of the volume is evident.

The book is clearly not intended as a text, and is written primarily for the specialist in the field. It is not suitable for beginners. However, every graduate student contemplating a thesis in the subject should be thoroughly familiar with the contents. Further, since it is precisely cosmic rays themselves which provide us with our only source particles of energies higher than can be produced in man-made accelerators, the entire subject of ultra high energy physics is based on a study of cosmic-ray phenomena. Hence the book will be of value to all those interested in this rapidly expanding field. The subject is presented on the level of articles in the Reviews of Modern Physics. It will be of value to those in allied fields who wish to inform themselves about current ideas on the subject. The publication will constitute a desirable addition to any physicist's bookshelf.

S. A. Korff
New York University

Modern Development of Chemotherapy

By E. Havinga, H. W. Julius, H. Veldstra, and K. C. Winkler. Pp. 175+xi, Figs. 31. Elsevier Publishing Company, Inc., Amsterdam, 1946. Price $3.50.

This volume is number four in a series of more than twenty monographs intended to record the advances made in various branches of scientific work in Holland during World War II. We cannot but be amazed at the nobility of spirit which showed itself by the perseverance in difficult activities in occupied countries during the war. This nobility is now shown again in the unique mixture of pride and generosity with which those activities are revealed to the rest of the world.

This little book summarizes the work of several Dutch laboratories up to about May 1945. In it are detailed numerous researches having to do primarily with sulfonamides, and to a very small extent with antibiotic chemotherapeutic agents. It is regrettable that this brave record can hardly be assured a permanent place in the scientific literature. Such a monograph is inevitably occupied with details too near the uncertain boundaries of knowledge to have a timeless factual value. This one is on the other hand, so limited in geographical coverage and (understandably enough) was long enough delayed in preparation that it is hardly a review of modern trends or recent advances. Especially is this true in the case of a field such as chemotherapy which is developing so rapidly all over the world.

The first and longest section deals with bacteriological investigations by Julius and Winkler on the mode of action of sulfonamides. This work is a well-conceived straightforward approach which has certainly foreshadowed many features of the theory that our more recent knowledge (particularly of the folic acids) has made more secure. Much of this approach is based upon bacterial growth curves which were probably determined more reliably than in almost any

similar study. Modifying the environments of the bacteria gave the opportunity to study the intimate effects of various inhibitors and activators. Wood's *para*-aminobenzoic acid displacement theory is re-examined with an admirable detachment. The authors insist that an antagonistic displacement of *para*-aminobenzoic acid by sulfonamide has never been demonstrated, only the reverse antagonism being known. The net result is that sulfonamides are viewed as interfering with a mechanism (involving in some way *para*-aminobenzoic acid) which leads to the synthesis of a peptone-like substance.

Here and elsewhere in the book, the authors discuss certain of the findings of workers elsewhere that were available to them through abstracts or otherwise. This is true even though in the preface it is stated that "foreign work will be referred to only in so far as it has a direct bearing on Dutch research work."

A section describing physico-chemical investigations on the sulfonamides by Havinga and Veldstra does not materially increase our knowledge of the mode of action of these substances. Certain studies were made of the titration curves, light absorption spectra, polarographic behavior, and the properties of surface films. The impression is given that these approaches were chiefly exploratory, based upon plausible but casual hypotheses. An interesting part of this section is the attempt to estimate the collision frequency of *para*-aminobenzoic acid or sulfonamide molecules with receptor spots upon a bacterial cell. If it is assumed that the former substance is required only at certain moments of the division cycle for normal growth to occur, then it may be easier to understand why the antagonists must be present in much higher concentration if they are to prevent growth.

The results of the testing of approximately seventy-five synthetic compounds related to sulfanilamide are given. There is a brief summary of clinical and animal testing of a few of these substances. Finally, the mold antibiotic "expansine" is described, a substance that appears to be identical with clavacin (and patulin) discovered elsewhere at about the same time.

This volume makes available in very satisfactory English translation a summary of brave and independent investigations.

ROLLIN D. HOTCHKISS
Rockefeller Institute

High Vacuum Technique

By J. YARWOOD. Second Edition. 15½×24 cm. John Wiley and Sons, Inc., New York, 1945. Price $2.75.

From the authors intention, which, as stated in the preface, is "to describe important industrial processes hitherto discussed only in scientific periodicals," it is difficult to discern to whom he addresses this addition to the "know-how" literature.

The author's intention "to introduce the latest developments . . . with special emphasis on the most recent work," is unfulfilled—the author does not, for example, discuss the palladium-window ion gauge for leak hunting, the silicone-diffusion pump oils, or Vycore.

There are instances where the author contributes but little to the subject he treats—for example, on page 82, after stating that silver oxidation can be followed by surface color changes the exposition concludes with: "The degree of oxidation is found only by experience based on previous experimental work . . . ."

The judgment of your reviewer does not always concur with that of the author on the value of the apparatus or of the procedures described and evaluated. It would be helpful to know which procedures the author knows first hand and intimately, and which he is merely re-writing, or reporting.

The author occasionally lets himself speak in the vernacular as: "The gun must be vacuum-stoved before mounting in the tube." In a book such as this the use of the vernacular seldom enlightens those who understand it and is unintelligible to those one would teach.

The chapter on the properties of materials does contribute to the author's stated intention, "to bring together in one volume the diverse facts regarding the relevant properties and uses of materials encountered in all types of vacuum work." However, his treatment of some materials, like copper, is certainly not up-to-date from the high vacuum point of view.

It is to be expected that engineers and experimental physicists will get substantial help and provocative suggestions from Yarwood's work. The references to the literature will be of value to some; several procedures are described which will be novel to others; and the subject matter is more modern than the "classics", to which the author refers.

JOHN D. STRONG
The Johns Hopkins University

Electrical Transmission in Steady State

By PAUL J. SELGIN. Pp. 427, Figs. 100, 14½×22 cm. McGraw-Hill Book Company, Inc., New York, 1946. Price $5.00.

This book, like many others recently published, is the outgrowth of notes developed in connection with courses taught for war-training purposes. For this reason the manner of presentation of the subject matter, as well as its selection, is not entirely what one would desire for ordinary undergraduate instruction in an electrical communications curriculum on a peacetime basis. The book is essentially one on the subject of transmission lines for use at high and ultra high frequencies, the first 332 pages out of a total of 416 being devoted to this topic. Following this material there is a chapter on inductively coupled circuits, a ten-page chapter on capacitive coupling, and two chapters, totalling 34 pages, on high frequency vacuum-tube amplifiers.

The first two chapters comprise a condensed review of some basic lumped-constant circuit principles, including such topics as matching and optimizing conditions for power transfer at junctions, transmission and insertion loss, reciprocity, Thévenin's and Norton's theorems, image parameters, etc. The steady-state behavior of transmission

lines is then dealt with through considering the limit approached by an increasing number of smaller and smaller lumped networks in cascade, and a detailed (rather involved) discussion is given of the frequency behavior of the attenuation and phase functions. At this point and throughout the remainder of the book, one has a very definite conviction that a student having no previous acquaintance with this subject would find the going very rugged indeed, unless considerable additional guidance were available from an experienced instructor.

The input impedance of the line is dealt with through a discussion of the mapping properties of the hyperbolic tangent function, followed by a consideration of the impedance transformations of analogous lumped networks based upon the circle properties of simple inversion. The bi-polar line chart is then introduced and applied to various conventional impedance-transformation problems, including the quarter-wave line as an impedance transformer. This discussion is generalized to a consideration of cascades of quarter-wave lines used to secure a more frequency insensitive impedance transformation, and an "optimum" design of such a transformer is given which, after several pages of involved algebra, finishes with the statement of an end result, the proof of which "although not particularly difficult, is beyond the scope of the present discussion" (footnote, page 203 . Single and double stub tuners are discussed with the help of the Smith Chart (not so called), and detailed treatment is given of the frequency sensitivity of such tuners, taking into account the effect of incidental dissipation and expressing these effects in terms of the "*Q*" of the system.

Chapter XI then turns to a consideration of a review of static field theory, a discussion that in the next chapter is extended to dynamic fields and Maxwell's equations. This material admittedly is too condensed to be helpful to the beginner, while for the reader with sufficient background to follow the argument, it fails to provide a picture that is compact and effective in presenting the essential relationships clearly and completely. While a reasonably good job is done here for readers who at this stage do not expect to acquire a proficient knowledge of these tools, there is left much room for improvement.

After some discussion concerning the relationship of lumped circuit theory to field theory, the author considers the propagation of plane waves and derives the uniform line equations from the field equations, extending this discussion to the consideration of the exponential tapered line and the exponential stub line.

The subject of inductively coupled, lumped tuned circuits given in the following chapter (XIV), and introduced through a consideration of self- and mutual inductances and the simple transformer, is dealt with in a manner as involved as any that this reviewer has seen to date (the average student must surely despair at this point). The succeeding short chapter on capacitive coupling is given primarily as a means for dealing with the inter-electrode capacitances of vacuum tubes, of which some basic principles are discussed in the concluding brief pages of this book.

A feature on which the author is to be complimented is the inclusion throughout the book of illustrative numerical examples fully worked out.

In view of some of the above rather harshly critical comments it is only fair to state in conclusion that for the purpose for which this material was originally intended, the accomplishment of the author ranks on the whole with the better text material of a similar nature. Now that war-training programs are over, however, it is to be hoped that more attention in textbook writing will be given to the needs of students following a more orderly and progressively stimulating program of education in basic circuit theory and closely related subjects.

E. A. GUILLEMIN
Massachusetts Institute of Technology

New Booklets

Fischer and Porter Company, Hatboro, Pennsylvania, has issued a 32-page booklet entitled *A New Era in Liquid and Gas Flow Measurement*, which describes the advantages of the flowrator meter for flow rate measurement. Address request to Department 6F-F of the company.

Burrell Technical Supply Company, 1936 Fifth Avenue, Pittsburgh 19, Pennsylvania, has published a bulletin on its *Junior Spectrophotometer—The Successor to Colorimeters*. 8 pages, free on request.

The Daven Company, 191 Central Avenue, Newark 4, New Jersey, announces the publication of a new bulletin of technical data, presenting information widely used in the design of sound equipment. 4 pages. Free on request. Write on company letterhead.

Tin Research Institute, Fraser Road, Greenford, Middlesex, England, issues at regular intervals (because of present conditions) a review entitled *Tin and Its Uses*. The issue of July 1947 contains 16 pages and has numerous photographs in color. Interested readers are invited to address a request to the Publications Department of the Institute, stating that they wish to receive, free of charge, any publications of the Tin Research Institute dealing with given subjects or products (naming them), and mentioning their own business connections and titles. The July 1947 issue may be obtained directly from the Battelle Memorial Institute, 505 King Avenue, Columbus, Ohio.

The Gaertner Scientific Corporation, 1201 Wrightwood Avenue, Chicago 14, Illinois, announces two new bulletins: 140–74, entitled *Dilatation Interferometer*, and an unnumbered booklet entitled *Survey of Precision Instruments*, which is intended to serve as a guide to the company's products. Both bulletins are eight pages in length and are free on request.

Interchemical Review for Summer 1947, published by the Interchemical Corporation, 432 West 45th Street, New York 19, New York, features "Acids, bases, salts—pH," by C. Ross Bloomquist, and "Printing inks for postage stamps," by Milton Zucker. 30 pages.

Eberbach and Son Company, Ann Arbor, Michigan, has published the fall issue of its house magazine, the *Announcer of Scientific Equipment.* The feature article is entitled "Functional design of laboratory glassware". Free on request.

The National Bureau of Standards has announced the publication of the following bulletins in the physics field. All are available at 10 cents per copy from the Superintendent of Documents, Government Printing Office, Washington 25, D. C.

RP 1807—*Solution of Problem of Producing Uniform Abrasion and Its Application to the Testing of Textiles*" by Herbert F. Schiefer.

RP 1808—*Chromaticities of Lovibond Glasses* by Geraldine W. Haupt and Florence L. Douglas.

RP 1813—*Resistance-Temperature Relation and Thermoelectric Properties of Uranium* by Andrew I. Dahl and Milton S. Van Dusen.

RP 1814—*Infared Absorption Spectrum of Carbon Disulfide* by Earle K. Plyler and Curtis J. Humphreys.

North American Philips Company, Inc., 100 East 42nd Street, New York 17, New York, has issued a 4-page folder entitled *X-Ray Diffraction Camera for Microtechniques.* The company states that it should be of value to those actively engaged in fiber research. Free on request.

The *RCA Review* Department of RCA Laboratories Division, Princeton, New Jersey, has published the first volume of its new *Engineering Book Series*, entitled *Patent Notes for Engineers.* Copies may be obtained from *RCA Review* at $2.50 per copy for the permanent clothbound edition (plus 20 cents per copy postage if mailing address is outside the United States). The book was written by the director of the company's patent department.

Here and There

New Appointments

Bruce S. Old has been appointed consultant to the Atomic Energy Commission, Division of Research, in the capacity of chief metallurgist. He will continue his present work with Arthur D. Little, Inc., on a part-time basis. Dr. Old will assist in organizing the work of the Commission in the metallurgical field.

Irving A. Denison has been named Chief of the Underground Corrosion Section of the National Bureau of Standards.

Bowen C. Dees (until recently an Assistant Professor of Physics at Rensselaer Polytechnic Institute) has accepted a position as physicist with the Economic and Scientific Section, under the Supreme Commander for the Allied Powers in Tokyo. He will survey and advise concerning the physical research being conducted in the university and commercial laboratories in Japan.

Ernest R. Hanson has joined the staff of Foster D. Snell, Inc., to direct research and development in the field of plastics and rubber.

Necrology

Dr. Selig Hecht, Professor of Biophysics at Columbia University, died in New York on September 18. A distinguished authority in the field of vision, Dr. Hecht had been an Associate Editor of the Journal of Applied Physics since 1943.

Awards

Warren A. Marrison, a member of the technical staff of Bell Telephone Laboratories, has been awarded the British Horological Institute's gold medal for 1947 in recognition of pioneer researches in the development of the quartz crystal clock, which has become the most accurate timekeeper in the world.

A. A. Knowlton, veteran physics professor at Reed College, Portland, Oregon, was recently voted a special award of $1,000 for distinguished teaching by directors of Research Corporation. The award is unique in that Dr. Knowlton, now in his thirty-third year at Reed, may spend it in any way he wishes. It was based on the extraordinary achievement of Dr. Knowlton's graduates. Specifically, the award stems from a recent study in the American Journal of Physics which showed that of all physicists granted Ph.D. degrees by American universities between 1936 and 1945, a disproportionate number had done their undergraduate work at one of two small colleges—Reed, and North Central College, Naperville, Illinois. (A similar award has been voted to Dr. Clifford N. Wall, formerly of North Central.)

Lincoln Arc Welding Foundation Award and Scholarship Program

The James F. Lincoln Arc Welding Foundation, Cleveland 1, Ohio, has issued a brochure outlining the continuing features of its ten-year award and scholarship program designed to help develop the arc welding industry. Under the award plan, engineering students of various colleges will submit papers on arc welded design. Under the scholarship plan, scholarships will be allocated to the schools in which the three highest award winners under the award program are registered. Awards will total $5,000 and scholarships, $1,750. Rules for the 1947–1948 competition may be obtained by addressing the Secretary of the Foundation at Cleveland 1, Ohio.

Research Corporation Reports on Grants

Research Corporation, which in late 1945 established the Frederick Gardner Cottrell Fund for grants in aid of postwar science, has announced that in the following year more than 100 grants were approved, totaling about $430,000. The grantee institutions are located in about thirty states, Alaska, and the District of Columbia. The awards were made largely to aid younger men just returned to academic research from wartime occupations.

Conference on the Administration of Research

A conference on the administration of research was held at The Pennsylvania State College October 6 and 7, 1947. It was sponsored by the School of Engineering of the College. Two hundred people registered, representing laboratories, both large and small, managed by industry, educational institutions, and governmental agencies. Proceedings of the conference will be published as soon as possible, at a price of $3. Persons who wish to have a copy and who did not have an opportunity to ask for it at the conference may order from Professor Kenneth L. Holderman, The Pennsylvania State College, State College, Pennsylvania.

Pittsburgh Physical Society Officers

The Physical Society of Pittsburgh has elected the following officers for the year 1947–1948: *President*, Dr. Frank Morgan, Gulf Research and Development Corporation; *Vice President*, Dr. E. Stickley, Pittsburgh Plate Glass Company; *Secretary-Treasurer*, Dr. F. A. Schwertz, Mellon Institute.

Bureau of Standards Establishes Atomic Physics Division

The National Bureau of Standards has formed a Division of Atomic Physics in which the main Bureau activities relating to atomic and molecular physics have been grouped together. The functions of the new division are the promotion of fundamental fact finding research and the precise determination of important fundamental standards in the field of atomic physics. Six sections make up the new division: spectroscopy, electronics, mass spectrometry, radioactivity, x-rays, and atomic physics. Dr. E. U. Condon, Director of the Bureau of Standards, has assumed charge of the new division, and Dr. Robert D. Huntoon has been named assistant chief.

Conference on the Use of Radioactive Isotopes in Agricultural Research

The Alabama Polytechnic Institute, in cooperation with the Oak Ridge Institute of Nuclear Studies, sponsored a three-day conference on the Use of Radioactive Isotopes in Agricultural Research at Auburn, Alabama, December 18–20, 1947. The attendance, through special invitations, consisted of representative scientists largely from the southeastern States.

Lalor Foundation Fellowship Program

The Lalor Foundation fellowship program at the Marine Biological Laboratory, inaugurated in 1947, will continue in 1948. Postdoctoral summer fellowships in the fields of biophysics, biochemistry, and physiological chemistry will be available. The fellowships are designed primarily to aid promising young investigators who can make maximum use of the facilities and opportunities provided at the Marine Biological Laboratory. In addition to laboratory facilities, the grants are intended to cover approximately the living expenses of the investigators at Woods Hole and necessary traveling expenses to and from Woods Hole. The committee administering the fellowships consists of Drs. Eric Ball, Kenneth Cole, Charles Packard, A. K. Parpart, and C. W. Metz (Chairman). Inquiries and applications should be addressed to the Director of the Marine Biological Laboratory, Woods Hole, Massachusetts. The applications should be received by December 31, 1947, but will be considered after this date.

Calendar of Meetings

December, 1947

29–31 American Physical Society (and its Division of High-Polymer Physics), American Association of Physics Teachers, *and* the American Association for the Advancement of Science, Chicago, Illinois

January, 1948

2– 3 American Physical Society Los Angeles, California
21–23 American Society of Civil Engineers, New York, New York
29–31 American Physical Society, New York, New York

March

1– 5 American Society for Testing Materials (Spring Meeting), Washington, D. C.
22–25 Institute of Radio Engineers, New York, New York

April

19–23 American Chemical Society, Chicago, Illinois
22–24 Acoustical Society of America, Washington, D. C.

Author Index to Volume 18

References with (L) are to Letters to the Editor.

Abbott, T. A. (see Nier, A. O.)—30
Adkins, John N. Book review—1134
Alpher, R. A. (see Hill, F. K.)—489 (L)
Altar, W. (see Coltman, J. W.)—530
Anderson, R. B. (see McCartney, J. T.)—902
Anthony, R. L. (see Wack, P. E.)—456
Archibald, W. J. Approximate solution of the differential equation of the ultracentrifuge—362
Armi, E. L., J. L. Johnson, R. C. Machler, and N. E. Polster. Application of the sliding thermocouple method to the determination of temperatures at the interface of a moving bullet and a gun barrel—88
Avery, W. H. and J. R. Morrison. Infra-red spectra of hydrocarbons. II. Analysis of octane mixtures by the use of infra-red spectra obtained at low temperatures—961

Barrett, R. L. (see Smith, C. S.)—177
Beck, Paul A. Comments on "Grain growth in alpha-brass"—1028 (L)
Bennett, G. S. Gyroscopic effects in a vibratory system—1110
Bennett, W. S. (see Smith, William V.)—1112
Bennett, Williard H. Cold cathode rectifier—479
Berg, O. E. and H. F. Kaiser. X-ray storage properties of the infra-red storage phosphor and application to radiography—343
Bidwell, C. C. and C. L. Hogan. Thermal conductivity of aluminum; solid and liquid states—776
Billmeyer, Fred W., Jr. Measurements of the refractive index of films—431
Birnbaum, H., H. Cohen, and S. S. Sidhu. X-ray diffraction studies of color variation of iron oxide pigments—27
Black, Sydney D. Book review—1032
Blewett, John P. Design of an air core synchrotron—976
—— Magnetic field configurations due to air core coils—968
Bloch, A. Inversion applied to the solution of 3-dimensional electromagnetic problems—1064
Bloch, F. (see Van Vleck, J. H.)—274
Bloom, Abraham (see Cohen, Victor W.)—847 (L)
Boegli, Charles P. Hydrodynamic lubrication of finite sliders—482
Bol, K. (see Marton, L.)—522
Booth, A. D. Two calculating machines for x-ray crystal structure analysis—664
Boothby, O. L. and R. M. Bozorth. New magnetic material of high permeability—173
Bouwkamp, C. J. and N. G. de Bruijn. Electrostatic field of a point charge inside a cylinder, in connection with wave guide theory—562
Bowie, O. L. Least-square application to relaxation methods—830
Boyer, R. F. Book review—787
Bozorth, R. M. (see Boothby, O. L.)—173
Brewington, G. P. On the action of cutting oils—260 (L)
Bridgman, P. W. Effect of hydrostatic pressure on the fracture of brittle substances—246
—— Reply to "Remarks on compressive and tensile strengths"—782 (L)
Brinkley, Stuart R., Jr. Heat transfer between a fluid and a porous solid generating heat—582
Brown, Orley E. Book review—687
—— Charts for computation of *d*-values in x-ray diffraction chemical analysis—191
Bruck, G. G. Modified cavity oscillator for the generation of microwaves—843 (L)
—— **and E. R. Wicher.** Slow transverse magnetic waves in cylindrical guides—766
Buechner, W. W. (see Lamar, E. S.)—22
Buffum, D. C. (see Hollomon, J. H.)—780 (L)
Burke, J. E. Grain growth in alpha-brass—1028 (L)

Carter, R. L. (see Smith, William V.)—1112
Chatterjee, G. P. and S. S. Sidhu. X-ray diffraction studies of chrome-steel slags—519
Cherry, Ruth (see Lilly, John C.)—613
Christ, C. L. Remarks on some recently developed devices for summing Fourier series for crystal structure analysis—1133 (L)
Christensen, Sabinus H. On the analysis of internal flow machinery—587 (L)
Chu, E. L. and W. W. Hansen. The theory of disk-loaded wave guides—996
Cobine, J. D. and C. J. Gallagher. Effects of magnetic field on oscillations and noise in hot-cathode arcs—110
Coggeshall, Norman D. Fringing flux corrections for magnetic focusing devices—855
Cohen, H. (see Birnbaum, H.)—27
Cohen, Victor W. and Abraham Bloom. Note on the reduction of microphonics in triodes—847 (L)
Coltman, J. W., E. G. Ebbighausen, and W. Altar. Physical properties of calcium tungstate x-ray screens—530
Cosslett, V. E. Particle "growth" in the electron microscope—844 (L)
Craggs, J. D., W. Hopwood, and J. M. Meek. On the localized afterglows observed with long sparks in various gases—919
Crout, Prescott D. Flux plotting method for obtaining fields satisfying Maxwell's equations, with applications to the magnetron—348
Cunningham, W. J. Graphical methods for evaluating Fourier integrals—656

Dakin, T. W. and C. N. Works. Microwave dielectric measurements—789
Daniel, J. H. (see Hanson, E. E.)—439
Darby, Paul (see Shortley, George)—116
Dart, S. L. and Eugene Guth. Elastic properties of cork. II. Stress-temperature relationship of compressed cork—470

Dart, S. L., Howard A. Robinson, and Eugene Guth. Elastic properties of cork. III. Hydrostatic and ordinary load-compression curves for cork—474
Davidson, Norman and James Hillier. Single crystal electron diffraction by micro-crystalline materials—499
Davis, M. E. (see Pekeris, C. L.)—838
De Bruijn, N. G. (see Bouwkamp, C. J.)—562
De Quevedo, José L. García (see Smith, William V.)—1112
Devaney, Richard (see Kaye, Wilbur)—912
Dewey, Jane M. Elastic constants of materials loaded with non-rigid fillers—578
—— Theory of filler reinforcement—132 (erratum)
Dicke, R. H. Computational method applicable to microwave networks—873
Dienes, G. J. Comments on "Sound-velocity determination of molecular weights"—848 (L)

Ebbighausen, E. G. (see Coltman, J. W.)—530
Elder, F. R., A. M. Gurewitsch, R. V. Langmuir, and H. C. Pollock. A 70-Mev synchrotron—810
Ellis, S. G. Films, resistant to organic solvents, for use in the electron microscope—846 (L)
—— Optics of three-electrode electron guns—879
Epstein, I. Motion of a conical coil spring—368
Evans, Lyle W. (see Schulman, James H.)—732
Eyring, Carl F. Book review—590

Fischer, Earl K. (see Lindsley, Charles H.)—988
Fitzgerald, James W. (see Weissler, Alfred)—434
Foldy, Leslie L. Book review—687
Frankel, Sidney. $TM_{0,1}$ mode in circular wave guides with two coaxial dielectrics—650
Froula, Henry C. Attachments for aligning a console electron microscope—850 (L)
—— Determination of magnification in electron micrographs—19 (L)

Gallagher, C. J. (see Cobine, J. D.)—110
Gamble, Edward H. (see Shortley, George)—116
Gerould, Charles H. Preparation and uses of silica replicas in electron microscopy—333
Ginther, Robert J. (see Schulman, James H.)—732
Glinski, G. Note on circular loop antennas with non-uniform current distribution—638
Goldberg, H. (see Van Wazer, J. R.)—207
Greenfield, M. (see Hudson, G.)—405
—— **and E. T. Habib.** High speed compression tests on copper—645
Gross, B. On creep and relaxation—212
Gurewitsch, A. M. (see Elder, F. R.)—810
Guth, Eugene (see Dart, S. L.)—470, 474
—— (see Wack, P. E.)—456

Habib, E. T. (see Greenfield, M.)—645
Hale, Donald H. and W. S. Huxford. Concerning estimates of the minimum sparking potential based upon the cathode work function—586 (L)
Hall, Cecil E. Objective aperture system for the electron microscope—588 (L)
Hall, Wayne, C. Electrostatic dischargers for aircraft—759
Halsey, George. Non-linear viscous elasticity and the Eyring shear model—1072
Hamermesh, M. (see Van Vleck, J. H.)—274
Hansen, W. W. (see Chu, E. L.)—996
Hanson, E. E. and J. H. Daniel. Instrument for measuring particle diameters and constructing histograms from electron micrographs—439
Harvey, E. Newton, William D. McElroy, and A. H. Whitely. On cavity formation in water—162
Havenhill, R. S. Book review—786
Heidenreich, R. D. Book review—685
—— **and W. Shockley.** Electron microscope and electron diffraction study of slip in metal crystals—1029 (L)
Hereford, Frank L., Jr. Acceleration of electrons by a resonant cavity—956
Herman, R. C. and C. F. Meyer. Thermoluminescence and conductivity of phosphors—258 (addendum and erratum)
Hicks, Bruce L., Donald J. Montgomery, and Robert H. Wasserman. On the one-dimensional theory of steady compressible fluid flow in ducts with friction and heat addition—891
Higgins, Thomas James and Henry Peter Messinger. Equations for the inductances of three-phase coaxial busses comprised of square tubular conductors—1009
Hill, F. K. and R. A. Alpher. Measurements of base pressure on a missile in free flight—489 (L)
Hillier, James (see Davidson, Norman)—499
—— **and E. G. Ramberg.** Magnetic electron microscope objective: contour phenomena and the attainment of high resolving power—48
Hogan, C. L. (see Bidwell, C. C.)—776
Hollomon, J. H., L. D. Jaffe, and D. C. Buffum. Stabilization, tempering, and relaxation in the austenite-martensite transformation—780 (L)
Hopwood, W. (see Craggs, J. D.)—919
Horsting, C. W. Carbide structures in carburized thoriated-tungsten filaments—95
Hotchkiss, Rollin D. Book review—1135
Hudson, G. and M. Greenfield. Speed of propagation of brittle cracks in steel—405
Humphreys, R. F., W. W. Watson, and D. L. Woernley. Ultrasonic modulation of a light beam—845 (L)
Hustrulid, A. (see Nier, A. O.)—30
Hutter, R. G. E. Electron beam deflection. Part I. Small-angle deflection theory—740
—— Part II. Applications of the small-angle deflection theory—797
Huxford, W. S. (see Hale, Donald H.)—586 (L)

Jacobs, H. and A. P. LaRocque. Minimum sparking potentials of barium, magnesium, and aluminum in argon—199
Jacobs, Robert B. and Herbert F. Zuhr. New developments in vacuum engineering—34
Jaffe, L. D. (see Hollomon, J. H.)—780 (L)
Jenkins, J. A. Book review—685
Johnson, J. L. (see Armi, E. L.)—88

Kac, Mark and A. J. F. Siegert. On the theory of noise in radio receivers with square law detectors—383
Kaiser, Herman F. European electron induction accelerators—1
—— (see Berg, O. E.)—343
Kaye, Wilbur and Richard Devaney. Apparatus for the observation of the Kerr effect with microsecond electrical pulses—912
Keilien, S. Incandescent lamps as electrical load for testing—769
Kerwin, Larkin. Use of the broadcast band in geologic mapping—407
King, Allen L. Waves in elastic tubes: velocity of the pulse wave in large arteries—595
King, Ronold W. P. Book review—1032
Kirkpatrick, Paul. Book review—851
Knudsen, Hans Lottrup. Pressure and oil flow in oil-filled cables at load variations—545
Korff, Serge A. Book review—1132

Lamar, E. S. and W. W. Buechner. Ion beams in high voltage tubes using differential pumping—22
Lamb, W. E. and M. Phillips. Space charge frequency dependence of magnetron cavity—230
Langmuir, R. V. (see Elder, F. R.)—810
LaRocque, A. P. (see Jacobs, H.)—199
Lawson, James L. (see Stone, Albert M.)—691
Legallais, Victor (see Lilly, John C.)—613
Letner, Harold R. and S. S. Sidhu. X-ray diffraction study of the silver-magnesium alloy system—833
Liebhafsky, H. A. and A. F. Winslow. Cesium chromate photo-tube pellets—1128
Lilly, John C., Victor Legallais, and Ruth Cherry. Variable capacitor for measurements of pressure and mechanical displacements. A theoretical analysis and its experimental evaluation—613
Lindsley, Charles H. and Earl K. Fischer. End-effect in rotational viscometers—988
Lipscomb, William N., T. R. Rubin, and J. H. Sturdivant. Investigation of a method for the analysis of smokes according to particle size—72
Ludloff, H. F. (see Mack, C. E., Jr.)—682 (L)
—— **and F. Reiche.** Linearized supersonic flow through ducts—681 (L)
Lukesh, Joseph S. Crystal pattern synthesis by an approximate summation of Fourier series—493
—— Semi-polar form of Fourier series and its use in crystal structure analysis—321
Lyons, W. James and Irven B. Prettyman. Measurement of the dynamic stretch-modulus and hysteresis of tire cords—586 (L)

McCartney, J. T. and R. B. Anderson. Crystalline aggregation of cobalt powder—902
McCuskey, S. W. Book review—686
McElroy, William D. (see Harvey, E. Newton)—162
Machler, R. C. (see Armi, E. L.)—88
Machlin, E. S. (see Nowick, A. S.)—79
Mack, C. E., Jr., H. F. Ludloff, and F. Reiche. Rigorous solution of linearized supersonic flow through ducts—682 (L)
McLachlan, N. W. Computation of the solutions of $(1+2\epsilon\cos 2z)y''+\theta y=0$; frequency modulation functions—723
Marin, Joseph. Creep deflections in columns—103
Marshall, Fitz-Hugh. Microsecond measurement of the phosphorescence of x-ray fluorescent screens—512
Marton, L. and K. Bol. Spherical aberration of compound magnetic lenses—522
Maxwell, E. Conductivity of metallic surfaces at microwave frequencies—629
—— Erratum—928
Meek, J. M. (see Craggs, J. D.)—919
Melvin, M. Avramy. Theory of automatic control systems—704
Messinger, Henry Peter (see Higgins, Thomas James)—1009
Meyer, C. F. (see Herman, R. C.)—258
Montgomery, Donald J. (see Hicks, Bruce L.)—891
Morris, Max. Book review—684
Morrison, H. L. Preliminary measurements relative to the onset of thermal convection currents in unconsolidated sands—849 (L)
Morrison, J. R. (see Avery, W. H.)—961
Morrison, Philip. Physics in 1946—133
Motz, J. (see Sack, H. S.)—450
Murata, K. J. (see Schulman, James H.)—732
Murray, Francis J. Linear equation solvers—426 (L)
Myers, S. B. Parallel plate optics for rapid scanning—221

Nelson, R. B. Magnetron oscillator for dielectric heating—356
Nier, A. O., C. M. Stevens, A. Hustrulid, and T. A. Abbott. Mass spectrometer for leak detection—30
Nowick, A. S. and E. S. Machlin. Dislocation theory as applied by N.A.C.A. to the creep of metals—79

Okress, E. C. A magnetron-resonator system—1098

Pakswer, S. Fatique of Ag-Cs_2O, Ag-Cs photoelectric surfaces—203
Parzen, Philip. Capacity per unit length and characteristic impedance of coaxial cables with one slightly noncircular conductor—774
Pekeris, C. L. Field of a microwave dipole antenna in the vicinity of the horizon—667
—— Part II—1025
—— **and M. E. Davis.** Preliminary analysis of microwave transmission data obtained on the San Diego coast under conditions of a surface duct—838
Pepinsky, R. Electronic computer for x-ray crystal structure analyses—601
Phillips, M. (see Lamb, W. E.)—230
Pollock, H. C. (see Elder, F. R.)—810
Polster, N. E. (see Armi, E. L.)—88
Prager, W. Introduction to the mathematical theory of plasticity—375
Prettyman, I. B. (see Lyons, W. James)—586 (L)

Prettyman, I. B. Book review—1032
Pritchard, Wilbur L. Quarter wave coupled wave-guide filters—862

Quimby, Edith H. Book review—851

Ramberg, E. G. (see Hillier, James)—48
Raub, H. L. (see Sack, H. S.)—450
Reiche, F. (see Ludloff, H. F.)—681 (L)
—— (see Mack, C. E., Jr.)—682 (L)
Resnick, Irving (see Weissler, Alfred)—434
Richards, D. O. (see Spitze, L. A.)—904
Richardson, John E. (see Swift, Irvin H.)—417
Rivlin, R. S. Torsion of a rubber cylinder—444
—— Erratum—837
Robinson, Howard A. (see Dart, S. L.)—474
Roess, L. C. (see Shull, C. G.)—295
—— **and C. G. Shull.** X-ray scattering at small angles by finely divided solids. II. Exact theory for random distributions of spheroidal particles—308
Rubin, T. R. (see Lipscomb, William N.)—72

Sack, H. S., J. Motz, H. L. Raub, and R. N. Work. Elastic losses in some high polymers as a function of frequency and temperature—450
Schmitt, Otto H. Cathode-ray presentation of three-dimensional data—819
Schulman, James H., Lyle W. Evans, Robert J. Ginther, and K. J. Murata. Sensitized luminescence of manganese-activated calcite—732
Seyfert, Carl K. Book review—930
Shaw, Milton C. Mechanism of cutting fluid action—683 (L)
Shelton, J. Reid. Book review—1134
Shive, J. N. Heating and cooling of bolometer elements—398
Shockley, W. (see Heidenreich, R. D.)—1029 (L)
Shortley, George, Royal Weller, Paul Darby, and Edward H. Gamble. Numerical solution of axisymmetrical problems, with applications to electrostatics and torsion—116
Shrader, Erwin F. Book review—787
Shull, C. G. (see Roess, L. C.)—308
—— **and L. C. Roess.** X-ray scattering at small angles by finely divided solids. I. General approximate theory and applications—295
Sidhu, S. S. (see Birnbaum, H.)—27
—— (see Chatterjee, G. P.)—519
—— (see Letner, Harold R.)—833
Siegert, A. J. F. (see Kac, Mark)—383
Smith, C. S. and R. L. Barrett. Apparatus and techniques for practical chemical identification by x-ray diffraction—177
Smith, William V., José L. García de Quevedo, R. L. Carter, and W. S. Bennett. Frequency stabilization of microwave oscillators by spectrum lines—1112
Sneddon, Ian N. Note on a boundary value problem of Reissner and Sagoci—130
Spitze, L. A. and D. O. Richards. Surface studies of glass. Part I. Contact angles—904
Sproull, Robert L. Excess noise in cavity magnetrons—314
Squire, Charles F. Book review—1031
Stephenson, R. J. Book review—590
Stevens, C. M. (see Nier, A. O.)—30
Stone, Albert M. and James L. Lawson. Infinite-rejection filters—691
Stone, William M. Note on a paper by Faust and Beck—414
Strong, John D. Book review—1036
Studley, Duane. Book review—590
Sturdivant, J. H. (see Lipscomb, William N.)—72
Swift, Irvin H. and John E. Richardson. Internal friction of zinc single crystals—417

Taylor, Nelson W. Mechanism of fracture of glass and similar brittle solids—943
Telkes, Maria. The efficiency of thermoelectric generators—1116
Thompson, Stanley. Remarks on compressive and tensile strengths—781 (L)
Townend, G. H. Direction of maximum crystal elongation during metal cutting—489 (L) and 784 (L)
Trump, John G. and R. J. van de Graaff. Insulation of high voltages in vacuum—327

Urick, R. J. A sound velocity method for determining the compressibility of finely divided substances—983

Valasek, Joseph. Book review—20
van de Graaff, R. J. (see Trump, John G.)—327
Van Driest, E. R. Streamlines for subsonic flow of a compressible fluid past a sphere—194
Van Vleck, J. H., F. Bloch, and M. Hamermesh. Theory of radar reflection from wires or thin metallic strips—274
Van Wazer, J. R. and H. Goldberg. Measurement of elasticity in fluids of low viscosity—207
Vonnegut, B. Nucleation of ice formation by silver iodide—593

Wack, P. E., R. L. Anthony, and E. Guth. Electrical conductivity of GR-S and natural rubber stocks loaded with Shawinigan and R-40 blacks—456
Walker, Eric A. Book review—428
—— Ordnance research laboratory—263
Warren, B. E. Book review—429
Wasserman, Robert H. (see Hicks, Bruce L.)—891
Watson, John L. Effect of electron bombardment upon carbon black—153
Watson, W. W. (see Humphreys, R. F.)—845 (L)
Waynick, A. H. Reduction of microphonics in triodes—239
Weil, Robert. Measurement of surface tension—426 (L)
Weissler, Alfred, James W. Fitzgerald, and Irving Resnick. Sound velocity method for determination of molecular weight of liquid polymers—434
Weller, Royal (see Shortley, George)—116
Weltmann, Ruth N. Initial oscillation on a rotational viscometer—933
Whitely, A. H. (see Harvey, E. Newton)—162
Wicher, E. R. (see Bruck, G. G.)—766

Wideröe, Rolf. European induction accelerators—783 (L)
Wilchinsky, Zigmond W. Approximation for absorption displacement in x-ray diffraction by highly absorbing cylindrical samples—260 (L)
—— Quantitative analysis of mixed powders with the Geiger-counter x-ray spectrometer—929 (L)
Winslow, A. F. (see Liebhafsky, H. A.)—1128
Wintner, Aurel. Stability and high frequency—941
Woernley, D. L. (see Humphreys, R. F.)—845 (L)
Wood, Elizabeth Armstrong. Conversion factor for *kX* units to angstrom units—929 (L)
Work, R. N. (see Sack, H. S.)—450
Works, C. N. Resonant cavities for dielectric measurements—605
—— (see Dakin, T. W.)—789

Yeagley, Henry L. The physical basis of bird navigation —1035

Zener, Clarence. Mechanical behavior of high damping metals—1022
Zuhr, Herbert F. (see Jacobs, Robert B.)—34

Subject Index to Volume 18

References with (L) are to Letters to the Editor.

Absorption displacement, Approximation for, in x-ray diffraction by highly absorbing cylindrical samples, Zigmond W. Wilchinsky—260 (L)

Acceleration of electrons by a resonant cavity, Frank L. Hereford, Jr.—956

Accelerators, European electron induction, Herman F. Kaiser—1

Accelerators, European induction, Rolf Wideröe—783 (L)

Action of cutting oils, G. P. Brewington—260 (L)

Ag-Cs_2O, Ag-Cs photoelectric surfaces, Fatigue of, S. Pakswer—203

Air core coils, Magnetic field configurations due to, John P. Blewett—968

Aircraft, Electrostatic dischargers for, Wayne C. Hall—759

Alpha-brass, Grain growth in, J. E. Burke—1028 (L)

—— Comments on, Paul A. Beck—1028 (L)

Aluminum, Minimum sparking potentials of barium, magnesium, and aluminum in argon, H. Jacobs and A. P. LaRocque—199

Aluminum, Thermal conductivity of; solid and liquid states, C. C. Bidwell and C. L. Hogan—776

Analysis of internal flow machinery, Sabinus H. Christensen—587 (L)

Angstrom units, Conversion factor for *kX* units to, Elizabeth Armstrong Wood—929 (L)

Antenna, Field of a microwave dipole antenna in the vicinity of the horizon, C. L. Pekeris—667

Antennas, Note on circular loop antennas with non-uniform current distribution, G. Glinski—638

Aperture system, Objective, for the electron microscope, Cecil E. Hall—588 (L)

Apparatus for the observation of the Kerr effect with microsecond electrical pulses, Wilbur Kaye and Richard Devaney—912

Apparatus and techniques for practical chemical identification by x-ray diffraction, C. S. Smith and R. L. Barrett—177

Application of the sliding thermocouple method to the determination of temperatures at the interface of a moving bullet and a gun barrel, E. L. Armi, J. L. Johnson, R. C. Machler, and N. E. Polster—88

Approximate solution of the differential equation of the ultracentrifuge, W. J. Archibald—362

Approximation for absorption displacement in x-ray diffraction by highly absorbing cylindrical samples, Zigmond W. Wilchinsky—260 (L)

Argon, Minimum sparking potentials of barium, magnesium, and aluminum in, H. Jacobs and A. P. LaRocque—199

Arteries, Waves in elastic tubes: velocity of the pulse wave in large arteries, Allen L. King—595

Attachments for aligning a console electron microscope, Henry C. Froula—850 (L)

Austenite-Martensite transformation, Stabilization, tempering, and relaxation in the, J. H. Hollomon, L. D. Jaffe, and D. C. Buffum—780 (L)

Automatic control systems, Theory of, M. Avramy Melvin—704

Axisymmetrical problems, Numerical solution of, with applications to electrostatics and torsion, George Shortley, Royal Weller, Paul Darby, and Edward H. Gamble—116

Barium, Minimum sparking potentials of barium, magnesium, and aluminum in argon, H. Jacobs and A. P. LaRocque—199

Bird navigation, Physical basis of, Henry L. Yeagley—1035

Bolometer elements, Heating and cooling of, J. N. Shive—398

Boundary value problem of Reissner and Sagoci, Note on a, Ian N. Sneddon—130

Brittle cracks in steel, Speed of propagation of, G. Hudson and M. Greenfield—405

Brittle substances, Effect of hydrostatic pressure on the fracture of, P. W. Bridgman—246

Broadcast band, Use of the, in geologic mapping, Larkin Kerwin—407

Bullet, Application of the sliding thermocouple method to the determination of temperatures at the interface of a moving bullet and a gun barrel, E. L. Armi, J. L. Johnson, R. C. Machler, and N. E. Polster—88

Calcite, manganese-activated, Sensitized luminescence of, James H. Schulman, Lyle W. Evans, Robert J. Ginther, and K. J. Murata—732

Calcium tungstate x-ray screens, Physical properties of, J. W. Coltman, E. G. Ebbighausen, and W. Altar—530

Calculating machines, Two, for x-ray crystal structure analysis, A. D. Booth—664

Capacitor, Variable, for measurements of pressure and mechanical displacements. A theoretical analysis and its experimental evaluation, John C. Lilly, Victor Legallais, and Ruth Cherry—613

Capacity per unit length and characteristic impedance of coaxial cables with one slightly non-circular conductor, Philip Parzen—774

Carbide structures in carburized thoriated-tungsten filaments, C. W. Horsting—95

Carbon black, Effect of electron bombardment upon, John L. Watson—153

Carburized thoriated-tungsten filaments, Carbide structures in, C. W. Horsting—95

Cathode, Cold cathode rectifier, Willard H. Bennett—479

Cathode-ray presentation of three-dimensional data, Otto H. Schmitt—819

Cathode work function, Estimates of the minimum sparking potential based upon the, Donald H. Hale and W. S. Huxford—586 (L)

Cavities, Resonant, for dielectric measurements, C. N. Works—605
Cavity formation in water, E. Newton Harvey, William D. McElroy, and A. H. Whitely—162
Cavity oscillator, Modified, for the generation of microwaves, George G. Bruck—843 (L)
Cavity, resonant, Acceleration of electrons by a, Frank L. Hereford, Jr.—956
Cesium chromate photo-tube pellets, H. A. Liebhafsky and A. F. Winslow—1128
Charts for computation of d-values in x-ray diffraction chemical analysis, O. E. Brown—191
Chemical identification, Apparatus and techniques for practical chemical identification by x-ray diffraction, C. S. Smith and R. L. Barrett—177
Chrome-steel slags, X-ray diffraction studies of, G. P. Chatterjee and S. S. Sidhu—519
Circular loop antennas with non-uniform current distribution, Note on, G. Glinski—638
Coaxial cables, Capacity per unit length and characteristic impedance of, with one slightly non-circular conductor, Philip Parzen—774
Cobalt powder, Crystalline aggregation of, J. T. McCartney and R. B. Anderson—902
Coil spring, conical, Motion of a, I. Epstein—368
Cold cathode rectifier, Willard H. Bennett—479
Color variation of iron oxide pigments, X-ray diffraction studies of, H. Birnbaum, H. Cohen, and S. S. Sidhu—27
Columns, Creep deflections in, Joseph Marin—103
Comments on "Grain growth in alpha-brass," Paul A. Beck—1028 (L)
Comments on "Sound-velocity determination of molecular weights," G. J. Dienes—848 (L)
Compression tests, High speed, on copper, M. Greenfield and E. T. Habib—645
Compressive and tensile strengths, Remarks on, Stanley Thompson—781 (L)
—— Reply to, P. W. Bridgman—782 (L)
Computation of the solutions of $(1+2\epsilon\cos 2z)y''+\theta y=0$; frequency modulation functions, N. W. McLachlan—723
Computational method applicable to microwave networks, R. H. Dicke—873
Computer, Electronic, for x-ray crystal structure analyses, R. Pepinsky—601
Conductivity of metallic surfaces at microwave frequencies, E. Maxwell—629
——Erratum—928
Console electron microscope, Attachments for aligning a, Henry C. Froula—850 (L)
Contour phenomena, Magnetic electron microscope objective: contour phenomena and the attainment of high resolving power, James Hillier and E. G. Ramberg—48
Conversion factor for kX units to angstrom units, Elizabeth Armstrong Wood—929 (L)
Copper, High speed compression tests on, M. Greenfield and E. T. Habib—645
Cork, Elastic properties of. II. Stress-temperature relationship of compressed cork, S. L. Dart and Eugene Guth—470
—— III. Hydrostatic and ordinary load-compression curves for cork, S. L. Dart, Howard A. Robinson, and Eugene Guth—474
Creep deflections in columns, Joseph Marin—103
Creep of metals, Dislocation theory as applied by N.A.C.A. to the, A. S. Nowick and E. S. Machlin—79
Creep and relaxation, B. Gross—212
Crystal electron diffraction, Single, by micro-crystalline materials, Norman Davidson and James Hillier—499
Crystal elongation, Direction of maximum crystal elongation during metal cutting, G. H. Townend—489 (L) and 784 (L)
Crystal pattern synthesis by an approximate summation of Fourier series, Joseph S. Lukesh—493
Crystal structure analyses, X-ray, Electronic computer for, R. Pepinsky—601
Crystal structure analysis, Recently developed devices for summing Fourier series for, C. L. Christ—1133 (L)
Crystal structure analysis, Semi-polar form of Fourier series and its use in, Joseph S. Lukesh—321
Crystal structure analysis, X-ray, Two calculating machines for, A. D. Booth—664
Crystalline aggregation of cobalt powder, J. T. McCartney and R. B. Anderson—902
Currents, thermal convection, in unconsolidated sands, Preliminary measurements relative to the onset of, H. L. Morrison—849 (L)
Cutting fluid action, Mechanism of, Milton C. Shaw—683 (L)
Cutting oils, Action of, G. P. Brewington—260 (L)
Cylindrical guides, Slow transverse magnetic waves in, G. G. Bruck and E. R. Wicher—766

Deflection, Electron beam. Part I. Small-angle deflection theory, R. G. E. Hutter—740
—— Part II. Applications of the small-angle deflection theory, R. G. E. Hutter—797
Deflections, Creep deflections in columns, Joseph Marin—103
Design of an air core synchrotron, J. P. Blewett—976
Determination of magnification in electron micrographs, Henry C. Froula—19 (L)
Dielectric heating, Magnetron oscillator for, R. B. Nelson—356
Dielectric measurements, Microwave, T. W. Dakin and C. N. Works—789
Dielectric measurements, Resonant cavities for, C. N. Works—605
Direction of maximum crystal elongation during metal cutting, G. H. Townend—489 (L) and 784 (L)
Dislocation theory as applied by N.A.C.A. to the creep of metals, A. S. Nowick and E. S. Machlin—79
Ducts, Linearized supersonic flow through, H. F. Ludloff and F. Reiche—681 (L)
Ducts, Rigorous solution of linearized supersonic flow through, C. E. Mack, Jr., H. F. Ludloff, and F. Reiche—682 (L)

Effect of electron bombardment upon carbon black, John L. Watson—153
Effect of hydrostatic pressure on the fracture of brittle substances, P. W. Bridgman—246
Effects of magnetic field on oscillations and noise in hot-cathode arcs, J. D. Cobine and C. J. Gallagher—110
Efficiency of thermoelectric generators, Maria Telkes—1116
Elastic constants of materials loaded with non-rigid fillers, Jane M. Dewey—578
Elastic losses in some high polymers as a function of frequency and temperature, H. S. Sack, J. Motz, H. L. Raub, and R. N. Work—450
Elastic properties of cork. II. Stress-temperature relationship of compressed cork, S. L. Dart and Eugene Guth—470
—— III. Hydrostatic and ordinary load-compression curves for cork, S. L. Dart, Howard A. Robinson, and Eugene Guth—474
Elastic tubes, Waves in: velocity of the pulse wave in large arteries, Allen L. King—595
Elasticity, Measurement of, in fluids of low viscosity, J. R. Van Wazer and H. Goldberg—207
Elasticity, Non-linear viscous, and the Eyring shear model, George Halsey—1072
Electrical conductivity of GR-S and natural rubber stocks loaded with Shawinigan and R-40 blacks, P. E. Wack, R. L. Anthony, and E. Guth—456
Electromagnetic problems, 3-dimensional, Inversion applied to the solution of, A. Bloch—1064
Electron beam deflection. Part I. Small-angle deflection theory, R. G. E. Hutter—740
—— Part II. Application of small-angle deflection theory, R. G. E. Hutter—797
Electron bombardment, Effect of, upon carbon black, John L. Watson—153
Electron diffraction, Single crystal, by micro-crystalline materials, Norman Davidson and James Hillier—499
Electron diffraction study of slip in metal crystals, Electron microscope and, R. D. Heidenreich and W. Shockley—1029 (L)
Electron guns, three-electrode, Optics of, S. G. Ellis—879
Electron induction accelerators, European, Herman F. Kaiser—1
Electron micrographs, Determination of magnification in, Henry C. Froula—19 (L)
Electron micrographs, Instrument for measuring particle diameters and constructing histograms from electron micrographs, E. E. Hanson and J. H. Daniel—439
Electron microscope, console, Attachments for aligning a, Henry C. Froula—850 (L)
Electron microscope and electron diffraction study of slip in metal crystals, R. D. Heidenreich and W. Shockley—1029 (L)
Electron microscope, Films, resistant to organic solvents, for use in the, S. G. Ellis—846 (L)
Electron microscope, Magnetic electron microscope objective: contour phenomena and the attainment of high resolving power, James Hillier and E. G. Ramberg—48
Electron microscope, Objective aperture system for the, Cecil E. Hall—588 (L)
Electron microscope, Particle "growth" in the, V. E. Cosslett—844 (L)
Electron Microscopy Society of America, Proceedings of —269
Electron microscopy, Preparation and uses of silica replicas in, Charles H. Gerould—333
Electronic computer for x-ray crystal structure analyses, R. Pepinsky—601
Electrons, Acceleration of, by a resonant cavity, Frank L. Hereford, Jr.—956
Electrostatic dischargers for aircraft, Wayne C. Hall—759
Electrostatic field of a point charge inside a cylinder, in connection with wave guide theory, C. J. Bouwkamp and N. G. de Bruijn—562
Electrostatics, Numerical solution of axisymmetrical problems, with applications to electrostatics and torsion, George Shortley, Royal Weller, Paul Darby, and Edward H. Gamble—116
End-effect in rotational viscometers, Charles H. Lindsley and Earl K. Fischer—988
Equation solvers, Linear, Francis J. Murray—426 (L)
Equations for the inductances of three-phase coaxial busses comprised of square tubular conductors, Thomas James Higgins and Henry Peter Messinger—1009
Estimates of the minimum sparking potential based upon the cathode work function, Donald H. Hale and W. S. Huxford—586 (L)
European electron induction accelerators, Herman F. Kaiser—1
European induction accelerators, Rolf Wideröe—783 (L)
Excess noise in cavity magnetrons, Robert L. Sproull—314
Eyring shear model, Non-linear viscous elasticity and the, George Halsey—1072

Fatigue of Ag-Cs_2O, Ag-Cs photoelectric surfaces, S. Pakswer—203
Faust and Beck, Note on a paper by, William M. Stone —414
Field of a microwave dipole antenna in the vicinity of the horizon, C. L. Pekeris—667
—— Part II—1025
Filaments, Carbide structures in carburized thoriated-tungsten filaments, C. W. Horsting—95
Filler reinforcement, Theory of, Jane M. Dewey—132 (erratum)
Fillers, Elastic constants of materials loaded with non-rigid fillers, Jane M. Dewey—578
Films, Measurements of the refractive index of, Fred W. Billmeyer, Jr.—431
Films, resistant to organic solvents, for use in the electron microscope, S. G. Ellis—846 (L)
Filters, Infinite-rejection, Albert M. Stone and James L. Lawson—691
Filters, Quarter wave coupled wave-guide, Wilbur L. Pritchard—862
Flow, Linearized supersonic, through ducts, H. F. Ludloff and F. Reiche—681 (L)

Flow, linearized supersonic, through ducts, Rigorous solution of, C. E. Mack, Jr., H. F. Ludloff, and F. Reiche—682 (L)
Fluid, compressible, Streamlines for subsonic flow of, past a sphere, E. R. Van Driest—194
Fluid flow, steady compressible, One-dimensional theory of, in ducts with friction and heat addition, Bruce L. Hicks, Donald J. Montgomery, and Robert H. Wasserman—891
Fluid, Mechanism of cutting fluid action, Milton C. Shaw—683 (L)
Fluids of low viscosity, Measurement of elasticity in, J. R. Van Wazer and H. Goldberg—207
Flux correction, Fringing, for magnetic focusing devices, Norman D. Coggeshall—855
Flux plotting method for obtaining fields satisfying Maxwell's equations, with applications to the magnetron, Prescott D. Crout—348
Fourier integrals, Graphical methods for evaluating, W. J. Cunningham—656
Fourier series, Crystal pattern synthesis by an approximate summation of, Joseph S. Lukesh—493
Fourier series, Recently developed devices for summing Fourier series for crystal structure analysis, C. L. Christ—1133 (L)
Fourier series, Semi-polar form of, and its use in crystal structure analysis, Joseph S. Lukesh—321
Fracture of brittle substances, Effect of hydrostatic pressure on, P. W. Bridgman—246
Frequency modulation functions, Computation of the solutions of $(1+2\epsilon\cos 2z)y''+\theta y=0$, N. W. McLachlan—723
Frequency stabilization of microwave oscillators by spectrum lines, William V. Smith, José L. García de Quevedo, R. L. Carter, and W. S. Bennett—1112
Fringing flux corrections for magnetic focusing devices, Norman D Coggeshall—855

Gases, On the localized afterglows observed with long sparks in various gases, J. D. Craggs, W. Hopwood, and J. M. Meek—919
Geiger-counter x-ray spectrometer, Quantitative analysis of mixed powders with the, Zigmond W. Wilchinsky—929 (L)
Generators, thermoelectric, Efficiency of, Marie Telkes—1116
Geologic mapping, Use of the broadcast band in, Larkin Kerwin—407
Glass, Mechanism of fracture of, and similar brittle solids, Nelson W. Taylor—943
Glass, Surface studies of. Part I. Contact angles, L. A. Spitze and D. O. Richards—904
Grain growth in alpha-brass, J. E. Burke—1028 (L)
——, Comments on, Paul A. Beck—1028 (L)
Graphical methods for evaluating Fourier integrals, W. J. Cunningham—656
GR-S, Electrical conductivity of GR-S and natural rubber stocks loaded with Shawinigan and R-40 blacks, P. E. Wack, R. L. Anthony, and E. Guth—456
Gun barrel, Application of the sliding thermocouple method to the determination of temperatures at the interface of a moving bullet and E. L. Armi, J. L. Johnson, R. C. Machler, and N. E. Polster—88
Gyroscopic effects in a vibratory system, G. S. Bennett—1110

Heat transfer between a fluid and a porous solid generating heat, Stuart R. Brinkley, Jr.—582
Heating and cooling of bolometer elements, J. N. Shive—398
High frequency, Stability and, Aurel Wintner—941
High speed compression tests on copper, M. Greenfield and E. T. Habib—645
High voltage tubes, Ion beams in high voltage tubes using differential pumping, E. S. Lamar and W. W. Buechner—22
High voltages, Insulation of, in vacuum, John G. Trump and R. J. van de Graaf—327
Histograms, Instrument for measuring particle diameters and constructing histograms from electron micrographs, E. E. Hanson and J. H. Daniel—439
Hot-cathode arcs, Effects of magnetic field on oscillations and noise in, J. D. Cobine and C. J. Gallagher—110
Hydrocarbons, Infra-red spectra of. II. Analysis of octane mixtures by the use of infra-red spectra obtained at low temperatures, W. H. Avery and J. R. Morrison—961
Hydrodynamic lubrication of finite sliders, Charles P. Boegli—482
Hydrostatic pressure, Effect of, on the fracture of brittle substances, P. W. Bridgman—246
Hysteresis of tire cords, Measurement of the dynamic stretch-modulus and, W. James Lyons and Irven B. Prettyman—586 (L)

Ice formation by silver iodide, Nucleation of, B. Vonnegut—593
Incandescent lamps as electrical load for testing, S. Keilien—769
Infinite-rejection filters, Albert M. Stone and James L. Lawson—691
Infra-red spectra of hydrocarbons. II. Analysis of octane mixtures by the use of infra-red spectra obtained at low temperatures, W. H. Avery and J. R. Morrison—961
Infra-red storage phosphor, X-ray storage properties of, and application to radiography, O. E. Berg and H. F. Kaiser—343
Initial oscillation on a rotational viscometer, Ruth N. Weltmann—933
Instrument for measuring particle diameters and constructing histograms from electron micrographs, E. E. Hanson and J. H. Daniel—439
Insulation of high voltages in vacuum, John G. Trump and R. J. van de Graaff—327
Internal flow machinery, Analysis of, Sabius H. Christensen—587 (L)
Internal friction of zinc single crystals, Irvin H. Swift and John E. Richardson—417

Introduction to the mathematical theory of plasticity, W. Prager—375
Inversion applied to the solution of 3-dimensional electromagnetic problems, A. Bloch—1064
Investigation of a method for the analysis of smokes according to particle size, William N. Lipscomb, T. R. Rubin, and J. H. Sturdivant—72
Ion beams in high voltage tubes using differential pumping, E. S. Lamar and W. W. Buechner—22
Iron oxide pigments, X-ray diffraction studies of color variation of, H. Birnbaum, H. Cohen, and S. S. Sidhu —27

Kerr effect, Apparatus for the observation of the, with microsecond electrical pulses, Wilbur Kaye and Richard Devaney—912
kX units, Conversion factor for, to angstrom units, Elizabeth Armstrong Wood—929 (L)

Leak detection, Mass spectrometer for, A. O. Nier, C. M. Stevens, A. Hustrulid, and T. A. Abbott—30
Least-square application to relaxation methods, O. L. Bowie—830
Light beam, Ultrasonic modulation of a, R. F. Humphreys, W. W. Watson, and D. L. Woernley—845
Linear equation solvers, Francis J. Murray—426 (L)
Linearized supersonic flow through ducts, H. F. Ludloff and F. Reiche—681 (L)
Linearized supersonic flow through ducts, Rigorous solution of, C. E. Mack, Jr., H. F. Ludloff, and F. Reiche—682 (L)
Localized afterglows observed with long sparks in various gases, J. D. Craggs, W. Hopwood, and J. M. Meek—919
Lubrication of finite sliders, Hydrodynamic, Charles P. Boegli—482

Magnesium alloy system, silver, X-ray diffraction study of the, Harold R. Letner and S. S. Sidhu—833
Magnesium, Minimum sparking potentials of barium, magnesium, and aluminum in argon, H. Jacobs and A. P. LaRocque—199
Magnetic electron microscope objective: contour phenomena and the attainment of high resolving power, James Hillier and E. G. Ramberg—48
Magnetic field configurations due to air core coils, John P. Blewett—968
Magnetic field, Effects of, on oscillations and noise in hot-cathode arcs, J. D. Cobine and C. J. Gallagher—110
Magnetic focusing devices, Fringing flux corrections for, Norman D. Coggeshall—855
Magnetic lenses, Spherical aberration of compound magnetic lenses, L. Morton and K. Bol—522
Magnetic material, New, of high permeability, O. L. Boothby and R. M. Bozorth—173
Magnetic waves, Slow transverse, in cylindrical guides, George G. Bruck and E. R. Wicher—766
Magnetron cavity, Space charge frequency dependence of, W. E. Lamb and M. Phillips—230
Magnetron, Flux plotting method for obtaining fields satisfying Maxwell's equations, with applications to the, Prescott D. Crout—348
Magnetron oscillator for dielectric heating, R. B. Nelson—356
Magnetron-resonator system, E. C. Okress—1098
Magnetrons, cavity, Excess noise in, Robert L. Sproull—314
Magnification, Determination of, in electron micrographs, Henry C. Froula—19 (L)
Manganese-activated calcite, Sensitized luminescence of, James H. Schulman, Lyle W. Evans, Robert J. Ginther, and K. J. Murata—732
Mass spectrometer for leak detection, A. O. Nier, C. M. Stevens, A. Hustrulid, and T. A. Abbott—30
Maxwell's equations, Flux plotting method for obtaining fields satisfying Maxwell's equations, with applications to the magnetron, Prescott D. Crout—348
Measurement of the dynamic stretch-modulus and hysteresis of tire cords, W. James Lyons and Irven B. Prettyman—586 (L)
Measurement of elasticity in fluids of low viscosity, J. R. Van Wazer and H. Goldberg—207
Measurement of surface tension, Robert Weil—426 (L)
Measurements of base pressure on a missile in free flight, F. K. Hill and R. A. Alpher—489 (L)
Measurements of the refractive index of films, Fred W. Billmeyer, Jr.—431
Mechanical behavior of high damping metals, Clarence Zener—1022
Mechanism of cutting fluid action, Milton C. Shaw—683 (L)
Mechanism of fracture of glass and similar brittle solids, Nelson W. Taylor—943
Metal crystals, Electron microscope and electron diffraction study of slip in, R. D. Heidenreich and W. Shockley —1029 (L)
Metal cutting, Direction of maximum crystal elongation during, G. H. Townend—489 (L) and 784 (L)
Metallic surfaces, Conductivity of, at microwave frequencies, E. Maxwell—629
—— Erratum—928
Metals, Dislocation theory as applied by N.A.C.A. to the creep of, A. S. Nowick and E. S. Machlin—79
Metals, Mechanical behavior of high damping metals, Clarence Zener—1022
Micro-crystalline materials, Single crystal electron diffraction by, Norman Davidson and James Hillier—499
Microphonics, Reduction of, in triodes, A. H. Waynick —239
Microphonics in triodes, Note on the reduction of, Victor W. Cohen and Abraham Bloom—847 (L)
Microsecond electrical pulses, Apparatus for the observation of the Kerr effect with, Wilbur Kaye and Richard Devaney—912
Microsecond measurement of the phosphorescence of x-ray fluorescent screens, Fitz-Hugh Marshall—512
Microwave dielectric measurements, T. W. Dakin and C. N. Works—789

Microwave dipole antenna, Field of a, in the vicinity of the horizon, C. L. Pekeris—667
—— Part II—1025
Microwave frequencies, Conductivity of metallic surfaces at, E. Maxwell—629
—— Erratum—928
Microwave networks, Computational method applicable to, R. H. Dicke—873
Microwave oscillators, Frequency stabilization of, by spectrum lines, William V. Smith, José L. García de Quevedo, R. L. Carter, and W. S. Bennett—1112
Microwave transmission data, Preliminary analysis of, obtained on the San Diego coast under conditions of surface duct, C. L. Pekeris and M. E. Davis—838
Microwaves, generation of, Modified cavity oscillator for the, George G. Bruck—843 (L)
Minimum sparking potentials of barium, magnesium, and aluminum in argon, H. Jacobs and A. P. LaRocque—199
Missile in free flight, Measurements of base pressure on a, F. K. Hill and R. A. Alpher—489 (L)
Modified cavity oscillator for the generation of microwaves, George G. Bruck—843 (L)
Molecular weight of liquid polymers, Sound velocity method for determination of, Alfred Weissler, James W. Fitzgerald, and Irving Resnick—434
Molecular weights, Comments on sound-velocity determination of, G. J. Dienes—848 (L)
Motion of a conical coil spring, I. Epstein—368

N.A.C.A., Dislocation theory as applied by N.A.C.A. to the creep of metals, A. S. Nowick and E. S. Machlin—79
New developments in vacuum engineering, Robert B. Jacobs and Herbert F. Zuhr—34
New magnetic material of high permeability, O. L. Boothby and R. M. Bozorth—173
Noise in radio receivers with square law detectors, Theory of, Mark Kac and A. J. F. Siegert—383
Non-linear viscous elasticity and the Eyring shear model, George Halsey—1072
Note on a boundary value problem of Reissner and Sagoci, Ian N. Sneddon—130
Note on circular loop antennas with non-uniform current distribution, G. Glinski—638
Note on a paper by Faust and Beck, William M. Stone—414
Note on the reduction of microphonics in triodes, Victor W. Cohen and Abraham Bloom—847 (L)
Nucleation of ice formation by silver iodide, B. Vonnegut—593
Numerical solution of axisymmetrical problems, with applications to electrostatics and torsion, George Shortley, Royal Weller, Paul Darby, and Edward H. Gamble—116

Objective aperture system for the electron microscope, Cecil E. Hall—588 (L)
Octane mixtures, Infra-red spectra of hydrocarbons. II. Analysis of octane mixtures by the use of infra-red spectra obtained at low temperatures, W. H. Avery and J. R. Morrison—961
Oil Flow in oil-filled cables, Pressure and, at load variations, Hans Lottrup Knudsen—545
Oils, Action of cutting oils, G. P. Brewington—260 (L)
One-dimensional theory of steady compressible fluid flow in ducts with friction and heat addition, Bruce L. Hicks, Donald J. Montgomery, and Robert H. Wasserman—891
Optics, Parallel plate, for rapid scanning, S. B. Myers—221
Optics of three-electrode electron guns, S. G. Ellis—879
Ordnance research laboratory, Eric A. Walker—263

Parallel plate optics for rapid scanning, S. B. Myers—221
Particle diameters, Instrument for measuring particle diameters and constructing histograms from electron micrographs, E. E. Hanson and J. H. Daniel—439
Particle "growth" in the electron microscope, V. E. Cosslett—844 (L)
Phosphorescence of x-ray fluorescent screens, Microsecond measurement of the, Fitz-Hugh Marshall—512
Phosphors, Thermoluminescence and conductivity of, R. C. Herman and C. F. Meyer—258 (addendum and erratum)
Photoelectric surfaces, Fatigue of Ag-Cs_2O, Ag-Cs photoelectric surfaces, S. Pakswer—203
Photo-tube pellets, Cesium chromate, H. A. Liebhafsky and A. F. Winslow—1128
Physical basis of bird navigation, Preliminary study of a, Henry L. Yeagley—1035
Physical properties of calcium tungstate x-ray screens, J. W. Coltman, E. G. Ebbighausen, and W. Altar—530
Physics in 1946, Philip Morrison—133
Plasticity, mathematical theory of, Introduction to, W. Prager—375
Polymers, Elastic losses in some high polymers as a function of frequency and temperature, H. S. Sack, J. Motz, H. L. Raub, and R. N. Work—450
Polymers, liquid, Sound velocity method for determination of molecular weight of, Alfred Weissler, James W. Fitzgerald, and Irving Resnick—434
Preliminary analysis of microwave transmission data obtained on the San Diego coast under conditions of a surface duct, C. L. Pekeris and M. E. Davis—838
Preliminary measurements relative to the onset of thermal convection currents in unconsolidated sands, H. L. Morrison—849 (L)
Preparation and uses of silica replicas in electron microscopy, Charles H. Gerould—333
Pressure and oil flow in oil-filled cables at load variations, Hans Lottrup Knudsen—545
Proceedings of the Electron Microscope Society of America—269

Quantitative analysis of mixed powders with the Geiger-counter x-ray spectrometer, Zigmond W. Wilchinsky—929 (L)
Quarter wave coupled wave-guide filters, Wilbur L. Pritchard—862

Radar reflection, Theory of, from wires or thin metallic strips, J. H. Van Vleck, F. Bloch, and M. Hamermesh—274

Radiography, X-ray storage properties of the infra-red storage phosphor and application to, O. E. Berg and H. F. Kaiser—343
Recently developed devices for summing Fourier series for crystal structure analysis, C. L. Christ—1133 (L)
Reduction of microphonics in triodes, A. H. Waynick—239
——, Note on the, Victor W. Cohen and Abraham Bloom —847 (L)
Refractive index of films, Measurements of the, Fred W. Billmeyer, Jr.—431
Reissner and Sagoci, Note on a boundary value problem of, Ian N. Sneddon—130
Relaxation, Creep and, B. Gross—212
Relaxation methods, Least-square application to, O. L. Bowie—830
Remarks on compressive and tensile strengths, Stanley Thompson—781 (L)
——, Reply to, P. W. Bridgman—782 (L)
Resonant cavities for dielectric measurements, C. N. Works—605
Resonator, Magnetron-resonator system, E. C. Okress—1098
R-40 blacks, Electrical conductivity of GR-S and natural rubber stocks loaded with Shawinigan and R-40 blacks, P. E. Wack, R. L. Anthony, and E. Guth—456
Rigorous solution of linearized supersonic flow through ducts, C. E. Mack, Jr., H. F. Ludloff, and F. Reiche—682 (L)
Rubber cylinder, Torsion of a, R. S. Rivlin—444
—— Erratum—837
Rubber, Electrical conductivity of GR-S and natural rubber stocks loaded with Shawinigan and R-40 blacks, P. E. Wack, R. L. Anthony, and E. Guth—456

Sagoci, Note on a boundary value problem of Reissner and, Ian N. Sneddon—130
Semi-polar form of Fourier series and its use in crystal structure analysis, Joseph S. Lukesh—321
Sensitized luminescence of manganese-activated calcite, James H. Schulman, Lyle W. Evans, Robert J. Ginther, and K. J. Murata—732
70-Mev synchrotron, F. R. Elder, A. M. Gurewitsch, R. V. Langmuir, and H. C. Pollock—810
Shawinigan blacks, Electrical conductivity of GR-S and natural rubber stocks loaded with Shawinigan and R-40 blacks, P. E. Wack, R. L. Anthony, and E. Guth—456
Silica replicas, Preparation and uses of, in electron microscopy, Charles H. Gerould—333
Silver iodide, Nucleation of ice formation by, B. Vonnegut —593
Silver-magnesium alloy system, X-ray diffraction study of the, Harold R. Letner and S. S. Sidhu—833
Single crystal electron diffraction by micro-crystalline materials, Norman Davidson and James Hillier—499
Sliders, finite, Hydrodynamic lubrications of, Charles P. Boegli—482
Slow transverse magnetic waves in cylindrical guides, G. G. Bruck and E. R. Wicher—766
Smokes, Investigation of a method for the analysis of smokes according to particle size, William N. Lipscomb, T. R. Rubin, and J. H. Sturdivant—72
"Sound-velocity determination of molecular weights," Comments on, G. J. Dienes—848 (L)
Sound velocity method for determination of molecular weight of liquid polymers, Alfred Weissler, James W. Fitzgerald, and Irving Resnick—434
Sound velocity method for determining the compressibility of finely divided substances, R. J. Urick—983
Space charge frequency dependence of magnetron cavity, W. E. Lamb and M. Phillips—230
Sparking potential, Estimates of the minimum sparking potential based upon the cathode work function, Donald H. Hale and W. S. Huxford—586 (L)
Spectrometer, Mass, for leak detection, A. O. Nier, C. M. Stevens, A. Hustrulid, and T. A. Abbott—30
Spectrometer, Quantitative analysis of mixed powders with the Geiger-counter x-ray spectrometer, Zigmond W. Wilchinsky—929 (L)
Speed of propagation of brittle cracks in steel, G. Hudson and M. Greenfield—405
Spherical aberration of compound magnetic lenses, L. Marton and K. Bol—522
Square law detectors, Theory of noise in radio receivers with, Mark Kac and A. J. F. Siegert—383
Stability and high frequency, Aurel Wintner—941
Stabilization, tempering, and relaxation in the austenite-martensite transformation, J. H. Hollomon, L. D. Jaffe, and D. C. Buffum—780 (L)
Steel, brittle cracks in, Speed of propagation of, G. Hudson and M. Greenfield—405
Streamlines for subsonic flow of a compressible fluid past a sphere, E. R. Van Driest—194
Strengths, compressive and tensile, Remarks on, Stanley Thompson—781 (L)
——, Reply to, P. W. Bridgman—782 (L)
Stretch-modulus and hysteresis of tire cords, dynamic, Measurement of, W. James Lyons and Irven B. Prettyman—586 (L)
Subsonic flow, Streamlines for, of a compressible fluid past a sphere, E. R. Van Driest—194
Surface studies of glass. Part I. Contact angles, L. A. Spitze and D. O. Richards—904
Surface tension, Measurement of, Robert Weil—426 (L)
Synchrotron, air core, Design of, J. P. Blewett—976
Synchrotron, 70-Mev, F. R. Elder, A. M. Gurewitsch, R. V. Langmuir, and H. C. Pollock—810

Temperatures, Application of the sliding thermocouple method to the determination of temperatures at the interface of a moving bullet and a gun barrel, A. L. Armi, J. L. Johnson, R. C. Machler, and N. E. Polster —88
Theory of automatic control systems, M. Avramy Melvin —704
Theory of disk-loaded wave guides, E. L. Chu and W. W. Hansen—996
Theory of filler reinforcement, Jane M. Dewey—132 (erratum)

Theory of noise in radio receivers with square law detectors, Mark Kac and A. J. F. Siegert—383
Theory of radar reflection from wires or thin metallic strips, J. H. Van Vleck, F. Bloch, and M. Hamermesh—274
Thermal conductivity of aluminum; solid and liquid states, C. C. Bidwell and C. L. Hogan—776
Thermal convection currents in unconsolidated sands, Preliminary measurements relative to the onset of, H. L. Morrison—849 (L)
Thermocouple, Application of the sliding thermocouple method to the determination of temperatures at the interface of a moving bullet and a gun barrel, E. L. Armi, J. L. Johnson, R. C. Machler, and N. E. Polster—88
Thermoelectric generators, Efficiency of, Maria Telkes—1116
Thermoluminescence and conductivity of phosphors, R. C. Herman and C. F. Meyer—258 (addendum and erratum)
Three-dimensional data, Cathode-ray presentation, Otto H. Schmitt—819
Thoriated-tungsten filaments, carburized, Carbide structures in, C. W. Horsting—95
Tire cords, Measurement of the dynamic stretch-modulus and hysteresis of, W. James Lyons and Irven B. Prettyman—586 (L)
$TM_{0,1}$ mode in circular wave guides with two coaxial dielectrics, Sidney Frankel—650
Torsion, Numerical solution of axisymmetrical problems, with applications to electrostatics and, George Shortley, Royal Weller, Paul Darby, and Edward H. Gamble—116
Torsion of a rubber cylinder, R. S. Rivlin—444
—— Erratum—837
Transmission data, microwave, Preliminary analysis of, obtained on the San Diego coast under conditions of a surface duct; C. L. Pekeris and M. E. Davis—838
Triodes, Reduction of microphonics in, A. H. Waynick—239
——, Note on, Victor W. Cohen and Abraham Bloom—847 (L)
Two calculating machines for x-ray crystal structure analysis, A. D. Booth—664

Ultracentrifuge, Approximate solution of the differential equation of the, W. J. Archibald—362
Ultrasonic modulation of a light beam, R. F. Humphreys, W. W. Watson, and D. L. Woernley—845 (L)
Use of the broadcast band in geologic mapping, Larkin Kerwin—407

Vacuum engineering, New developments in, Robert B. Jacobs and Herbert F. Zuhr—34
Vacuum, Insulation of high voltages in, John G. Trump and R. J. van de Graaff—327
Variable capacitor for measurements of pressure and mechanical displacements. A theoretical analysis and its experimental evaluation, John C. Lilly, Victor Legallais, and Ruth Cherry—613
Vibratory system, Gyroscopic effects in a, G. S. Bennett—1110
Viscometer, rotational, Initial oscillation on a, Ruth N. Weltmann—933
Viscometers, rotational, End-effects in, Charles H. Lindsley and Earl K. Fischer—988
Viscous elasticity, Non-linear, and the Eyring shear model, George Halsey—1072

Wave guide theory, Electrostatic field of a point charge inside a cylinder, in connection with, C. J. Bouwkamp and N. G. de Bruijn—562
Wave guides, disk-loaded, Theory of, E. L. Chu and W. W. Hansen—996
Wave guides, $TM_{0,1}$ mode in circular wave guides with two coaxial dielectrics, Sidney Frankel—650
Waves in elastic tubes: velocity of the pulse wave in large arteries, Allen L. King—595

X-ray crystal structure analyses, Electronic computer for, R. Pepinsky—601
X-ray crystal structure analysis, Two calculating machines for, A. D. Booth—664
X-ray diffraction, Apparatus and techniques for practical chemical identification by, C. S. Smith and R. L. Barrett—177
X-ray diffraction, Approximation for absorption displacement in, by highly absorbing cylindrical samples, Zigmond W. Wilchinsky—260 (L)
X-ray diffraction chemical analysis, Charts for computation of d-values in, O. E. Brown—191
X-ray diffraction studies of chrome-steel slags, G. P. Chatterjee and S. S. Sidhu—519
X-ray diffraction studies of color variation of iron oxide pigments, H. Birnbaum, H. Cohen, and S. S. Sidhu—27
X-ray diffraction study of the silver-magnesium alloy system, Harold R. Letner and S. S. Sidhu—833
X-ray fluorescent screens, Microsecond measurement of the phosphorescence of, Fitz-Hugh Marshall—512
X-ray scattering at small angles by finely divided solids. I. General approximate theory and applications, C. G. Shull and L. C. Roess—295
—— II. Exact theory for random distributions of spheroidal particles, L. C. Roess and C. G. Shull—308
X-Ray screens, calcium tungstate, Physical properties of, J. W. Coltman, E. G. Ebbighausen, and W. Altar—530
X-ray storage properties of the infra-red storage phosphor and application to radiography, O. E. Berg and H. F. Kaiser—343

Zinc single crystals, Internal friction of, Irvin H. Swift and John E. Richardson—417

"Console" type: magnification 500 X and 5,000 X; useful photographic enlargement to 100,000 diameters.

"Universal" type: adjustable magnifications to 20,000 X; sharp photographic enlargement to 100,000 diameters.

HELPING GREAT COMPANIES PLAN TOMORROW'S PRODUCTS

RCA ELECTRON MICROSCOPES multiply vision 100,000 times

An ore company sees the detailed structure of alumina particles for the first time . . . determines the best size for a rubber reinforcing agent. *A steel company* improves pearlite surfaces because of new crystalline knowledge disclosed under 10,000 times magnification. *A zinc company* learns what zinc pigments really look like structurally . . . keys its production accordingly. *A plastics manufacturer* studies polymerization processes . . . develops new molding materials.

And so it goes. The RCA Electron Microscope reveals long-held secrets of particle size, shape and structure. Its enormous resolving power and depth of focus permit easy visual and photographic inspections hitherto impossible . . . magnifications up to 100,000 X!

We'll gladly help you evaluate the benefits of the electron microscope for any job. Write Dept. 44-L.

RCA

SCIENTIFIC INSTRUMENTS

RADIO CORPORATION of AMERICA

ENGINEERING PRODUCTS DEPARTMENT, CAMDEN, N.J.

In Canada: RCA VICTOR Company Limited, Montreal

Portable PACKAGED POWER!

NEW VOLTBOX by SUPERIOR ELECTRIC

PORTABLE

• Light • Handsome • Flexible

PACKAGED

- Cast aluminum case
- Powerstat variable transformer
- Easy to read voltmeter
- Superior Binding Posts
- Output receptacles
- "On-Off" switch
- "Line-Load" switch
- Renewable fuse
- Six (6) foot cord-plug

VOLTBASE

VOLTBASE POWERSTAT MOUNTED

POWER

	Type UC1M	Type UC2M
INPUT:	115 volts, 50/60 cycles, single phase	230 volts, 50/60 cycles, single phase
OUTPUT:	0-135 volts, 7.5 amps. 1000 va.	0-270 volts, 3.0 amps. 810 va.
PRICE:	$46.00 F.O.B. Bristol	$52.00 F.O.B. Bristol

• Easy to operate • Continuously adjustable output voltage
• Overload protection • Practical power for the laboratory

For those users who have POWERSTAT variable transformers types 116 or 216, the VOLTBASE is available. When used with the POWERSTAT, the VOLTBASE offers the features of the VOLTBOX. Type UCB1 is designed for use with POWERSTAT type 116 and type UCB2 is used with POWERSTAT type 216. The ratings of the VOLTBASES are the same as their respective POWERSTAT. For further information regarding these new products and their uses,

Write SUPERIOR ELECTRIC, 1205 Laurel Street, BRISTOL, CONN.

THE SUPERIOR ELECTRIC CO.
BRISTOL, CONNECTICUT

POWERSTAT VARIABLE TRANSFORMERS • VOLTBOX A·C POWER SUPPLY • STABILINE VOLTAGE REGULATORS

Select DPI HIGH VACUUM OILS for their 9 ESSENTIAL QUALITIES

1. Low vapor pressures. **2.** Narrow boiling ranges. **3.** Stability. **4.** Ease of fractionation and recovery. **5.** Low operating cost. **6.** Uniformity. **7.** Low viscosity. **8.** Easy vaporization. **9.** Nontoxic vapors.

PUMPING FLUIDS play a big part in attaining the maximum operating efficiency of high vacuum equipment. The wide variety of DPI high vacuum equipment has been designed to accomplish specific tasks . . . and a complete series of oils—esters, hydrocarbons, and silicones—has been provided and classified according to the unique characteristics so that each piece of that equipment may be supplied with the oil to enable it to do its job at its best.

Similarly, DPI vacuum greases, ideal for lubrication of stopcocks, ground glass joints, and other vacuum seals, should be carefully selected for their special properties.

DP INC

For full information on DPI high vacuum oils and greases write—

Vacuum Equipment Division

DISTILLATION PRODUCTS, INC.
Rochester 13, N. Y.

Silicone News

DC SILICONE

SILICONE DIFFUSION PUMP FLUIDS Improve Adhesion of Metal Films

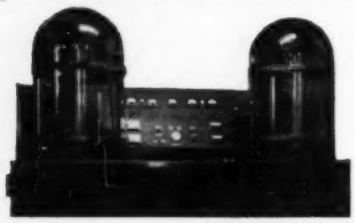

COURTESY DUPLATE CANADA, LTD.

Use of DC 703 in production units for the thermal evaporation of metallic and non-metallic films indicates that the exceptional heat stability of this DC Silicone Diffusion Pump Fluid results in better adhesion of magnesium fluoride films to glass.

After using DC 703 for the past year in two production units for evaporating magnesium fluoride and rhodium, Dr. Bateson of Duplate Canada Ltd., Oshawa, Ontario, reports that he has had no difficulty in producing equal or higher vacuum with pumping speeds equal to those of a high grade organic pumping fluid.

Even more significant are Dr. Bateson's observations that backstreaming seems to be reduced by use of DC 703; that the Silicone-vapor which does migrate into the system is more heat-stable; and that primary adhesion of magnesium fluoride films to glass is therefore improved. Preliminary observations also indicate that use of DC 703 results in brighter first surface mirrors. That DC 703 causes less contamination of the system is further indicated by these aluminum shields. Both were normally exposed to the heaters in the bell jar for 9 months. Shield at left, exposed to DC 703, is quite clean. The other shield, exposed to a high grade organic pumping fluid, is covered with a dark brown deposit. May we also remind you of DC 702. Both DC 702 and DC 703 are useful in electron microscopes, high vacuum dehydration and in evacuating electronic tubes. Write for pamphlet No. G 9-5.

DOW CORNING CORPORATION
MIDLAND, MICHIGAN
New York • Chicago • Cleveland • Los Angeles
In Canada: Fiberglas Canada, Ltd., Toronto
In England: Albright and Wilson, Ltd., London

Dow Corning
FIRST IN SILICONES

Fundamental Electronics and Vacuum Tubes

Revised Edition

By ARTHUR L. ALBERT
Professor of Communication Engineering, Oregon State College

This text for electrical engineering training provides a sound foundation in electronic theory and its principal applications in both the communications and power fields. All underlying theory is very fully and clearly explained, and at the end of the discussion of each step in theory illustrative applications are described.

To be published in the fall.

$5.00 (probable)

Powder Metallurgy

By PAUL SCHWARZKOPF

This important new book for metallurgists is, in effect the revised and expanded notebook of one of the pioneer powder metallurgists—a man whose life work has been an integral part of the whole scientific and industrial development of powder metallurgy and one who is in the fortunate position of having no restrictions on the disposal of his knowledge. The book contains a great deal of invaluable information about the industrial processing of metal powders and the products obtainable. It also contains a review of the theories on which powder metallurgy is based.

Published October 28, 1947.

$8.00

THE MACMILLAN COMPANY New York 11

Higher x-ray magnification

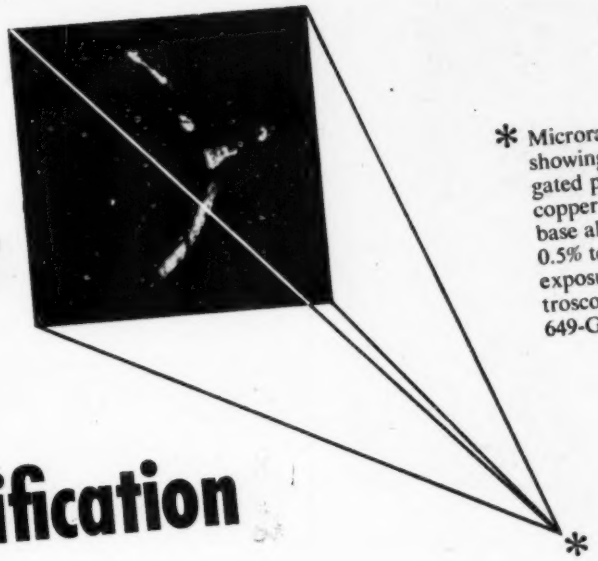

* Microradiograph at 400X showing shape of segregated phase particle of copper telluride in copper base alloy containing 0.5% tellurium. Original exposure on Kodak Spectroscopic Plate, Type 649-GH.

...with the **Kodak** emulsion that can carry the most information per millimeter

Ever use microradiography?

It's microscopy by x-rays. Photography makes it possible, even though x-rays can't be bent like light or electrons to form images in microscopes. Contact radiographs of thin specimens, made with soft x-radiation, are optically magnified and viewed directly in the microscope or as photomicrographs.

If the original image is on the remarkable Kodak Spectroscopic Plate, Type 649-GH, magnification can be boosted to explore finer subsurface structures than ever before. (The resolving power of this plate for visible light is more than 1000 lines per millimeter!)

For metallurgists, microradiography supplements metallography. By proper choice of kilovoltage and tube target, they select the characteristic radiation that best differentiates between elements to show concentration gradients around segregate phases.

Microradiography has been used to distinguish natural from cultured pearls, to study distribution of inorganic spray materials on foliage, and in many other diverse applications. Possibly it can help *you* in problems of three-dimensional microcomposition.

Equipment required is readily available and simple, like the vacuum exposure holder for good specimen-emulsion contact that Kodak can tell you how to make. And of course we shall be glad to supply full information about photographic materials.

EASTMAN KODAK COMPANY
Rochester 4, N. Y.

Kodak cordially invites you to visit Booth 55 at the A.A.A.S. Meeting at the Stevens Hotel in Chicago, December 26-31.

MICRORADIOGRAPHY
...another important function of photography

Kodak

YOUR POTENTIOMETRIC INSTRUMENTS HAVE A HEART TOO!

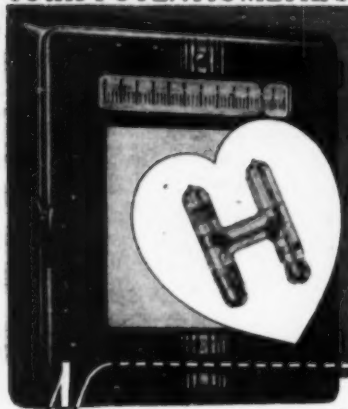

NO matter how perfect otherwise, the human organism isn't much good without a dependable heart. The same is true of your automatic temperature and pH control instruments. The "heart" of most such instruments for the past quarter century has been the Eplab Standard Cell. It is a "yardstick" for translation of voltage to temperature or pH. The first American commercial cell of its type, constantly improved by research, it is "as standard as sterling". Get ACCURATE temperature or pH control with potentiometers and make sure the standard cells are EPLAB.

The Eppley Laboratory, Inc. SCIENTIFIC INSTRUMENTS NEWPORT, RHODE ISLAND, U. S. A.

EPLAB Standard CELLS
FOR POTENTIOMETRIC INSTRUMENTS

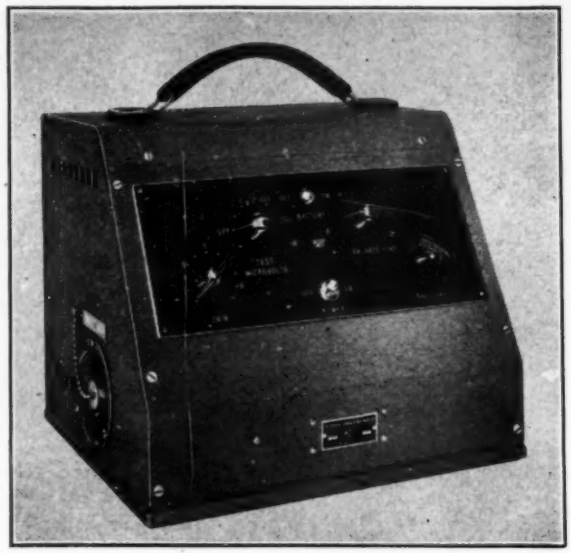

An Electronic Replacement for the Galvanometer

For many years, the suspension galvanometer has been the established means for measurements in the microvolt and fractional microvolt region. However, it is both slow in response, extremely sensitive to vibrations and, consequently, unsuitable for many applications

The Model 53 contact modulated amplifier is capable of duplicating or bettering the performance of any galvanometer system. It is compact, portable and unaffected by vibrations and its output is suitable for actuating standard d.c. meters and relays. Its speed of response permits its use for the measurements of small, rapidly varying voltages and alternating currents up to ten cycles per second. The stability and freedom from drift of the amplifier combined with its rugged construction enables it to meet the requirements of process control equipment.

We shall be pleased to discuss with you the possible application of the amplifier to your particular problems.

P E C

THE PERKIN-ELMER CORP.
GLENBROOK, CONN.

for DISTORTION and BRIDGE MEASUREMENTS at 2 to 15,000 Cycles

● This highly stable oscillator with unusually low distortion is of the resistance-tuned type and operates on the inverse feedback principle developed by General Radio.

The Type 1301-A Low-Distortion Oscillator is especially suitable as an a-f power source for bridge use, for general distortion measurements, to obtain frequency characteristics and to make rapid measurements of distortion in broadcast transmitter systems.

FEATURES

- **WIDE FREQUENCY RANGE**—20 to 15,000 cycles (with Range Extension Unit, 2 to 15,000 cycles)
- **CONVENIENT TO USE**—27 fixed-frequencies, selected by two push-button switches, in logarithmic steps—any desired frequency between steps obtained by plugging in external resistors
- **THREE OUTPUT IMPEDANCES**—600-ohm balanced to ground; 600-ohm unbalanced; 5,000-ohm unbalanced
- **EXCEPTIONALLY PURE WAVEFORM**—Distortion not more than following percentages: with 5,000-ohm output 0.1% from 40 to 7,500 cycles; 0.15% at other frequencies. With 600-ohm output 0.1% from 40 to 7,500 cycles; 0.25% from 20 to 40 cycles and 0.15% above 7,500 cycles.
- **HIGH STABILITY**—Frequency is not affected by changes in load or plate supply voltage. Drift less than 0.02% per hour after few minutes operation
- **ACCURATE FREQUENCY CALIBRATION**—Adjusted to within $1\frac{1}{2}\% \pm 0.1$ cycle
- **NO TEMPERATURE OR HUMIDITY EFFECTS**—In ordinary climatic changes, operation is unaffected

TYPE 1301-A LOW DISTORTION OSCILLATOR . . $395.00

● *The normal range of this oscillator is 20 to 15,000 cycles. The Range Extension Unit (above) lowers this range by a full decade to 2 to 15 cycles, greatly extending its usefulness to frequencies considerably below that heretofore practicable.*

With its very high stability, unusually low distortion and many operating conveniences, the Type 1301-A Oscillator fills a universal need in distortion and bridge measurements.

TYPE 1301-A RANGE EXTENSION UNIT . . $70.00

GENERAL RADIO COMPANY Cambridge 39, Massachusetts

90 West St., New York 6 — 920 S. Michigan Ave., Chicago 5 — 950 N. Highland Ave., Los Angeles 38

CENCO

TRADE MARK REG. U. S. PAT. OFF.

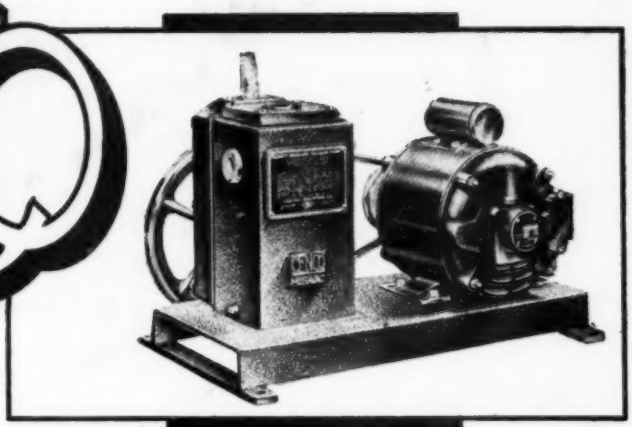

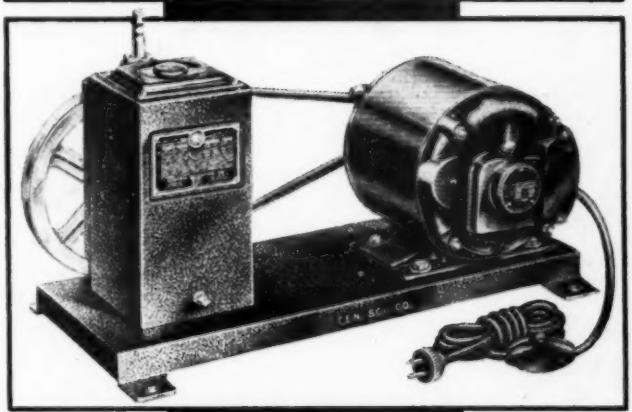

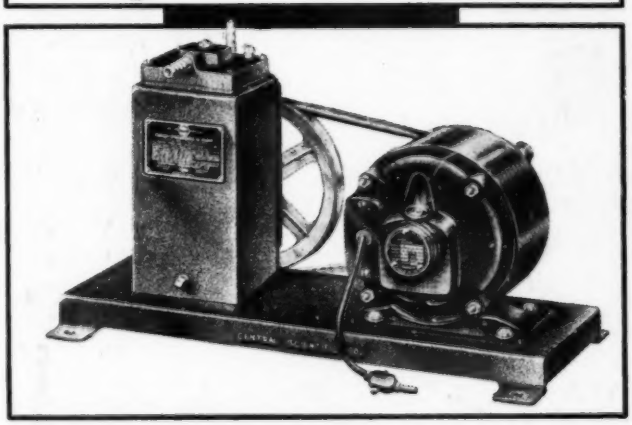

1. **Precision built.**
2. **Minimum number of moving parts.**
3. **Long and trouble-free service.**
4. **Efficient in operation with high speed-to-size ratio.**
5. **High factor of merit.**
6. **Self-lubricated.**
7. **Low cost.**

Cenco High-Vacuum Pumps are precision built for maximum pumping speed and minimum pressure. Engineered with the fewest number of moving parts possible, these pumps combine efficiency and long-life operation with high pumping speed-to-size ratio. Compactness, air-cooling, self-lubrication, trouble-free service, and low cost are other factors worth noting. Technical information on Cenco Vacuum Pumps and accessories may be found in Cenco's new Bulletin 10. Included in this 48-page pamphlet are suggestions for planning a high-vacuum system; information on pumping speed; explanation of merit factor, connections and speed of evacuation, low pressure technique, and other data, together with a complete listing of Cenco mechanical pumps, D-P diffusion pumps and Cenco gages, oils, traps, and other vacuum accessories.

Write attention Dept. Y for copy of Bulletin No. 10 on high vacuum equipment.

SERVING SCIENCE

CENTRAL SCIENTIFIC COMPANY

CENTRAL SCIENTIFIC COMPANY

Scientific CENCO *Apparatus*

1700 IRVING PARK ROAD, CHICAGO 13

NEW YORK BOSTON SAN FRANCISCO NEWARK LOS ANGELES TORONTO MONTREAL

LANCASTER PRESS, INC., LANCASTER, PA.